

**KINETICS OF COIL OVERLAP IN IONOMER  
BLENDS BY  $^1\text{H}$  NMR IN  $\text{DMSO}_{\text{d}6}$**

by

**Francis Bossé**

**A thesis submitted to the Faculty of Graduate Studies and Research in partial fulfillment  
of the requirements for the degree of Master of Science.**

**Department of Chemistry  
McGill University  
Montréal, Québec  
Canada**

**December 1990**

**© Francis Bossé**

## ABSTRACT

### KINETICS OF COIL OVERLAP IN IONOMER BLENDS BY $^1\text{H}$ NMR IN $\text{DMSO}_{d6}$

$^1\text{H}$  nuclear magnetic resonance (NMR) studies were carried out on blends of lightly sulfonated polystyrenes (PS-SSA) [5 to 15 mole % sulfonation] of molecular weight (MW's) ranging from 5000 to 100,000, with poly(methyl methacrylate-co-4-vinyl pyridine) (PMMA-4VP) copolymers [5 to 11 mole %] of MW=100,000.

The process of coil overlap was monitored as a function of time by the acquisition of a proton spectra, which showed the gradual disappearance of the original methoxy signal and the appearance of a new signal originating from the shielded methoxy protons. The contributions of the two species were separated using a deconvolution program.

In order to propose a complete model for the coil overlap phenomenon, parameters that can influence the kinetics of the process were studied. The parameters included the water content of the solution, the ion content of copolymers, the temperature, the MW of PS-SSA and the total polymer concentration.

It was found that the water content had no influence on the shielding process. The study of all the other parameters showed that the overlap was occurring through a complex mechanism. It was determined that the *true order* ( $n_c$ ) for the shielding process was second-order, reflecting the early stages of the mixing process. In the stage in which the "ladder" like complex is produced, the experimental data can be best represented by a kinetic expression containing two opposing first order reactions.

## RÉSUMÉ

La cinétique de recouvrement de chaînes par l'observation du déplacement chimique du groupement méthoxy du PMMA-4VP, pour des mélanges de polymères ioniques en solution de  $\text{DMSO}_{d6}$  par RMN  $^1\text{H}$ .

Des études de résonance magnétique nucléaire  $^1\text{H}$  (RMN) ont porté sur des mélanges de polystyrène légèrement sulfoné (PS-SSA) [5 à 11 mole % de sulfonation] ayant un poids moléculaire (PM) de 5000 à 100,000 avec un copolymère de poly(méthacrylate de méthyl-co-vinylpyridine) (PMMA-4VP) [5 à 11 mole % de 4VP] de PM=100,000.

Le procédé de recouvrement de chaînes a été observé par l'acquisition de spectres de RMN  $^1\text{H}$ , qui montraient la disparition graduelle du signal originant des groupements méthoxys et l'apparition d'un nouveau signal provenant des groupements méthoxys blindés. Les contributions respectives des deux espèces ont été séparées à l'aide d'un programme de déconvolution.

Afin de proposer un modèle complet pour le phénomène de recouvrement de chaînes, les paramètres pouvant influencer le procédé ont été étudiés. Ces paramètres sont la présence d'eau en solution, le contenu ionique des copolymères, la température, le PM du PS-SSA et la concentration totale des copolymères.

Il a été observé que la présence d'eau en solution n'avait pas d'influence sur le procédé. L'étude de tous les autres paramètres nous indique que la réaction se produit par un mécanisme complexe. L'ordre réel ( $n_c$ ) de la réaction a été déterminé comme étant du 2<sup>ème</sup> ordre, mais la meilleure corrélation entre les résultats expérimentaux et les expressions des lois de la cinétique a été obtenue en assumant un mécanisme pour lequel deux réactions d'ordre un s'opposent.

## **FOREWORD**

<b>Chapter 1</b>	<b>Introduction</b>
<b>Chapter 2</b>	<b>Experimental</b>
<b>Chapter 3</b>	<b>Inherent limitations</b>
<b>Chapter 4</b>	<b>Order determination</b>
<b>Chapter 5</b>	<b>Quantitative kinetics - Results and discussion</b>
<b>Chapter 6</b>	<b>Contribution to original knowledge and suggestion for future work</b>

**References are followed by :**

<b>Appendix 1</b>	<b>Deconvolution Process</b>
<b>Appendix 2</b>	<b>Supporting data for the appendix 1</b>
<b>Appendix 3</b>	<b>Formatting program written in fortran, for the transferred nmr files (NMRMOD)</b>
<b>Appendix 4</b>	<b>Deconvolution program written in Fortran (FIT)</b>
<b>Appendix 5</b>	<b>Calculation of the mean distances between two coils in solution</b>
<b>Appendix 6</b>	<b>Supporting Data</b>



## TABLE OF CONTENTS

	Page
ABSTRACT	
RÉSUMÉ	
FOREWORD	
TABLE OF CONTENTS	
ACKNOWLEDGMENTS	
LIST OF TABLES	
LIST OF FIGURES	
LIST OF SYMBOLS	
<u>CHAPTER 1 GENERAL INTRODUCTION</u>	1
1.1 Thermodynamic Basis of Miscibility of Polymer Blends	3
1.1.1 Entropy and Enthalpy Changes upon Mixing of Small Molecules	4
1.1.2 Entropy and Enthalpy Changes upon Mixing of Macromolecules	6
1.2 The Blending Process	8
1.3 Introduction to Chemical Kinetics	10
1.3.1 Rate of Reaction	11
1.3.2 Order of a Reaction	11
1.3.3 The Arrhenius Law	12
1.4 Methods for Determining the Order of a Reaction	13

1.4.1	The Integration Method	13
1.4.2	The Differential Method	14
1.5	Outline of the Thesis	17
	<b><u>CHAPTER 2 EXPERIMENTAL</u></b>	<b>18</b>
2.1	Syntheses	18
2.1.1	Synthesis of PS-SSA	18
2.1.2	Synthesis of PMMA-4VP	19
2.2	Polymer Characterization	19
2.2.1	Characterization of the Molecular Weight and Polydispersity of the PS	19
2.2.2	Characterization of the acid content of PS-SSA	20
2.2.3	Characterization of the base content of PMMA-4VP	23
2.3	Blending Techniques	23
2.4	The NMR Instrumental Method	24
2.5	Introduction to Deconvolution	26
2.5.1	Data Transfer	26
2.5.2	Data Manipulation	27
2.5.3	The Deconvolution Process	27
2.5.4	Quantitative Results of the Deconvolution	30
2.5.4.1	Lineshape of the PMMA-4VP Methoxy Groups	31
2.5.4.2	Lineshape of the PMMA-4VP Methoxy Groups in the Blend	38

2.5.4.3 Application of the Deconvolution to a Typical Lineshape for Shielding Experiments	39
---	----

<b><u>CHAPTER 3 EXPERIMENTAL LIMITATIONS</u></b>	<b>41</b>
3.1 Introduction	41
3.2 Water Content	41
3.3 Temperature	42
3.4 Total Polymer Concentration	44
3.5 PS-SSA Molecular Weight	45
3.6 Ion Content	48
3.7 Electrolyte Effect	50
3.8 Conclusion	51

<b><u>CHAPTER 4 ORDER DETERMINATION</u></b>	<b>53</b>
4.1 Derivation Method	53
4.1.1 Determination of the true order ( $n_c$ )	53
4.1.2 Determination of the order according to time ( $n_t$ )	55
4.1.3 Comparison between $n_t$ and $n_c$	56
4.2 The Integration Method	57
4.3 Opposing Reactions	58
4.3.1 First-Order Opposing Reactions	58
4.3.2 Second-Order Forward First-Order Opposing Reaction	60

4.3.3 Applications of First and Second-Order Scheme to the Time-Concentration Curves	61
4.4 Mechanism for the Shielding Process	74
4.5 Conclusion	78
<b>CHAPTER 5 <u>QUANTITATIVE KINETICS-RESULTS AND DISCUSSION</u></b>	<b>80</b>
5.1 Introduction	80
5.2 Parameters Affecting the Shielding Process for Blends Containing PS-SSA of MW= $10^4$	80
5.2.1 Temperature	81
5.2.2 SSA Content	83
5.2.3 Total Polymer Concentration	85
5.3 Parameters Affecting the Shielding Process for Blends Containing PS-SSA of MW= $10^5$	88
5.3.1 Temperature	89
5.3.2 SSA Content	90
5.3.3 Total Polymer Concentration	92
5.4 The Shielding Process at 80°C for an Equimolar Blend Equilibrated at 150°C	93
5.5 Summary and Conclusions for the Influence of the Experimental Parameters on the Coil Overlap Process	95

<b>CHAPTER 6</b>	<b><u>CONTRIBUTION TO ORIGINAL KNOWLEDGE</u></b>	<b>101</b>
	<b><u>AND SUGGESTION FOR FUTURE WORK</u></b>	
<b>6.1</b>	<b>Contribution to Original Knowledge</b>	<b>101</b>
<b>6.2</b>	<b>Suggestion for Future Work</b>	<b>104</b>
<b>REFERENCES</b>		<b>107</b>
<b>Appendix 1</b>	<b>Deconvolution Process</b>	<b>111</b>
<b>Appendix 2</b>	<b>Supporting data for the appendix 1</b>	<b>119</b>
<b>Appendix 3</b>	<b>Formatting program written in fortran, for the transferred nmr files (NMRMOD)</b>	<b>149</b>
<b>Appendix 4</b>	<b>Deconvolution program written in Fortran (FIT)</b>	<b>155</b>
<b>Appendix 5</b>	<b>Calculation of the mean distances between two coils in solution</b>	<b>203</b>
<b>Appendix 6</b>	<b>Supporting Data</b>	<b>205</b>

## **ACKNOWLEDGEMENTS**

**The contributions of the following persons are most sincerely appreciated and recognized :**

**Dr. Adi Eisenberg for the opportunity to conduct this research, for his support, enlightening discussions, and financial support;**

**Dr. Almeria Natansohn for her most helpful suggestions and discussions relating to many aspects of this work;**

**Dr. Françoise Sauriol for her suggestions and discussions relating to experimental aspect of this work;**

**Nathalie Asselin for her love, patience, encouragement, as well as the proofreading, and many helpful suggestions concerning this thesis;**

**Bryn Hird, Jean-Pierre Gouin, Alain Desjardins and all the other fellow graduate students and summer students who created a friendly and workable environment;**

**The staff of the various workshops of the Chemistry Department; Mr. Roland Gaulin warrants special mention for maintaining the equipment in good working condition;**

**Les Fonds pour la Formation de Chercheurs et l'Aide à la Recherche (Québec), and McGill University for financial support;**

**The Natural Sciences and Engineering Research Council (Canada) and the Imperial Oil for financial support of laboratory supplies and equipments.**

## LIST OF TABLES

Table	Page	Title
1	15	Summary of rate equations
2.1	20	Molecular weights and polydispersity indices for the PS samples
2.2	21	Ion content determination for PS-SSA
2.3	22	Ion content determination after water extraction for PS-SSA
2.4	23	Ion content determination for PMMA-4VP
2.5	34	Deconvoluted shoulder area for the methoxy $^1\text{H}$ NMR signal of PMMA-4VP as a function of temperature
3.1	47	Summary of $\Gamma$ and $\Delta\Gamma$ values for blends containing a PS-SSA of low MW, with no observable shielded methoxy group signal
3.2	49	Summary of $\Gamma$ and $\Delta\Gamma$ values for blends containing a PMMA-4VP of low ion content, with no observable shielded methoxy group signals
3.3	52	Summary of the experimental ranges over which the kinetic runs for the shielding process of the methoxy group signal can be performed, as a function of the investigated parameters
4.1	56	Determination of the order according to time ( $n_t$ ) for two series of equimolar mixtures of PS-SSA 10 mole % with PMMA-4VP 11 mole % (MW= $10^5$ ), at 85°C
4.2	70	Summary of the rate constants for a mechanism in which a first-order or a second-order forward reaction is opposed to a first-order backward reaction, for various mixtures of PMMA-4VP 11 mole % (MW= $10^5$ ) with PS-SSA, in 0.5 ml of $\text{DMSO}_{\text{d}6}$
5.1	82	Effect of Temperature Rate constants for equimolar blends (0.10 M) of PMMA-4VP 11 mole % (MW = $10^5$ ) with PS-SSA 10 mole % (MW = $10^4$ ) in 0.5 ml of $\text{DMSO}_{\text{d}6}$

<b>Table</b>	<b>Page</b>	<b>Title</b>
5.2	84	Effect of SSA content Rate constants for equimolar blends (0.10 M) of PMMA-4VP 11 mole % (MW = $10^5$ ) with PS-SSA (MW = $10^4$ ) in 0.5 ml of DMSO <sub>d6</sub> at 85°C
5.3	87	Effect of total polymer concentration Rate constants for equimolar blends of PMMA-4VP 11 mole % (MW = $10^5$ ) with PS-SSA 10 mole % (MW = $10^4$ ) in 0.5 ml of DMSO <sub>d6</sub> at 85°C
5.4	90	Effect of temperature Rate constants for equimolar blends (0.10 M) of PMMA-4VP 11 mole % (MW = $10^5$ ) with PS-SSA 10 mole % (MW = $10^5$ ) in 0.5 ml of DMSO <sub>d6</sub>
5.5	91	Effect of SSA content Rate constants for equimolar blends of PMMA-4VP 11 mole % (MW = $10^5$ ) with PS-SSA (MW = $10^5$ ) in 0.5 ml of DMSO <sub>d6</sub> at 85°C
5.6	93	Effect of total polymer concentration Rate constants for the experimental total polymer concentration range, for equimolar blends of PMMA-4VP 11 mole % (MW = $10^5$ ) with PS-SSA 10 mole % (MW = $10^5$ ) in 0.5 ml of DMSO <sub>d6</sub> at 85°C



## LIST OF FIGURES

Figure	Page	Title
1	9	Illustration of the mixing process and the resulting proton transfer for PMMA-4VP and PS-SSA.
2.1	25	a) Experimental array of preacquisition delay (PAD) in seconds. b) Profile of the S2PUL pulse sequence.
2.2	35	$^1\text{H}$ NMR spectrum for the methoxy groups from PMMA-4VP at $120^\circ\text{C}$
2.3	36	$^1\text{H}$ NMR spectrum for the methoxy groups from PMMA-4VP at $85^\circ\text{C}$
2.4	37	$^1\text{H}$ NMR spectrum for the methoxy groups for a blend of PS-SSA 10% of $\text{MW} = 10^4$ with PMMA-4VP 11% of $\text{MW} = 10^5$ in $\text{DMSO}_{\text{d}6}$ at $85^\circ\text{C}$ (contact time = 30 min.). The peaks labeled A ( $\approx 3.57$ ppm) and B ( $\approx 3.52$ ppm) are, respectively, the unshielded and the shielded methoxy signal.
2.5	40	Example of a $^1\text{H}$ NMR stack spectra for a typical shielding experiment for a blend of PS-SSA (5 mole %) of $\text{MW} = 10^4$ with PMMA-4VP (11 mole %) of $\text{MW} = 10^5$ in $\text{DMSO}_{\text{d}6}$ at $85^\circ\text{C}$ . The contact times correspond to the PAD defined in section 2.4 minute with one minute added to each delay time. A ( $\approx 3.57$ ppm) and B ( $\approx 3.52$ ppm) are respectively the unshielded and the shielded ( $\approx 3.52$ ppm) methoxy group signals, and C ( $\approx 3.15$ ppm) is the signal due to traces of water.
3.1	43	Spectrum obtained by the addition of $\text{D}_2\text{O}$ to the equilibrated polymer solution; elapsed time 1.5 hrs at $T = 85^\circ\text{C}$ . The percentage figures refers to volume $\text{D}_2\text{O}$ / volume $\text{DMSO}_{\text{d}6} \times 100$ . The peaks labeled A ( $\approx 3.57$ ppm), B ( $\approx 3.52$ ppm) and C (3.2 to 3.0 ppm range) are respectively, the unshielded methoxy, the shielded methoxy and the water peak.
4.1	54	Determination of the true order ( $n_c$ ) for equimolar blends of PMMA-4VP 11 mole % ( $\text{MW}=10^5$ ) with PS-SSA 10 mole % ( $\text{MW}=10^4$ , $\text{MW}=10^5$ ) at $85^\circ\text{C}$ in $\text{DMSO}_{\text{d}6}$ .

Figure	Page	Title
4.2	62	Time-concentration curves for various equimolar starting concentrations of PMMA-4VP 11 mole % of MW= $10^5$ with PS-SSA 10 mole % of MW= $10^5$ , at 85°C. The concentration on the vertical axis refers to the unshielded methoxy groups signal.
4.3	63	Time-concentration curves for equimolar mixtures of PMMA-4VP 11 mole % with PS-SSA of MW= $10^5$ at 85°C. Each curve represents a distinct sulfonation level. The solution contains 5 mg of both copolymers per 0.5 ml of DMSO <sub>d6</sub> (0.10 M). The concentration of the vertical axis refers to the unshielded methoxy groups signal.
4.4	64	Time-concentration curves for equimolar mixtures of PMMA-4VP 11 mole % with PS-SSA 10 mole % of MW= $10^5$ at various temperatures. The DMSO <sub>d6</sub> solution contains 5 mg of both copolymers per 0.5 ml (0.10 M). Vertical shifts of 0.025, 0.05, 0.02, 0 and 0 were respectively introduced on the curves from 70°C to 95°C. The concentration on the vertical axis refers to the unshielded methoxy groups signal.
4.5	65	Time-concentration curves for mixtures of various equimolar starting concentrations of PMMA-4VP 11 mole % of MW= $10^5$ with PS-SSA 10 mole % of MW= $10^4$ , at 85°C. Vertical shifts of 0, 0.01 and 0.020 were respectively introduced on the curves from 0.15 M to 0.05 M. The concentration on the vertical axis refers to the unshielded methoxy groups signal.
4.6	66	Time-concentration curves for equimolar mixtures of PMMA-4VP 11 mole % with PS-SSA of MW= $10^4$ at 85°C. Each curve represents a distinct sulfonation level. The solution contains 5 mg of both copolymers per 0.5 ml of DMSO <sub>d6</sub> (0.10 M). The concentration on the vertical axis refers to the unshielded methoxy groups signal.
4.7	67	Time-concentration curves for equimolar mixtures of PMMA-4VP 11mole % with PS-SSA 10 mole % of MW= $10^4$ at various temperatures. The solution of DMSO <sub>d6</sub> (0.5 ml) contained 5 mg of both copolymers. The concentration on the vertical axis refers to the unshielded methoxy groups signal.

Figure	Page	Title
4.8	71	Plots of equations 4.5 and 4.8 for an equimolar mixture of PMMA-4VP 11 mole % with PS-SSA 10 mole % of MW=10 <sup>5</sup> , at 85°C. The DMSO <sub>d6</sub> solution contains 2.5 mg of both copolymers per 0.5 ml (0.05 M).
4.9	72	Plot of equation 4.11 for an equimolar mixture of PMMA-4VP 11 mole % with PS-SSA 10 mole % of MW=10 <sup>5</sup> , at 85°C, The DMSO <sub>d6</sub> solution contains 2.5 mg of both copolymers per 0.5 ml (0.05 M).
4.10	73	Time-concentration curve for the equimolar mixture (0.05 M) of PMMA-4VP 11 mole % of MW=10 <sup>5</sup> with PS-SSA 10 mole % of MW= 10 <sup>4</sup> , at 85°C. The concentration on the vertical axis refers to the shielded methoxy groups signal.
5.1	96	Plot of $\ln(X_e/X_e - X)$ vs time for an EQB (0.10M) containing PMMA-4VP 11 mole % (MW=10 <sup>5</sup> ) with PS-SSA 10 mole % (MW= 10 <sup>5</sup> ), at 80°C.

## LIST OF SYMBOLS

$A$	= preexponential factor
$a_0$	= initial concentration
$\text{\AA}$	= angstrom
$B(T)$	= temperature-dependent preexponential factor
$C^*$	= polymer concentration at which coil interpenetration begins
DMSO	= dimethyl sulfoxide
DMSO <sub>d6</sub>	= deuterated dimethyl sulfoxide
$E$	= internal energy
EA	= ethyl acrylate
EQB	= equilibrated blend at a preset temperature
exp	= function which returns the value of $e$ (base of natural logarithm) raised to the value of the argument
$E_{AA}, E_{BB}, E_{AB}$	= energy required to separate two A molecules, two B molecules, and an A molecule from a B molecule.
$E_a$	= activation energy
$G$	= Gibbs free energy
$h_{av}$	= average end-to-end distance of a polymer chain
$(\bar{h}^2)^{1/2}$	= rms average of the separation between the two ends of the polymer chain
$H$	= enthalpy
$^1\text{H}$	= proton
$k$	= rate constant
$k_{-1}$	= rate constant for the back reaction of the initiation process
$k_{-2}$	= rate constant for the back reaction of the cascade process

$k_{-3}$	= rate constant for the back reaction of the spatial reorganization process
$K_{-1}$	= apparent rate constant for the deshielding process
$k_1$	= rate constant for the forward reaction of the initiation process
$k_2$	= rate constant for the forward reaction of the cascade process
$k_3$	= rate constant for the forward reaction of the spatial reorganization process
$K_1$	= apparent rate constant for the shielding process
$K_T$	= apparent rate constant for the global process
$l$	= bond length
$\ln$	= logarithm to the base e (2.718281828)
$\log$	= logarithm to the base 10
$M$	= mole liter <sup>-1</sup>
$M$	= mole of repeat units liter <sup>-1</sup>
$M_i$	= unstable intermediate referring to component i
$MW$	= molecular weight, in atomic mass units
$n$	= order of a reaction
$n_c$	= order according to concentration
$n_t$	= order according to time
$N_{AV}$	= Avogadro's number
$NMR$	= nuclear magnetic resonance
$NOE$	= nuclear Overhauser effect
$NOESY$	= nuclear Overhauser effect pulse sequence
$P$	= pressure
$PEA$	= poly(ethyl acrylate)

PMMA-4VP	= poly(methyl methacrylate-co-4-vinylpyridine)
4VP	= 4-vinyl pyridine
PS	= poly(styrene)
PS-SSA	= poly(styrene-co-styrene sulfonic acid)
$r$	= degree of polymerization in the equation for the entropy of mixing
$R$	= ideal gas constant
rms	= root mean square
$S$	= entropy
$T$	= temperature
$t$	= time
$V$	= volume
$V_r$	= molar volume of a reference segment
$W_{AB}$	= interchange energy
$x$	= concentration of the products (general) at time = $t$
$X$	= concentration of the shielded methoxy groups at time = $t$
$X_e$	= equilibrium concentration of the shielded methoxy groups
$X_A, X_B$	= mole fraction of component A and B
$\nu_{1/2}$	= half width of a band or peak at half height
$\phi_i$	= volume fraction of component $i$
$\sigma$	= number of segments in a polymer chain
$\Gamma$	= width of a band at half height
$\Gamma_{1/2}$	= width of a band at half height divided by two
$\Theta$	= angle between the positive direction of successive bonds in a polymer chain

## CHAPTER 1. GENERAL INTRODUCTION

Since major improvements in polymer properties can be achieved by blending, this area has been subject of increasing interest over the last few decades.<sup>1-8</sup> The potential of this approach can be appreciated when one considers the improvement in the properties of metallic alloys over those of pure metals. However, most polymer pairs are not miscible<sup>9-11</sup>, and the blends formed from such pairs tend to phase separate. The lack of strong cohesive forces between the phases in such blends gives rise to poor mechanical properties, which greatly limits the number of industrial applications of these materials. A few methods are described in the literature that lead to miscibility enhancement in polymer blends<sup>30</sup>. One of these, explored extensively in our laboratory, consists of introducing appropriate ionic groups onto each polymer chain. The first example<sup>12</sup> of the series of papers published on this topic dealt with the immiscible pair poly(styrene) (PS) and poly(ethyl acrylate) (PEA). When a copolymer of EA with 5 mol % of 4-vinylpyridine (4VP) was mixed with a lightly sulfonated poly(styrene) (PS-SSA) containing 5 mol % of sulfonic acid groups, the proton from the styrene sulfonic acid unit was transferred to the pyridine ring, forming an ion pair which rendered this polymer pair miscible.

It is evident that the concentration of interacting groups has to be equimolar in order to obtain maximum interaction. Studies on different polymer pairs suggest that a minimum of 4 mol % of interacting groups was necessary in order to achieve miscibility in two different polymer pairs<sup>13</sup>, i.e. to obtain a single glass transition temperature for the blend measured by dynamic mechanical studies.

Many techniques can be used to determine the extent of phase separation in polymer blends, however, each of these methods is sensitive to domains of specific sizes.

For instance, glass transition temperature measurements reveal homogeneity over dimensions down to 100 Å, whereas film transparency indicates homogeneity at a level of ca. 1000 Å. However, in order to achieve a better understanding of the parameters influencing the miscibility of polymer blends, they must be studied down to a molecular level, and this has been recently feasible by two spectroscopic techniques NMR<sup>14-15</sup> and fluorescence<sup>16-29</sup>.

In a previous study by A. Natansohn and A. Eisenberg, <sup>1</sup>H NMR spectroscopy was used to probe the miscibility of a blend of poly(methyl methacrylate-co-4VP) [PMMA-4VP] with poly(styrene-co-styrene sulfonic acid) [PS-SSA] in DMSO solution.<sup>30</sup> This technique was useful because the methoxy proton signal of MMA is very sensitive to any aromatic shielding effect, in this particular case to the effect of the aromatic rings of the styrene units. It was previously demonstrated<sup>31</sup> that the proton transfer from the SSA group to the pyridine ring takes place very rapidly; by contrast, it was found<sup>30</sup> that the mixing of the two types of polymers is a slow process dictated by the segmental motion in solution. For a system containing ca. 11 mole % of ionic groups on each polymer at a 2% total concentration in DMSO, the coil overlap took ca. two hours at 85°C. The coil overlap process could be followed by monitoring the chemical shift of the methoxy signal in the proton spectra, or by measuring the area of the cross-peak that appears in the 2D-NOESY spectrum between the methoxy and aromatic signals, but the second procedure is more time consuming. The best method to obtain quantitative information about the interpolymer interaction is by measuring the one dimensional NOE effects.<sup>31</sup> Correlation of the magnitude of the NOE effect with the relaxation times can give detailed information on intermolecular distances. The one- and two-dimensional NOE-correlated spectra demonstrated the presence of dipolar coupling through space between the methoxy protons of the PMMA-4VP and the aromatic protons



of the PS-SSA, and this requires an interchain distance of about 4Å.

From the previous study it was clearly demonstrated that the blending process occurs in DMSO solution, and from the aromatic shielding effect on the methoxy protons in PMMA, it was seen that the majority of those protons were indeed close to the aromatic rings of the PS-SSA. However, the detailed mechanism and the parameters influencing the coil overlap or interpenetration remained unknown. To explore this problem, the  $^1\text{H}$  NMR aromatic shielding phenomenon can be utilized to perform kinetic experiments. Thus, the purpose of this investigation is to elucidate the kinetics of the process in greater details, and this will be the subject of this thesis.

Before proceeding further, a general overview of the topics that are directly related to the subject matter of this thesis will be given. Section 1.1 will give the thermodynamic basis of miscibility of two dissimilar polymer chain. Section 1.2 will describe the specific interaction that has been used to enhance the miscibility, and finally sections 1.3 and 1.4 will review chemical kinetic principles and methods that will be essential to the comprehension of the proposed model.

### 1.1 Thermodynamic Basis of Miscibility of Polymer Blends

For systems at constant pressure and temperature, the thermodynamic function that determines the chemical equilibrium is the Gibbs free energy (G):

$$G = H - TS$$

where H is the enthalpy, T the temperature and S the entropy of the system under consideration. A reaction will be spontaneous if the change of the free energy is negative ( $\Delta G < 0$ ). If we consider the variation of the free energy upon isothermal mixing two

components A and B, we can write:

$$\Delta G_M = \Delta H_M + T\Delta S_M \quad (1.1)$$

where  $\Delta H_M$  is the change in the enthalpy and  $\Delta S_M$  is the change in the entropy upon mixing. If we assume that the volume remains constant upon mixing ( $\Delta V_M = 0$ ), which is usually the case for solutions, the enthalpic term can be related to the internal energy variation upon mixing ( $\Delta E_M$ ):

$$\Delta H_M = \Delta E_M + P \Delta V_M = \Delta E_M \quad (1.2)$$

where P is the pressure.

Thus, to a first approximation, we may say that the miscibility will be influenced only by the two contributions to the free energy of mixing, which are the internal energy and the entropy of mixing. The influence of these two contributions on the miscibility will be discussed for two separate cases, small molecules and macromolecules.

### 1.1.1 Entropy and Enthalpy Changes upon Mixing of Small Molecules

The energy change upon mixing is related to the cohesive forces holding the individual component molecules A and B to their neighbors in the pure state as compared to the solution. If  $E_{AA}$  (or  $E_{BB}$ ) is the minimum energy required to break the contact between two of the pure molecules (A or B), and  $E_{AB}$  the minimum energy that is necessary to break the contact between an A molecule and its B-type neighbor in the solution, then, according to the regular solution theory<sup>32</sup>,  $\Delta E_M$  per mole of molecules can be expressed as:

$$\Delta E_M = N_{AV} X_A X_B z [1/2 (E_{AA} + E_{BB}) - E_{AB}] \quad (1.3)$$

where  $X_A$  and  $X_B$  are the mole fractions of components A and B, respectively,  $N_{AV}$  is Avogadro's number, and  $z$  is a constant dependent on the geometry of the molecular arrangement in the solution and in the pure states. The factor in brackets is referred to as the interchange energy ( $W_{AB}$ ), and its sign determines that of  $\Delta E_M$ . Consequently, from equation (1.2), the enthalpy of mixing can be related to the attractive forces that are holding molecules in their environment as it changes from the pure state to the solution state. It is a measure of the antipathy between the components: a positive value is an indication that the molecules prefer to be in the pure state, while a negative value indicates that the molecules prefer being mixed.

The variation in entropy upon mixing ( $\Delta S_M$ ) can be estimated by evaluating the change in the combinatorial entropy, using the lattice model of the strictly regular solution theory. The expression for the variation of entropy of mixing per mole of molecules in the solution<sup>32</sup> is

$$\Delta S_M = -R [X_A \ln(X_A) + X_B \ln(X_B)] \quad (1.4)$$

where  $R$  is the ideal gas constant. The value of the entropic term is always negative, so it will always contribute to decrease the Gibbs free energy upon mixing.

Although the assumptions used in the derivation of the regular solution theory are not always met in practice, equation (1.2) and (1.3) will still enable us to get a qualitative understanding of the driving force leading to mixing. In theory, the entropic term of equation (1.4) will depend only on the initial composition of the solution, while the enthalpic term will depend only on the interactions between the molecules in solution. This model leads us to three distinct situations:

1)  $\Delta H_M = 0$  : This occurs when the average strength of A-B interactions are equivalent to the mean strength of A-A and B-B interactions. This mixing process is athermal and

the mixing is only due to the entropic contribution that will render  $\Delta G_M$  negative.

2)  $\Delta H_M < 0$  : This is due to some specific interactions occurring between A and B molecules, the average strength of the A-B interactions are greater than those for the A-A and B-B interactions. The mixing is exothermic, because both contributions will render  $\Delta G_M$  negative, resulting in a one phase solution.

3)  $\Delta H_M > 0$  : This case is encountered when the A and B molecules "dislike" one another in the solution state, thus the mixing process is endothermic. In such cases, the sign of  $\Delta G_M$  would depend on the relative magnitude of the entropic and enthalpic terms. Usually, in the case of small molecules, the enthalpic contribution is smaller than the entropic one. Thus, if the positive contribution of  $\Delta H_M$  to  $\Delta G_M$  is counterbalanced by negative contribution of  $\Delta S_M$ , mixing will occur.

From the previous cases, it can be stated that unless the small molecules to be mixed are very dissimilar in terms of the strength of cohesive forces holding them concerned, the Gibbs free energy of mixing will always be negative and favor mixing, because of the large entropy increase upon mixing.

### 1.1.2 Entropy and Enthalpy Changes upon Mixing of Macromolecules

The thermodynamic treatment of mixing polymers is more complex than that given by the regular solution theory. Using the lattice model to express the combinatorial entropy of mixing, it is assumed that for small molecules there is no limitation on the neighbor that can occupy a site in the lattice. This is not the case for macromolecules due to their segmental nature. Thus the number of possible arrangements in the lattice are greatly reduced for macromolecules, and this implies that the combinatorial entropy of mixing to  $\Delta G_M$  will drastically differ from that obtained for

small molecules.

Applying the Flory-Huggins theory of polymer solutions<sup>33</sup> to mixtures of polymer, Scott expressed the enthalpy and entropy of mixing (per unit volume of solution) of two polymers<sup>34</sup> as

$$\Delta H_M/V = z \phi_1 \phi_2 \quad (1.5)$$

$$\Delta S_M/V = -(R/V_r) [\phi_1/r_1 \ln(\phi_1) + \phi_2/r_2 \ln(\phi_2)] \quad (1.6)$$

where  $V$  is the volume of the mixture,  $\phi_i$  is the volume fraction of component  $i$ ,  $V_r$  is the molar volume of a reference segment, and  $r$  is the degree of polymerization in terms of the reference segment. The presence of the  $r_i$  terms in the denominator implies that  $\Delta S_M$  will decrease as the degree of polymerization increases, thus it is expected that for high molecular weight (MW) blends of polymers, the entropic contribution to the mixing process will eventually be negligible.

This simple theory leads essentially to the same conclusions as more involved models<sup>35-37</sup>, which is that for polymers of high MW, above ca. several thousand, the combinatorial entropy variation associated with mixing becomes unimportant, as opposed to solutions of low MW molecules where it is often the major driving force for mixing. The enthalpy of mixing, on the other hand, is primarily dependent on the energy variation associated with the nearest neighbor interactions during mixing, and, as a first approximation, we can assume that this is independent of MW. Accordingly, miscibility can usually be achieved if the enthalpy of mixing is negative ( $\Delta H_M < 0$ ). Thus, the favorable electrostatic interaction that occurs when appropriate ionic groups are introduced onto each polymer chain, is the driving force that enables the two dissimilar polymeric chains to mix and form the blend.

## 1.2 The Blending Process

As we have seen in section 1.1.2, because of the negligible contribution from the entropy change upon mixing, specific interactions between two dissimilar polymer chains are very helpful in order to achieve miscibility. Thus, the blending process occurring between the PS-SSA and the PMMA-4VP is due to proton transfer which occurs between the SSA and the 4VP, which in turn, generates the oppositely charged ions which are the driving force responsible for the miscibility of the PS-SSA and PMMA-4VP. The formation of those ion pairs drags both chains close to one another, which is schematically represented in figure 1.

This blending process can be monitored by NMR in  $\text{DMSO}_{d6}$  solutions, and has been found to be surprisingly long, ca. one hour<sup>30</sup>. From a NMR proton spectrum, it is possible to quantify the concentration of chain segments that are close to one another by the appearance of a second peak for the PMMA methoxy signal. This new upfield methoxy signal is due to aromatic shielding caused by the presence of the benzene ring of the PS in the neighborhood of the methoxy groups. This phenomenon is due to the large closed loop of  $\Pi$  electrons on the benzene ring. When the ring is placed in a magnetic field, electron circulation over the entire  $\Pi$  system causes a powerful induced field. This induced field will create, in the case of the benzene ring, a cone of anisotropy that will induce shielding upon the methoxy groups that are under its influence.

Assuming that the peak area is proportional to the concentration, when both contributions to the methoxy lineshape are detectable, it is possible by a mathematical deconvolution process to obtain two independent areas. This will enable us to perform quantitative kinetics of the blending process, and since the blending is performed in solution, we can look at it as the interpenetration of two coils.

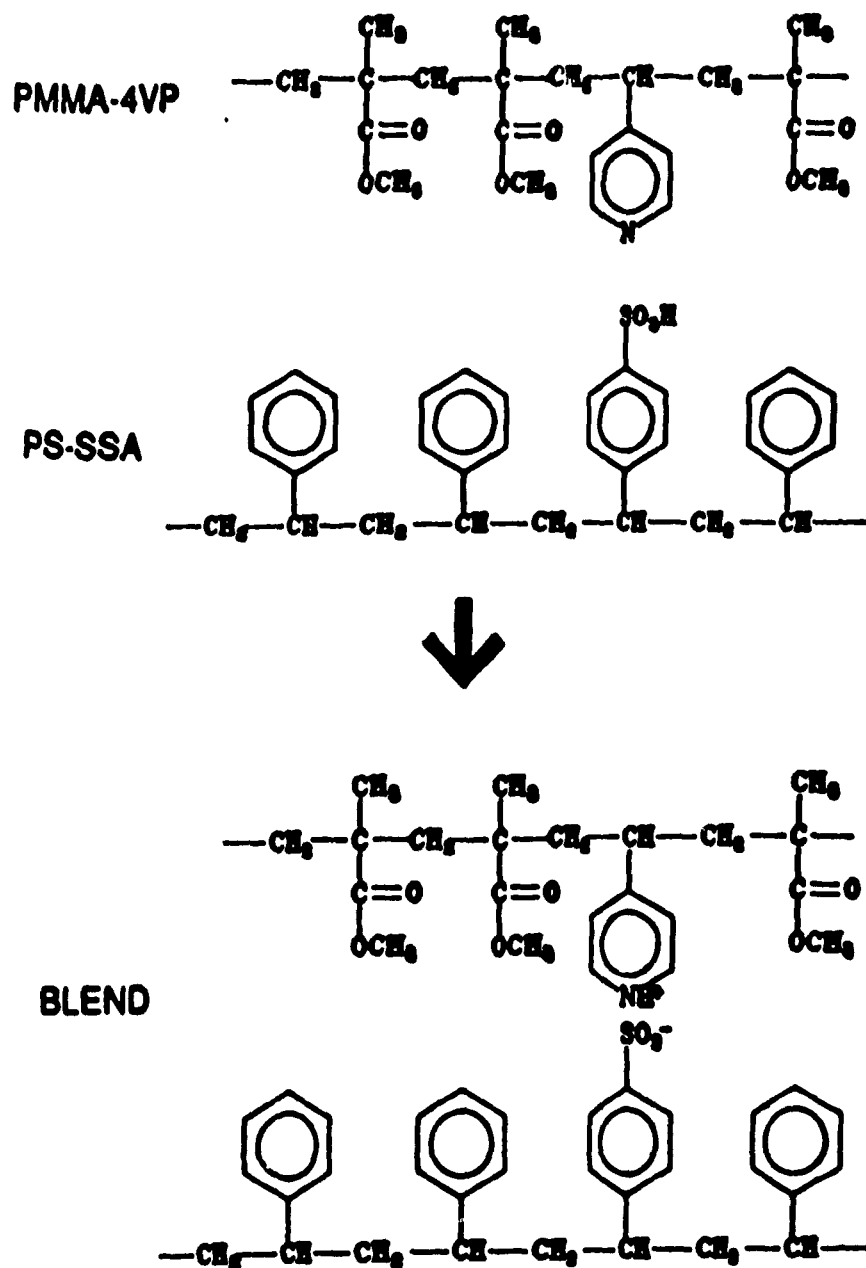


**Figure 1** Illustration of the mixing process and the resulting proton transfer for PMMA-4VP and PS-SSA.

### 1.3 INTRODUCTION TO CHEMICAL KINETICS

The subject of chemical kinetics is concerned with the quantitative study of the rates of chemical reactions and the factors on which they depend. Historically, a few investigations were carried out before the beginning of the last century: those studies involved rate determinations, but little attempt was made to interpret these results in terms of exact laws. Among these early studies may be mentioned the experiments of Kirchhoff<sup>38</sup> on the hydrolysis of starch by dilute acids, and Thénard's investigation<sup>39</sup> of the rate of decomposition of hydrogen peroxide in presence of alkalis.

In the years 1865 to 1867 Hartcourt and Esson<sup>40,41</sup> published the results of their investigations on the reaction between potassium permanganate and oxalic acid. Detailed experimental studies of the rate of this reaction were performed by Hartcourt, and the results were analyzed mathematically by Esson. Expressions for the extent of reaction as a function of time were worked out for a "*first-order*" reaction, in which the rate is proportional to the concentration of only one reacting substance, and for a "*second-order*" reaction, in which the rate is proportional to the product of two concentrations.

In 1889, an important breakthrough was made by Arrhenius<sup>42</sup>, who explained the large increase in the rate that was very often observed when the temperature was increased. This development will be discussed in some detail in section 1.3.3, and most of the remainder of the present introduction will be devoted to the definition and the expression of laws that can relate the concentration and the rate of reaction.



### 1.3.1 Rate of Reaction

The rate of a reaction , which may also be called its velocity or speed, may be expressed in terms of the concentration of any reactant or any product of the reaction. It may also be expressed as the rate of decrease of the concentration of the reactants, or as the rate of increase of the products of the reaction. Thus if a reactant has a concentration  $c$  at any time  $t$ , the rate is given by  $-dc/dt$ , or  $dx/dt$  if the product is referred to as  $x$ . It is clear from this formulation that the rate must have the units of concentration divided by time. The time is usually expressed in seconds or minutes, and the concentration most frequently in moles liter<sup>-1</sup> (M); in such cases, the units for the rate are M sec.<sup>-1</sup> or M minute<sup>-1</sup>.

### 1.3.2 Order of a Reaction

Usually, the rate of a reaction varies with the concentrations of the reacting species, and this variation can be characterized by stating the order of the reaction. In general, it is found experimentally that the rate of a reaction is proportional to the  $\alpha$  power of the concentration of one of the reactants A, to the  $\beta$  power of the concentration of B, etc.,

$$\text{Rate} = k c_A^\alpha c_B^\beta \dots \quad (1.7)$$

the overall order of the reaction can be express as

$$n = \alpha + \beta + \dots \quad (1.8)$$

and such a reaction is said to be of the order  $\alpha$  with respect to A, and  $\beta$  with respect to B, etc.

For the sake of completeness, it is important to mention that by no means all reactions can be spoken of as having an order. In many cases the relationship between the rate and the concentrations can not be represented by equation (1.7); frequently, for example, concentrations appear also in the denominator of the rate expression. Such complex rate expressions arise as a result of the fact that the reaction occurs by a complex mechanism, that involves a certain number of steps. However, it is beyond the scope of this introduction to develop the related equations for those reactions.

### 1.3.3 The Arrhenius Law

All theories of chemical kinetics bear a close relationship to the Arrhenius law,

$$k = A e^{-E_a / RT} \quad (1.9)$$

where  $k$  is the rate constant,  $A$  the preexponential factor,  $E_a$  the activation energy,  $R$  the ideal gas constant and  $T$  the temperature. Equation (1.9) was originally an empirical and macroscopic law relating the rate constant to the temperature. The great virtue of this law is its simplicity; it involves only two parameters, the experimental activation energy  $E_a$  and the preexponential or frequency factor  $A$ . It is satisfactory that few experimental results show significant deviations from the law. However, the precise meaning of the parameters  $E_a$  and  $A$  is by no mean simple and straightforward.

Arrhenius<sup>43</sup> and van't Hoff<sup>44</sup> originally interpreted  $E_a$  as simply the height of the energy barrier which has to be overcome in order for the reaction to occur. This concept is basically correct, but is oversimplified since we know that the probability that a reaction will occur is a rather complex function of the various kinds of energy in the reacting molecules, and the relative configuration of the reactant molecules when the collision takes place. Various attempts to take this into account can be summarized by

the following equation,

$$k = B(T) e^{-E_0/RT} \quad (1.10)$$

where  $E_0$  is the threshold, i.e., the lowest relative translational energy at which reaction can occur. The preexponential factor  $B(T)$  is now temperature-dependent, its form depending on the specific assumptions made in the theory about which part of the total energy of the system contributes towards the reaction. Since this depends upon the nature of the reaction, most versions of equation (1.10) are not widely applicable; however, it remains a convenient way to rationalize results that deviate from the Arrhenius law.

#### 1.4 Methods for Determining the Order of a Reaction

##### 1.4.1 The Integration Method

In the kinetic study of a reaction, the concentration of one or more of the products (or reactants) is determined at various times. If this concentration is plotted as a function of time, a smooth curve should be obtained. The slope of this curve is the rate of reaction ( $-dc/dt$  or  $dx/dt$ ). The method of integration is commonly employed and involves using expressions relating the concentration to the time for reactions of various orders, and fitting the appropriate expression to the experimental data.

A reaction that is of the  $n$ th order and involves substances that initially have a concentration  $a_0$ , may be represented schematically as



If  $x$  is the amount of  $A$  per unit volume that has disappeared in time  $t$ , the amount of  $A$

remaining is  $a_0 - x$ ; the rate of disappearance of A or appearance of X is thus

$$-\frac{d(a_0 - x)}{dt} = \frac{dx}{dt} = k(a_0 - x)^n \quad (1.12)$$

Equation (1.12) must be integrated using the boundary condition that  $x = 0$  when  $t = 0$ .

For  $n \neq 1$ , the solution for the rate constant  $k$  is

$$k = \frac{1}{t(n-1)} \left[ \frac{1}{(a_0 - x)^{n-1}} - \frac{1}{a_0^{n-1}} \right] \quad (1.13)$$

If  $n = 1$ , the solution is

$$k = \frac{1}{t} \ln \frac{a_0}{a_0 - x} \quad (1.14)$$

The integrated rate equations for various values of  $n$  are given in Table 1.

In order to use the integration method, we start with a differential rate equation that is believed to apply to the reaction under consideration. The integrated equation is then applied to the kinetic data, by graphical means. If there is a good fit over a wide range of the relevant variables (concentration and time), we may conclude that the equation chosen is applicable, and the rate constant can be calculated. If the fit is not good, the procedure is repeated with another equation until the fit is satisfactory. Even though trial and error is evidently involved, it remains a valuable method.

#### 1.4.2 The Differential Method

In the differential method, which was suggested by van't Hoff<sup>22</sup>, the actual rates of reactions can be determined by measuring the slope of concentration-time curves.

Table 1 Summary of rate equations

RATE EQUATION		
Order	Differential form	integrated form
0	$\frac{dx}{dt} = k$	$k = \frac{x}{t}$
1/2	$\frac{dx}{dt} = k(a_0 - x)^{1/2}$	$k = \frac{2}{t} [a_0^{1/2} - (a_0 - x)^{1/2}]$
1	$\frac{dx}{dt} = k(a_0 - x)$	$k = \frac{1}{t} \ln \frac{a_0}{a_0 - x}$
3/2	$\frac{dx}{dt} = k(a_0 - x)^{3/2}$	$k = \frac{2}{t} \left  \frac{1}{(a_0 - x)^{1/2}} - \frac{1}{a_0^{1/2}} \right $
2	$\frac{dx}{dt} = k(a_0 - x)^2$	$k = \frac{1}{t} \frac{x}{a_0(a_0 - x)}$

In each case the rate constant  $k$  refers to the disappearance of reactants.

The rate of a reaction may be related to the concentration of a reactant by the equation.

$$v = kc^n \quad (1.15)$$

Taking the natural logarithms,

$$\ln v = \ln k + n \ln c \quad (1.16)$$

If the velocity is measured at various initial concentrations, and a log-log plot of the initial rate of reaction as a function of the initial concentration is prepared, we should have a straight line with a slope equal to  $n_c$  (see below for definition). This procedure of dealing with initial rates avoids possible complications due to interference by products, and leads to an order which corresponds to the simplest type of situation. In view of this, Letort<sup>23</sup> has referred to the order determined in this way as the *order with respect to concentration* or the *true order*. The symbol  $n_c$  will be used to denote this order.

The second procedure involves considering a single run, and measuring slopes at various times corresponding to different values of the reactant concentrations. For a double logarithmic plot of the rate of reaction as a function of the corresponding reactant concentrations, the slope is equal to  $n_t$ , which can be referred as the *order with respect of time*, because the time is now varying.

Comparing these two orders ( $n_t$  and  $n_c$ ) can help us to draw some qualitative conclusion about the mechanism. If the *true order*  $n_c$  is equal to the *order with respect of time*  $n_t$  then this is an indication that there is no complexity in the mechanism. If the order  $n_c$  is greater than  $n_t$ , this can be related to the fact that the rate is falling less rapidly with time than expected on the basis of the true order, and the reaction is then said to be *autocatalytic*. If the *order with respect of time*  $n_t$  is greater than the *true order*  $n_c$ , this means that some intermediate in the reaction is acting as an inhibitor.

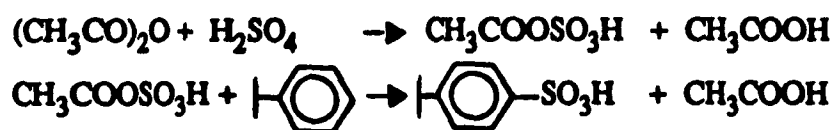
## 1.5 Outline of the Thesis

The purpose of this investigation, is to at elucidate the kinetics of the coil overlap process in oppositely charged ionomers in greater detail. The investigated parameters are the water content, molecular weight, polymer concentration, temperature, and ion content. Establishing the influence of those parameters on the rate may enable us to postulate a mechanism to account for the shielding process. In chapter 3 a description is given for the parameter ranges over which reproducible quantitative kinetic experiments can be performed. Chapter 4 will be dedicated to the determination of the order of the process, while chapter 5 will be a discussion on the effects of those parameters on the kinetics of the coil overlap process. Chapter 6 will be the global conclusion.

## CHAPTER 2. EXPERIMENTAL

### 2.1.1 Synthesis of Sulfonated PS

Monodisperse acid copolymers based on PS were synthesized according to an established procedure suggested by the patent of Makowski and al.<sup>46</sup> This procedure was used to sulfonate monodisperse polystyrene samples (Polyscience) with molecular weights between 5000 and 100,000. Acetyl sulfate ( $\text{CH}_3\text{COOSO}_3\text{H}$ ) is formed by the reaction of the acetic anhydride with sulfuric acid, which then sulfonates the benzene ring in the para position:



In a typical sulfonation reaction, 1.5 grams of PS were dissolved in 10 ml of 1,2-dichloroethane at 55°C. The required amount of acetic anhydride (A&C American Chemical, reagent grade) was added to the stirred solution, followed by the required amount of concentrated  $\text{H}_2\text{SO}_4$  (Fisher Scientific, 98% by weight). The positioning of the sulfonic acid groups on the aromatic units is claimed to occur in the para position at random along the chain. In order to obtain the right percentage of sulfonation, an excess of 15% of  $\text{H}_2\text{SO}_4$  and acetic anhydride was used. The extent of sulfonation was varied between 5 and 15 mole % of SSA units.

The reaction mixture was maintained at 55°C for one hour, after which the reaction was terminated by the addition of 2 ml of methanol. The solution was then poured dropwise into a beaker containing 100 ml of boiling water, in order to flash off the 1,2-dichloroethane.



After filtration, the PS-SSA was dried under reduced pressure (1 mm Hg) at 60°C for one day. The PS-SSA was then redissolved in a benzene/methanol mixture (90/10 v/v) and freeze dried.

#### 2.1.2 Synthesis of PMMA-4VP

Copolymers of PMMA-4VP of 4.7, 7.3 and 11.1 mol% VP were obtained through the courtesy of Denis Duchesne.<sup>47</sup> Polymers prepared by methods utilized in that study were found to have a viscosity average molecular weight ( $M_v$ ) of  $10^5$ .

### 2.2 Polymer Characterization

#### 2.2.1 Characterization of the Molecular Weight and Polydispersity of the PS

The characterization was performed by gas permeation chromatography (GPC) on a Varian 5000 liquid chromatograph. The solvent used for the standardization curve was tetrahydrofuran (THF) [Chemlab spectroscopic grade]. Solutions of 2% by weight of monodisperse PS were prepared. After filtration, 50  $\mu$ l of the solution were injected into the column. The flow was kept constant at 0.5 ml/min., and the temperature of the column was maintained at 25°C.

The three monodisperse PS (Polyscience) samples were used as received. The MW=5000 sample was passed through two Ultrastyrigel columns in series ( $10^3$  Å and  $10^4$  Å from Waters Associates), while for the MW=15,000 and 100,000 samples the Ultrastyrigel  $10^4$  Å and  $10^5$  Å were utilized. THF was used as the solvent. The

standardization curve was obtained using 5 monodisperse PS standards (Varian TSK kit) ranging from 500 to 20,000 MW for the MW=5000 material, and from 10,000 to 1,300,000 MW for the two others.

The analyses were performed in duplicate and the results averaged. The molecular weight peak, the weight-average MW (Mw), the number-average MW (Mn) and the polydispersity indices are given in table 2.1.

**Table 2.1** Molecular weights and polydispersity indices for the PS samples

<b>Peak MW</b>	<b>Mn</b>	<b>Mw</b>	<b>Polydispersity Index</b>
<b>4400</b>	<b>4200</b>	<b>5000</b>	<b>1.18</b>
<b>12000</b>	<b>12000</b>	<b>13000</b>	<b>1.10</b>
<b>107000</b>	<b>100000</b>	<b>105000</b>	<b>1.07</b>

### 2.2.2 Characterization of the acid content of PS-SSA

The procedure for the determination of the sulfonic acid content in the copolymers was obtained from the literature.<sup>48</sup> The polymer to be characterized was dried under reduced pressure at 60°C until constant weight was achieved. A weighed amount of the dried PS-SSA was dissolved in a benzene/methanol (90/10 v/v) mixed solvent to yield a 2% (w/w) solution. Before titrating, two drops of phenolphthalein indicator (1 g of phenolphthalein/liter of ethanol) were then added to the solution. The titrant (dilute methanolic NaOH) was added until the end-point was reached, which was characterized by a persistent pink coloration of the solution. The titration procedure was

repeated for a blank consisting of the same quantity of mixed solvent and phenolphthalein, the volume resulting from the blank titration was then subtracted from the amount necessary to reach the end-point in the case of the PS-SSA solutions. The PS-SSA titrations were performed in triplicate and the average deviation in the SSA content was less than 1%.

**Table 2.2** Ion content determination for PS-SSA

<b>Mn</b>	<b>Ion Content (%)</b>	<b>mean # of SSA units per chain</b>
<b>2000</b>	<b>24.9</b>	<b>5</b>
<b>4200</b>	<b>7.7</b>	<b>3</b>
	<b>10.2</b>	<b>4</b>
	<b>14.9</b>	<b>6</b>
	<b>20.7</b>	<b>8</b>
<b>9800</b>	<b>16.0</b>	<b>15</b>
<b>12000</b>	<b>5.3</b>	<b>6</b>
	<b>8.3</b>	<b>10</b>
	<b>10.5</b>	<b>12</b>
	<b>13.8</b>	<b>16</b>
<b>100000</b>	<b>7.7</b>	<b>74</b>
	<b>10.0</b>	<b>96</b>
	<b>14.7</b>	<b>141</b>

In order to ascertain whether any unreacted  $\text{H}_2\text{SO}_4$  remained from the sulfonation reaction, two samples were refluxed in a Soxhlet extractor for one week. The solvent used for the extraction was distilled water. Two samples of PS-SSA of  $\text{MW} = 10^5$

were used, since the materials of lower molecular weight are too soluble in water to be extracted over a long period of time. In each experiment, 0.2 g of PS-SSA were weighted in a cellulose receptacle and then placed in the top part of the soxhlet, which had been previously filled with distilled water ( $\approx 250$  ml). Water was considered a satisfactory extractant for these material in view of their high ion content and their small particle sizes. At comparable equivalent weights, it is known that perfluorosulfonates are excellent ion conductors.<sup>49</sup> Thus, it is reasonable that for these high ion content polymers, the water should be able to swell the materials and extract the residual sulfuric acid.

After one week of extraction, the dried samples of PS-SSA were titrated using the same procedure. Results from the titration of the PS-SSA ( $MW = 10^5$ ) with ion contents of 10.0% and 14.7%, are given in table 2.3, and from these results it was concluded that there was no evidence of residual  $H_2SO_4$  in the copolymer.

**Table 2.3** Ion content determination after water extraction for PS-SSA

<b>MW</b>	<b>Without Extraction Ion Content (%)</b>	<b>With Extraction Ion Content (%)</b>
<b><math>10^5</math></b>	<b>10.0</b>	<b>10.0</b>
<b><math>10^5</math></b>	<b>14.7</b>	<b>14.8</b>

### 2.2.3 Characterization of the Base Content of PMMA-4VP.

The vinylpyridine content was determined by a potentiometric titration using a solution of perchloric acid in glacial acetic acid according to established procedure;<sup>50</sup> the results are given in table 2.4.

**Table 2.4** Ion content determination for PMMA-4VP

<b>Mv</b>	<b>Ion Content (%)</b>	<b>mean # of 4VP units per chain</b>
<b>100000</b>	<b>4.7</b>	<b>45</b>
	<b>7.3</b>	<b>69</b>
	<b>11.1</b>	<b>106</b>

### 2.3 Blending Technique

Solutions of the blends were prepared using two procedures. The first was only used in the exploratory stage of the project, while the second was employed for the quantitative kinetic studies. For the exploratory work, the two dried copolymers were added sequentially to a predried NMR tube to a total weight of 12 mg; subsequently, 0.5 ml of DMSO<sub>d6</sub> was added in a glove bag under nitrogen. The sample was then placed directly in the NMR probe at the preset temperature.

The reproducibility achieved in the early stages of the NMR runs using this procedure was not satisfactory, because the copolymers were not always dissolving at the same rate. Thus, the second method was developed in order to eliminate the problem.

For the procedure used in the quantitative kinetics runs, equimolar quantities of the two dried copolymers were weighted separately to a total of 10 mg. The PMMA-4VP was then placed in a predried NMR tube, and the PS-SSA in a predried vial. Subsequently, 0.25 ml of  $\text{DMSO}_{d6}$  was added to each copolymer. Both copolymer solutions were then placed for 15 minutes in a thermostatted bath set at the experimental temperature. Subsequently, the PS-SSA solution was injected with a syringe into the NMR tube containing the PMMA-4VP solution, and the NMR tube was immediately placed in the probe at the experimental temperature.

#### 2.4 The NMR Instrumental Method

All NMR spectra were registered in  $\text{DMSO}_{d6}$  solution on a Varian XL-300 spectrometer. The deuterated DMSO (Aldrich; 99.96% deuterated) was used as received.

The pulse sequence employed was a standard S2PUL as illustrated in figure 2.1. The only modification to this pulse sequence was needed when the experimental temperature was varied; this sometimes necessitated the modification of the array PAD (preacquisition delay), but in more than 90% of the runs the array of PAD was as in figure 2.1.

a)

PAD ARRAY	
INDEX	TIME (sec.)
1	0
2	60
3	60
4	60
5	60
6	60
7	180
8	240
9	240
10	240
11	540
12	540
13	540
14	840
15	840
16	840
17	840
18	840

b)

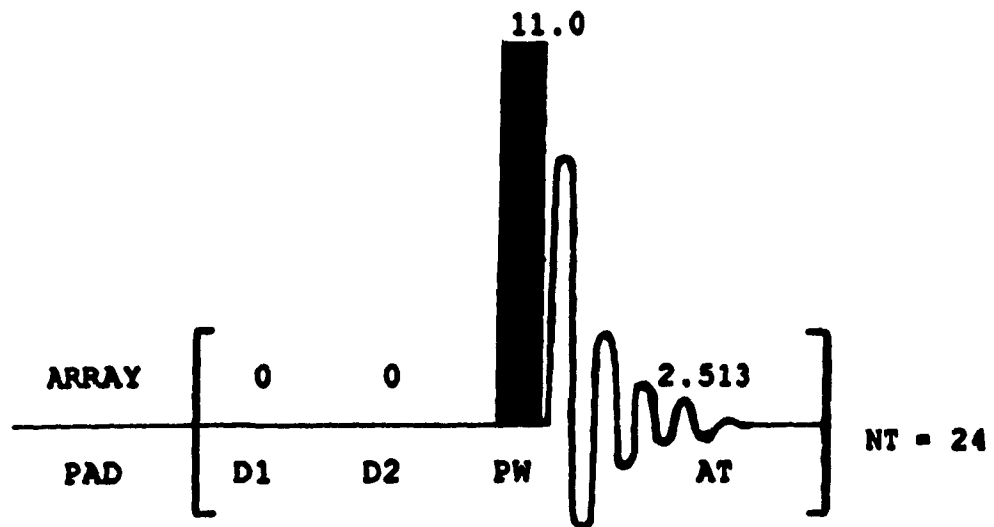


**Figure 2.1** a) Experimental array of preacquisition delay (PAD) in seconds.

b) Profile of the S2PUL pulse sequence.

## 2.5 Introduction to Deconvolution

The deconvolution process involves the separation of a complex curve into a certain number of independent contributions, which, when added to the proper baseline, will restructure the original lineshape. The procedure used to achieve the deconvolution of the superposed  $^1\text{H}$  NMR signal of the two methoxy groups, as well as the principles behind the deconvolution, will be described in greater detail in section 2.5.3 and 2.5.4.

### 2.5.1 Data Transfer

In order to perform the deconvolution of the NMR spectrum on a personal computer (AST AT), the experimental data from the NMR spectrometer had to be retrieved. The transfer was not trivial, since there was no communication package on the NMR spectrometer. Moreover, the disk format used by the disk operating system [DOS] of the spectrometer and IBM DOS are incompatible. The transfer was made possible by the implementation of a macro-command to the NMR spectrometer.<sup>51</sup> This macro-command basically transfers portions of a spectrum, by sending to the RS-232 I/O peripheral port of the spectrometer an array of real numbers, which corresponds to the relative intensity of the data points that are included in the range. The data were captured by the PC with a communication software (Procomm) set at a baud rate of 9600 with an even parity (one stop byte/seven data bytes), using the physical setup described in reference 51.



### **2.5.2 Data Manipulation**

All the transferred ASCII files have the same format, an example of which can be found in appendix 1 A and 2 A. For practical reasons, these files require major modifications in order to be usable. Those modifications were done using the Fortran program NMRMOD (appendix 3). This program performs four modifications on the original file. The first is the removal of all the extra (non-numerical) characters. The second operation involves the creation of an alternate chemical shift axis, which is, in fact, directly related to the number of transferred points. The third modification is introduced when a smoothing (moving average) operation is performed on the intensity values. Finally, the intensity is rescaled in order to eliminate negative values and to obtain a maximum value less than 1000.

### **2.5.3 Deconvolution Process**

The deconvolution of the modified experimental NMR spectrum files which had been generated by NMRMOD was performed by the Fortran program FIT. The documented Fortran listing of FIT can be found in appendix 4. Before describing the applications of this program, it is useful to describe in greater detail the principles that enable one to perform the deconvolution.

The program FIT deconvolutes a given lineshape by performing a non-linear least-squares estimation of a combination of two common idealized band shapes, Lorentzian and Gaussian. An algebraic expression modeling those two distributions is obtainable using three non-linear parameters: the mean, the standard deviation and the relative height, which can be related, respectively, to the position, the half width at half

height ( $\nu_{1/2}$ ) and the height of an experimental band.

The deconvolution process is based on the algorithm developed by Marquardt,<sup>52,53</sup> which, for the sake of completeness, will be explained in some detail here. The equations relating the three non-linear parameters to the intensity of a given band are well known<sup>54</sup>,

$$\text{Lorentzian: } \Phi = \Phi_{\max} \frac{\Gamma_{1/2}^2}{\Gamma_{1/2}^2 + (\nu - \nu_{\max})^2} \quad (2.1)$$

$$\text{Gaussian : } \Phi = \Phi_{\max} \exp \frac{-(\ln 2) (\nu - \nu_{\max})^2}{\Gamma_{1/2}^2} \quad (2.2)$$

where  $\Phi$  is the intensity,  $\Phi_{\max}$  is the height for the intensity maximum,  $\Gamma_{1/2}$  is the width at half height divided by two ( $\nu_{1/2}$ ) and  $\nu_{\max}$  the position of the maximum of the band.

The algorithm does an iterative minimization of the  $\Phi$  function using a *steepest-descent* procedure. In effect, this approach seeks to calculate corrections such that at each iteration, the value of the gradient of the parametrized  $\Phi$  function will be maximum. Thus, the positive quantity  $\Phi$  can be conceived as defining a "contour surface" as the unknown parameters are varied, the *steepest-descent* procedure determines the corrections which are in the steepest downhill direction from the current trial values. The *steepest-descent* direction, which is the rate of change of the function  $\Phi$  with respect to each of the intensity parameters evaluated at the  $r^{\text{th}}$  trial ( $r$ ), can be expressed as

$$(\delta\Phi/\delta\Phi_{\max})^{(r)}, (\delta\Phi/\delta\Gamma)^{(r)}, (\delta\Phi/\delta\nu_{\max})^{(r)} \quad (2.3)$$

and as an example, the *steepest-descent* correction on  $\Gamma$  can be expressed as

$$\Gamma^{(r+1)} = \Gamma^{(r)} + \Delta\Gamma^{(r)} \quad (2.4)$$

We can easily imagine that the contour lines of the volume generated by the  $\Phi$  function are not even approximately spherical, because each of the parameters does not have the same influence on the intensity. Thus, the contour lines will be elongated and irregular, and this will generate a football shaped volume containing a certain number of depressions. In such cases, the *steepest-descent* direction at any trial value near a local minimum of the function (trough) is nearly at right angles to the direction from the current point to the real minimum of  $\Phi$ . Thus, the path taken by the basic *steepest-descent* procedure (equation 2.4) is a zig-zag path which crosses and recrosses the bottom of the trough on successive trials, slowing down the determination of the minimum. This difficulty was removed by normalizing equation 2.4 as suggested in reference 53, which led to the following expression,

$$\Gamma^{(r+1)} = \Gamma^{(r)} + \alpha^{(r)} N_{\Gamma}^{(r)} \quad (2.5)$$

where  $N_{\Gamma}^{(r)}$  is the normalized value of the partial derivative (equation 2.3) after multiplication by a factor  $[1+(\Gamma^{(r)})^2]$ , and  $\alpha^{(r)}$  is the step size, which determines the absolute magnitude of the correction.

The selected convergence criterion for the experimental spectrum is the  $\text{Khi}^2$  test, which is a standard procedure to verify the adjustment of a series of experimental observations to a given statistical model.<sup>55</sup>

The iteration process can be summarized as follows

- 1- Add the baseline to the estimated bands.
- 2- Compute the partial derivative according to the three parameters.
- 3- Set the iteration counter to zero
- 4- Do 10 iterations using the Marquardt algorithm

- 5- If a band has gone negative try to fix this band and go to step 3.
- 6- If the  $Khi^2$  value did not improve, divide alpha by 4 and go to step 1
- 7- If after 10 iterations the  $Khi^2$  value is still improving keep those parameters and go to step 1.
- 8- When  $\Delta Khi^2$  reaches  $10^{-5}$  then the iteration process stops.

After step 7, the deconvolution process is completed and the final parameters for the baseline and the bands are saved.

#### 2.5.4 Quantitative Results of the Deconvolution

Since the three parameters defining the individual contribution for each idealized band are known, one should be able to derive an equation relating the  $\Gamma$  and  $\Phi_{\max}$  to the area under the curve. This can not be done in our case, because, for practical and computational reasons, the half width value was employed in the  $\Phi$  function used to perform the regression, instead of the  $\Gamma$  value as defined in equation 2.1 and 2.2. This statistical bias introduced in the evaluation function does not modify the confidence level (95%) or the validity of the fit, but leads to a  $\Phi_{\max}$  that can not be directly related to the area of the theoretical band lineshape.

A well known and documented algorithm due to Simpson<sup>56</sup> has been used to evaluate the area of the individual bands. Thus, knowing the concentration at time  $t = 0$  for the PMMA-4VP and the area of each band at time  $t$ , one can express the concentration of the unshielded methoxy signal as the ratio of the unshielded peak to the total methoxy signal multiplied by the original PMMA-4VP concentration.

In order to enable us to calculate the precise confidence level of the fit, the  $Khi^2$

value for the deconvolution process should be calculated using the square root value of the intensity instead of the intensity itself, and then normalized. This was not done because the computational time involved in this calculation and because negative intensity values can occur during the deconvolution process. If one still wants to have a quantitative idea on the accuracy of the fit, one can calculate the correlation coefficient on the total fitted range. In the present case, this coefficient was always greater than 0.99.

#### 2.5.4.1 Lineshape of the PMMA-4VP Methoxy Groups

Before one can attempt qualitative or quantitative kinetics, it is necessary to explore and define the real lineshape of the methoxy group in pure PMMA-4VP, in the absence of the PS-SSA. Moreover, since the experiments are carried out over a relatively wide range of temperature, it is crucial to know the influence of the temperature on the methoxy group lineshape. This was achieved by the acquisition of  $^1\text{H}$  spectra of the pure PMMA-4VP [5 mg/0.5 ml  $\text{DMSO-d}_6$ ] over an temperature interval from 60°C to 120°C in increments of 5°C. From figure 2.2, one can see that the lineshape of the pure PMMA-4VP methoxy groups at 120°C is not due to a single theoretical band, but is composed of several such bands. The individual features of the main methoxy signal that appear in the range of 3.62 ppm to 3.50 ppm, were assigned to methoxy groups in MMA sequences and to those in cosyndiotactic MMA-4VP sequences in terms of pentads.<sup>57</sup> Thus, this signal is composed of features due to the following sequences; 11111, 21111, 12111, 22111, 21112, 12121 and 21212, where the index 1 and 2 refer, respectively, to the MMA and 4VP monomers. At 120°C, these seven independent contributions can be assigned to the following bands: the shoulder

observable at  $\sim 3.61$  ppm is due to the 11111 sequences, the two main peaks at 3.60 ppm and 3.59 ppm to the 21111 and 12111 sequences, respectively, and the shoulder at  $\sim 3.57$  ppm to the 22111 sequences, while the broad signal centered around 3.54 ppm to results from a combination of the three remaining sequences (21112, 12121 and 21212). These assignments were made on the basis of the relative induced shielding from the 4VP nitrogens atoms on the PMMA methoxy groups, as discussed by Natansohn, Maxim and Feldman.<sup>54</sup>

For temperatures lower then  $120^{\circ}\text{C}$ , two observations can be made about the methoxy group lineshape. First, the position of those bands is shifting to lower fields with decreasing temperature. Second, the two main bands attributed to the 21111 and 12111 sequences coalesce at temperatures lower then  $120^{\circ}\text{C}$ . Furthermore, as one can see from figure 2.3, which is the methoxy groups lineshape at  $85^{\circ}\text{C}$ , the two signals which appear at 3.58 ppm and 3.57 ppm almost form one band, and for temperature below  $85^{\circ}\text{C}$ , only one featureless signal is observable for the two sequences.

Empirically, it was found that for temperature  $\geq 85^{\circ}\text{C}$ , the methoxy group lineshape can be approximated using three Lorentzian bands, while for spectra taken below that temperature only two Lorentzian bands are required. For temperature  $\geq 85^{\circ}\text{C}$ , this procedure neglects the two shoulders attributed to the 11111 and 22111 sequences, and only three bands, i.e. the two sharp signals attributed to the 21111 and 12111 sequences and the shoulder that is the combination of three sequences (21112, 12121 and 21212). For temperature under  $85^{\circ}\text{C}$ , we are also neglecting the two shoulders (11111 and 22111), and assuming that the 21111 and 12111 can be fitted by only one Lorentzian band. The validity of this approach was verified by the deconvolution of the methoxy group lineshape obtained for each temperature; an excellent correlation ( $\geq 0.99$ ) between the experimental spectrum and the fitted lineshape

was obtained. From this fact it can be concluded that the contribution to the total lineshape of the two shoulders due to the 11111 and 22111 sequences can be neglected, and that a minimum number of bands (2 or 3) could satisfactorily duplicate the experimental lineshape of the methoxy groups. Furthermore, it should be pointed out that in presence of the aromatic shielding the signal from the methoxy groups gets averaged, and only two bands can be observed; a relatively sharp and intense peak at  $\approx 3.57$  ppm at the broad shoulder centered at  $\approx 3.52$  ppm.

Deconvolution of the methoxy group lineshape indicates that the contributions of each of the methoxy bands to the total area are temperature independent, which is reasonable, since they are due to the sequences included in the polymer chain. Thus, one can calculate the mean % area of the shoulder to the total area of the homopolymer methoxy signal as a function of temperature, which was found to be  $27.3 \pm 1.2$ . Obtaining the relative area contribution of the shoulder to the total area of the homopolymer methoxy signal enables one to calculate a factor that, when multiplied by the area of the main methoxy peak (21111 and 12111 sequences), will give the total area of the homopolymer methoxy signal; this factor was found to be  $1.38 \pm 0.06$ . For PMMA blends in which aromatic shielding is present, the determination of a factor that relates the total area of the homopolymer methoxy signal to the main peak located at approximately 3.57 ppm will become essential. Area ratios reported in table 2.5, are the area ratio of the homopolymer methoxy group shoulder ( $\approx 3.2$  ppm) composed of the three cosyndiotactic sequences 21112, 12121 and 21212 to the total area of the methoxy signal. Table 2.5 also contains the correction factors that enables one to obtain the total area of the homopolymer methoxy group signal from the area of the main peak (21111 and 12111 sequences).

**Table 2.5** Deconvoluted shoulder area for the methoxy  $^1\text{H}$  NMR signal of PMMA-4VP as a function of temperature

Temperature (°C)	Shoulder Area (%)	Correction Factor for the Total Area
60	27.7	1.38
65	28.5	1.40
70	29.2	1.41
75	27.4	1.38
80	27.1	1.37
85	30.8	1.45
90	31.0	1.45
95	31.6	1.46
100	28.4	1.40
105	20.9	1.26
110	26.0	1.35
115	22.7	1.29
120	24.4	1.32
mean value:	$27.3 \pm 1.2$	$1.38 \pm 0.06$



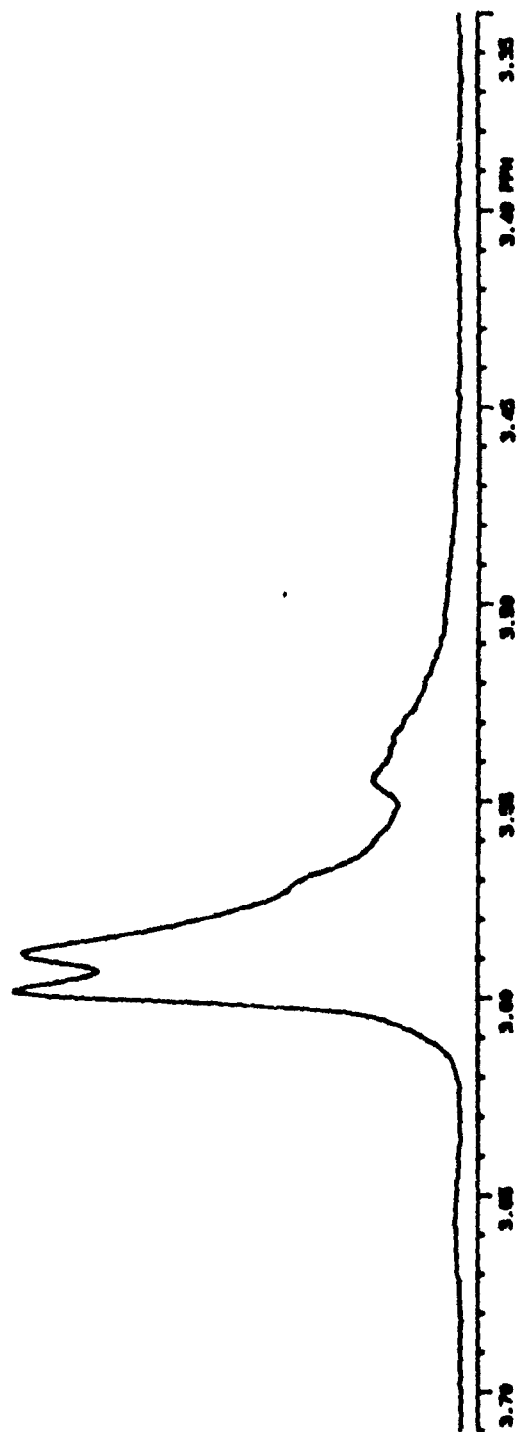
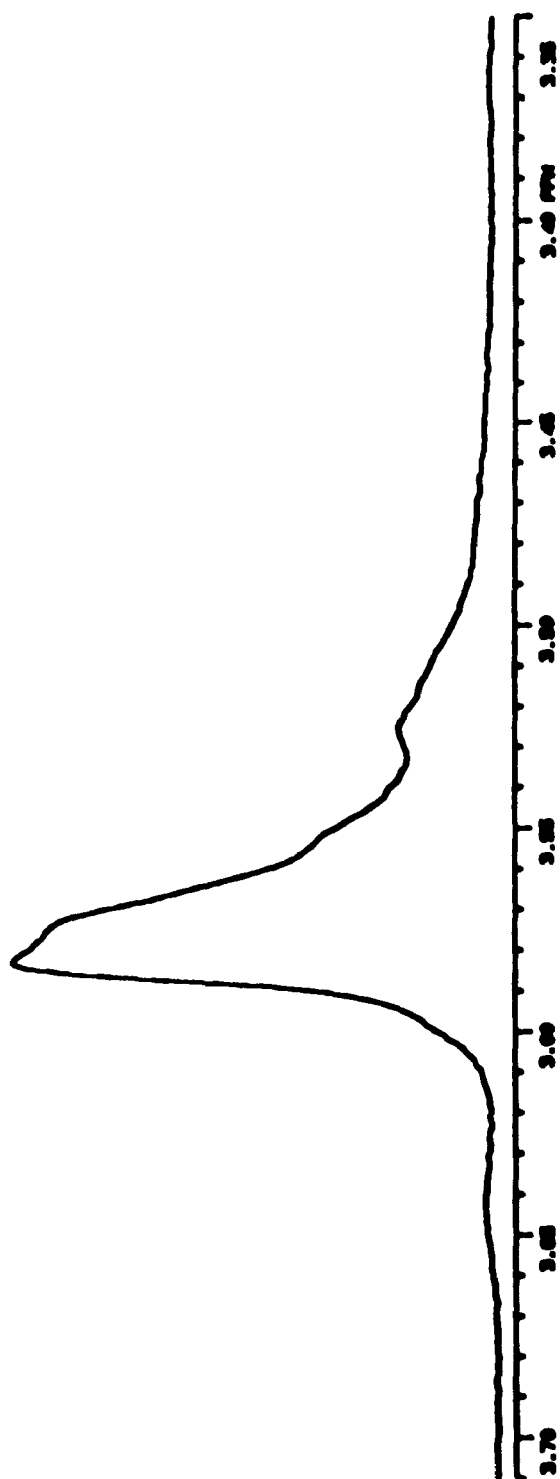
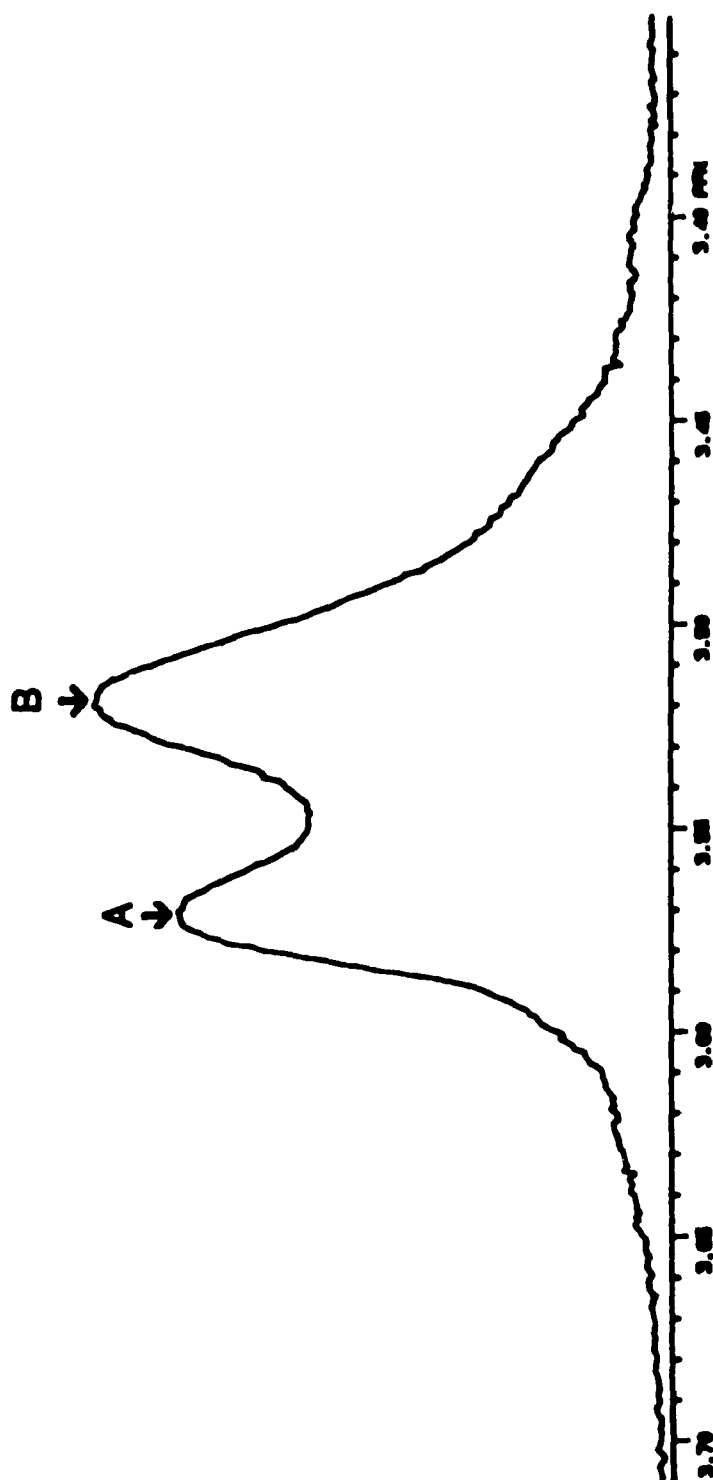


Figure 2.2  $^1\text{H}$  NMR spectrum for the methoxy groups from PMMA-4VP at 120°C



**Figure 2.3**  $^1\text{H}$  NMR spectrum for the methoxy groups from PMMA-4VP at 85°C



**Figure 2.4**  $^1\text{H}$  NMR spectrum for the methoxy groups for a blend of PS-SSA 10% of MW =  $10^4$  with PMMA-4VP 11% of MW =  $10^5$  in  $\text{DMSO}_{d6}$  at  $85^\circ\text{C}$  (contact time = 30 min.). The peaks labeled A ( $\sim 3.57$  ppm) and B ( $\sim 3.52$  ppm) are, respectively, the unshielded and the shielded methoxy signal.

#### 2.5.4.2 Lineshape of the PMMA-4VP Methoxy Groups in the Blend

For a blend of PMMA with another polymer containing aromatic groups, the lineshape for the methoxy group indicates that it is composed of two superimposed signals, i.e the unshielded methoxy signal ( $\approx 3.57$  ppm) and the shielded methoxy signal ( $\approx 3.52$  ppm). This is illustrated for an equimolar blend of PS-SSA (10 mole %) of  $MW = 10^4$  with PMMA-4VP (11 mole %) of  $MW = 10^5$  in  $DMSO_{d6}$  at  $85^\circ C$  (contact time = 30 min.) in figure 2.4. A comparison of the methoxy signal in the homopolymer at  $85^\circ C$  (figure 2.3) with that obtained for the blend at the same temperature (figure 2.4) clearly indicates that the shoulder in the homopolymer methoxy signal, located at approximately 3.52 ppm, lies at approximately the same position as that of the shielded methoxy signal, and since the latter is quite large, the shoulder can be buried. This presents us with a major complication for the quantitative analysis of the areas due to the unshielded and shielded methoxy groups. A simple deconvolution into two Gaussians or two Lorentzians would not be correct in this particular case, since we know that the unshielded peak is composed of the peak and the shoulder; therefore, we cannot reconstruct the unshielded peak by itself. However, one does have information related to the relative areas of the shoulder and the unshielded peak.

For convenience, it was judged advantageous not to subtract the shoulder area from that of the shielded peak, but instead to add it to unshielded signal. Furthermore, from the relative area of the unshielded methoxy peak, one can obtain the concentration of the pure methoxy in solution at any given time. This concentration is, in fact, the only parameter required to establish the time-concentration curves.

The procedure that was adopted consists of the following steps: The two peaks for the blends spectrum were deconvoluted into two Lorentzian bands, then the relative % area of the unshielded methoxy group signal to the total area of the methoxy signal

was calculated. Multiplication of the % area of the unshielded methoxy peak by the factor determined in the previous section ( $1.38 \pm 0.06$ ), gives one the total % area of the unshielded methoxy signal.

#### 2.5.4.3 Application of the Deconvolution to a Typical Lineshape for Shielding Experiments

In order to minimize the acquisition time,  $^1\text{H}$  NMR spectra were monitored for the spectral range included between 3.9 ppm and 2.9 ppm. As one can see from figure 2.5, the lineshape of the acquired spectrum is composed of three major signals: A ( $\approx 3.57$  ppm) and B ( $\approx 3.52$  ppm) are respectively, the unshielded and the shielded ( $\approx 3.52$  ppm) methoxy group signal, and C ( $\approx 3.15$  ppm) is the signal due to traces of water. Using a parabolic baseline, the two overlapping methoxy signals and the water peak were deconvoluted as three Lorentzian bands. In all cases, a correlation coefficient greater or equal to 0.99 was achieved. Thus, it can be concluded that there is no significant difference between the experimental and the deconvoluted lineshape. Furthermore, the end value of the  $\text{Khi}^2$  obtained by the deconvolution process qualitatively indicates that the maximum error in the area of individual bands is of the order of  $\pm 2.5\%$  (confidence level of 95%).

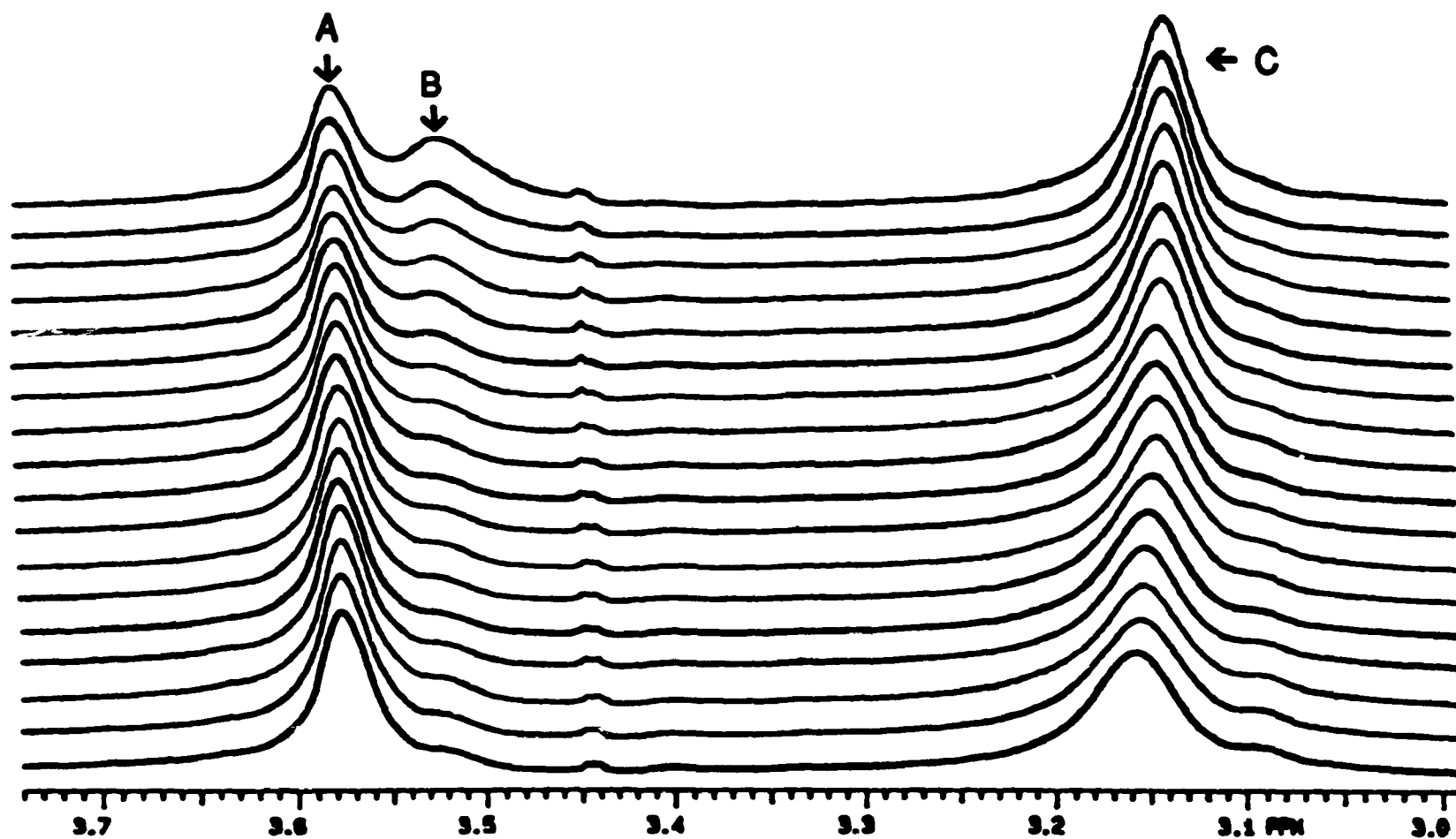


**Figure 2.5** Example of a  $^1\text{H}$  NMR stack spectra for a typical shielding experiment for a blend of PS-SSA (5 mole %) of  $\text{MW} = 10^4$  with PMMA-4VP (11 mole %) of  $\text{MW} = 10^5$  in  $\text{DMSO}_{d6}$  at  $85^\circ\text{C}$ . The contact times correspond to the PAD defined in section 2.4 minute with one minute added to each delay time. A ( $\approx 3.57$  ppm) and B ( $\approx 3.52$  ppm) are respectively the unshielded and the shielded ( $\approx 3.52$  ppm) methoxy group signals, and C ( $\approx 3.15$  ppm) is the signal due to traces of water.

## CHAPTER 3. INHERENT LIMITATIONS

### 3.1 Introduction

In order to obtain quantitative kinetic results for the coil overlap process, it was necessary to perform a preliminary study of the parameters that influence this process. Moreover, before proposing any working hypotheses on the mechanism, one first has to obtain a complete qualitative picture of the process. Finally, one has to define the experimental ranges over which the signal from the methoxy groups could be observed. These topics are the subject of the present chapter.

### 3.2. Water Content.

The first parameter concerns the presence of water. For a small amount of water, it can be assumed that the water is uniformly distributed throughout the DMSO. After polymer addition, it seems reasonable that the water should concentrate preferentially in the vicinity of the ionic groups, and since water tends to solvate the ion pairs, an increased amount of water might be able to disrupt the intermixing process for the non-ionic part of the polymer chains. If this were the case, no shielding would be observed. Moreover, if the above considerations are correct, deshielding would be expected on addition of water to an equilibrated blend (EQB), i.e. a polymer solution that had previously reached the equilibrium state.

Since it is known that the addition of even trace quantities of water (0.2 % v/v) produces a signal very intense compared to that due to the polymer, the decision was made to use D<sub>2</sub>O instead. Chemically, the effect will be the same, but from the NMR point of view, one will detect only a very weak proton signal because of the small

amount of  $\text{H}_2\text{O}$  in the  $\text{D}_2\text{O}$ . The experiments involved an equimolar blend of PS-SSA 10 mole % and PMMA-4VP 11 mole % in  $\text{DMSO}_{d6}$  at  $85^\circ\text{C}$ . The samples, to which either 0.001, or 0.01, or 0.04 ml (0.2, 0.8, and 2 % v/v) of  $\text{D}_2\text{O}$  were added, were allowed to reach equilibrium ( $\approx 100$  minutes).

For the three blends, it was empirically observed that a maximum in the intensity for the shielded methoxy signal was obtained in about one hour, after which the signal remained constant. From figure 3.1, which contains the EQB (contact time of 1.5 hours) for the three shielding experiments, one can see three major peaks, A, B and C, which are, respectively, the unshielded methoxy signal ( $\approx 3.57$  ppm), the shielded methoxy signal (3.52 ppm) and the water peak (3.2 to 3.0 ppm region). This figure shows that shielding has occurred even in the presence of large amounts of water. Moreover, further addition of  $\text{D}_2\text{O}$  (up to 5 % v/v) to the EQB did not induce deshielding. From these results, it is clear that the presence of small quantities of water in the solvent or the polymers does not have a major influence on the coil overlap process.

### 3.3. Temperature

Temperature can have two possible effects. On one hand it favors molecular motion, and therefore would tend to increase the rate of the coil overlap process. However, an increase in temperature effectively decreases the importance of the coulombic interactions between the ions, and therewith also the driving force for the mixing process. For this reason, it is necessary to explore the temperature dependence of the shielding process, since we cannot predict the relative importance of these two effects at any temperature.



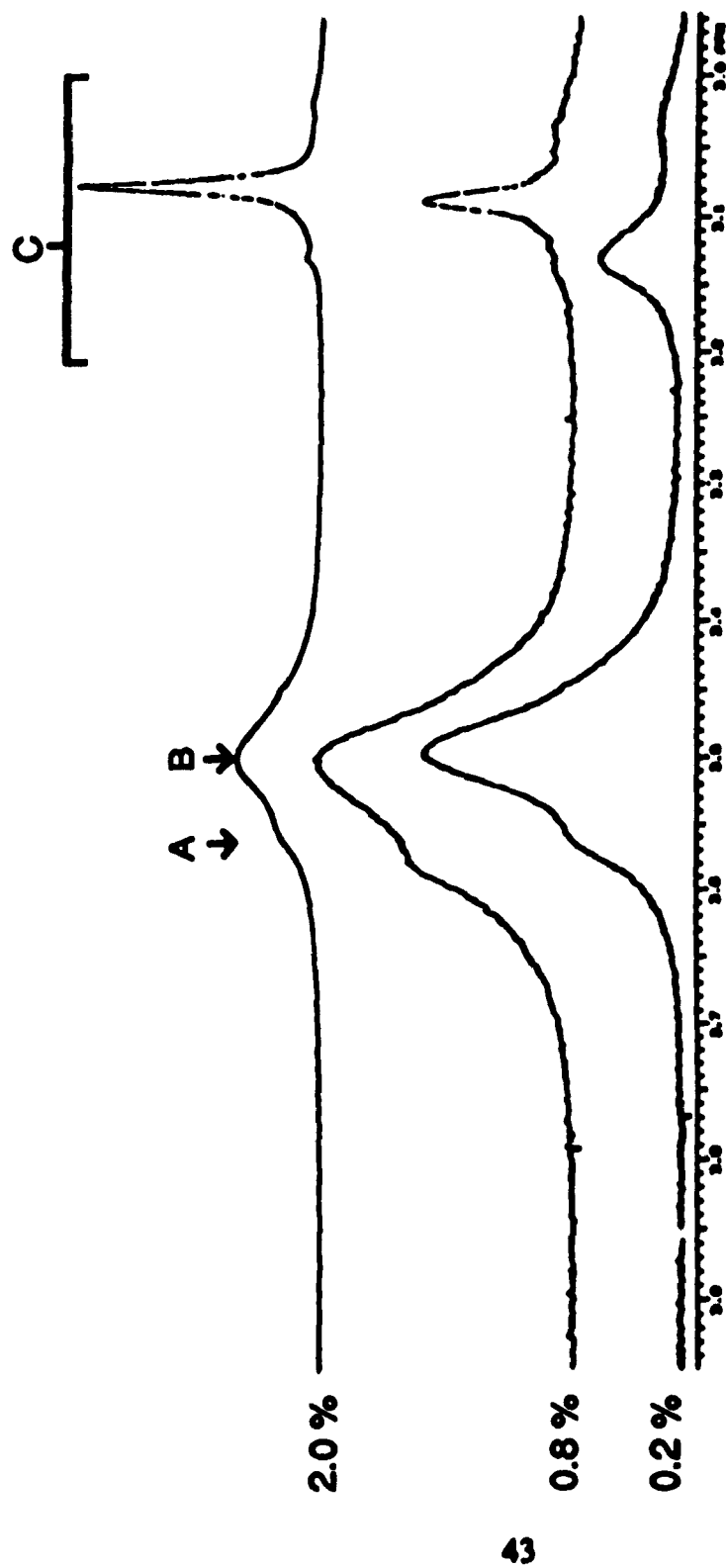


**Figure 3.1** Spectrum obtained by the addition of  $D_2O$  to the equilibrated polymer solution; elapsed time 1.5 hrs at  $T = 85^\circ C$ . The percentage figures refers to volume  $D_2O$  / volume  $DMSO_{d6} \times 100$ . The peaks labeled A ( $\approx 3.57$  ppm), B ( $\approx 3.52$  ppm) and C (3.2 to 3.0 ppm range) are respectively, the unshielded methoxy, the shielded methoxy and the water peak.

As can be expected, the solvent selected for the measurements imposes a major limitation on the accessible temperature range. The criteria for solvent selection are quite severe, in that the solvent must be relatively high boiling, so as to allow a wide temperature range to be studied, while at the same time it must retain its ability to solvate both polymers and the polymer mixture. Empirically, DMSO<sub>d6</sub> was found to be the only solvent which could be used in this study.<sup>30</sup> At the low temperature end, the limit is imposed by the solubility of the polymers in DMSO. It was found that below 70°C the signal to noise ratio was too low, so that 70°C was selected as the minimum temperature. At the upper limit, the boiling of the solvent imposes the most severe limitation. Formation of bubbles, which occurs somewhat earlier, limited the upper temperature to 150°C.<sup>57,58</sup>

Another observation made at elevated temperature relates to deshielding. It was found that for mixtures which were allowed to equilibrate at 85°C, an increase in temperature to about 100°C caused the size of the shielded methoxy peak to decrease. This shows that above 100°C the thermal motion is sufficiently energetic to disrupt the shielding process. Therefore, in this study of the shielding process itself, the temperature range of 70°C to 95°C was most suitable.

For temperatures higher than 100°C, the deshielding rates increase monotonously with temperature. However, while complete deshielding could be achieved, this process is quite slow, taking more than one hour at the highest temperature (150°C).

### 3.4 Total Polymer Concentration

It was found that 0.5 ml of DMSO<sub>d6</sub> at 85°C could not dissolve more than 10 mg of each polymer. Furthermore, for blends containing less than 2.5 mg of PS-SSA or PMMA-4VP in 0.5 ml of DMSO<sub>d6</sub>, i.e a concentration of 0.05 M, the signal to noise ratio

was too low to allow us to perform quantitative kinetic experiments. Thus, the experimental concentration range that was selected to perform the quantitative kinetics is 0.05 to 0.15 M for each polymer.

Two significant observations emerge from the preliminary experiments. First, an induction period of the order of 5 minutes was observed. This period is the time elapsed between the mixing of the two dissimilar chains in solution and the first detectable appearance of the shielded methoxy signal. During this period, the process probably is diffusion-controlled, since a certain quantity of the dissimilar copolymer chains have to find one another in solution, to yield the shielded methoxy signal.

Second, after the induction period, the rate of the coil overlap process increased as the polymer concentration increased. This behaviour cannot be rationalized if this stage of the coil overlap process is diffusion-controlled. Hence, it can be assumed that the coil overlap process during this stage must be governed by another mechanism, which requires only the spatial reorganization of the two dissimilar chains, in order to achieve electroneutrality.

### 3.5 Molecular Weight

To study the effects of the molecular weight on the shielding process, blends containing PS-SSA of MW's of 2000, 5000, 9600, 12,000, 100,000 with PMMA-4VP 11 mole % of MW=100,000, were investigated at 85°C. Three blends for each ion content listed in table 2.2 were monitored for more than one hour.

For the blends containing PS-SSA of low MW, i.e. of MW = 2000 and 5000, no resolvable shielded methoxy group signal was observed. The absence of a shielded peak for these low MW blends does not rule out the possibility that some shielding may be present, since it is well known that the extent of the shielding and the position of the

shielded methoxy peak are a function of the distance and the orientation of the PS ring to the methoxy group of the PMMA chain.<sup>34</sup> The  $X_e$  concentration is directly proportional to the degree of compatibilization between the two dissimilar chains. The diminution of the  $X_e$  concentration, down to the point where it can no longer be observed, i.e. for low MW blends of PS-SSA, can be rationalized by invoking the following explanation: The  $X_e$  value can be described as an average of all the contributions of the PS benzene rings to the chemical shift. Therefore, so one can assume, that at equilibrium, the mean distance between two dissimilar copolymer chains increases for blends with decreasing MW of PS-SSA, leading to a reduction of the effective number of methoxy groups that are close to the benzene ring of the PS. This increase in the mean distance for these blends can be attributed to two factors. First, due to the higher mobility of the low MW's PS-SSA chains, the thermal motions of these chains, in solution, can be sufficient to pull the two dissimilar chains apart. Second, the mismatch in chain contour between the PMMA-4VP and the low MW PS-SSA leads to a reduction of the effective shielding effect of the PS benzene rings on the PMMA methoxy groups. The two dissimilar chains are no longer in the right spatial configuration to observe the shielded methoxy, which leads to a large number of methoxy groups without optimal shielding.

A convenient way to determine whether there is a shielding effect in these blends is to compare the width at half height ( $\Gamma$ ) of the main methoxy peak signal ( $\approx 3.57$  ppm) for the homopolymer of PMMA-4VP at 85°C, with that obtained for the blend. If some shielding is present in the blend as seen in the methoxy group lineshape, one can expect a greater  $\Gamma$  value. The  $\Gamma$  value for the main peak due to the methoxy group of the homopolymer is  $0.025 \pm 0.01$  ppm. One can subtract this value from the  $\Gamma$  value of the blend main peak, and obtain the difference ( $\Delta\Gamma$ ), which is a qualitative indication on the presence of the shielding effect. Table 3.1 reports the  $\Gamma$  and the  $\Delta\Gamma$  values for the blends of low MW PS-SSA, which were equilibrated for more than three hours. From these  $\Delta\Gamma$

values, one can see that a shielding effect is present for all these blends, which implies that proton transfer occurred at least to a certain extent.

For blends containing PS-SSA with a  $MW \geq 9600$ , two observations can be made. First, a shielded methoxy group signal is observable for the blends containing PS-SSA of the three highest molecular weight, i.e. 9600, 12,000 and 100,000. Second, the shielded methoxy concentration at equilibrium ( $X_e$ ) increases with increasing MW. Thus, the quantitative shielding experiments will be performed on blends containing PS-SSA with a MW greater than  $10^4$ .

**Table 3.1** Summary of  $\Gamma$  and  $\Delta\Gamma$  values for blends containing a PS-SSA of low MW, with no observable shielded methoxy group signal

MW	Blends Composition				$\Gamma$ (ppm)	$\Delta\Gamma$ (ppm)
	PS-SSA Ion Content (%)	Weight (mg)	PMMA-4VP Ion Content (%)	(MW= $10^5$ ) Weight (mg)		
2000	25	2.2	11	5.0	0.027	0.002
2000	25	5.0	11	5.0	0.030	0.005
5000	10	5.1	11	5.0	0.038	0.013
5000	15	3.7	11	5.0	0.032	0.007
5000	15	5.0	11	5.0	0.039	0.014
5000	20	2.8	11	5.0	0.031	0.006
5000	20	5.0	11	5.0	0.037	0.012

### 3.6 Ion Content

The effects of the ion content on the shielding process, were studied for a range of copolymers blends containing 5 to 11 mole % of 4VP and 5 to 15 mole % of SSA in  $\text{DMSO}_{d6}$ , at  $85^\circ\text{C}$ .

For blends with a PMMA-4VP ion content of less than 11 mole %, i.e. 5 and 7 mole %, no shielded methoxy peak was observed. The absence of the shielded peak due to the methoxy groups, even though a certain number of methoxy groups are close to the PS benzene rings, can be due to the fact that the concentration of the unshielded methoxy groups is too high. In addition, the mean distance between two ionic sites on the PMMA-4VP chain increases when the ion content is lowered. This mismatch between the ionic sites on the two copolymer chains can also lead to an effective diminution of the shielding effect.

Using the procedure described in section 3.5, one can evaluate the presence of the shielding effect for these low ion content PMMA-4VP blends. The  $\Gamma$  and  $\Delta\Gamma$  values for the equilibrated blends (contact time  $\geq 3$  hours) of PMMA-4VP with a low ion content are reported in table 3.2. From the  $\Delta\Gamma$  values, one can see that a shielding effect is present for all these blends. This implies that proton transfer did occur, even though no apparent shielded methoxy peak can be observed.

For blends containing PS-SSA of 5 to 15 mole %, with PMMA-4VP 11 mole %, two observations can be made. First, a shielded methoxy peak is present for all these blends. Second, the  $X_e$  value associated with the shielded methoxy peak increases with increasing SSA content. Therefore, appropriate blends for the study of the shielding process contain PS-SSA with an ion content ranging from 5 to 15 mole %, with a PMMA-4VP 11 mole %.

**Table 3.2** Summary of  $\Gamma$  and  $\Delta\Gamma$  values for blends containing a PMMA-4VP of low ion content, with no observable shielded methoxy group signals

MW	Blends Composition				$\Gamma$ (ppm)	$\Delta\Gamma$ (ppm)
	PS-SSA Ion Content (%)	Weight (mg)	PMMA-4VP (MW=10 <sup>5</sup> ) Ion Content (%)	Weight (mg)		
10 <sup>5</sup>	10	3.2	5	6.8	0.030	0.005
10 <sup>5</sup>	10	5.0	5	5.0	0.032	0.007
10 <sup>5</sup>	10	4.3	7	5.8	0.032	0.007
10 <sup>5</sup>	10	5.0	7	5.0	0.035	0.010

### 3.7 Electrolyte Effect

Even though the extraction studies described earlier showed that no residual  $\text{H}_2\text{SO}_4$  was present in this system, it was of interest to explore whether the addition of  $\text{H}_2\text{SO}_4$  or other electrolytes could prevent shielding. To test this, small amounts of 0.5 N  $\text{H}_2\text{SO}_4$  in  $\text{DMSO}_{\text{d}6}$  were added to an equimolar EQB containing PMMA-4VP 11 mole % ( $\text{MW}=10^5$ ) and PS-SSA 10 mole % ( $\text{MW}=10^5$ ) in 0.5 ml of  $\text{DMSO}_{\text{d}6}$  at  $85^\circ\text{C}$ . The spectra were followed for one hour.

After the first addition of 0.001 ml of the  $\text{H}_2\text{SO}_4$  solution to the EQB, we have a ratio of 1  $\text{H}^+$  cation to 10 4VP anions; no significant deshielding was observed at this point. After the second addition of 0.001 ml, i.e. 2  $\text{H}^+$  cations to 10 4VP anions, partial deshielding was observed. The deshielding process is rapid and the concentration of the shielded methoxy signal does not change with time after the first spectrum is obtained. After the third addition of 0.002 ml, i.e. 4  $\text{H}^+$  cations to 10 4VP anions, deshielding is almost complete. For a ratio of 8  $\text{H}^+$  cations to 10 4VP anions, complete deshielding is observed. Thus, it is clear that addition of sulfuric acid can cause deshielding, even at low concentrations.

This seems reasonable in view of the fact that sulfonate microanions can now be paired with the pyridinium cations, thus, eliminating the driving force which keeps the two polymer chains next to each other. The anions from the styrene are no longer needed to balance the cations of the vinylpyridine.

From this experiment, it can be concluded that while significant amounts of sulfuric acid do cause deshielding, they do not do so at low concentration, i.e. when the electrolyte concentration is of the order of one tenth of the PS-SSA ion content in solution. Trace quantities, in other words, would not be expected to have an effect on the coil overlap process, since they do not disrupt the equilibrium concentration of the



shielded methoxy groups. To confirm that the observed deshielding was indeed electrostatic in origin, the experiment was repeated with other electrolytes such as NaOH or p -toluenesulfonic acid. Solutions of 0.1 M of each electrolytes were added to an EQB, and, as in the case of the sulfuric acid experiment, deshielding was again observed at similar concentrations, confirming that electrolytes can induce deshielding.

### 3.8 Conclusion

In this chapter, it was shown that the water content of the  $\text{DMSO}_{d6}$  solutions did not have a significant effect on the shielding process. Experiments were also described which determined that trace quantities of electrolytes did not affect the shielding process, while electrolyte concentrations of the order of the polymer ion content in solution could completely disrupt the shielding process.

Furthermore, the experimental ranges over which the kinetics of the shielding process for the methoxy signal can be performed, were determined for blends of PS-SSA and PMMA-4VP in  $\text{DMSO}_{d6}$ , and are summarized in table 3.3.

**Table 3.3** Summary of the experimental ranges over which the kinetic runs for the shielding process of the methoxy group signal can be performed, as a function of the investigated parameters.

EXPERIMENTAL PARAMETERS	RANGE
Temperature	70°C to 95°C
Concentration of each Copolymer in 0.5 ml of DMSO <sub>d6</sub>	0.05 M to 0.15 M
Molecular Weight for the PS-SSA Copolymer	12,000 and 100,000
Molecular Weight for the PMMA-4VP Copolymer	≈ 100,000
Ionic Content for the PS-SSA Copolymer	5 to 15 mole %
Ionic Content for the PMMA-4VP Copolymer	11 mole %

## CHAPTER 4. ORDER DETERMINATION

There are many methods which can be used to determine the order of a reaction. In this chapter, two methods will be described in detail, the derivation method<sup>45</sup> and the integration method.<sup>61</sup> However, it should be stress that there are a number of others.<sup>62,63,64</sup>

### 4.1 Derivation Method

The method was previously described in section 1.4.2. It is considered to be the most reliable,<sup>65</sup> since the true order of the reaction and the initial rate can be graphically measured from the plot of the relevant variables of equation 1.16. It gives the order of the reaction without possible competing effects of the products.

#### 4.1.1 Determination of the true order ( $n_c$ )

The true order was determined for two series of experiments utilizing equimolar blends containing, respectively, PS-SSA 10 mole % of  $MW = 10^4$  and of  $MW = 10^5$ , to which PMMA-4VP 11 mole % of three different concentrations (0.05, 0.10 and 0.15 M) were added. Figure 4.1 is a plot of  $\ln v$  vs  $\ln a_0$ , as described in equation 1.16, for the two sets of experiments. From the slope of this linear equation, one can obtain the true order of the reaction ( $n_c$ ). Thus, for runs utilizing equimolar mixtures of the PS-SSA  $MW = 10^4$  and  $MW = 10^5$ ,  $n_c$  is equal to  $2.4 \pm 0.2$  and  $2.9 \pm 0.2$ , respectively.

## Determination of the true order

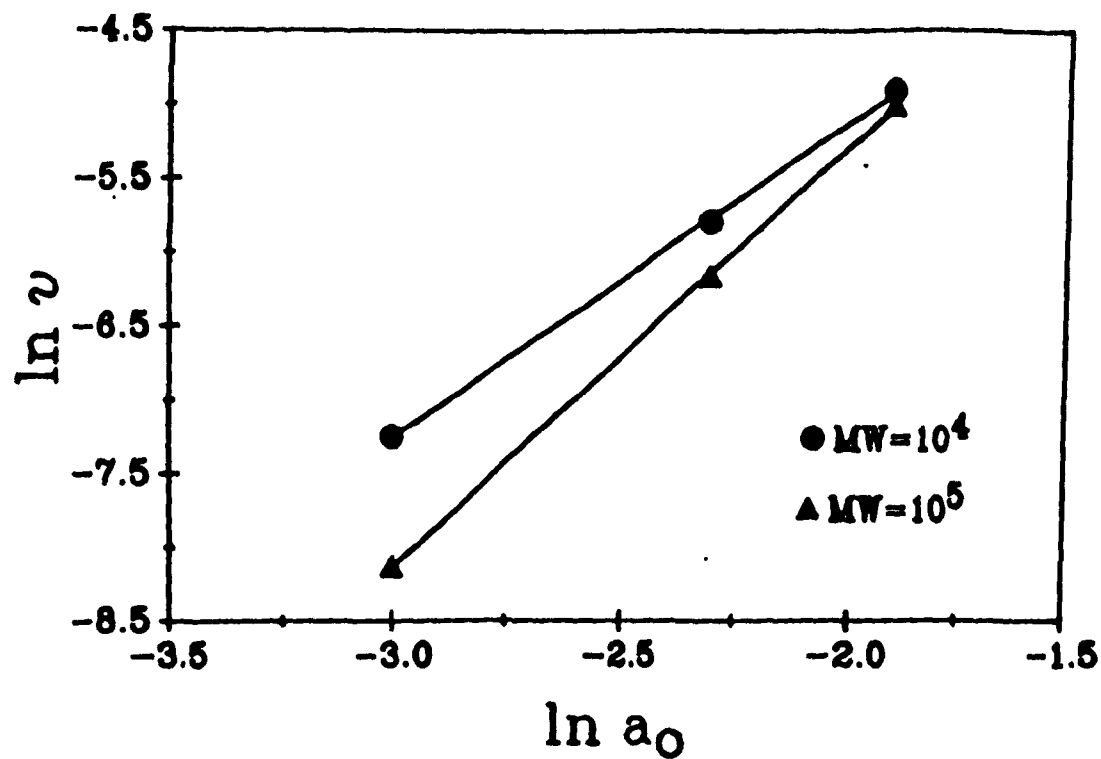


**Figure 4.1** Determination of the true order ( $n_c$ ) for equimolar blends of PMMA-4VP 11 mole % (MW=10<sup>5</sup>) with PS-SSA 10 mole % (MW=10<sup>4</sup>, MW=10<sup>5</sup>) at 85°C in DMSO<sub>66</sub>.

#### 4.1.2 Determination of the order according to time ( $n_t$ )

The determination of  $n_t$ , described on page 16, involves the measurement of tangents to a concentration-time curve. These determinations are fraught with experimental uncertainties. As a result of this, the determination of  $n_t$  from independent kinetic runs usually leads to significant discrepancies between the various determinations. Thus, for curves in which the concentration varies monotonously with time, the best procedure to obtain constant  $n_t$  values between different experiments is to perform the differentiation systematically at the same concentrations, i.e. 25%, 50%, 75% of the initial concentration of PMMA-4VP.<sup>66</sup> This was done here, by smoothing the data (moving average), and then performing a polynomial regression on the concentration-time curve. From the differentiation of the fitted equation ( $-dc/dt$ ), one can calculate the value of the tangents to the curve at any concentration. Using this procedure, the mean values of  $n_t$  were obtained for two series of equimolar blends (table 4.1), i.e. the two series previously used in section 4.1.1. These values are equal to  $1.22 \pm 0.05$  and  $1.10 \pm 0.08$  for the blends containing PS-SSA 10 mole % of  $MW = 10^4$  and  $MW = 10^5$ , respectively. Thus, the order according to time obtained in both cases is lower than the true order.

Table 4.1 Determination of the order according to time ( $n_t$ ) for two series of equimolar mixtures of PS-SSA 10 mole % with PMMA-4VP 11 mole % (MW= $10^5$ ), at 85°C.

PMMA-4VP CONCENTRATION (M)	PS-SSA MW= $10^4$	$n_t$ PS-SSA MW= $10^5$
0.05	1.21	1.10
0.10	1.27	1.18
0.15	1.18	1.02
Mean value :		
	1.22± 0.05	1.10± 0.08

#### 4.1.3 Comparison between $n_t$ and $n_c$

The fact that the order with respect to time ( $n_t$ ) is lower than that with respect to concentration ( $n_c$ ) means that, as the reaction proceeds, the rate (dc/dt) is falling off less rapidly with time than expected on the basis the true order. Therefore, this abnormal difference in the rate of reaction can be rationalized by assuming that some intermediate in the reaction is acting as a catalyst, or by assuming that the mechanism is complex, and that it involves more than one reaction.<sup>66</sup>

It was shown previously that two competing reactions are involved in the coil overlap process, this can be a possible explanation for the difference between  $n_c$  and  $n_t$ . Due to the back reaction contained in the process, the equilibrium concentration will be smaller than for a non-complex process containing only a forward reaction. Thus, this displacement in the equilibrium position leads to the observed discrepancy between the true order and according to time ( $n_c > n_t$ ).

Such reactions do not permit the assignment of an order, since their rates are not simple power functions of the concentrations.<sup>65,68</sup> Thus, in this case,  $n_t$  can only be considered as a pseudo-order that describes the concentration-time curves. Moreover, it indicates the type of complication that is occurring for a given process.

#### 4.2 The Integration Method

This method is not applicable to the coil overlap process, since it is known that the process contains two contributions, i.e. a forward reaction that can be observed by the appearance of the shielded signal from the PMMA methoxy group, and a backward reaction that can cause the deshielding of the PMMA-4VP methoxy signal. The contribution of the backward reaction to a process can only be omitted if the rate constant for the forward reaction is 100 times bigger than for the rate constant of the back reaction.<sup>65,66</sup> It will be shown, in chapter 5, that one cannot neglect the deshielding contribution to the coil overlap process. Thus, this method cannot be used for the present purpose. Although this method is mentioned here for the sake of comprehension and completeness, since this method will be used in section 4 of chapter 5.

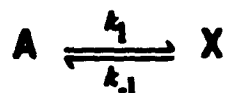
In order to use this method, we must start with a differential rate equation (table 1) that is believed to apply to the reaction under consideration. This integrated equation is then applied to the kinetic data, by graphical means. If there is good agreement between the points and a given kinetic equation, one can conclude that this equation is applicable, and that one can obtain the rate constant. If the correlation between the equation and the experimental data is not acceptable, the procedure is repeated with another equation until a satisfactory fit is achieved.

The main criterion for accepting or rejecting an order found by this method is that the kinetic data as treated by the equation must be linear, over a wide range of the relevant variables (concentration and time), i.e. = 80 % of the time required for a given process to reach steady state.

### 4.3 Opposing Reaction

#### 4.3.1 First-Order Opposing Reactions

From the experiments performed in chapter 3, it was observed that the shielding process is reversible; the reaction therefore does not go to completion. The simplest kinetic expression to describe this behaviour can be derived from a mechanism in which two first-order reactions are opposing each other. This leads to the following expression



where  $k_1$  and  $k_{-1}$  are the rate constants for the forward and reverse directions respectively,  $A$  is the concentration of the PMMA-4VP as determined from the unshielded methoxy signal (or the uninvolved PS-SSA segments, and  $X$  the concentration of the shielded methoxy groups in the PMMA-4VP, which, in turn, is equal to the concentration of the strongly interacting group segments in the blend. From the previous equation, one can obtain the equation for the net rate of production of  $X$

$$\frac{dx}{dt} = k_1(a_0 - x) - k_{-1}x \quad (4.1)$$



where  $a_0$  is the concentration of A at  $t = 0$  and  $x$  the concentration of X after a time  $t$ .

Since  $x$  is being produced by the forward reaction and removed by the reverse reaction, at equilibrium, when  $dx/dt$  is equal to 0 (with  $X_e$  denoting the equilibrium concentration of X), one can write the following expression:

$$k_1 (a_0 - X_e) = k_{-1} X_e \quad (4.2)$$

which can be rearranged to

$$k_{-1} = [k_1 (a_0 - X_e)] / X_e \quad (4.3)$$

substituting equation 4.3 into equation 4.1 gives

$$\frac{dx}{dt} = \frac{k_1 a_0}{X_e} (X_e - x) \quad (4.4)$$

Integration of equation 4.4 using the boundary condition of  $x = 0$  at  $t = 0$  gives

$$k_1 t = \frac{X_e}{a_0} \ln \frac{X_e}{X_e - x} \quad (4.5)$$

For practical purposes, it is convenient to present equation 4.5 in a different form.

Rearrangement of equation 4.2 yields

$$X_e(k_1 + k_{-1}) = k_1 a_0 \quad (4.6)$$

which can be rearranged to

$$\frac{X_e}{a_0} = \frac{k_1}{k_1 + k_{-1}} \quad (4.7)$$

Substitution of equation 4.7 in equation 4.5 gives

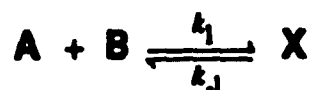
$$k_1 + k_{-1} = \frac{1}{t} \ln \frac{X_e}{X_e - x} \quad (4.8)$$

Comparison of this equation with equation 1.14, which was applicable to a simple first order reaction, shows that the two are formally analogous, with  $X_e$  replacing  $a_0$ , and  $k_1 + k_{-1}$  ( $k_t$ ) replacing  $k$ .

By expressing the data from the time-concentration curves as suggested by equation 4.5, i.e. by plotting the RHS of equation 4.5 as a function of time, one can obtain the rate constant  $k_1$  from the slope. Using the same procedure, one can obtain the rate constant  $k_{-1}$  from equation 4.8. The rate constant  $k_{-1}$  can then be calculated by subtracting  $k_1$  from  $k_t$ .

#### 4.3.2 Second-Order Forward First-Order Opposing Reaction

The formation of the blend involves two distinct chemical species, therefore, it is reasonable to explore the possibility that the blend formation involves a second order forward reaction and a first order backward reaction. This can be expressed by:



Assuming that the concentrations of both A and B are equal, one can obtain the net rate from the stoichiometric equation, which can be expressed as:

$$\frac{dx}{dt} = k_1(a_0 - x)^2 - k_{-1}x \quad (4.9)$$

Since  $x$  is being produced by the forward reaction and removed by the reverse reaction, at equilibrium, when  $dx/dt$  is equal to 0 (with  $X_e$  denoting the equilibrium concentration of  $X$ ), one can write

$$k_1 = \frac{k_1(a_0 - X_\theta)^2}{X_\theta} \quad (4.10)$$

Integration of equation 4.9 using the boundary condition of  $x = 0$  at  $t = 0$ , gives

$$k_1 t = \frac{X_\theta}{(a_0^2 - X_\theta^2)} \ln \frac{a_0 X_\theta + x(a_0 - X_\theta)}{a_0(X_\theta - x)} \quad (4.11)$$

One can obtain the rate constant  $k_1$ , by plotting the RHS of equation 4.11 against time. The rate constant  $k_{-1}$ , in turn, can be calculated by substituting the value for  $k_1$  into equation 4.10.

#### 4.3.3 Application of the First and Second-Order Scheme to the Time-Concentration Curves

The plots of equations 4.5, 4.8 and 4.11 that are needed to obtain the rate constants for a process involving both a forward and backward reaction that are opposing one another were reviewed in section 4.3.1 and 4.3.2. These equations were utilized for the mixing process of the present system. The 4VP content and the molecular weight of the PMMA-4VP were kept constant, i.e. a VP content of 11 mole % and a molecular weight of  $10^5$ . The experimental parameters having an influence on the kinetic process were investigated for two PS-SSA samples of molecular weights of  $10^5$  and  $10^4$ , i.e. for materials which yielded a resolvable NMR  $^1\text{H}$  shielded methoxy signal in the blend. The time-concentration curves for the PS-SSA blends of  $\text{MW} = 10^5$  and  $\text{MW} = 10^4$  as a function of the total polymer concentration, the ion content and the temperature can be found in figures 4.2 to 4.4 and figures 4.5 to 4.7, respectively.

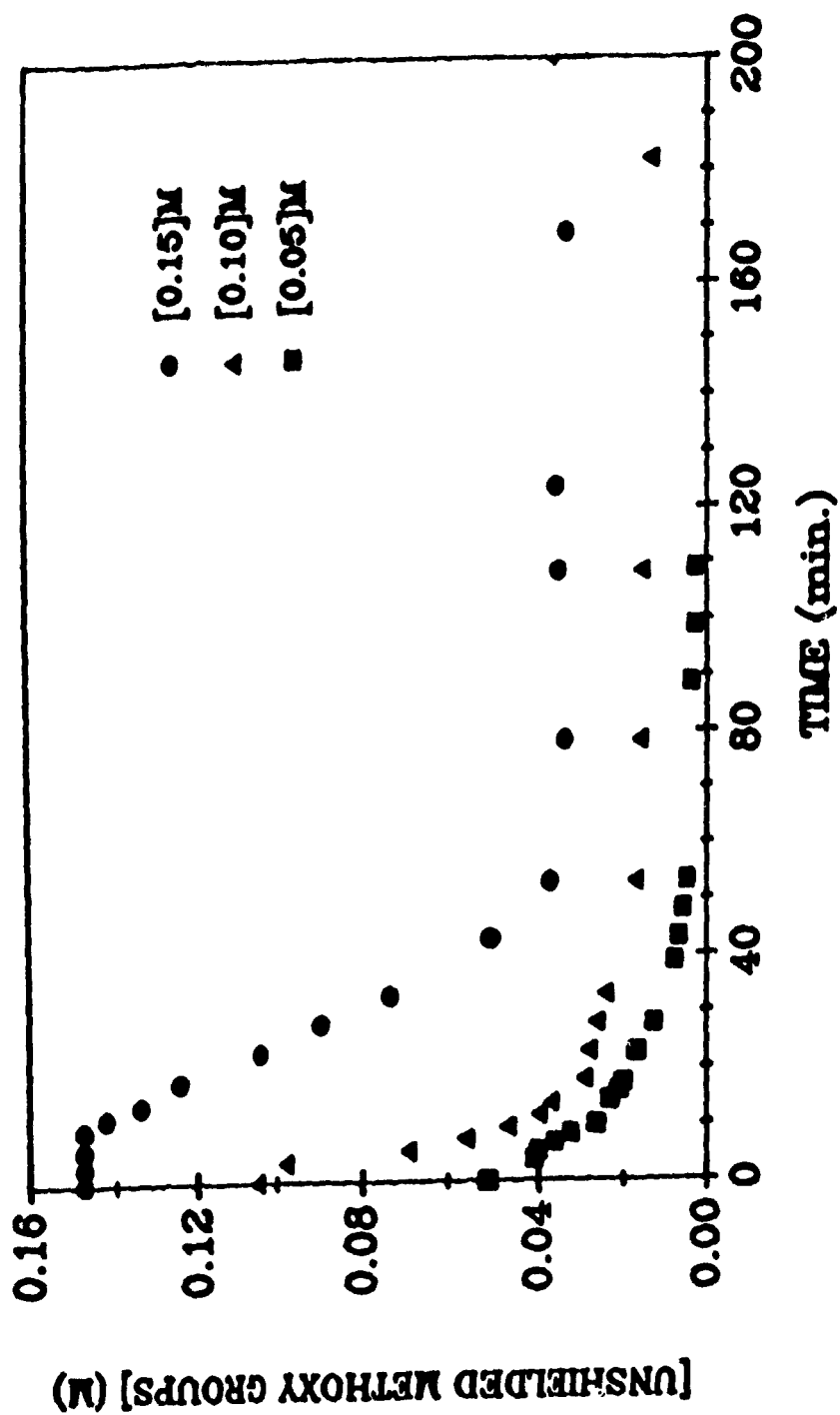


Figure 4.2 Time-concentration curves for various equimolar starting concentrations of PMMA-4VP 11 mole % of MW=10<sup>5</sup> with PS-SSA 10 mole % of MW=10<sup>5</sup>, at 85°C. The concentration of the vertical axis refers to the unshielded methoxy groups signal.

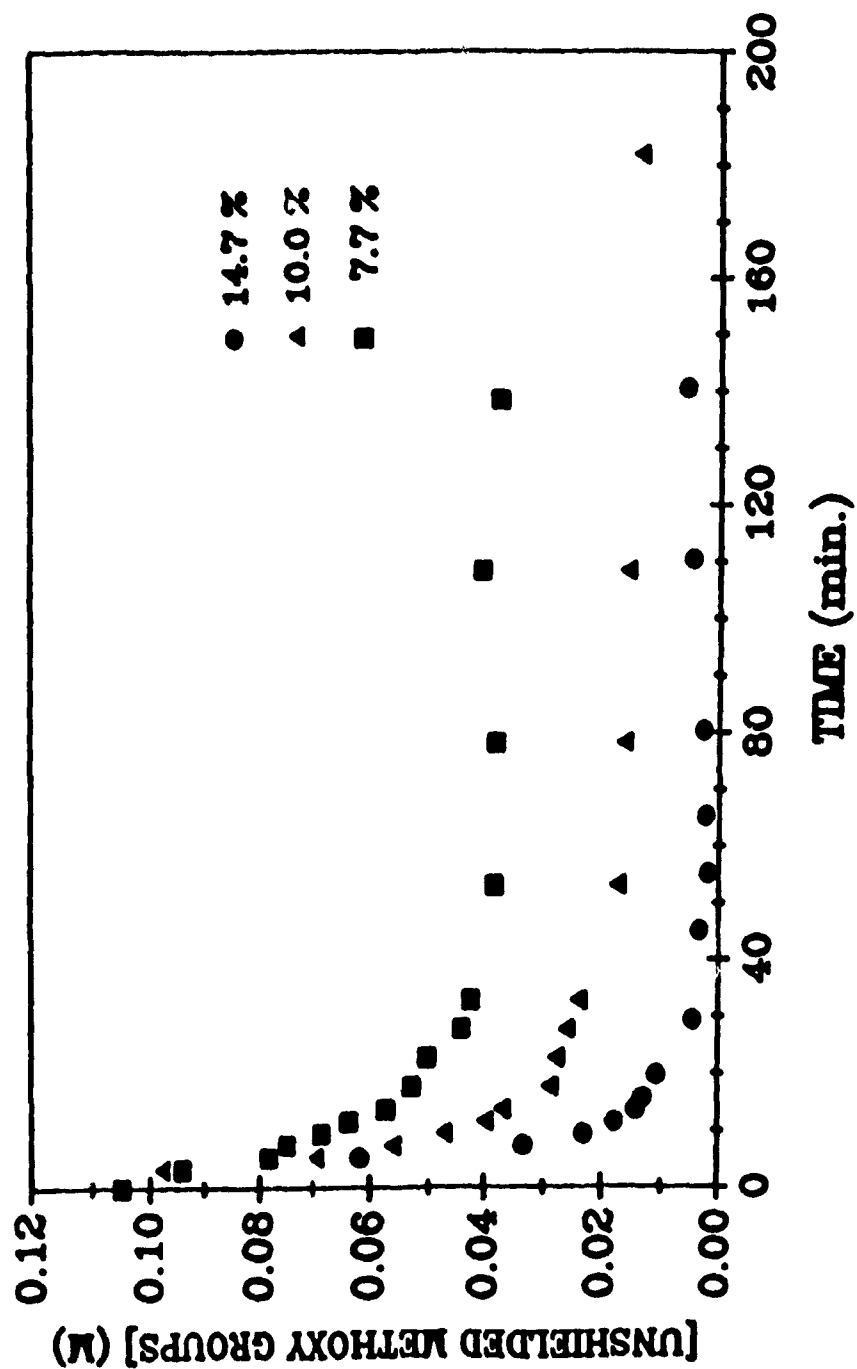


Figure 4.3 Time-concentration curves for equimolar mixtures of PMMA-4VP 11 mole % with a PS-SSA of MW=10<sup>5</sup>, at 85°C. Each curve represents a distinct sulfonation level. The solution contains 5 mg of both copolymer per 0.5 ml of DMSO-d<sub>6</sub> (0.10 M). The concentration of the vertical axis refers to the unshielded methoxy groups signal.

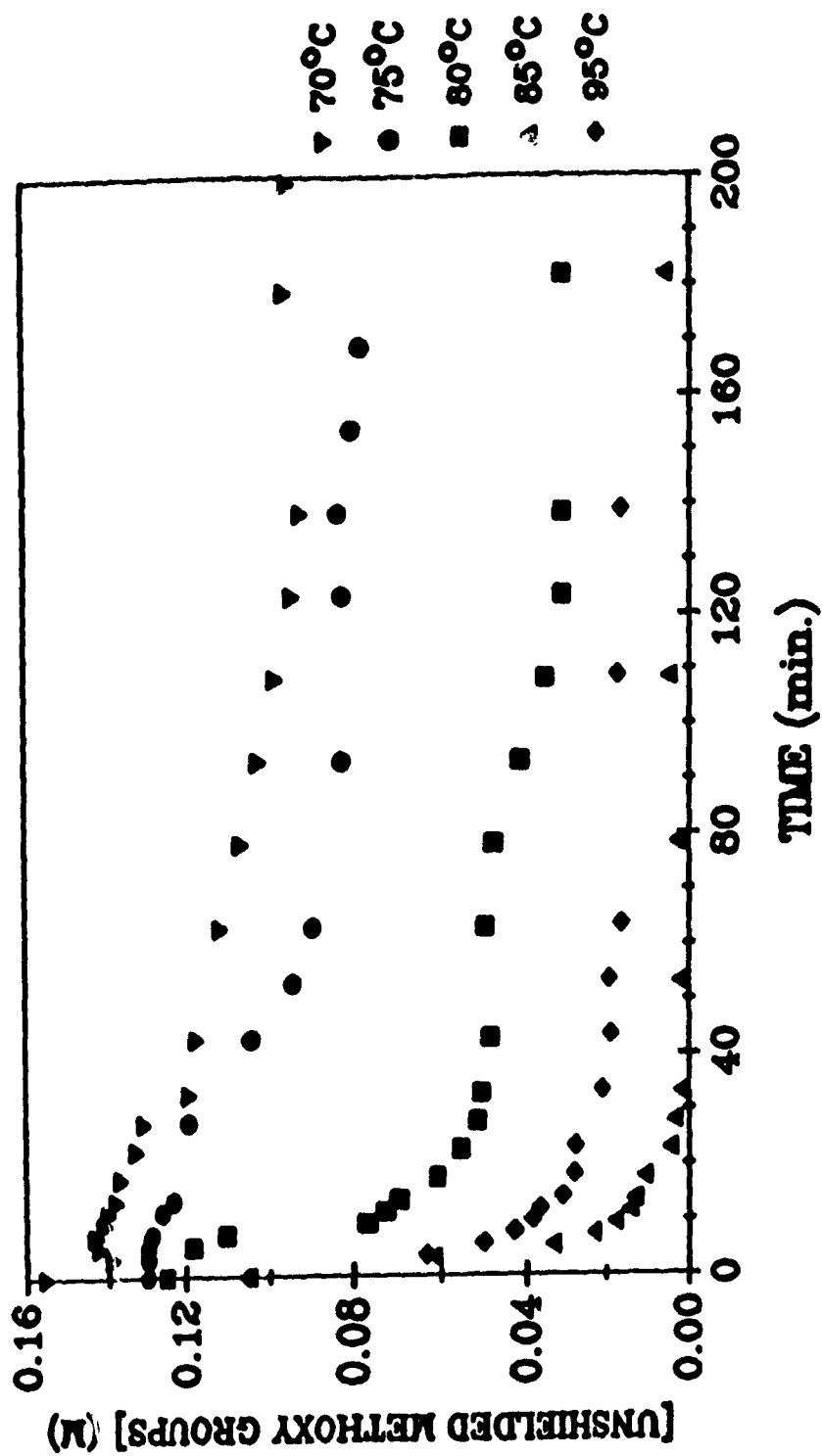
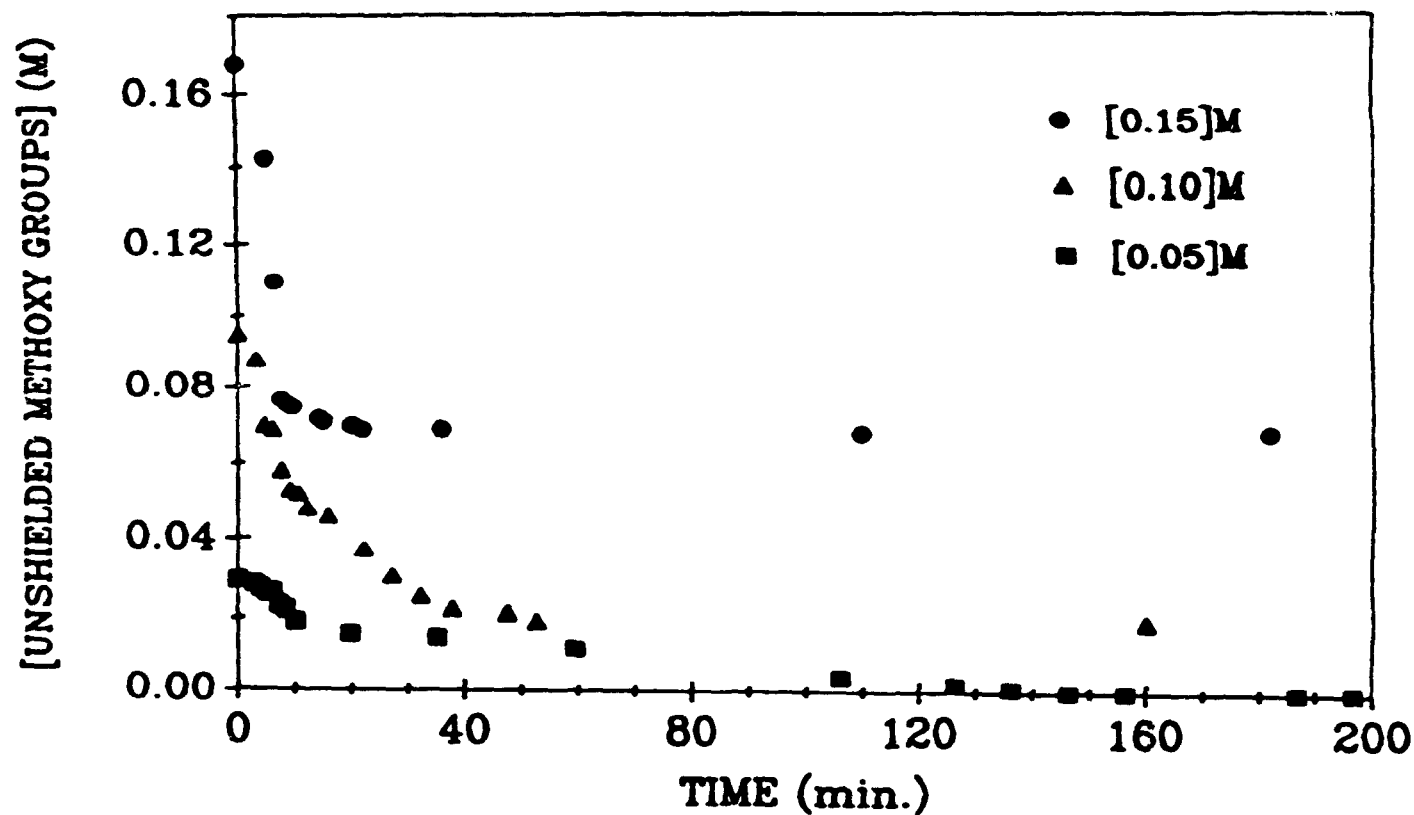


Figure 4.4 Time-concentration curves for equimolar mixtures of PMMA-4VP 11 mole % with PS-SSA 10 mole % of  $MW=10^5$ , at various temperatures. The  $DMSO_{d6}$  solution contains 5 mg of both copolymers per 0.5 ml (0.10 M). Vertical shifts of 0.025, 0.05, 0.02, 0 and 0 were respectively introduced on the curves from 70°C to 95°C. The concentration of the vertical axis refers to the unshielded methoxy groups signal.



**Figure 4.5** Time-concentration curves for mixtures of various equimolar starting concentrations of PMMA-4VP 11 mole % of MW=10<sup>5</sup> with PS-SSA 10 mole % of MW= 10<sup>4</sup>, at 85°C . Vertical shifts of 0, 0.01 and 0.020 were respectively introduced on the curves from 0.15 M to 0.05 M. The concentration of the vertical axis refers to the unshielded methoxy groups signal.

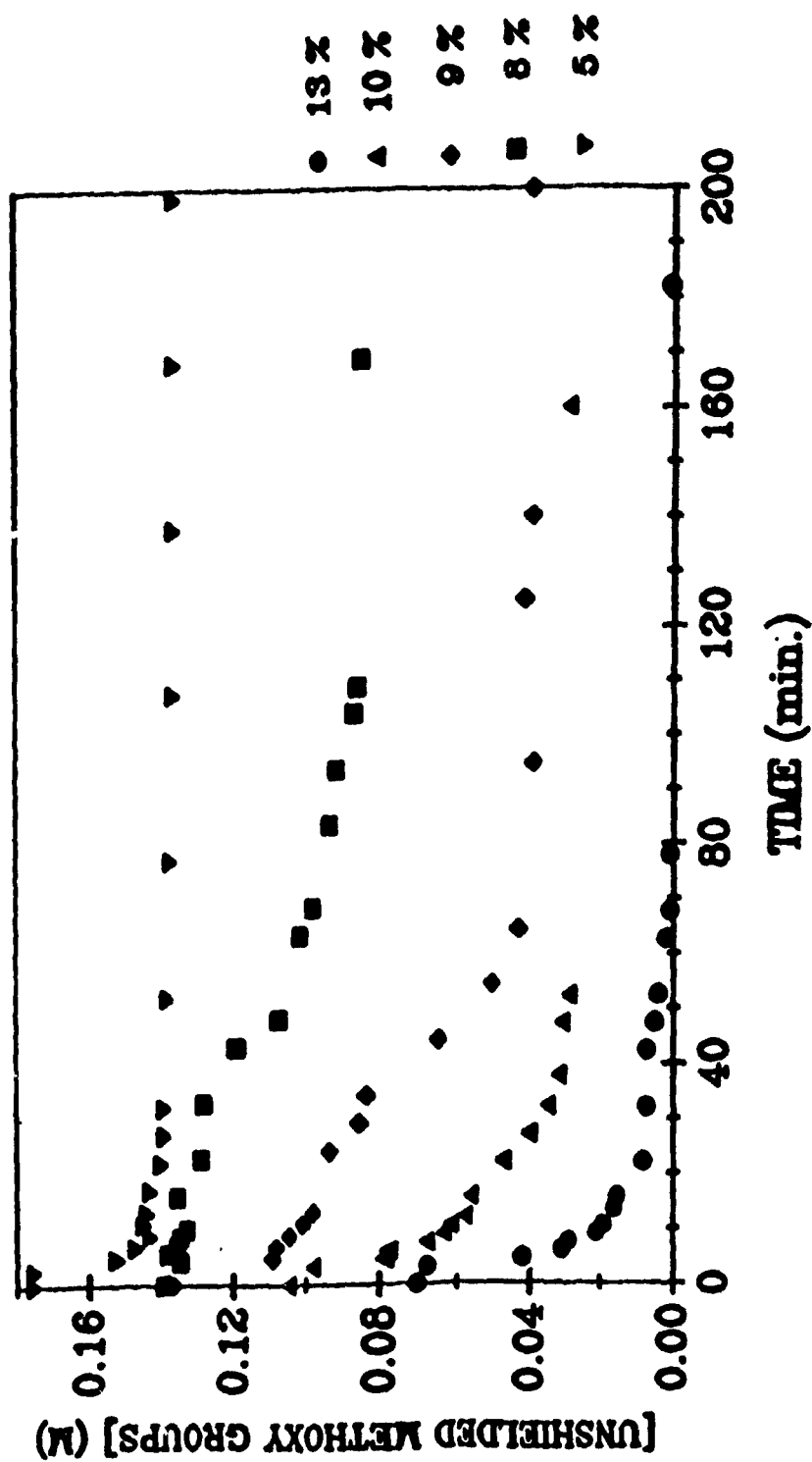


Figure 4.6 Time-concentration curves for equimolar mixtures of PMMA-4VP 11 mole % with a PS-SSA of  $MW=10^4$ , at  $85^\circ\text{C}$ . Each curve represents a distinct sulfonation level. The solution contains 5 mg of both copolymer per 0.5 ml of  $\text{DMSO}_{d6}$  (0.10 M). The concentration of the vertical axis refers to the unshielded methoxy groups signal.



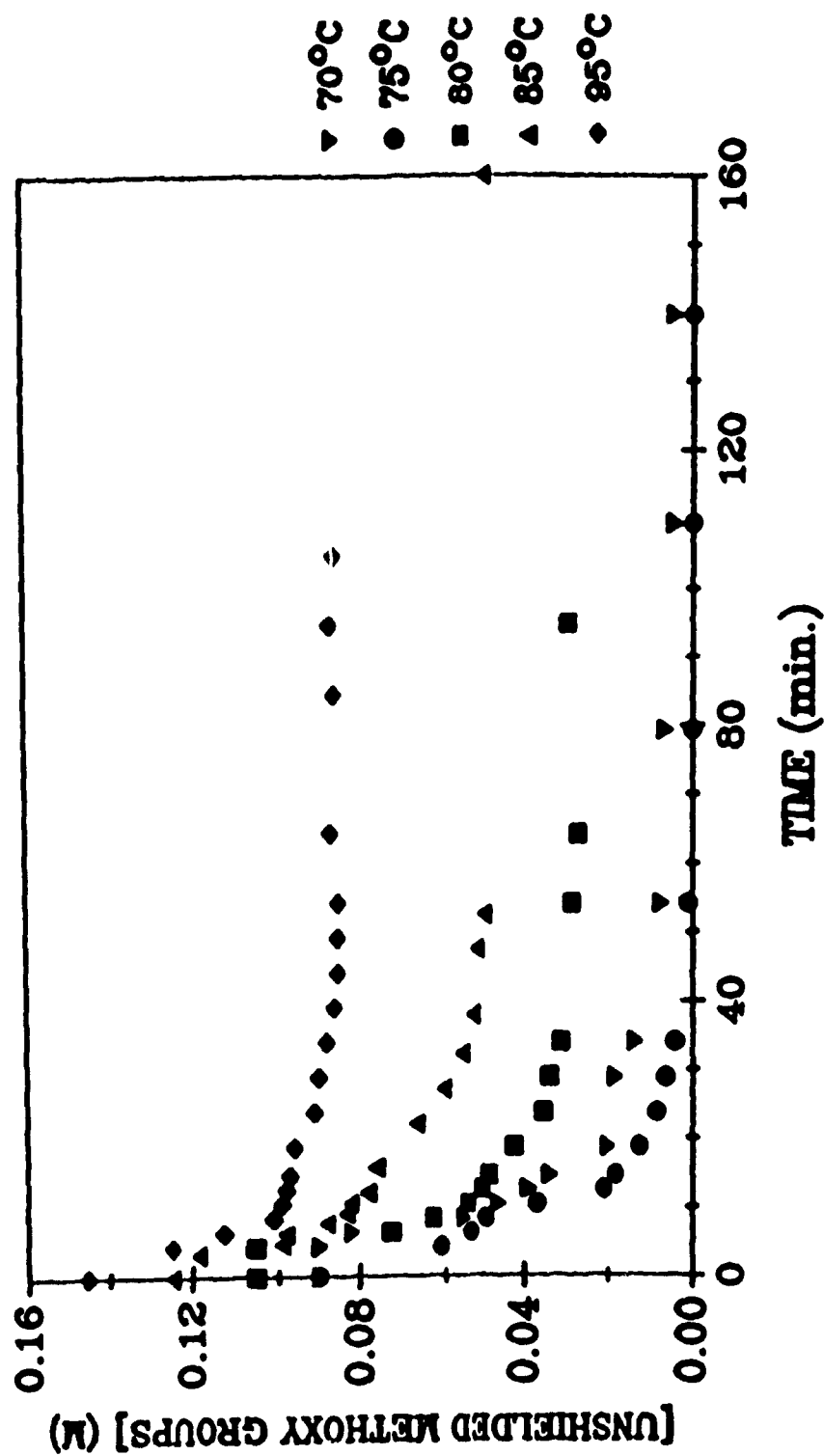


Figure 4.7 Time-concentration curves for equimolar mixtures of PMMA-4VP 11mole % with P<sub>n</sub>SSA 10 mole % of MW=10<sup>4</sup> at various temperature. The solution of DMSO<sub>d6</sub> (0.5 ml) contained 5 mg of both copolymers. The concentration of the vertical axis refers to the unshielded methoxy groups signal.

These time-concentration curves were graphically analyzed using equations 4.5 and 4.11. Typical plots that were used to determine the first-order and second-order rate constants can be found in figure 4.8 and 4.9 respectively. These plots are for an equimolar mixture (0.05 M) containing PMMA-4VP 11 mole % ( $MW=10^5$ ) with a PS-SSA 10 mole % of  $MW=10^5$  (squares in figure 4.5). The equilibrium concentration of the shielded methoxy groups ( $X_e$ ) is equal to 0.030 M (figure 4.10), and is attained after  $\approx 135$  minutes, i.e. when the variation in concentrations are less than 5% of the equilibrium concentration. The correlation coefficient obtained for the determination of  $k_1$  for this mixture using two first-order opposing reactions is 0.996, compared to 0.983 for a second-order forward reaction with an opposing first-order back reaction.

The rate constants for the forward reaction, their correlation coefficients, and the difference between their correlation coefficient ( $\Delta CC$ ) are reported in table 4.2. One can see from table 4.2 that the worst correlation coefficient for a mechanism containing a first-order or second-order forward reaction with a first order opposing reaction is equal to 0.971 and 0.897, respectively. The mean correlation coefficients, calculated for these mixtures, are respectively equal to  $0.988 \pm 0.008$  and  $0.967 \pm 0.027$  for the first- and second-order mechanism. Comparison between the calculated standard deviation for these two mechanisms (0.008 vs 0.027) shows a smaller discrepancy for the first-order correlation coefficient. Moreover, the positive  $\Delta CC$  values indicate that, with the exception of one mixture, the best correlation is achieved with the first-order equation. It is important to note that the induction periods that are observed in the time-concentration curves were not included in the linear regression, since during this time period the concentration of the product either remained below the experimental limit of detection, or was simply not produced at all.<sup>65-68</sup> All the above arguments about the correlation coefficients, the standard deviation of these coefficients, and the  $\Delta CC$  criterion, lead to

the conclusion that a mechanism containing two first-order opposing reactions gives the best fit.

Another argument can be invoked to illustrate the preference for a mechanism containing a first-order forward reaction over one with a second-order forward reaction. For a first-order plot (equation 4.5), it is known that the points which fit the regression line best can be found in the first two thirds of the reaction,<sup>66</sup> while for a second-order plot (equation 4.11), they can be found in the first half of the reaction.<sup>66</sup> Thus, if one compares the fit of the experimental points to the regression line in those regions, one will have an additional criterion for the quality of the correlation.

For a first-order mechanism, two third of the equilibrium concentration of shielded methoxy groups ( $X_e$ ) is produced after 60 minutes, i.e., when the concentration of shielded methoxy groups is equal to 0.020 M (figure 4.10). While, for a second-order mechanism, half of the  $X_e$  concentration of shielded methoxy (0.015 M) will be produced after 35 minutes (figure 4.10). Thus for the second-order plot (figure 4.9), one can see that half of the points are far from the regression line in the 4 to 35 minutes region, while for the first-order plot (figure 4.8), over the 4 to 60 minutes time scale, only one point is far from the regression line (10 minutes). Furthermore, it was generally observed for the first-order opposing reactions, that the deviations from equation 4.5 were very small, over the entire time scale of the experiments. Therefore, it can be concluded that the best fit is obtained with a mechanism containing two first-order opposing reactions.

**Table 4.2** Summary of the rate constants for a mechanism in which a first-order or a second-order forward reaction is opposed to a first-order backward reaction, for various mixtures of PMMA-4VP 11 mole % (MW=  $10^5$ ) with PS-SSA, in 0.5 ml of DMSO<sub>66</sub>.

BLEND DESCRIPTION				RATE CONSTANTS				ACC
PS-SSA CONCENTRATION (M)	PS-SSA MW	PS-SSA ION CONTENT (mole %)	TEMPERATURE (°C)	FIRST-ORDER $k_1$ (min <sup>-1</sup> )	CORRELATION COEFFICIENT	SECOND-ORDER $k_1$ (M <sup>-1</sup> min <sup>-1</sup> )	CORRELATION COEFFICIENT	
0.05	10 <sup>5</sup>	10.0	85	0.042±0.001	0.996	1.29±0.04	0.990	0.006
0.10	10 <sup>5</sup>	10.0	85	0.089±0.002	0.998	1.52±0.05	0.983	0.015
0.15	10 <sup>5</sup>	10.0	85	0.034±0.002	0.991	0.47±0.02	0.974	0.017
0.10	10 <sup>5</sup>	10.0	70	0.012±0.001	0.992	0.14±0.02	0.988	0.004
0.10	10 <sup>5</sup>	10.0	75	0.028±0.001	0.986	0.16±0.01	0.982	0.004
0.10	10 <sup>5</sup>	10.0	80	0.055±0.003	0.989	0.90±0.05	0.988	0.001
0.10	10 <sup>5</sup>	10.0	95	0.118±0.009	0.991	1.62±0.11	0.991	0.000
0.10	10 <sup>5</sup>	7.7	85	0.054±0.001	0.997	1.06±0.11	0.983	0.014
0.10	10 <sup>5</sup>	14.7	85	0.163±0.013	0.987	6.57±0.44	0.982	0.005
0.05	10 <sup>4</sup>	10.0	85	0.011±0.001	0.992	0.57±0.03	0.973	0.019
0.10	10 <sup>4</sup>	10.0	85	0.057±0.003	0.987	0.93±0.07	0.970	0.017
0.15	10 <sup>4</sup>	10.0	85	0.173±0.015	0.978	1.64±0.15	0.961	0.017
0.10	10 <sup>4</sup>	10.0	70	0.041±0.005	0.971	0.84±0.11	0.951	0.020
0.10	10 <sup>4</sup>	10.0	75	0.066±0.003	0.988	0.99±0.05	0.975	0.013
0.10	10 <sup>4</sup>	10.0	80	0.078±0.004	0.989	1.57±0.09	0.990	0.001
0.10	10 <sup>4</sup>	10.0	95	0.034±0.001	0.994	0.55±0.04	0.969	0.025
0.10	10 <sup>4</sup>	5.3	85	0.010±0.001	0.985	0.29±0.03	0.926	0.059
0.10	10 <sup>4</sup>	8.3	85	0.013±0.001	0.981	0.26±0.04	0.907	0.074
0.10	10 <sup>4</sup>	9.2	85	0.036±0.001	0.995	0.59±0.09	0.897	0.098
0.10	10 <sup>4</sup>	13.8	85	0.121±0.015	0.957	0.29±0.03	0.926	0.015
Mean value:					0.988±.008		0.967±.027	0.021±.025

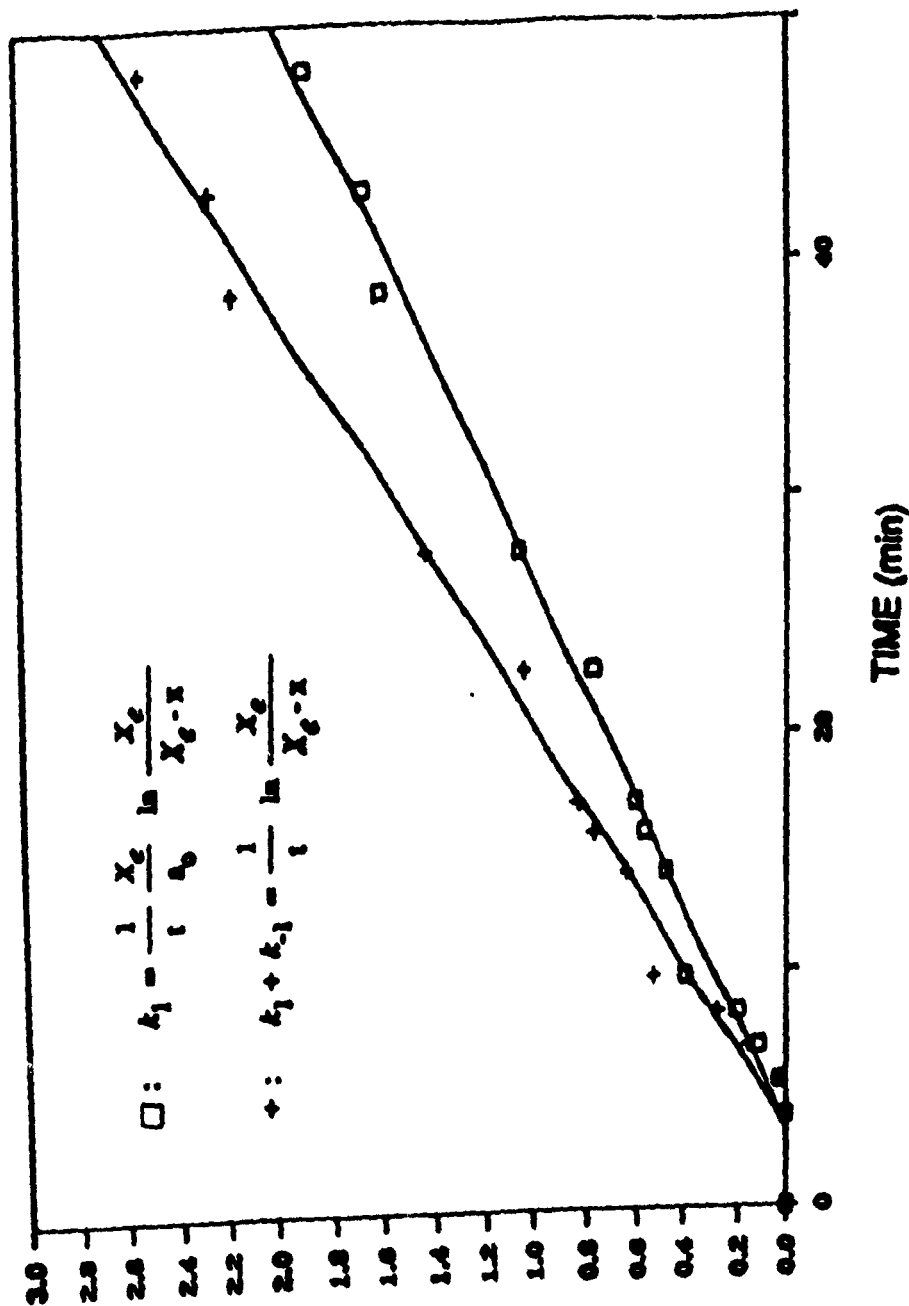


Figure 4.3 Plot of equation 4.5 and 4.3 for an equimolar mixture of PMAA-VVP 11 mole % with PS-SSA 10 mole % of MW=10<sup>5</sup>, at 35°C. The DMSO<sub>0.5</sub> solution contains 2.5 mg of both copolymer per 0.5 ml (0.05 M).

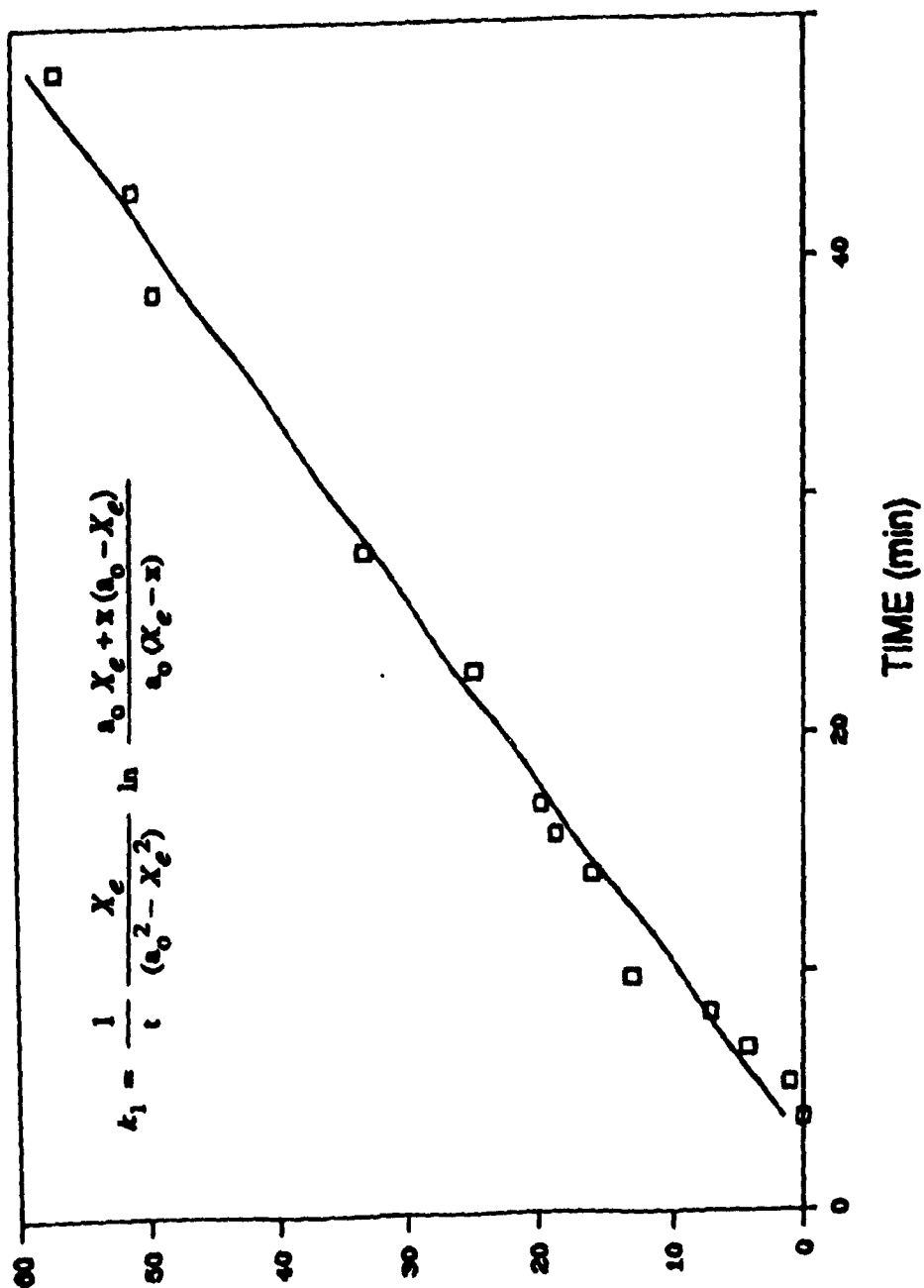
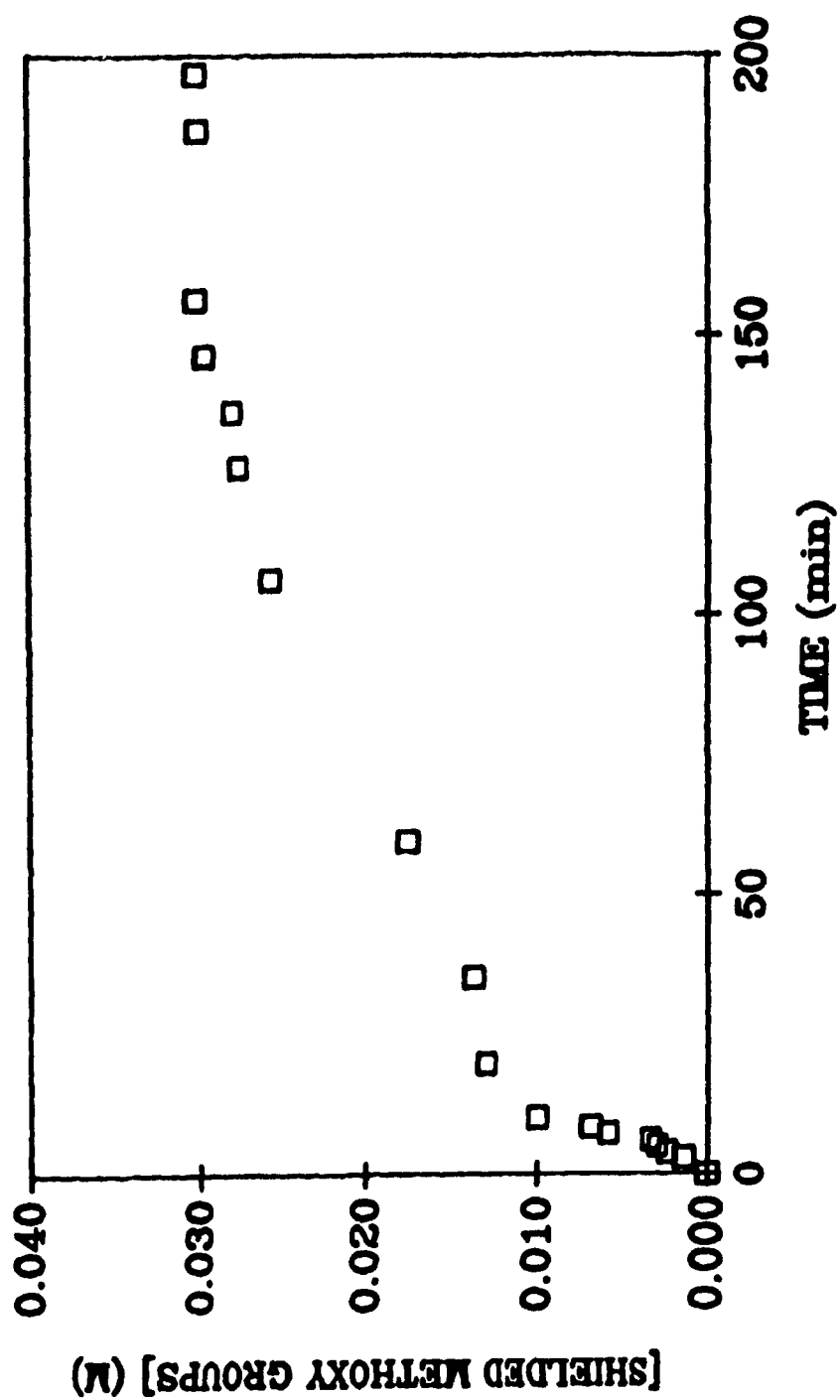


Figure 4.9 Plot of equation 4.11 for an equimolar mixture of PMMA-4VP 11 mole % with PS-SSA 10 mole % of MW=10<sup>5</sup>, at 85°C. The DMSO<sub>66</sub> solution contains 2.5 mg of both copolymer per 0.5 ml (0.05 M).



**Figure 4.10** Time-concentration curve for the equimolar mixture (0.05 M) of PMMA-4VP 11 mole % of MW=10<sup>5</sup> with PS-SSA 10 mole % of MW=10<sup>4</sup>, at 85°C. The concentration of the vertical axis refers to the shielded methoxy groups signal.

#### 4.4 Mechanism of the Shielding Process

Before discussing the effects of the experimental parameters on the kinetics of shielding, it is useful to explore in somewhat greater detail the physical significance of the apparent rate constants  $K_1$  and  $K_{-1}$ . This can best be achieved by considering a possible reaction mechanism for the mixing process of the coils.

However, even before suggesting an overall mechanism, it is important to review all the experimental observations that can be used to justify the mechanism. It is well known that most proton transfer reactions can be characterized as very rapid processes in which equilibrium is established essentially instantaneously.<sup>69</sup> From other studies, on model compounds in DMSO, it is known that the proton transfer from relatively weak acids (carboxylic, or sulfonic) to the nitrogen atom of a substituted pyridine ring is fast ( $\approx 10^{-7}$  sec.),<sup>69,70</sup> and that it occurs when the two species are at distance of the order of 10-100 Å.<sup>69</sup> Thus, one can expect, for the present system, an analogous behaviour for the proton transfer from the SSA to the 4VP.

From the present experimental results, it was observed that the complete coil overlap process was fully reversible, and that therefore all the forward reactions contained in the mechanism must have their opposed backward reactions. Generally, the solutions are dilute. This implies that at  $t=0$ , the coils must be separated by a large distance. A crude estimate of these distances can be obtained, and examples of the calculations are presented in appendix 5. These distances are of the order of 200 Å and 100 Å for mixtures containing PS-SSA samples of molecular weights of  $10^5$  and  $10^4$ , respectively.

Since the solutions are quite dilute, when two dissimilar chains collide or segments are at a distance of less than 10 Å, proton transfer from a sulfonic acid group



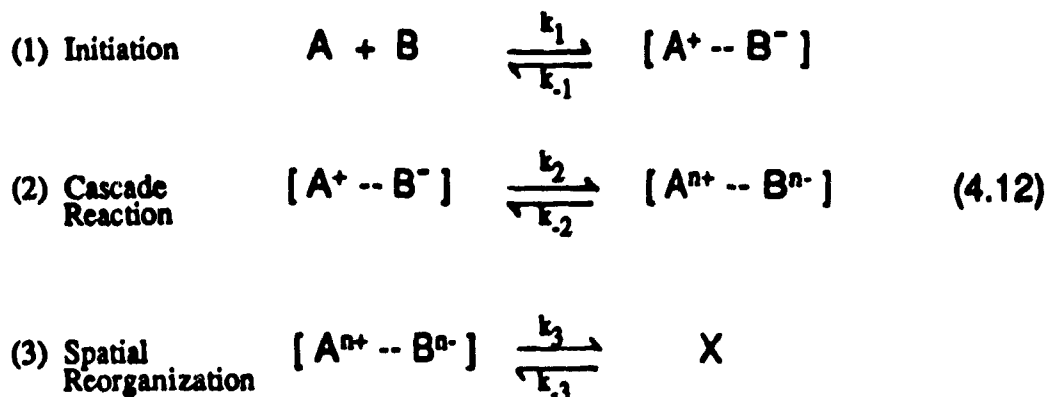
from the PS-SSA (B) chain to a vinylpyridine group of the PMMA-4VP (A) chain can occur. As soon as even one event has taken place, one can assume that the two dissimilar chains form a complex and that the shielding process can now proceed between the two dissimilar chains within that complex. This is valid for two dissimilar chains of equivalent molecular weights. The formation of that initial complex  $[A^+ \cdots B^-]$ , is the first step (initiation) of the proposed mechanism.

As soon as this initial complex is formed, a cascade reaction will be initiated, and most of the remaining protons of the SSA groups from the PS-SSA chain will be transferred more or less randomly to the nearest VP units in the complex. This random ion pairing reaction between the two dissimilar chains involved in the initial complex constitutes the second step of the mechanism. In a previous study, Natansohn and Eisenberg investigated the present system by  $^1\text{H}$  NMR. They concluded that the vast majority of the protons from the SSA were interacting with the pyridine rings of the PMMA-4VP chains, even in the early stage stages of the mixing process.<sup>30</sup> Thus, the formation of this complex  $([A^{s+} \cdots B^{s-}])$  is rapid, and is mostly complete by the time that the first  $^1\text{H}$  NMR spectrum is acquired (less than 2 min.). There is strong electrostatic interaction between the chains. However, it must be stressed that the vast majority of the methoxy groups are not yet shielded at that point.

The third step of the mechanism can be attributed to the spatial reorganization of the two dissimilar chains involved in the  $[A^{s+} \cdots B^{s-}]$  complex. This reorganization of the complex is a slow process dictated in part by the segmental motions of the chains in solution. Some of the ion pairs in the  $[A^{s+} \cdots B^{s-}]$  complex will come apart, and reform

in such a way as to form a "ladder" like complex (X). Thus, the presence of the shielded methoxy signal, observed in  $^1\text{H}$  NMR, can be interpreted as the appearance of a certain quantity of the ladder complex in the solution.

These three steps can be represented by the following equations



The over-all reaction is obtained by adding the 3 equations of set (4.12)



In order to simplify the equations for the derivation of the apparent rate constants,  $[\text{A}^+ \cdots \text{B}^-]$  and  $[\text{A}^{n+} \cdots \text{B}^{n-}]$  will be replaced by  $M_1$  and  $M_2$ , respectively in the subsequent equations.

The individual rate equation for the stable species are then

$$\begin{array}{ll}
 \text{(1)} & -d\text{A} / dt = k_1 [\text{A}] [\text{B}] - k_{-1} M_1 \\
 \text{(2)} & -d\text{B} / dt = k_1 [\text{A}] [\text{B}] - k_{-1} M_1 \\
 \text{(3)} & d\text{X} / dt = k_3 M_2 - k_{-3} \text{X}
 \end{array} \quad (4.14)$$

and for the "unstable" intermediates

$$\begin{aligned} (1) \quad dM_1 / dt &= k_1 [A][B] + k_{-2} M_2 - (k_{-1} + k_2) M_1 \\ (2) \quad dM_2 / dt &= k_2 M_1 + k_{-3} X - (k_{-2} + k_3) M_2 \end{aligned} \quad (4.15)$$

in addition, one can obtain the stoichiometric relation

$$\text{moles of A used} = M_1 = (a_0 - X) \quad (4.16)$$

If one assumes that  $X$ ,  $M_1$ , and  $M_2$  are equal to zero at  $t = 0$ , and that the concentrations of intermediates  $M_1$  and  $M_2$  are at all time much less than the concentrations of reactants and product, one can apply the stationary-state concept to equation 4.15 and obtain the following expressions for the intermediates

$$\begin{aligned} (1) \quad M_1 &= \frac{k_1 [A][B] + k_{-2} M_2}{(k_{-1} + k_2)} \\ (2) \quad M_2 &= \frac{k_2 M_1 + k_{-3} X}{(k_{-2} + k_3)} \end{aligned} \quad (4.17)$$

by substituting the expression for  $M_2$  (equation 4.17.2) into equation 4.14.3, one obtains

$$dX / dt = [k_3 / (k_{-2} + k_3)] [k_2 M_1 + k_{-3} X] - k_{-3} X \quad (4.18)$$

rearrangement of equation 4.18 and substitution for  $M_1$  of its value from equation 4.16, gives

$$\frac{dX}{dt} = \frac{k_2 k_3}{k_{-2} + k_3} (a_0 - X_e) - \left[ k_{-3} - \frac{k_{-3}}{k_{-2} + k_3} \right] X_e \quad (4.19)$$

A comparison of this equation with equation 4.1, which was applied to a mechanism in which two first-order reactions are opposing each other, shows that they are formally analogous. The integration of equation 4.19 will give rise to an expression having the same form as equation 4.8, in which  $[k_2 k_3 / (k_2 + k_3)]$  and  $[k_{-3} - (k_{-3} / (k_2 + k_3))]$  are replaced by  $K_1$  and  $K_{-1}$  respectively.

From equation 4.19, it is clear that only the rate constants  $k_2$  (random chain of proton transfers) and  $k_3$  (spatial reorganization) will have a major influence on the apparent rate constant ( $K_1$ ) characterizing the forward reaction. For the backward reaction, one can expect that only  $k_{-3}$  will have a major effect on the observed apparent constant  $K_{-1}$ , since it is the difference between  $k_{-3}$  and a fraction of  $k_{-3}$   $[(k_3 / (k_2 + k_3))]$ .

#### 4.5 Conclusion

From the derivation method, it has been established that the true orders ( $n_c$ ) of the processes, for mixtures containing PS-SSA of MW=10<sup>4</sup> and MW=10<sup>5</sup>, respectively, were equal to 2.4 and 2.9. From the comparison of  $n_c$  with  $n_t$ , it was confirmed that more than one simple forward reaction should be required to describe the mixing process.

Since the mixing process was found to be fully reversible, the kinetic expression describing the process ought to contain at least one backward reaction. From the value of the correlation coefficient, and the quality of the fit criterion, a mechanism in which two first-order reactions are opposing one another (equation 4.5) was favored over one containing a second-order forward reaction and first-order back reaction (equation 4.11).

Application of equation 4.5 enables one to obtain the rate constants for the mixing process. However, these are only apparent rate constants, since they contain all the individual rate constants included in the overall process. Thus, the application of equation 4.5 can be envisaged as a mathematical subterfuge, that enables one to obtain quantitative information on the system, without having to characterize all the individual rate constants of the process.

The physical significance of the apparent rate constants  $K_1$  and  $K_{-1}$  was obtained by suggesting a mechanism containing three steps. The first step occurs when one proton from the SSA is transferred to the 4VP, i.e., the two dissimilar chains are close to one another and are attached by one contact point ( $[A^+ \cdots B^-]$ ). The second step can be envisaged as a cascade reaction occurring within the initial complex. This reaction involves the transfer of a vast majority of the SSA protons from the PS chain to the 4VP units of the PMMA-4VP chain ( $[A^{2+} \cdots B^{2-}]$ ). The last step of the mechanism consists of a spatial reorganization of the complex formed during the second step. This spatial reorganization of the  $[A^{2+} \cdots B^{2-}]$  species leads to the formation of a ladder like complex (X).

The first two steps are rapid, and are completed by the time that the first  $^1\text{H}$  NMR spectrum is acquired; by contrast, the third step is a slow, because it involves segmental motions of strongly interacting chains. Thus, the appearance of the shielded methoxy signal from the PMMA, which can be observed by  $^1\text{H}$  NMR, can be attributed mostly to the formation of the ladder like complex in solution.

From the proposed mechanism, one can derive an equation which relates the individual rate constants of the process to the apparent rate constants  $K_1$  and  $K_{-1}$ . It was found that  $K_1$  and  $K_{-1}$  could be expressed as  $[k_2 k_3 / (k_2 + k_3)]$  and  $[k_{-3} - (k_{-3} / (k_2 + k_3))]$ , respectively.

## CHAPTER 5. QUANTITATIVE KINETICS - RESULTS AND DISCUSSION

### 5.1 Introduction

This chapter will examine the kinetic results obtained in the studies of the effects of various experimental parameters on the shielding and deshielding process for mixtures of two copolymers, specifically, of PS-SSA and PMMA-4VP in  $\text{DMSO}_{d6}$ . As previously mentioned, the data gathered so far on the coil overlap process of the copolymer mixtures lead to the conclusion that the mechanism is analogous to an overall reaction containing two first order reactions that are opposing one another. Using the procedure described in section 4.3.1, one can obtain the rate constants for each processes. Comparison of these calculated rate constants will enable one to quantify the influence of each experimental parameter on the coil overlap process.

### 5.2 Parameters Affecting the Shielding Process for Blends Containing PS-SSA of $\text{MW}=10^4$

In this section, three experimental parameters influencing the coil overlap process will be discussed. For all these mixtures, the PMMA-4VP copolymer will be identical, i.e, the 4VP content will be equal to 11 mole %, and the molecular weight to  $10^5$ . For the second copolymer involved in the mixing process (PS-SSA), only the MW ( $10^4$ ) will remain constant, while the other experimental parameters will be modified, one at a time. In section 5.2.1 to 5.2.3, the influence of the temperature, the SSA content and the total polymer concentration will be discussed. It is important to note that in order to form the  $[A^{2+} \cdots B^{2-}]$  complex, more than one PS-SSA chain per PMMA-4VP chain will be required. This implies that the ladder-like complex (X) will probably contain several independent sections that have gone through spatial reorganization, which is not the case if the two dissimilar chains are of similar molecular weights molecular.

### 5.2.1 Temperature

In section 3.3, it was shown that the temperature has two opposed effects which are competing during the coil overlap process. On one hand, an increase in temperature favors molecular motions, and therefore will tend to increase the rate at which the two dissimilar chains will find one another in solution. It may also favor, to a certain extent, the spatial reorganization of the ladder complex. However, an increase in temperature will effectively decrease the importance of the coulombic interactions between the ions, and therewith the driving force for the mixing process.

Therefore, on the basis of the proposed mechanism, two possible cases can be envisaged in terms of their effect on the apparent rate constant of the shielding process, i.e.  $K_1$  (see equation 4.12 to 4.19 for details). First, if the disruptive effects of the molecular motions of the two dissimilar chains involved in the  $[A^{n+} \cdots B^{n-}]$  complex are not dominant, it is expected that the value of  $K_1$  will increase as the temperature increases. However, if the disruptive effects are dominant, the value of the apparent rate constant for the shielding process will decrease, since it is a product of two rate constants ( $k_2$  and  $k_3$ ) for two processes that will be inhibited by an increase in temperature. The apparent deshielding rate constants  $K_{-1}$  and  $k_{-2}$  should have approximately the same values, since the temperature is not high enough to cause a major disruption of the coulombic interaction. Consequently, for a certain temperature range, the value of the rate constant for the total coil overlap process ( $K_T$ ), will show the same trend as  $K_1$ , since it is a summation of a quantity that is variable ( $K_1$ ) and a constant ( $K_{-1}$ ).

Five equimolar mixtures (0.10 M in repeat units of each copolymer) of PMMA-4VP with PS-SSA of 10 mole % in 0.5ml of  $DMSO_{d6}$  were used to perform this study at various temperatures. For these five blends, rate constants were determined for the

following processes i.e., shielding ( $K_1$ ), deshielding ( $K_{-1}$ ) and the total process ( $K_T$ ). Moreover, the equilibrium constant ( $k_{eq}$ ) was calculated, i.e the ratio of  $K_1$  to  $K_{-1}$ . The results are reported in table 5.1.

From these results, one can see that as the temperature increases, the value for the shielding and the total rate constants are increasing up to 80°C. On the other hand, the value of the rate the constant for the deshielding process remains almost constant. Consequently, values obtained for the equilibrium constants ( $k_{eq}$ ) show the same trend as  $K_1$ , i.e, increasing up to 80°C, then decreasing as the temperature increases further.

**Table 5.1** Effect of Temperature  
Rate constants for equimolar blends (0.10 M) of PMMA-4VP 11 mole % (MW =  $10^5$ ) with PS-SSA 10 mole % (MW =  $10^4$ ) in 0.5 ml of DMSO<sub>d6</sub>.

TEMPERATURE (°C)	RATE CONSTANTS (min <sup>-1</sup> )			
	TOTAL ( $K_T$ )	SHIELDING ( $K_1$ )	DESHIELDING ( $K_{-1}$ )	EQUILIBRIUM ( $k_{eq}$ )
70	0.060	0.040	0.020	2.0
75	0.089	0.066	0.023	2.9
80	0.090	0.078	0.012	6.5
85	0.079	0.057	0.022	2.6
95	0.060	0.034	0.026	1.3

These results show that in this system, an increase in temperature will favor the shielding process up to 80°C. However, for higher temperatures, the disruptive effects of the segmental motions of the chains become dominant over the coulombic interactions between the ion pairs. The decrease in the apparent shielding rate constant for temperature higher than 80°C can be attributed mostly to that effect.



### 5.2.2 SSA Content

Since the coulombic interactions between the ions are the driving force for the mixing process, it is expected that the value of the apparent shielding rate constant should increase with increasing SSA content. This increase is obviously due to the presence of a greater number of reactive sites on the PS-SSA chain. It should be recalled that the apparent rate constants in equation 4.9 are related to the concentration of polymer chains, not of the functional groups. Clearly, the probability of the occurrence of proton transfer increases with increasing SSA content, which implies that rate constant  $k_2$  will increase. One can also anticipate that the value of  $k_{-2}$  will decrease, while the value of  $k_3$  should remain almost unchanged with increasing SSA contents, since  $k_3$  is mostly a function of the segmental motions of the chains; adding more ions on a PS chain should not have a major effect on the rate constant  $k_3$ . Thus, all the rate constants which contribute to  $K_1$  behave so as to lead to an increase of the value of the rate constant as the SSA ion content increases. Moreover, it is known that the apparent rate constant for the deshielding process is, to a certain extent, a measure of the effectiveness of the shielding effect. Therefore, if the coulombic interactions are strong enough, it is expected for these low molecular weight PS-SSA chains that less material will go through spatial reorganization. This will tend to increase the value of  $K_{-1}$  with increasing SSA contents.

Five equimolar blends (0.10 M) of PMMA-4VP with PS-SSA of various SSA contents in 0.5ml of  $\text{DMSO}_{d6}$  at  $85^\circ\text{C}$  were used to perform this study. For these five blends, as in section 5.2.1, the following rate constants were determined, i.e.,  $K_1$ ,  $K_{-1}$ ,  $K_T$ , and  $k_{eq}$ . Values of these rate constants are reported in table 5.2.

One can see from the results in table 5.2 that as the ion content of the PS-SSA

chains increases, the shielding, the deshielding and the total rate constants are increasing. On the other hand, the rate constant of the shielding process increases slightly more rapidly than that of the deshielding process. From the value of  $k_{eq}$ , one can see that its value increases until the ionic content of the two dissimilar chains is equal, and then levels off.

**Table 5.2** Effect of SSA content

Rate constants for equimolar blends (0.10 M) of PMMA-4VP 11 mole % (MW =  $10^5$ ) with PS-SSA (MW =  $10^4$ ) in 0.5 ml of DMSO<sub>d6</sub> at 85°C.

SSA CONTENT (mole %)	RATIO (%4VP/ %SSA)	RATE CONSTANTS (min <sup>-1</sup> )			
		TOTAL ( $K_T$ )	SHIELDING ( $K_1$ )	DESHIELDING ( $K_{-1}$ )	EQUILIBRIUM ( $k_{eq}$ )
5.3	2.1	0.027	0.010	0.017	0.6
8.3	1.3	0.025	0.013	0.012	1.1
9.2	1.2	0.060	0.036	0.017	2.1
10.5	1.1	0.079	0.057	0.022	2.6
13.8	0.8	0.170	0.120	0.050	2.4

These results show that in this system, an increase in SSA content will favor the shielding process up to point where the ion content of the dissimilar chains are equal. On the other hand, the SSA contents do not affect the apparent deshielding rate constant for symmetrical mixtures or those in which the 4VP / SSA mole % ratio > 1. However, when there is an excess of SSA groups in the mixture, the rate constant  $K_{-1}$  increases drastically. This observation can be rationalized by recalling a previous comment on the nature of this rate constant.  $K_{-1}$  can be directly related to the effectiveness or the extent of the shielding; at equilibrium, this implies that the value of the apparent rate constant will

increase, if the quantity of shielded methoxy groups is decreased. Clearly, it means that for asymmetric mixtures of low 4VP/SSA values, a smaller quantity of the ladder-like complex is formed than for symmetric mixtures. This may be due to the fact that in asymmetric systems, the ladder complex is formed too rapidly, and since it is formed with a certain number of PS-SSA ( $\approx 10$ ) chains per PMMA-4VP chain, these strongly interacting chains will, to a certain extent, prefer to undergo a minimum of spatial reorganization.

The facts that the initial ionic interactions from random pairing are more effective, and that the contour length of the two dissimilar chains are quite different, can produce a large number of mismatched PS-SSA segments (PS-SSA chains dangling at the ends of a PMMA chain). Thus, the formation of the ladder-like complex is favored by an increase of the SSA content. However, for the non-symmetric mixture in which an excess of SSA groups is present,  $K_1$  increases and the formation of the ladder-like complex is slightly inhibited.

### 5.2.3 Total Polymer Concentration

In section 3.4, it was shown that after the induction period, the rate of the coil overlap process increased as the polymer concentration increased. It was concluded that the coil overlap process during this stage was governed by the spatial reorganization of the two dissimilar chains.

Thus, it is expected that the value of the apparent shielding rate constant should increase with an increase in concentration. This increase is obviously due to the presence of a greater number of chains in solution. Clearly, the collision probability of two

dissimilar chains increases with increasing concentrations. Thus the same arguments can be made as in section 5.2.2. The value of the rate constant  $k_2$  will increase greatly, the value of  $k_{-2}$  will decrease, while the value of  $k_3$  should remain almost unchanged with increasing concentrations. Thus, all the rate constants which contribute to  $K_1$  behave in such a way as to increase of the value of the rate constant, as the concentration increases. Moreover, it is known that the apparent rate constant for the deshielding process is, to a certain extent, a measure of the effectiveness of the shielding effect. Therefore, as suggested in section 5.2.2, if the coulombic interactions are strong enough, it is expected for these low molecular weight PS-SSA chains that less material will go through spatial reorganization. This will tend to increase the value of  $K_{-1}$  with increasing total polymer concentrations.

Three equimolar blends (0.05 M, 0.10 M and 0.15 M) of PMMA-4VP with PS-SSA of 10 mole % in 0.5ml of  $\text{DMSO}_{d6}$  at  $85^\circ\text{C}$  were used to perform this study. For these three blends, as in section 5.2.1,  $K_1$ ,  $K_{-1}$ ,  $K_T$ , and  $k_{eq}$  were calculated. Values of these rate constants are reported in table 5.3.

One can see from the results in table 5.3 that as the concentration of the two copolymer chains increases, the shielding, the deshielding and the total rate constants are increasing. On the other hand, the rate of the deshielding process increases more rapidly than that of the shielding process. This is clearly illustrated by the trend of the calculated values of  $k_{eq}$ , which first increase and then decrease as the concentration is increased.

**Table 5.3** Effect of total polymer concentration  
Rate constants for equimolar blends of PMMA-4VP 11 mole % (MW =  $10^5$ ) with PS-SSA 10 mole % (MW =  $10^4$ ) in 0.5 ml of DMSO<sub>d6</sub> at 85°C.

TOTAL POLYMER CONCENTRATION (M)	RATE CONSTANTS (min <sup>-1</sup> )			
	TOTAL ( $K_T$ )	SHIELDING ( $K_1$ )	DESHIELDING ( $K_{-1}$ )	EQUILIBRIUM ( $k_{eq}$ )
0.10	0.018	0.011	0.007	1.5
0.20	0.079	0.057	0.022	2.6
0.30	0.250	0.170	0.080	2.1

These results show that in this system, an increase in concentration will favor the rate of the shielding and the deshielding processes. However, the value of  $K_{-1}$  increases more rapidly than for  $K_1$ . An estimate of the initial distances between two dissimilar coils in solution (Appendix 5), gives a better picture of what is happening when the concentration is increased. For the mixtures containing a total concentration of 0.10 and 0.20 M, the average distances between two dissimilar chains are greater than the sizes of the coils themselves. However, this is not the case for the mixture containing a total concentration of 0.30 M, for which it can be calculated that the distance is less than the size of the coil. Thus, one can conceive that there is a threshold concentration below which the formation of the ladder-like complex will be inhibited. At this point, more than one PS-SSA chain can interact with a given PMMA-4VP chain (and possibly vice versa). This will result in occasional "catastrophic" pairing of chains that will lead to the formation of a microgel. This species will be highly entangled, the entanglement being reinforced by the strongly interacting ion pairs. It is conceivable that portions of this complex will not be able to go through spatial reorganization.

One can conclude that an increase in concentrations leads to an increase in the value of the rate constants. However, it seems that the pure ladder-like complex will be produced only for dilute solutions.

### 5.3 Parameters affecting the shielding process for blends containing PS-SSA of MW=10<sup>5</sup>

In this section, three experimental parameters influencing the coil overlap process will be discussed. Mixtures of PMMA-4VP and PS-SSA were prepared as described in section 5.2. The parameters of the PMMA-4VP chains and the molecular weight (10<sup>5</sup>) of the PS-SSA will be kept constant, while the other experimental parameters, i.e. the temperature, the SSA content and the total polymer concentration will be varied. The results will be discussed in section 5.3.1 to 5.3.3.

It is important to note that in this case, in order to form the [ A<sup>n+</sup> -- B<sup>n-</sup> ] complex, only one PS-SSA chain per PMMA-4VP chain will be required. This implies that the ladder-like complex (X) will probably contain only two dissimilar chains, in which the various sections have undergone spatial reorganization. Thus, compared to a mixture containing a relatively low molecular weight PS-SSA, one can expect that a longer period of time will be needed in order to reach the equilibrium shielded methoxy group concentration (X<sub>e</sub>), i.e smaller values of K<sub>1</sub> will be encountered. Moreover, the values of the apparent deshielding rate constant K<sub>-1</sub> are expected to be smaller than for the mixtures containing a low molecular weight PS-SSA.

### 5.3.1 Temperature

For these two relatively high molecular weight copolymers, it is reasonable that an increase in temperature should not decrease the value of the apparent shielding constant, since the chains will now be able to go through spatial reorganization more effectively. The disruptive effects of the temperature may be strong enough to break some of the specific ion-ion interactions, but not strong enough to break all of them. The two dissimilar chains will stay much closer to one another than in the case of a low molecular weight PS-SSA. Thus, the spatial reorganization that requires some kind of cooperative motions between the two dissimilar chains will be favored if the two chains are staying close to one another.

Five equimolar mixtures (0.10 M) of PMMA-4VP with PS-SSA of 10 mole % (in 0.5ml of DMSO<sub>d6</sub>) were used to perform this study at various temperatures. As before, values of the rate constants were determined for the shielding process ( $K_1$ ), the deshielding process ( $K_{-1}$ ) and the total process ( $K_T$ ), and the equilibrium constant ( $k_{eq}$ ) was calculated. The results are reported in table 5.4.

From these results, one can see that as the temperature increases, the values for the shielding and the total rate constants increase monotonously. On the other hand, the values of the rate constants for the deshielding process increase only slightly with temperature. Values obtained for  $k_{eq}$  show the same trend as those observed for the mixtures containing chains of PS-SSA of low molecular weight, i.e they increase up to 80°C, then decrease as the temperature increases further.

**Table 5.4** Effect of temperature

Rate constants for equimolar blends (0.10 M) of PMMA-4VP 11 mole % (MW =  $10^5$ ) with PS-SSA 10 mole % (MW =  $10^5$ ) in 0.5 ml of DMSO<sub>d6</sub>.

TEMPERATURE (°C)	RATE CONSTANTS (min <sup>-1</sup> )			
	TOTAL ( $K_T$ )	SHIELDING ( $K_1$ )	DESHIELDING ( $K_{-1}$ )	EQUILIBRIUM ( $k_{eq}$ )
70	0.020	0.011	0.009	1.2
75	0.028	0.014	0.014	1.0
80	0.061	0.055	0.006	9.2
85	0.102	0.089	0.013	6.8
95	0.139	0.118	0.021	5.6

These results show that in this system an increase in temperature will accelerate both the shielding and the deshielding process. Using the arguments of section 5.2.1, one can say that with increasing temperature the disruptive effects of the segmental motion will be strong enough to reduce the quantity of ladder like complex formed when steady state is achieved, but not strong enough to inhibit the shielding process.

### 5.3.2 SSA Content

The coulombic interactions between the ions are the driving force for the mixing process. Thus, using the same arguments, that were used in section 5.2.2, one can expect  $K_1$  to increase with increasing SSA contents. Furthermore, from section 5.3.1, it is known that at 85°C and above significant disruptions occur to the ion-ion interactions. Thus, two kind of behavior can be envisaged for  $K_{-1}$ . In the case of major disruptions,



values of  $K_{-1}$  will remain constant or increase with increasing SSA contents. On the other hand, if the disruptive effects are minor, it is expected that the values of  $K_{-1}$  will decrease.

Three equimolar blends (0.10 M) of PMMA-4VP with PS-SSA of various SSA contents in 0.5ml of  $\text{DMSO}_{d6}$  at  $85^\circ\text{C}$  were used to perform this study. For these three blends, as in section. 5.3.1, the constants  $K_1$ ,  $K_{-1}$ ,  $K_T$ , and  $k_{eq}$  were determined. Values of these rate constants are summarized in table 5.5.

**Table 5.5** Effect of SSA content

Rate constants for equimolar blends of PMMA-4VP 11 mole % ( $MW = 10^5$ ) with PS-SSA ( $MW = 10^5$ ) in 0.5 ml of  $\text{DMSO}_{d6}$  at  $85^\circ\text{C}$ .

SSA CONTENT (mole %)	RATIO (%4VP/%SSA)	RATE CONSTANTS ( $\text{min}^{-1}$ )			
		TOTAL ( $K_T$ )	SHIELDING ( $K_1$ )	DESHIELDING ( $K_{-1}$ )	EQUILIBRIUM ( $k_{eq}$ )
7.7	1.4	0.084	0.054	0.030	1.8
10.0	1.1	0.102	0.089	0.013	6.8
14.7	0.8	0.166	0.163	0.003	55

One can see, from the results in table 5.5, that as the ion content of the PS-SSA chains increases, the shielding and the total rate constants are increasing. On the other hand, the values of the constants for the deshielding process drastically decrease with SSA content. From the  $k_{eq}$ , one is able to observe that its value increases exponentially with increasing SSA contents.

These results show that in this system, an increase in SSA content will favor the shielding process. On the other hand, for increasing SSA contents the apparent deshielding rate constants are greatly reduced. Thus, at 85°C the disruptive effects of the temperature are minor, and they only contribute to favor the formation of ladder-like complex.

### 5.3.3 Total Polymer Concentration

From the arguments of section 5.2.3, it is expected that the values of the apparent shielding rate constants should increase with polymer concentration. On the other hand,  $K_{-1}$  values should remain constant. Furthermore, for these high molecular weight polymers, it is conceivable that occasional "catastrophic" pairing of the dissimilar chains will occur at high concentration, leading to the formation of microgels.

Three equimolar blends (0.05 M, 0.10 M and 0.15 M) of PMMA-4VP with PS-SSA 10 mole % in 0.5ml of DMSO<sub>d6</sub> at 85°C were used to perform this study. For these three blends, as in section 5.3.1,  $K_1$ ,  $K_{-1}$ ,  $K_T$ , and  $k_{eq}$  were calculated. These rate constants are reported in table 5.6.

One can see from the results in table 5.6 that as the total concentration of the two copolymer chains increases up to 0.20 M, the shielding and the total rate constants are increasing. On the other hand, the rate constant of the deshielding process remains approximately constant. This is illustrated by the trend of the calculated values of  $k_{eq}$ , which are increasing as the concentration is increased. For mixtures containing a total polymer concentration of 0.30 M, precipitation always occurred.

**Table 5.6 Effect of total polymer concentration**  
Rate constants for the experimental total polymer concentration range, for equimolar blends of PMMA-4VP 11 mole % (MW =  $10^5$ ) with PS-SSA 10 mole % (MW =  $10^5$ ) in 0.5 ml of DMSO<sub>d6</sub> at 85°C.

TOTAL POLYMER CONCENTRATION (M)	RATE CONSTANTS (min <sup>-1</sup> )			
	TOTAL ( $K_T$ )	SHIELDING ( $K_1$ )	DESHIELDING ( $K_{-1}$ )	EQUILIBRIUM ( $k_{eq}$ )
10	0.084	0.042	0.015	2.8
20	0.102	0.089	0.013	6.8
30*	0.044	0.034	0.010	3.4

\* indicates that precipitation is occurring during the experiment.

These results, show that in this system, an increase in concentration will accelerate the shielding process. On the other hand, the deshielding process is not affected by an increase in concentration. Moreover, since precipitation occurs for total concentrations of 0.30 M, it seems that the ladder-like complex will be formed only in the case of solutions that have a concentration below  $C^*$ .

#### 5.4 The Shielding Process at 80°C for an Equimolar Blend Equilibrated at 150°C.

It was established in section 3.3 that for an equilibrated blend, it takes  $\approx 1$  hour at 150°C to observe the complete disappearance of the signal due to the shielded methoxy groups. This deshielding effect is mainly due to the fact that the two interacting groups involved in the shielding process are at a distance greater than 5 Å. Furthermore, if no specific ion-ion interactions were present in the mixture, one should observe for the

methoxy lineshape two sharp signals due to the 21111 and 12111 cosyndiotactic sequences. In fact, the  $^1\text{H}$  NMR spectrum of these mixtures only shows one broad featureless methoxy signal. This seems to indicate that the PS-SSA chain and the PMMA-4VP are still close to one another.

Two extreme cases can be envisaged to rationalize the presence of the interactions. First, the two dissimilar chains are far from one another, however, due to random collisions between the coils the interactions are present. Second, the chains are still close to one another forming a ladder-like complex, but the mean distances are greater than  $5 \text{ \AA}$ .

In the first case, it is clear that the mechanism for the coil overlap process on the cooling of the mixture will be quite similar to a standard shielding experiment. By contrast, for the second case, since the chains are already involved in a ladder-like complex, the shielding process will be independent of the concentration of the reactants (order 0).

This experiment was performed in triplicate, using equimolar blends (0.10M) containing PMMA-4VP 11 mole % ( $\text{MW}=10^5$ ) with PS-SSA 10 mole % ( $\text{MW}=10^5$ ). The  $^1\text{H}$  NMR spectra were observed at  $80^\circ\text{C}$  until the equilibrium concentration of shielded methoxy groups was reached. These blends were then removed from the NMR probe, and placed in a thermostated bath for three more hours at  $80^\circ\text{C}$  (EQB). These EQB were then monitored at  $150^\circ\text{C}$  until complete deshielding was obtained. The NMR probe temperature was then set to  $80^\circ\text{C}$ , followed immediately by the acquisition of the spectra.

Experimentally, it was observed that the  $X_e$  concentration is reached in  $\sim 45$  minutes, i.e. half the time required for a standard shielding experiment at  $80^\circ\text{C}$ . This qualitative observation implies that the coils are not far from one another. Moreover, using the procedure described in section 4.1.2, one can calculate the order according to

time ( $n_t$ ) for the process. For the three experiments, the plots of  $\ln(-dC/dt)$  vs  $\ln(C)$  do not lead to a straight line (correlation coefficient  $\leq 0.4$ ), which indicates that the process does not have an order with respect to the unshielded methoxy concentration, or that the order of the reaction is equal to 0.<sup>66</sup>

In order to ascertain that the order of this process is zero, one can plot  $\ln(X_e/X_e - X)$  vs time, where  $X_e$  is the equilibrium concentration of the shielded methoxy groups, and  $X$  the concentration of the shielded methoxy groups at a given time.<sup>65-66</sup> Figure 5.1, which is an example of these plots, shows that a good correlation (0.996) can be obtained for a zero-order process.

Thus, one may conclude that at 150°C, the two dissimilar chains are close to one another, even though they are at a distance greater than 5 Å. Furthermore, the zero-order process observed for the reshielding experiments at 80°C indicates that the two dissimilar chains are still in a ladder-like complex.

## 5.5 Influence of the Experimental Parameters on the Coil Overlap Process - Summary and Conclusions

For the sake of completeness and clarity, this section will summarize the major effects of the experimental parameters on the coil overlap process. Comparison between the rate constants for the two types of mixtures, i.e. the mixtures containing the low molecular weights PS-SSA chains ( $10^4$ ) and the high molecular weights chains ( $10^5$ ), will enable one to elucidate some of these effects. The relevant rate constants needed to compare the two types of mixtures are the apparent rate constants for the shielding ( $K_1$ ) and the deshielding, ( $K_{-1}$ ) processes, since the apparent rate constants for the global process ( $K_T$ ) and the equilibrium constants ( $k_{eq}$ ) are calculated from these two constants.

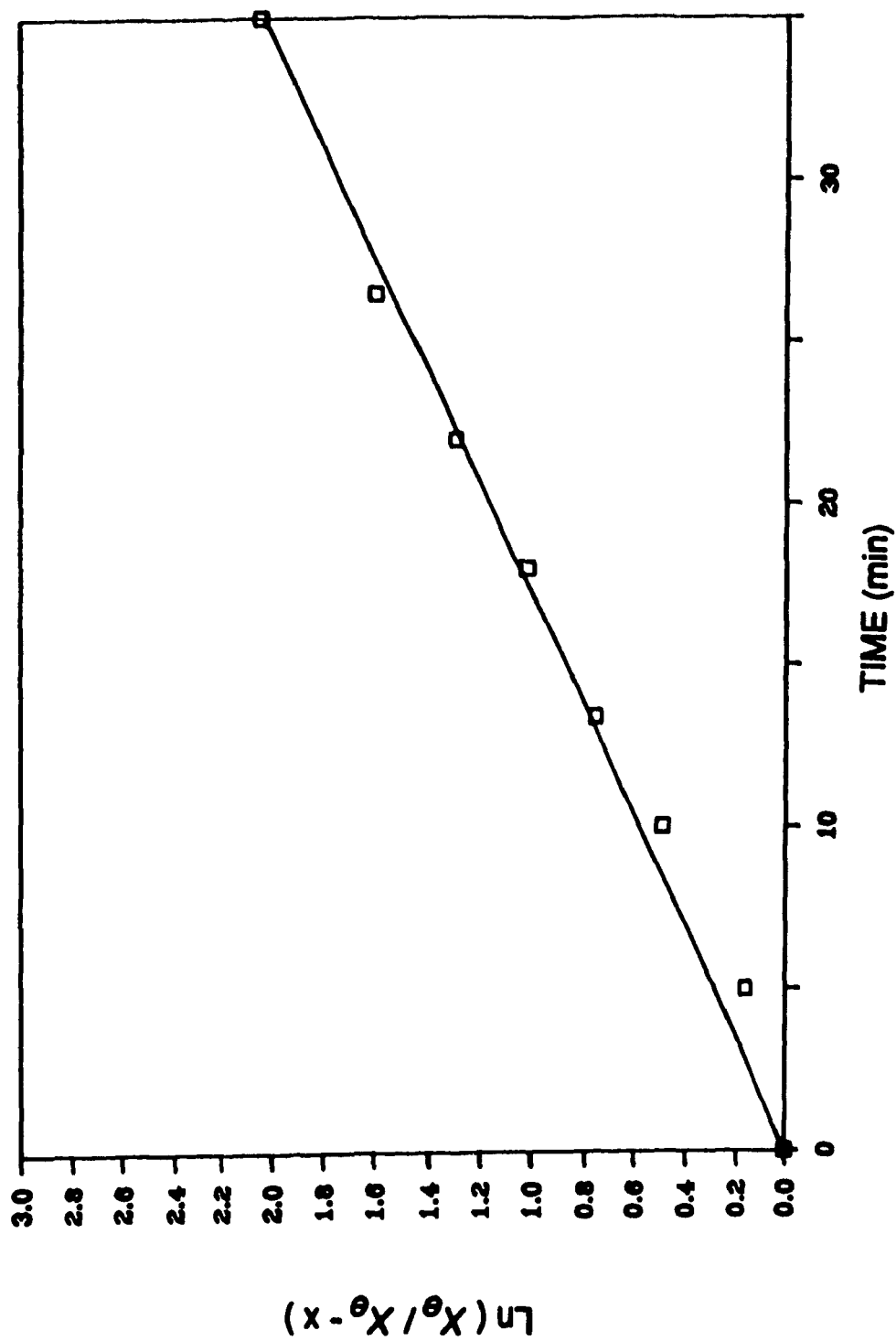


Figure 5.1 Plot of  $\ln(X_0/X - X)$  vs time for an EQB (0.10M) containing PMMA-4VP 11 mole % (MW=10<sup>5</sup>) with PS-SSA 10 mole % (MW=10<sup>5</sup>), at 80°C.

The specific effects of the temperature can be obtained from a comparison between the values of the apparent rate constants  $K_1$  and  $K_{-1}$  reported in tables 5.1 and 5.4. For the low molecular weight mixtures, one can see that the values of  $K_1$  increase up to 85°C and then decrease for higher temperatures. By contrast, for high molecular weight mixtures these values increase monotonously with temperature. This implies that the disruptive effects induced by temperature will not inhibit the shielding process for blends containing PS-SSA chains of high molecular weights. However, for low molecular weight mixtures a threshold in temperature exists at which the shielding process will be hampered. From tables 5.1 and 5.4, one can see that the temperature does not have a major effect on  $K_{-1}$ . However, it should be pointed out that the values of  $K_{-1}$  are always higher for the low molecular weights mixtures. This indicates that the equilibrium concentration of shielded methoxy groups (ladder-like complex) is higher for the high molecular weights mixtures.

For mixtures containing high molecular weight PS-SSA chains, it can be concluded that an increase in temperature will favor the global coil overlap process, but not necessarily the formation of the ladder-like complex. For the low molecular weight mixtures it is clear that at high temperatures the global process is inhibited. Thus, to obtain the largest quantity of shielded methoxy groups for a given mixture, two conditions must be met. First, the molecular weight of the PS-SSA chain must be high enough to counteract the disruptive effects of the temperature. Second, the temperature must be high enough to favor the spatial reorganization of the two dissimilar chains without inhibiting the process, i.e. 85°C.

To understand the effects of the SSA content on the coil overlap process, one must compare the values of the apparent rate constants  $K_1$  and  $K_{-1}$  reported in tables 5.2 and 5.5. The values obtained for the apparent rate constants  $K_1$  for the mixtures

containing the low and the high molecular weight PS-SSA chains show that in both systems an increase in SSA content accelerates the shielding process. For an equivalent ratio (%4VP / %SSA in this tables), the subtraction of the  $K_1$  values of table 5.2 from those of table 5.5 give a constant value ( $\approx 0.4$ ). This implies that an increase in the SSA content will produce the same effect on  $K_1$ , independent of the molecular weight. However, for systems containing the high MW PS-SSA chains, the shielding process will be favored compared to those containing the low MW chains. By contrast, the behaviour of the rate constants  $K_{-1}$  differs drastically for the two systems. For the low molecular weight system, the values of  $K_1$  increase with increasing SSA contents, while for the mixtures containing the high MW chains, the  $K_{-1}$  values decrease.

Thus, it can be concluded that by increasing the SSA content, one will always increase the rate of the global process. However, the optimal quantity of shielded methoxy groups will be produced for a system containing two dissimilar chains of comparable and high molecular weights. This molecular weight effect is probably due to the existence of a match between the contour lengths of the two high molecular weight dissimilar chains. Moreover, these high MW chains must bear a relatively large quantity of SSA and 4VP on their backbone ( $\geq 10$  mole%) in order to produce the highest quantity of shielded methoxy groups. A low concentration of functional groups leads presumably to a greater mean distance between the two dissimilar chains, which implicates that a lower quantity of shielded methoxy groups is achieved at steady-state.

Comparisons of the values of  $K_1$  from tables 5.3 and 5.6 enables one to understand the effects of the total polymer concentration on the shielding process, while a comparison between the  $K_{-1}$  values from these tables enables one to explain the effects of total concentration on the deshielding process. These two independent comparisons can then be related to the global process. This discussion will



exclude the mixtures in which precipitation occurs, i.e. those for which the total polymer concentration is 0.30 M for the blend containing the high molecular PS-SSA ( $10^5$ ). However, it is clear that if the total polymer concentration is too high, the interpenetration of coils will inhibit the formation of the ladder-like complex. Moreover, this will lead to a diminution of the equilibrium concentration of shielded methoxy groups.

The  $K_1$  values for both systems exhibit the same trend, i.e. increasing with increasing polymer concentrations. Subtraction of the  $K_1$  values reported in table 5.3 from those of table 5.6, for the systems containing total polymer concentrations of 0.10 M and 0.20 M gives 0.31 and 0.32, respectively. Since, the values from these subtractions are almost equal, one can say that an increase in concentration has the same effect on both systems. However, for equivalent concentrations, systems containing two dissimilar chains of  $MW=10^5$  show higher values for the apparent rate of shielding. Thus, if the molecular weight of the PS-SSA chain is increased, the rate of shielding process will also increase, in parallel with the effect of increasing SSA content.

By contrast, increasing the total polymer concentration will produce opposite effects on the apparent deshielding constants for the two systems. From table 5.3 (low MW PS-SSA chains), one can see that the values for  $K_{-1}$  increase with increasing concentrations. This behaviour was rationalized in section 5.2.3 by invoking the formation of microgels due to the serious interpenetration occurring for the polymer coils with increasing polymer concentrations. On the other hand, for the mixtures containing the PS-SSA of  $MW=10^5$ , an increase in concentration will not produce a major effect on the  $K_{-1}$  values. This indicates that an increase in concentration will only have a major effect on the deshielding process for the mixtures containing low MW PS-SSA chains.

Thus, one can conclude that in both systems an increase in total polymer

concentration will lead to an increase in the rate of the global process. However, this increase does not imply that more shielded methoxy groups will be present at steady-state. On the contrary, for systems containing PS-SSA chains of  $MW=10^4$ , the equilibrium concentration of shielded methoxy groups decreases with increasing concentration, while for the mixtures containing PS-SSA chains of  $MW=10^5$ , an increase in concentration leads to the precipitation of the product. This implies that in order to obtain an optimal concentration of shielded methoxy groups, the solution must be in the semi-dilute regime, i.e. without coil interpenetration at  $t=0$ . Moreover, if the mixture is in semi-dilute region, the optimal shielding will be achieved with high molecular weights PS-SSA chains.

From this discussion, one can summarize the effects of the individual parameters on the coil overlap process as follows. First, the high molecular weight PS-SSA chains ( $MW=10^5$ ) will give the highest rate for the shielding process, and, by extension, also for the global process. High molecular weight chains will also lead to optimal production of species in which the methoxy groups are shielded, which is presumably due to the fact that the contour lengths of the two dissimilar chains are equivalent. Second, an increase in temperature, or in SSA content, or in total polymer concentration will always increase the rate of the global process. Third, at high temperatures ( $\geq 85^\circ\text{C}$ ), the disruptive effects of temperature will inhibit, to a certain extent, the formation of shielded methoxy groups. The extent of this disruption is molecular weight dependent, i.e. it will be a major disruption only in the case of a low molecular weight PS-SSA chains. Finally, increasing the SSA content or the total polymer concentration will produce a maximum concentration of shielded methoxy groups only for high MW systems.

## Chapter 6     CONTRIBUTION TO ORIGINAL KNOWLEDGE AND SUGGESTION FOR FUTURE WORK

### 6.1     Contribution to Original Knowledge

A brief resume of the major results presented in the preceding chapters is given here. For the sake of convenience, the presentation is divided into three parts. The first part is a summary of the qualitative results. The second part summarizes of the quantitative results obtained for the mixtures containing PS-SSA chains of low and high molecular weights. In the last section, suggestions for future work will be proposed.

To my knowledge, this study constitutes the first report on the kinetics of coil overlap in ionomer blends. Apart from the work of Natansohn and Eisenberg, this appears to be the only report that quantifies the effects of various parameters on the interpenetration of two dissimilar but interacting coils in solution, i.e. mixtures containing copolymers of PMMA-4VP with PS-SSA in DMSO<sub>d6</sub>.

In the early stages of this work, it was shown that the water content of the DMSO<sub>d6</sub> solutions did not have a significant effect on the shielding process. Moreover, experiments were performed in order to determine the effects of electrolytes on the coil overlap process. It was observed that trace quantities of electrolytes did not affect the shielding process. By contrast, it was found that electrolyte concentrations of the order of the polymer ion content in the solution could completely disrupt the process. It was also observed that the coil overlap process was fully reversible for equilibrated blends. Moreover, for these equilibrated blends, it was observed that major disruptions could be induced at temperatures higher than 100°C. The extent of the disruption could even lead to the complete disappearance of the shielded methoxy signal (1 hour at 150°C). From the quantitative kinetics studies of similar systems, i.e. equimolar blends (0.10M)

containing PMMA-4VP 11 mole % ( $MW=10^5$ ) with PS-SSA 10 mole % ( $MW=10^5$ ), it was found that the disruptive effects of temperature were strong enough to pull apart the two dissimilar chains to distances greater than 5 Å, but not enough to lead to the complete destruction of the complex. The experimental ranges over which the kinetics of the shielding process could be performed, were determined. It was found, for the experimental parameters, that the observation of this phenomenon was only possible on a small window.

The quantitative studies were performed using two molecular weights of PS-SSA with a PMMA-4VP copolymer, in which three experimental parameters were varied, i.e. the total polymer concentration, the temperature and the total polymer concentration. For the mixtures, the 4VP content of the PMMA-4VP was kept constant, at 11 mole %, and so was the molecular weight at  $10^5$ . The first type of mixture contains low MW PS-SSA chains ( $MW=10^4$ ), while the second system contains relatively high molecular weight PS-SSA chains ( $MW=10^5$ ).

Application of the derivation method to these two systems lead to the determination of the true order ( $n_c$ ) of the process. The true order of the reaction was found to be equal to 2.4 for the low MW PS-SSA chains, and 2.9 for the high MW mixture. From the comparison of  $n_c$  with  $n_p$  it was confirmed that more than one simple forward reaction is required to describe the mixing process. From the value of the correlation coefficient, and the quality of the fit criterion, a mechanism in which two first-order reactions are opposing one another (equation 4.5) was favored over one containing a second-order forward reaction and first-order back reaction (equation 4.11).

The physical significance of the apparent rate constants  $K_1$  and  $K_{-1}$ , contained in equation 4.5, was obtained by suggesting a mechanism containing three steps. The first step occurs when one proton from the SSA is transferred to a 4VP. The second step can

be envisaged as a cascade reaction occurring within the initial complex, in which the majority of the remaining SSA protons are transferred from the PS chain to the 4VP units of the PMMA-4VP chain. The last step of the mechanism consists of a spatial reorganization of the complex formed during the second step, and this spatial reorganization most probably leads to the formation of a ladder like complex (X).

From the proposed mechanism, an equation which relates the individual rate constants of the process to the apparent rate constants  $K_1$  and  $K_{-1}$  was derived. It was found that  $K_1$  and  $K_{-1}$  could be expressed as  $[k_2 k_3 / (k_2 + k_3)]$  and  $[k_{-3} - (k_{-3} / (k_2 + k_3))]$ , respectively.

This mechanism is operative, since the effects of the experimental parameters on the shielding process can be rationalized by comparing the apparent rate constant. Moreover, from the comparison of each parameter between the two PS-SSA systems, it was possible to obtain a better comprehension of the effects of the PS-SSA chain length on the coil overlap process. It was found that the highest rate for both the shielding and the global processes could be observed in systems containing the high MW PS-SSA chains. Moreover, the equilibrium concentration of shielded methoxy groups is always higher in these systems. Thus, the molecular weight of the PS-SSA chains is a very important parameter.

It was found that the temperatures higher or equal to 85°C lead to the disruptions of the shielding process. However, major disruptions were only observed for mixtures containing PS-SSA chains of MW=10<sup>4</sup>. With increasing SSA contents, it was found that the values for the shielding process and the global process always increase. For the systems containing PS-SSA chains of MW=10<sup>4</sup>, the extent of the shielding effect will increase up to the point where the number of SSA is equal to the number of 4VP groups. However, when an excess of SSA to 4VP groups is present, the equilibrium

concentration of shielded methoxy groups is reduced. By contrast, for systems containing the high molecular weight PS-SSA chains, the equilibrium concentration of shielded methoxy groups increases exponentially with increasing SSA content.

Finally, it was observed that an increase in total polymer concentration leads two majors effects. First, it increases the rate of the shielding process and the rate of the global process, but not necessarily the concentrations of shielded methoxy groups present at steady-state. Second, for the low MW systems, it was found that for increasing polymer concentrations, decreasing equilibrium concentrations of shielded methoxy groups were produced. However, for the systems containing the PS-SSA chains of  $MW=10^5$ , in which no precipitation occurred, an increase in concentration does not affect the extent of the shielding effect.

## 6.2 Suggestion for Future Work

In this report a global picture of the coil overlap process was developed for a very specific system. However, the characterization of this phenomenon could lead to a wide variety of studies. This section contains the summary of these studies, which are divided in three parts. The first type of study will be perform to confirm certain hypothesis contained in the current work. The second type of studies involve the current system. However, studying this system with a new experimental method should enable one to obtain new insights on the coil overlap process. Finally, the last type of suggestion will be related to investigation of completely new copolymer pairs.

First, in order to obtain a greater understanding of the effects of the molecular weight of the PS-SSA chains on the process one should performed some complementary studies. In this report, it was clearly established that the quantity of shielded methoxy

groups present at equilibrium was increasing with the MW of the PS-SSA chains. This effect was rationalized by invoking the increase in the match between the contour length of the two interacting chains. In order to confirm this hypothesis, it would be interesting to study mixtures in which the molecular weight of the PS-SSA chains will be higher than the molecular weight of the PMMA, i.e. a MW =  $5 \times 10^5$  and  $1 \times 10^5$  for the PS-SSA chains and the PMMA chains, respectively. Compared to the mixtures in which the MW of both chains are equal ( $1 \times 10^5$ ), one should observe a diminution of the concentration of shielded methoxy groups present at steady state. On the other hand, the equilibrium concentration of shielded methoxy should be similar to those observed for mixtures containing the low MW PS-SSA chains.

In order to characterize the ladder-like complex, it may prove interesting to perform static light scattering studies on these mixtures. From these studies one should be able to obtain the shape and the MW of the complex present at steady state.

Second, studies of the coil overlap process using other instrumental technics should leads to interesting results. Compared to the NMR study that probes the process to the molecular level, technics like dynamic light scattering and viscosity, should give information on the coil as a whole. From the dynamic light scattering one should observed an increase in the intensity of the scattered light with time, since the formation of the ladder-like complex will lead to an increase in the average volume occupied by one scattering center. Thus, using this technic, qualitative and quantitative studies of the coil overlap process are feasible.

Viscometry is the second experimental technic that can be used to investigate the process. From the proposed model, one can expect that the volume occupied by the molecules to decrease in time, since the coil overlap process leads to a diminution of the number of species in solution. If this increase in volume is significant, it should be

possible to perform dynamic viscosity measurements (viscosity vs time) of these mixtures. From these studies one could confirm some of the results contained in this report, i.e. time required to achieve steady state, influence of the temperature...

Third, using the same experimental procedure, it should be interesting to investigate new systems in which the shielding effect can be observed, i.e. systems containing copolymer pairs like PS-SSA with poly(ethyl methacrylate-co-VP) or PS-SSA with poly(isobutyl methacrylate-co-VP). Moreover, using a more powerful NMR instruments (400-600 MHz) one should be able to study polymer pairs in which the shielding effect is very weak, i.e. systems containing copolymer pairs like poly(ethylene oxides) with PS-SSA, any functionalized polyurethane with PS-SSA... Moreover, these systems could also be investigated using the experimental technics previously described.



## REFERENCES

1. T. Sulzberg, R. J. Cotter, *J. Polym. Sci. Part A-1*, **8**, 2747 (1970)
2. S. Krause, *J. Macromol. Sci.-Rev.*, **C7**, 251 (1972).
3. D. Klempner and K. C. Frisch, *Polymer Alloys: Blends, Blocks, Grafts and Interpenetrating Networks*, Polymer Science and Technology, **10**, Plenum Press, New York (1977)
4. D. R. Paul and S. Newman, *Polymer Blends*, **1** and **2**, Academic Press, New York (1978).
5. H. Morawetz, F. Amrani, *Macromolecules*, **11**(1), 281-2 (1978).
6. O. Olabisi, L. M. Robenson and M. T. Shaw, *Polymer-Polymer Miscibility*, Academic Press, New York (1979).
7. J. S. Higgins, D. J. Walsh, *Polym. Eng. Sci.*, **24**(8), 555-62 (1984).
8. J. A. Schroeder, F. E. Karasz, W. J. MacKnight, *Polymer*, **26**(12), 1795-800 (1985).
9. L. A. Utracki and R. A. Weiss, *ACS symp. series*, **395** (1989).
10. M. Nishimoto, H. Keskkula, D. R. Paul, *Polymer*, **30**(7), 1279-86 (1989).
11. T. S. Ellis, *Macromolecules*, **22**(2), 742-54 (1989).
12. P. Smith and A. Eisenberg, *J. polym. Sci., Polym. Lett. Ed.*, **21**, 223 (1983).
13. P. Smith, *Ph.D. thesis*, McGill University 1985.
14. M. B. Djordjevic and R. S. Porter, *Polym. Eng. Sci.*, **23**, 650 (1983)
15. D. C. Douglass and V. J. McBrierty, *Polym. Eng. Sci.*, **19**, 1054 (1979).
16. C. T. Chen and H. Morawetz, *Macromolecules*, **22**(1), 159-64 (1989).
17. F. Mikes, H. Morawetz, J. Labsky, and K. Dennis, *Sb. Vys. Sk. Chem.-Technol.*, **9**, 93-109 (1983).
18. F. Mikes, H. Morawetz, K. S. Dennis, *Macromolecules*, **17**(1), 60-3 (1984).
19. H. Morawetz, *Polym. Eng. Sci.*, **23**(12), 689-92 (1983).
20. J. Jachowicz, H. Morawetz, *Macromolecules*, **15**(3), 828-31 (1983)

21. M. A. Winnik, O. Pekcan, L. Chen, M. D. Croucher, *Macromolecules*, 21(1), 55-9 (1988).
22. L. S. Egan, M. A. Winnik, M. D. Croucher, *Polym. Eng. Sci.*, 26(1), 15-27 (1986).
23. Y. H. Jeng, C. W. Frank, *Adv. Polym. Blends Alloys Technol.*, 2, 81-99 (1989).
24. K. A. Peterson, M. B. Zimmt, M. D. Fayer, Y. H. Jeng, C. W. Frank, *Macromolecules*, 22(2), 874-9 (1989).
25. W. T. Tang, G. Hadziioannou, B. A. Smith, C. W. Frank, *Polymer*, 29(7), 1313-17 (1988).
26. Y. H. Jeng, M. L. Shi, W. C. Tao, C. W. Frank, *Polym. Prepr. (Am. Chem. Soc., Div. Polym. Chem.)*, 27(2), 212-13 (1986).
27. J. W. Thomas Jr, C. W. Frank, D. A. Holden, J. E. Guillet, *J. Polym. Sci., Polym. Phys. Ed.*, 20(9), 1749-53 (1982).
28. C. W. Frank, M. A. Gashgari, *Polym. Prepr., Am. Chem. Soc., Div. Polym. Chem.*, 21(2), 42-3 (1980).
29. C. W. Frank, M. A. Gashgari, *Ann. N. Y. Acad. Sci.*, 366 (Lumin. Biol. Synth. Macromol.), 387-403 (1981).
30. A. Natansohn and A. Eisenberg, *Macromolecules*, 20(2), 323 (1987).
31. J.K.M. Sanders and J.D. Merish, *Progr. NMR Spectrosc.*, 15, 353 (1982).
32. H. Tompa, *Polymer Solutions*, Butterworth, London (1956).
33. P.J. Flory, *Principles of Polymer Chemistry*, Cornell, New York (1962).
34. R.L. Scott, *J. Chem. Phys.*, 17, 279 (1949).
35. S. Krause, Chapter 2 in ref. 1
36. D. Patterson and A. Robard, *Macromolecules*, 11, 690 (1978).
37. T.K. Kwei and T.T. Wang, Chapter 4 in ref. 1
38. J. Kirchhoff, *Schweigger's J.*, 4, 108 (1912).
39. J. Thénard, *Ann. chim. et phys.*, (2) 9, 314 (1818).
40. A. V. Hartcourt and W. Esson, *Proc. Roy. Soc. (London)*, 14, 470 (1865).
41. A. V. Hartcourt and W. Esson, *Phil. Trans.*, 156, 193 (1866); 157, 117 (1867).

42. C. M. Guldberg and P. Waage, "*Études sur les affinités chimiques*," Brogger and Christie, Christinia (Oslo), 1897.
43. S. Arrhenius, *Z. Physik. Chem.*, **4**, 226 (1889).
44. J. H. van't Hoff, "*Études de dynamique chimique*," p. 87, F. Muller and Company, Amsterdam, 1884.
45. M. Letort, *J. Chim. Phys.*, **34**, 206 (1937); *Bull. Soc. Cim. France*, **9**, 1 (1942).
46. H.S. Makowski, R.D. Lundberg, and G.H. Singhal, *U.S. Patent 3,870,841* (1975)
47. Duchesne, D. *Ph.D. Thesis*, McGill University, 1985.
48. N. Z. Erdi and H. Morawetz, *J. Colloid Sci.*, **19**, 708 (1964).
49. A. Eisenberg and H. L. Yeager, *ACS symp. series*, **180** (1982).
50. J. E. Burleigh, O. F. McKinney, M. G. Barker, *Analytical Chem.*, **31**, 10, 1684 (1959).
51. S. Patt, *Magnetic Moments*, **3**, Vol. 1, 12 (1987)
52. D.W. Marquardt, *Chem. Eng. Prog.*, **55**, 65 (1959).
53. D.W. Marquardt, *J. Soc. Indust. Appl. Math.*, (2) **11**, 431 (1963).
54. D.C. Harris and M.D. Bertolucci, *Symmetry and Spectroscopy*, Oxford University Press, New York (1978).
55. G. Baillargeon and J. Rainville, *Introduction a la Statistique Appliquee 3<sup>rd</sup> ed.*, Les Editions SMG, Trois-Rivieres (1976).
56. I. Poole, M. Borchers and S. Cook, *Some Common Basic Programs*, Osborne/ McGraw-Hill, California (1981).
57. A. Natansohn, S. Maxim, D. Feldman, *Eur. Polym. J.*, **14**, 283 (1978).
58. A. Natansohn Ph. D., Private Communication.
59. F. Sauriol Ph. D., Private Communication.
60. F.W. Wehrli and T. Wirthlin, *Interpretation of Carbon-13 NMR Spectra*, Heyden, London (1980).
61. A.A. Frost and R.G. Pearson, *Kinetics and Mechanism*, 2<sup>nd</sup> ed., John-Wiley & Sons, Inc., 14-15 (1961).
62. W. Ostwald, *Z. Chem.*, **2**, 127 (1888).

63. E.A. Guggenheim, *Phil. Mag.*, **1**, 538 (1926).
64. J.M. Sturtevant, *J. Am. Chem. Soc.*, **59**, 699 (1937).
65. S.W. Benson, *The Foundations of Chemical Kinetics*, McGraw-Hill Book Company, Inc., New York (1960).
66. K.J. Laidler, *Chemical Kinetics*, 3<sup>rd</sup> ed., Harper & Row, New York (1987).
67. K.J. Laidler, *Theories of Chemical Reaction Rates*, McGraw-Hill, Inc., New York (1969).
68. A.A. Frost and R.G. Pearson, *Kinetics and Mechanism*, 2<sup>nd</sup> ed., John Wiley & Sons, Inc., New York (1965).
69. R. Stewart, *The Proton: Applications to Organic Chemistry*, Academic Press, Inc., Orlando (1985).
70. G.W. Klumpp, *Reactivity in Organic Chemistry*, A. Wiley-Interscience Publication, New York (1982).
71. C. Tanford, *Physical Chemistry of Macromolecules*, John Wiley & Sons, Inc., New York (1961).

## Appendix 1

### Deconvolution Process

This appendix will give an example of the deconvolution process for a NMR spectrum. The example under consideration involves an equimolar mixture (0.10 M) of PMMA-4VP 11 mole% (MW= $10^5$ ) with PS-SSA 10 mole% (MW= $10^4$ ) in DMSO<sub>d6</sub> at 85°C. The contact time for this solution is equal to 15.9 min. The supporting data for these plots will be given in appendix 2.

#### A) The $^1\text{H}$ NMR Spectrum

Three bands can be observed in this  $^1\text{H}$  NMR spectrum (figure 1A). The bands are centered at 3.57 ppm, 3.52 ppm and 3.11 ppm, corresponding to the unshielded methoxy groups, the shielded methoxy groups and the signal due to residual water, respectively.

#### B) Resulting $^1\text{H}$ NMR Spectrum Obtained From the Program NMRMOD

Figure 1B corresponds to the plot of the modified intensity values for the spectrum shown in appendix 1 A. Three major modifications to transferred NMR spectrum files are introduced by the program NMRMOD. First, it formats the transferred file. Second, it smooth and rescale the intensity values. Third, it creates an alternate chemical shift axis. The details, regarding this program are given in appendix 3. The bands centered at ~360, ~420 and ~888 correspond to the unshielded methoxy groups, the shielded methoxy groups and the signal due to residual water, respectively.

**C) Plot of the range on which the deconvolution will be performed**

The next step of the process involves the selection of the portion to be analyzed. This is shown in figure 1C and corresponds to the spectral region (3.0 to ~3.7 ppm), for the NMR spectrum of appendix 1A, on which the program FIT was used to deconvolute the three bands.

**D) Plot of the Deconvoluted Spectrum**

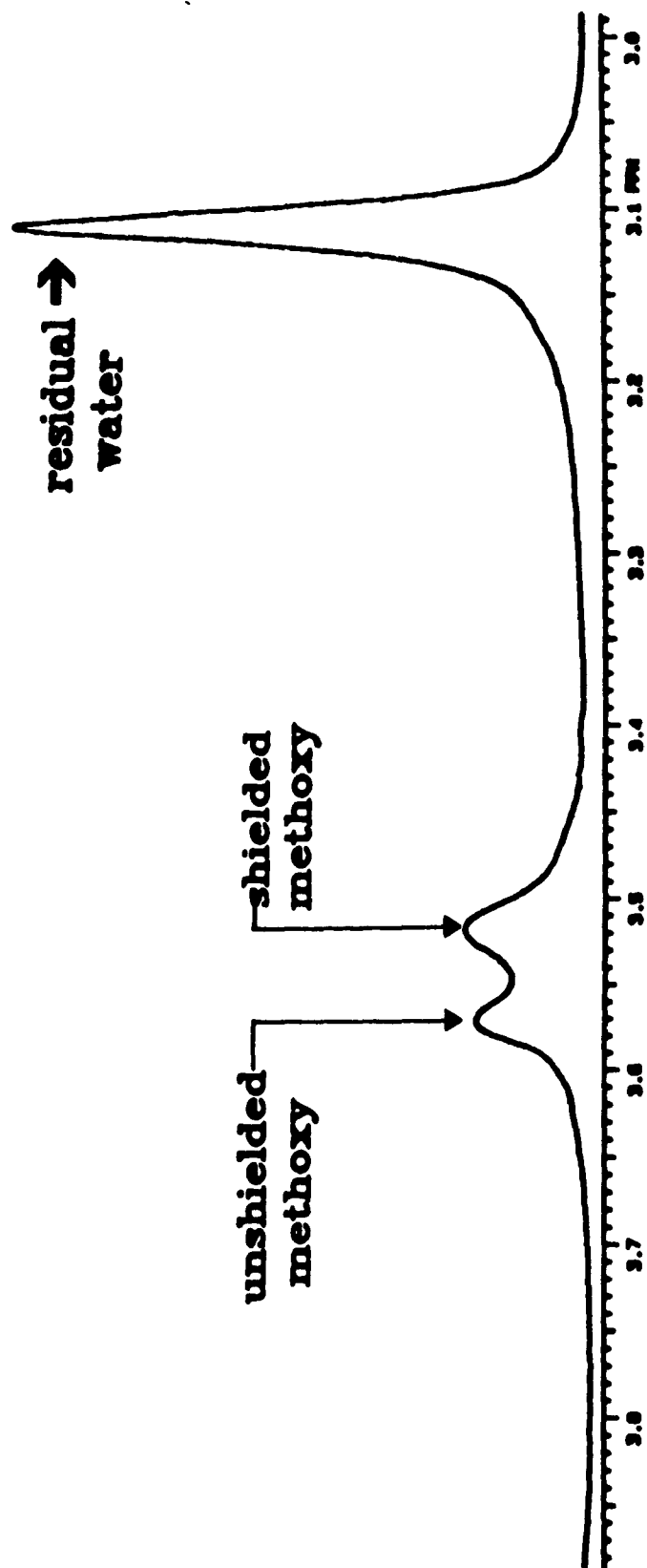
This plot corresponds to the final stage of the deconvolution process. The deconvoluted spectrum was obtained after 5 iterations. The  $\chi^2$  value based on 849 degrees of freedom (861 points - 12 parameters) is equal to 4199.5. The correlation coefficient is equal to 0.998. The value of this coefficient being very close to 1 indicates that the correlation is very high between the experimental and the deconvoluted spectrum.

**E) Plot of the Three Individual Bands**

This plot represents the specific contribution of the three deconvoluted bands to the deconvoluted lineshape illustrated in appendix 1D. The quantitative results obtained from the deconvolution are the position, the area and the width at half height for each bands. These values are summarized table 1A.

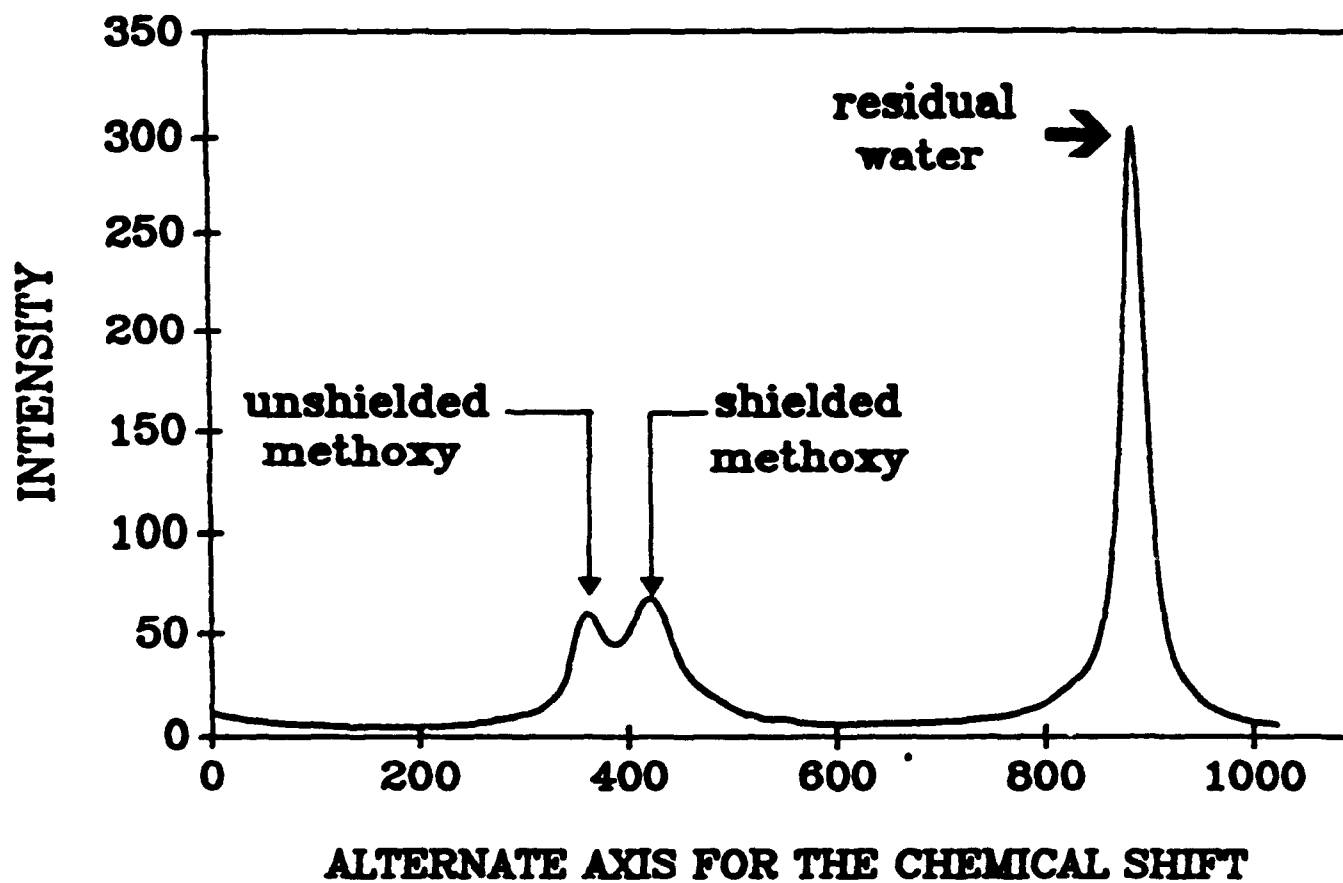
**Table 1A Summary of the quantitative results for the deconvoluted bands.**

PEAK LABEL	POSITION	AREA	WIDTH AT HALF HEIGHT
UNSHIELDED METHOXY	360.00	3133.75	17.59
SHIELDED METHOXY	420.00	6412.59	29.24
RESIDUAL WATER	886.69	12138.43	13.83

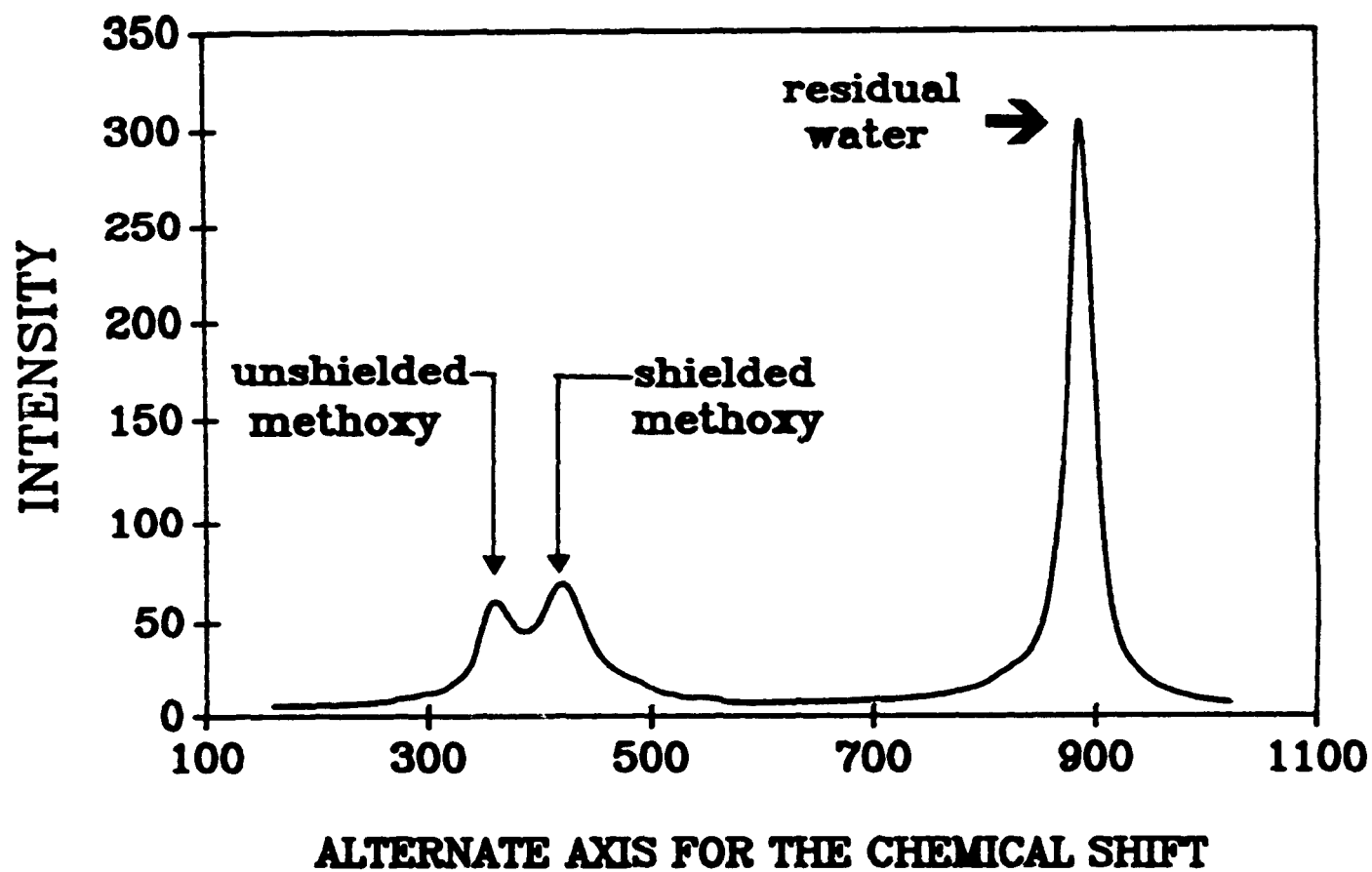


A)  $^1\text{H}$  NMR Spectrum

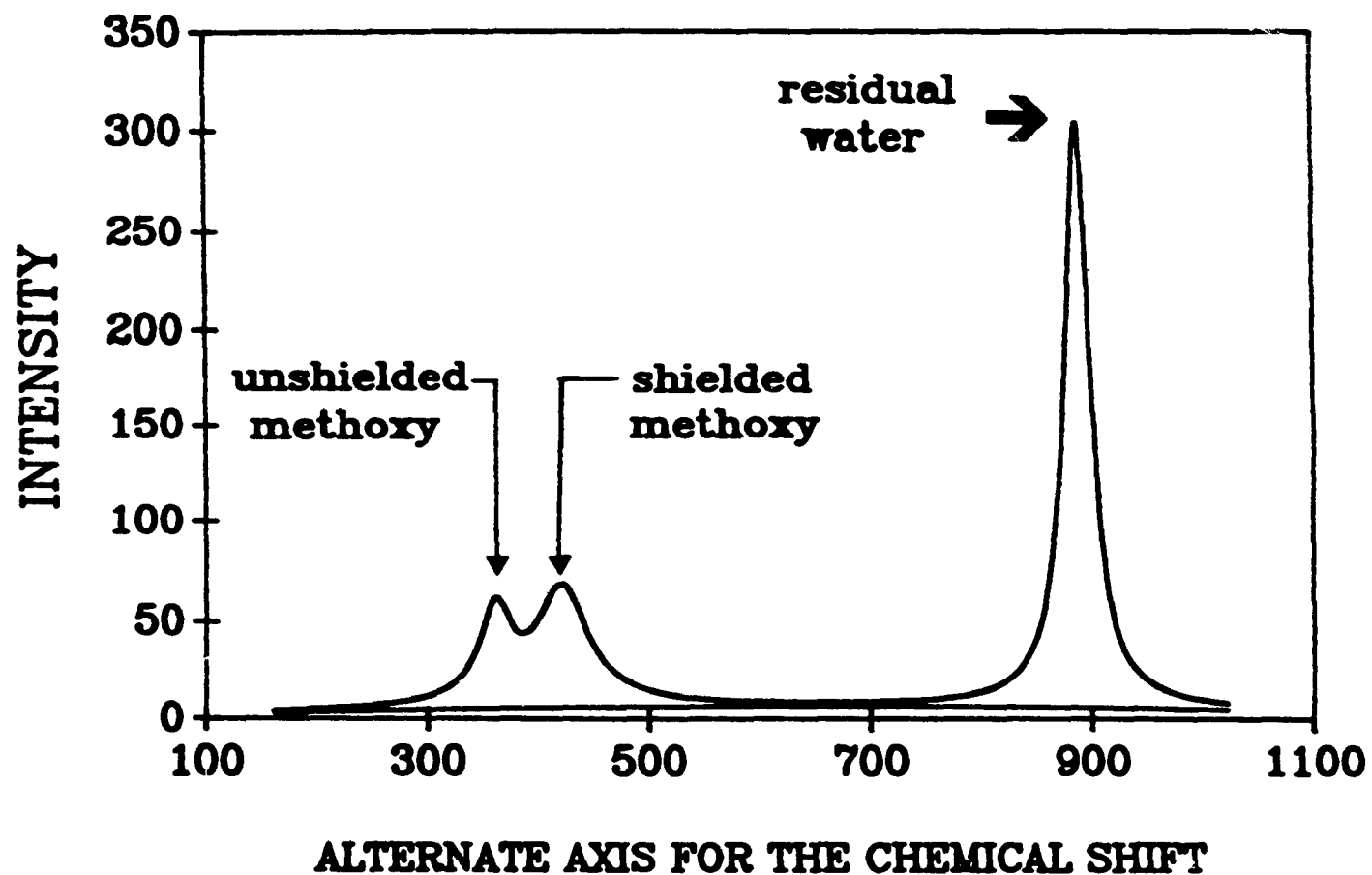




B) Resulting  $^1\text{H}$  NMR Spectrum Obtained From the Program NMRMOD

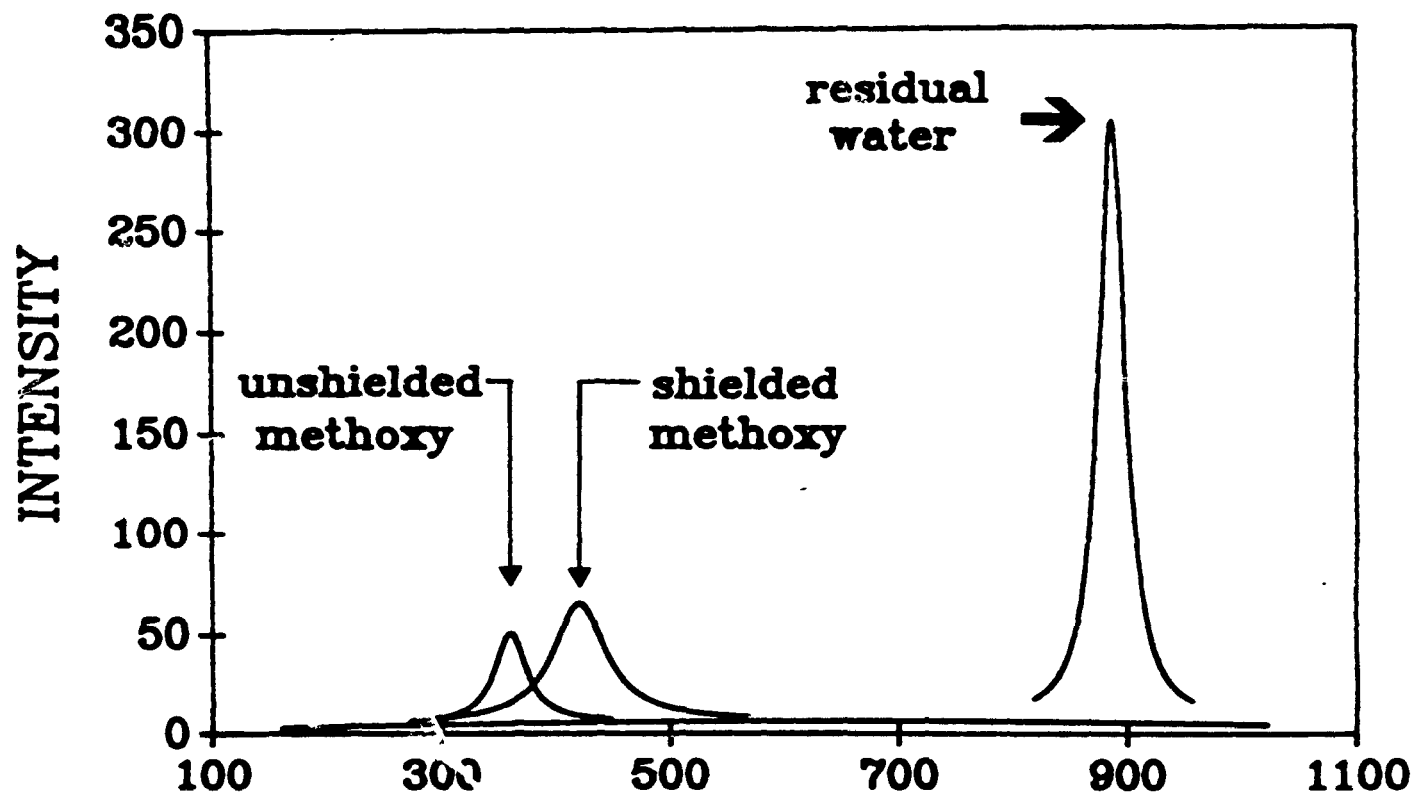


C) Plot of the range on which the deconvolution will be performed



D) Plot of the Deconvoluted Spectrum

## DECONVOLUTED BANDS AND BASELINE



ALTERNATE AXIS FOR THE CHEMICAL SHIFT

E) Plot of the Three Individual Bands

## Appendix 2

Appendix 2 contains the supporting data for the figures shown in the appendix 1, i.e. for the equimolar mixture (0.10 M) of PMMA-4VP 11 mole% (MW=10<sup>5</sup>) with PS-SSA 10 mole% (MW=10<sup>4</sup>) in DMSO<sub>d6</sub>, at 85°C. The contact time is equal to 15.9 minutes.

### A) Example of the Transferred NMR File.

These data correspond to the transferred NMR file for the spectrum shown in appendix 1 A. The four lines at the beginning, i.e. CATFCB + 5 numbers and PHASFL + 7 numbers, indicate how the spectrum intensity values are stored on the hard drive of the NMR work station. The intensity values for the transferred files are always in two columns. For the sake of clarity, these values are reported with an index, which is directly related to the number of transferred points. These data points are reported in three columns.

CATFCB  
8 10 72 1 1792

PHASFL SECTOR 6 10  
2 10 0 3 512

INDEX	INTENSITY	INDEX	INTENSITY	INDEX	INTENSITY
1	1.593493E 06	13	-3.032940E 05	25	-6.428689E 05
2	1.744744E 06	14	5.471950E 05	26	-1.182328E 06
3	1.147794E 06	15	-2.717200E 05	27	-1.048611E 06
4	8.450849E 05	16	3.007300E 04	28	-8.779400E 05
5	1.225881E 06	17	-3.421350E 05	29	-1.188547E 06
6	1.107776E 06	18	1.327300E 04	30	-1.689932E 06
7	8.406800E 05	19	-5.153430E 05	31	-1.433666E 06
8	9.292119E 05	20	-1.548060E 05	32	-1.354774E 06
9	1.977970E 05	21	1.352490E 05	33	-1.778008E 06
10	1.433710E 05	22	-1.068348E 06	34	-1.817226E 06
11	7.412940E 05	23	-3.457340E 05	35	-2.111353E 06
12	4.417080E 05	24	-8.002189E 05	36	-1.780370E 06

INDEX	INTENSITY
37	-1.773875E 06
38	-1.753990E 06
39	-2.453460E 06
40	-2.058860E 06
41	-1.965845E 06
42	-1.894961E 06
43	-2.124985E 06
44	-2.528966E 06
45	-2.558317E 06
46	-2.323599E 06
47	-2.554828E 06
48	-2.094312E 06
49	-2.556862E 06
50	-3.062421E 06
51	-2.680414E 06
52	-2.594885E 06
53	-2.908954E 06
54	-3.274930E 06
55	-2.963016E 06
56	-2.649243E 06
57	-2.845542E 06
58	-3.036674E 06
59	-3.353132E 06
60	-2.859826E 06
61	-2.481942E 06
62	-3.385609E 06
63	-3.251828E 06
64	-3.193121E 06
65	-3.649051E 06
66	-3.344005E 06
67	-3.448801E 06
68	-3.381536E 06
69	-3.472836E 06
70	-3.700916E 06
71	-3.521901E 06
72	-3.529954E 06
73	-3.980874E 06
74	-4.031401E 06
75	-3.379051E 06
76	-3.710818E 06
77	-3.502234E 06
78	-3.683263E 06
79	-3.602356E 06
80	-3.405990E 06
81	-3.848045E 06
82	-3.839108E 06
83	-4.120822E 06
84	-3.747963E 06
85	-4.154325E 06
86	-4.256790E 06

INDEX	INTENSITY
87	-3.881750E 06
88	-3.739470E 06
89	-3.234778E 06
90	-3.809262E 06
91	-4.183726E 06
92	-4.320710E 06
93	-3.963277E 06
94	-3.848443E 06
95	-4.073345E 06
96	-4.043034E 06
97	-3.767601E 06
98	-4.186433E 06
99	-4.579635E 06
100	-4.310004E 06
101	-4.520681E 06
102	-4.101437E 06
103	-4.063047E 06
104	-4.672721E 06
105	-4.036283E 06
106	-3.966511E 06
107	-4.313579E 06
108	-4.617248E 06
109	-4.459062E 06
110	-4.373131E 06
111	-4.835947E 06
112	-4.575925E 06
113	-4.739975E 06
114	-4.978780E 06
115	-4.574089E 06
116	-4.732652E 06
117	-5.065693E 06
118	-4.717228E 06
119	-4.769837E 06
120	-4.981494E 06
121	-4.500993E 06
122	-4.960470E 06
123	-4.544831E 06
124	-4.221273E 06
125	-4.522893E 06
126	-4.892525E 06
127	-5.008969E 06
128	-4.807330E 06
129	-4.640331E 06
130	-5.064605E 06
131	-5.197710E 06
132	-5.522430E 06
133	-5.115481E 06
134	-4.856325E 06
135	-5.109581E 06
136	-5.139182E 06

INDEX	INTENSITY
137	-5.640967E 06
138	-4.844641E 06
139	-4.462897E 06
140	-5.053628E 06
141	-4.364701E 06
142	-4.728442E 06
143	-4.436753E 06
144	-4.892265E 06
145	-4.784160E 06
146	-5.179697E 06
147	-5.080574E 06
148	-5.021255E 06
149	-4.824505E 06
150	-5.140021E 06
151	-4.873468E 06
152	-4.784097E 06
153	-5.055588E 06
154	-4.833153E 06
155	-4.602221E 06
156	-4.825065E 06
157	-4.927387E 06
158	-4.418680E 06
159	-4.512790E 06
160	-5.041196E 06
161	-4.907790E 06
162	-5.226093E 06
163	-5.328455E 06
164	-4.862495E 06
165	-5.346771E 06
166	-5.301023E 06
167	-4.938175E 06
168	-4.900518E 06
169	-5.294136E 06
170	-4.894581E 06
171	-5.031767E 06
172	-4.690386E 06
173	-5.315509E 06
174	-4.808466E 06
175	-5.533160E 06
176	-5.061508E 06
177	-5.031340E 06
178	-4.360963E 06
179	-4.963570E 06
180	-5.395955E 06
181	-5.073095E 06
182	-5.180723E 06
183	-5.274258E 06
184	-5.073842E 06
185	-4.904816E 06
186	-4.525407E 06

INDEX	INTENSITY
187	-5.176163E 06
188	-4.693251E 06
189	-5.043421E 06
190	-4.551687E 06
191	-4.911070E 06
192	-4.997040E 06
193	-5.149593E 06
194	-4.469878E 06
195	-5.192311E 06
196	-5.284894E 06
197	-5.157493E 06
198	-5.036430E 06
199	-5.228035E 06
200	-4.745777E 06
201	-4.882783E 06
202	-5.161914E 06
203	-4.811674E 06
204	-4.731421E 06
205	-4.522743E 06
206	-4.886113E 06
207	-5.237597E 06
208	-5.311906E 06
209	-4.926954E 06
210	-4.314926E 06
211	-4.619997E 06
212	-4.789137E 06
213	-4.584693E 06
214	-4.680578E 06
215	-4.925765E 06
216	-4.479620E 06
217	-4.904996E 06
218	-4.738540E 06
219	-4.795431E 06
220	-4.243533E 06
221	-4.078265E 06
222	-4.259958E 06
223	-4.553427E 06
224	-4.512152E 06
225	-4.161750E 06
226	-4.364414E 06
227	-4.563620E 06
228	-4.390221E 06
229	-4.224784E 06
230	-4.300723E 06
231	-4.142920E 06
232	-3.693199E 06
233	-4.093139E 06
234	-3.833805E 06
235	-4.041498E 06
236	-4.101846E 06

INDEX	INTENSITY
237	-3.914547E 06
238	-3.439633E 06
239	-3.959036E 06
240	-3.516035E 06
241	-3.935081E 06
242	-3.762960E 06
243	-3.567845E 06
244	-3.723974E 06
245	-3.821479E 06
246	-3.586593E 06
247	-3.495951E 06
248	-3.409728E 06
249	-3.426936E 06
250	-3.178741E 06
251	-3.535574E 06
252	-3.317253E 06
253	-3.903317E 06
254	-3.011772E 06
255	-2.937155E 06
256	-2.929015E 06
257	-2.715170E 06
258	-3.051009E 06
259	-3.386530E 06
260	-2.959943E 06
261	-2.562876E 06
262	-2.836330E 06
263	-2.788164E 06
264	-2.985777E 06
265	-2.497919E 06
266	-2.336545E 06
267	-2.322218E 06
268	-2.529042E 06
269	-2.384620E 06
270	-1.850454E 06
271	-1.830729E 06
272	-1.281905E 06
273	-1.062991E 06
274	-1.693212E 06
275	-1.087577E 06
276	-1.926415E 06
277	-1.221614E 06
278	-1.521631E 06
279	-1.207367E 06
280	-1.040799E 06
281	-1.196168E 06
282	-3.761040E 05
283	-6.221320E 05
284	-8.857219E 05
285	-3.214980E 05
286	-2.078850E 05

INDEX	INTENSITY
287	-1.163536E 06
288	6.587170E 05
289	-1.790400E 05
290	2.603880E 05
291	2.081190E 05
292	5.086130E 05
293	4.008420E 05
294	9.171750E 05
295	1.131907E 06
296	9.860059E 05
297	1.263645E 06
298	1.396494E 06
299	1.646607E 06
300	1.713725E 06
301	1.849343E 06
302	9.680309E 05
303	1.241813E 06
304	1.453006E 06
305	2.199075E 06
306	1.541795E 06
307	2.014392E 06
308	1.624541E 06
309	2.163040E 06
310	2.515347E 06
311	2.892565E 06
312	2.750588E 06
313	2.940182E 06
314	3.262212E 06
315	3.362359E 06
316	3.471448E 06
317	4.063661E 06
318	4.819227E 06
319	5.070064E 06
320	5.428571E 06
321	5.293873E 06
322	6.531867E 06
323	6.737684E 06
324	7.395505E 06
325	8.089606E 06
326	7.717168E 06
327	8.411449E 06
328	9.378627E 06
329	9.944659E 06
330	1.031484E 07
331	1.049711E 07
332	1.142169E 07
333	1.161785E 07
334	1.255478E 07
335	1.336077E 07
336	1.452378E 07

INDEX	INTENSITY	INDEX	INTENSITY	INDEX	INTENSITY
337	1.546849E 07	387	3.499857E 07	437	4.379120E 07
338	1.630246E 07	388	3.491586E 07	438	4.253089E 07
339	1.721886E 07	389	3.449225E 07	439	4.171708E 07
340	1.844377E 07	390	3.526105E 07	440	3.998640E 07
341	1.993645E 07	391	3.500076E 07	441	3.839736E 07
342	2.182956E 07	392	3.531499E 07	442	3.734219E 07
343	2.394744E 07	393	3.593377E 07	443	3.575537E 07
344	2.586969E 07	394	3.646116E 07	444	3.446659E 07
345	2.823650E 07	395	3.691205E 07	445	3.342564E 07
346	3.009161E 07	396	3.760961E 07	446	3.187899E 07
347	3.253871E 07	397	3.783496E 07	447	3.095783E 07
348	3.438966E 07	398	3.823500E 07	448	2.982417E 07
349	3.700181E 07	399	3.999949E 07	449	2.898666E 07
350	3.886847E 07	400	4.013345E 07	450	2.729430E 07
351	4.128979E 07	401	4.047944E 07	451	2.653713E 07
352	4.241324E 07	402	4.191912E 07	452	2.554469E 07
353	4.507878E 07	403	4.354228E 07	453	2.441875E 07
354	4.574276E 07	404	4.411313E 07	454	2.349178E 07
355	4.739441E 07	405	4.503850E 07	455	2.323581E 07
356	4.805315E 07	406	4.680853E 07	456	2.146597E 07
357	4.885771E 07	407	4.766551E 07	457	2.113635E 07
358	4.973646E 07	408	4.908674E 07	458	2.056411E 07
359	4.986414E 07	409	5.087042E 07	459	1.962505E 07
360	5.015700E 07	410	5.193369E 07	460	1.923036E 07
361	4.978306E 07	411	5.278076E 07	461	1.850780E 07
362	5.033295E 07	412	5.350764E 07	462	1.789963E 07
363	4.946173E 07	413	5.445527E 07	463	1.725426E 07
364	4.930803E 07	414	5.531793E 07	464	1.641406E 07
365	4.899194E 07	415	5.673304E 07	465	1.590642E 07
366	4.874333E 07	416	5.692480E 07	466	1.612962E 07
367	4.773967E 07	417	5.761607E 07	467	1.506449E 07
368	4.669455E 07	418	5.798642E 07	468	1.443545E 07
369	4.603001E 07	419	5.774734E 07	469	1.438555E 07
370	4.490745E 07	420	5.868550E 07	470	1.445062E 07
371	4.393842E 07	421	5.829944E 07	471	1.338556E 07
372	4.307142E 07	422	5.811078E 07	472	1.312576E 07
373	4.180565E 07	423	5.820989E 07	473	1.332000E 07
374	4.116244E 07	424	5.776974E 07	474	1.215687E 07
375	4.038154E 07	425	5.763383E 07	475	1.227145E 07
376	3.940178E 07	426	5.697542E 07	476	1.200526E 07
377	3.842794E 07	427	5.634091E 07	477	1.099364E 07
378	3.782341E 07	428	5.520286E 07	478	1.128185E 07
379	3.706943E 07	429	5.434805E 07	479	1.081120E 07
380	3.635272E 07	430	5.335804E 07	480	1.054722E 07
381	3.611610E 07	431	5.188508E 07	481	1.008567E 07
382	3.568771E 07	432	5.085048E 07	482	1.002176E 07
383	3.540682E 07	433	4.942570E 07	483	9.622513E 06
384	3.489916E 07	434	4.829903E 07	484	9.448681E 06
385	3.494989E 07	435	4.675872E 07	485	9.107851E 06
386	3.472601E 07	436	4.567151E 07	486	8.951875E 06



INDEX	INTENSITY	INDEX	INTENSITY	INDEX	INTENSITY
487	8.436217E 06	537	-1.459801E 06	587	-3.824156E 06
488	7.970793E 06	538	-1.584195E 06	588	-3.924931E 06
489	7.503764E 06	539	-1.399036E 06	589	-3.563688E 06
490	7.395735E 06	540	-9.876450E 05	590	-3.518192E 06
491	7.556789E 06	541	-5.988850E 05	591	-3.487431E 06
492	6.904911E 06	542	-9.457620E 05	592	-3.152788E 06
493	6.978714E 06	543	-7.647000E 05	593	-3.906375E 06
494	6.210865E 06	544	-1.080387E 06	594	-3.571797E 06
495	5.690240E 06	545	-9.101590E 05	595	-3.518608E 06
496	5.505385E 06	546	-1.224194E 06	596	-3.333734E 06
497	5.373300E 06	547	-1.228401E 06	597	-3.512352E 06
498	4.757496E 06	548	-7.828850E 05	598	-3.570131E 06
499	4.139108E 06	549	-5.053300E 05	599	-3.587069E 06
500	4.702280E 06	550	-9.539870E 05	600	-3.321514E 06
501	4.366639E 06	551	-1.491018E 06	601	-3.796654E 06
502	3.813589E 06	552	-1.250205E 06	602	-3.087763E 06
503	3.910658E 06	553	-1.209622E 06	603	-3.230945E 06
504	3.307926E 06	554	-1.220927E 06	604	-3.659329E 06
505	2.747876E 06	555	-1.730417E 06	605	-3.623287E 06
506	2.737522E 06	556	-1.425844E 06	606	-3.729894E 06
507	2.494922E 06	557	-1.456906E 06	607	-3.446839E 06
508	1.955001E 06	558	-1.812317E 06	608	-3.703805E 06
509	2.043903E 06	559	-1.905884E 06	609	-3.366439E 06
510	1.940520E 06	560	-2.124135E 06	610	-3.567466E 06
511	1.740795E 06	561	-2.102951E 06	611	-3.639407E 06
512	1.657989E 06	562	-2.678724E 06	612	-3.234864E 06
513	1.020470E 05	563	-2.267626E 06	613	-2.827060E 06
514	1.403108E 06	564	-2.948282E 06	614	-3.421128E 06
515	1.174156E 06	565	-2.744245E 06	615	-3.567140E 06
516	6.043330E 05	566	-3.191989E 06	616	-3.332764E 06
517	7.489891E 05	567	-2.733034E 06	617	-3.295733E 06
518	1.094834E 06	568	-2.912060E 06	618	-3.928382E 06
519	5.733810E 05	569	-3.229830E 06	619	-2.926492E 06
520	9.340809E 05	570	-3.515533E 06	620	-3.563376E 06
521	8.032100E 05	571	-3.139957E 06	621	-3.638320E 06
522	8.607570E 05	572	-3.345491E 06	622	-3.052277E 06
523	1.658280E 05	573	-3.254988E 06	623	-3.520472E 06
524	-1.930670E 05	574	-3.143462E 06	624	-3.137693E 06
525	3.556230E 05	575	-3.348818E 06	625	-3.244387E 06
526	-5.292610E 05	576	-3.581128E 06	626	-2.624514E 06
527	-5.443630E 05	577	-3.387507E 06	627	-4.174563E 06
528	-1.013224E 06	578	-3.302832E 06	628	-3.186881E 06
529	-7.981880E 05	579	-3.042883E 06	629	-3.721242E 06
530	-7.844230E 05	580	-4.080921E 06	630	-3.675779E 06
531	-1.035019E 06	581	-3.124237E 06	631	-2.879473E 06
532	-9.989769E 05	582	-3.768111E 06	632	-3.062542E 06
533	-1.256735E 06	583	-3.868468E 06	633	-3.170173E 06
534	-6.134530E 05	584	-3.620981E 06	634	-3.195250E 06
535	-1.100236E 06	585	-3.048106E 06	635	-3.253962E 06
536	-6.989120E 05	586	-3.962363E 06	636	-2.780289E 06

INDEX	INTENSITY
637	-3.427060E 06
638	-3.518106E 06
639	-3.107017E 06
640	-3.118637E 06
641	-3.228165E 06
642	-2.989054E 06
643	-2.808373E 06
644	-3.393312E 06
645	-2.778499E 06
646	-2.850123E 06
647	-3.344378E 06
648	-3.158608E 06
649	-2.598873E 06
650	-3.286611E 06
651	-2.822616E 06
652	-3.063080E 06
653	-2.724819E 06
654	-3.098531E 06
655	-2.995664E 06
656	-2.765487E 06
657	-3.291957E 06
658	-2.636932E 06
659	-2.891653E 06
660	-3.151157E 06
661	-3.413816E 06
662	-2.989766E 06
663	-2.715093E 06
664	-2.876252E 06
665	-2.588362E 06
666	-2.716837E 06
667	-3.121868E 06
668	-2.581387E 06
669	-2.658289E 06
670	-3.033639E 06
671	-2.250519E 06
672	-2.936521E 06
673	-2.969361E 06
674	-2.821160E 06
675	-2.937990E 06
676	-2.813276E 06
677	-3.060239E 06
678	-3.013829E 06
679	-2.289345E 06
680	-2.603885E 06
681	-2.836073E 06
682	-2.269837E 06
683	-2.699171E 06
684	-2.366471E 06
685	-2.456585E 06
686	-2.715597E 06

INDEX	INTENSITY
687	-2.571048E 06
688	-1.942913E 06
689	-2.349477E 06
690	-2.683898E 06
691	-2.483823E 06
692	-2.308236E 06
693	-2.610838E 06
694	-2.430239E 06
695	-2.831975E 06
696	-2.239098E 06
697	-2.244534E 06
698	-1.761384E 06
699	-2.426794E 06
700	-1.639051E 06
701	-2.487488E 06
702	-1.970329E 06
703	-2.119729E 06
704	-2.183426E 06
705	-1.494608E 06
706	-2.080655E 06
707	-2.293680E 06
708	-1.815897E 06
709	-2.057461E 06
710	-1.981055E 06
711	-2.039063E 06
712	-2.167336E 06
713	-1.546805E 06
714	-1.839794E 06
715	-2.169432E 06
716	-1.827143E 06
717	-2.311734E 06
718	-2.183728E 06
719	-1.557703E 06
720	-1.745027E 06
721	-1.743973E 06
722	-1.271295E 06
723	-1.979722E 06
724	-1.944038E 06
725	-1.576289E 06
726	-1.214786E 06
727	-1.423836E 06
728	-1.288954E 06
729	-1.309092E 06
730	-9.571279E 05
731	-1.247916E 06
732	-1.639628E 06
733	-1.022397E 06
734	-9.361370E 05
735	-1.063691E 06
736	-1.514796E 06

INDEX	INTENSITY
737	-9.436160E 05
738	-2.094900E 05
739	-1.183429E 06
740	-4.836770E 05
741	-7.665370E 05
742	-7.510630E 05
743	-5.219630E 05
744	-6.531589E 05
745	-7.002770E 05
746	-8.202340E 05
747	-2.503550E 05
748	-1.670010E 05
749	-8.112310E 05
750	-1.133300E 05
751	-3.251490E 05
752	-6.669500E 04
753	2.596010E 05
754	4.665000E 04
755	2.891510E 05
756	-1.583930E 05
757	7.290091E 05
758	3.398260E 05
759	3.409530E 05
760	9.529829E 05
761	4.777340E 05
762	7.963521E 05
763	6.209860E 05
764	1.024990E 06
765	8.833621E 05
766	8.205670E 05
767	1.491153E 06
768	1.619895E 06
769	1.432574E 06
770	1.339998E 06
771	1.711311E 06
772	1.798788E 06
773	2.218452E 06
774	2.193009E 06
775	2.338913E 06
776	2.416506E 06
777	2.384292E 06
778	2.570042E 06
779	3.215460E 06
780	2.642658E 06
781	3.490647E 06
782	3.246270E 06
783	3.162086E 06
784	3.628959E 06
785	3.652585E 06
786	4.161630E 06
787	3.890558E 06

INDEX	INTENSITY	INDEX	INTENSITY	INDEX	INTENSITY
788	4.135995E 06	838	2.303662E 07	888	2.956135E 08
789	4.163233E 06	839	2.341788E 07	889	2.946905E 08
790	4.873484E 06	840	2.353183E 07	890	2.898950E 08
791	4.344814E 06	841	2.443801E 07	891	2.823920E 08
792	5.045713E 06	842	2.544288E 07	892	2.731575E 08
793	4.679994E 06	843	2.597184E 07	893	2.611065E 08
794	5.350776E 06	844	2.767900E 07	894	2.468635E 08
795	5.803290E 06	845	2.856979E 07	895	2.326260E 08
796	5.955127E 06	846	2.936486E 07	896	2.173072E 08
797	5.850802E 06	847	3.051290E 07	897	2.025297E 08
798	5.910937E 06	848	3.217985E 07	898	1.869871E 08
799	6.491410E 06	849	3.326265E 07	899	1.717634E 08
800	7.057728E 06	850	3.456648E 07	900	1.582457E 08
801	7.248407E 06	851	3.735421E 07	901	1.458582E 08
802	7.583446E 06	852	3.818146E 07	902	1.339085E 08
803	8.025131E 06	853	4.059643E 07	903	1.226709E 08
804	8.093622E 06	854	4.272602E 07	904	1.124758E 08
805	8.337684E 06	855	4.480348E 07	905	1.034153E 08
806	9.040428E 06	856	4.720924E 07	906	9.542950E 07
807	9.683150E 06	857	5.030437E 07	907	8.749034E 07
808	9.778025E 06	858	5.336091E 07	908	8.068331E 07
809	1.056894E 07	859	5.612099E 07	909	7.500182E 07
810	1.066209E 07	860	5.958797E 07	910	6.923395E 07
811	1.083363E 07	861	6.341843E 07	911	6.381433E 07
812	1.150504E 07	862	6.775272E 07	912	5.975686E 07
813	1.187302E 07	863	7.184395E 07	913	5.531898E 07
814	1.291206E 07	864	7.706557E 07	914	5.152152E 07
815	1.263137E 07	865	8.171103E 07	915	4.754854E 07
816	1.295177E 07	866	8.710766E 07	916	4.508772E 07
817	1.386550E 07	867	9.347999E 07	917	4.229067E 07
818	1.360092E 07	868	9.989089E 07	918	3.938595E 07
819	1.412383E 07	869	1.066509E 08	919	3.742264E 07
820	1.460765E 07	870	1.130515E 08	920	3.513731E 07
821	1.475481E 07	871	1.217718E 08	921	3.310077E 07
822	1.518463E 07	872	1.297688E 08	922	3.163118E 07
823	1.555408E 07	873	1.389599E 08	923	2.942910E 07
824	1.617306E 07	874	1.489399E 08	924	2.827254E 07
825	1.739085E 07	875	1.591930E 08	925	2.698013E 07
826	1.733573E 07	876	1.706013E 08	926	2.558446E 07
827	1.758674E 07	877	1.825152E 08	927	2.472263E 07
828	1.825815E 07	878	1.954258E 08	928	2.390034E 07
829	1.842242E 07	879	2.084587E 08	929	2.182400E 07
830	1.904344E 07	880	2.219222E 08	930	2.128632E 07
831	1.887350E 07	881	2.357203E 08	931	2.073040E 07
832	1.922261E 07	882	2.483082E 08	932	1.917548E 07
833	1.975193E 07	883	2.620808E 08	933	1.898722E 07
834	2.111994E 07	884	2.721306E 08	934	1.785596E 07
835	2.076323E 07	885	2.825137E 08	935	1.746208E 07
836	2.148485E 07	886	2.892836E 08	936	1.713113E 07
837	2.184328E 07	887	2.943152E 08	937	1.590800E 07

INDEX	INTENSITY
938	1.530014E 07
939	1.477815E 07
940	1.437433E 07
941	1.357873E 07
942	1.310544E 07
943	1.253141E 07
944	1.203068E 07
945	1.077091E 07
946	1.040335E 07
947	1.005915E 07
948	1.049424E 07
949	8.476349E 06
950	8.535190E 06
951	7.993719E 06
952	7.765414E 06
953	7.760540E 06
954	6.844453E 06
955	6.195218E 06
956	5.585591E 06
957	6.107377E 06
958	5.317793E 06
959	4.904741E 06
960	4.824190E 06
961	4.610653E 06
962	4.724810E 06
963	3.826991E 06
964	3.708614E 06
965	3.549071E 06
966	2.526562E 06
967	3.239316E 06
968	2.907525E 06
969	2.793860E 06
970	2.496977E 06
971	2.168408E 06
972	1.426037E 06
973	1.434197E 06
974	1.280167E 06
975	1.269601E 06
976	6.233500E 05
977	1.023188E 06
978	6.436960E 05
979	2.476550E 05
980	5.905010E 05
981	2.632010E 05
982	-2.005880E 05
983	-1.732980E 05
984	2.255610E 05
985	-3.586970E 05
986	-8.297031E 05
987	-7.520920E 05
988	-1.166621E 06

INDEX	INTENSITY
989	-9.372109E 05
990	-1.324544E 06
991	-1.356814E 06
992	-1.282849E 06
993	-1.586745E 06
994	-1.952834E 06
995	-1.423266E 06
996	-1.999191E 06
997	-2.248431E 06
998	-1.833851E 06
999	-2.393144E 06
1000	-2.469784E 06
1001	-1.906074E 06
1002	-2.539697E 06
1003	-2.567431E 06
1004	-2.636042E 06
1005	-2.608506E 06
1006	-2.076081E 06
1007	-2.854624E 06
1008	-2.790833E 06
1009	-2.618348E 06
1010	-3.495380E 06
1011	-2.995031E 06
1012	-2.957466E 06
1013	-3.357550E 06
1014	-2.727382E 06
1015	-2.866488E 06
1016	-3.055382E 06
1017	-3.440568E 06
1018	-3.387892E 06
1019	-3.541929E 06
1020	-3.292242E 06
1021	-3.820525E 06
1022	-3.679132E 06
1023	-3.143180E 06
1024	-3.770512E 06

### B) Example of a Formatted NMR File.

Processing the transferred NMR file (Appendix 2-A) with the program NMRMOD, one obtains a data file that is compatible with the deconvolution program (FIT). The first line contains the description of the X axis, i.e. the minimum and maximum values, the increment between points, and the number of points. The second line contains the minimum and maximum values in intensity. The file then contains the intensity values in one column. In this appendix, for the sake of clarity and convenience, two modifications were introduced. First, the transfer index (number of the point) is shown. Second, the intensity values are reported in three columns instead of one. The plot of the intensity values as a function of the transfer index (alternate chemical shift) was shown in the appendix 1 B.

2            1023            1.00            1022

4.71            304.73

INDEX	INTENSITY	INDEX	INTENSITY	INDEX	INTENSITY
2	11.52	20	9.74	38	8.06
3	11.37	21	9.69	39	7.99
4	11.09	22	9.71	40	7.77
5	11.01	23	9.18	41	8.01
6	11.10	24	9.47	42	8.01
7	11.00	25	9.14	43	7.89
8	10.70	26	9.12	44	7.67
9	10.55	27	8.93	45	7.52
10	10.32	28	8.96	46	7.50
11	10.37	29	8.84	47	7.68
12	10.41	30	8.62	48	7.56
13	10.28	31	8.46	49	7.55
14	9.92	32	8.50	50	7.29
15	10.21	33	8.42	51	7.15
16	9.79	34	8.13	52	7.28
17	9.93	35	8.12	53	7.16
18	9.70	36	8.06	54	6.99
19	9.84	37	8.23	55	6.96

INDEX INTENSITY

56 7.14  
57 7.20  
58 6.98  
59 6.93  
60 6.99  
61 7.10  
62 7.10  
63 6.70  
64 6.66  
65 6.66  
66 6.48  
67 6.62  
68 6.56  
69 6.52  
70 6.46  
71 6.39  
72 6.36  
73 6.23  
74 6.16  
75 6.21  
76 6.51  
77 6.35  
78 6.43  
79 6.41  
80 6.39  
81 6.38  
82 6.09  
83 6.11  
84 5.96  
85 6.02  
86 5.89  
87 5.97  
88 6.32  
89 6.37  
90 6.38  
91 5.97  
92 5.84  
93 5.89  
94 6.04  
95 6.05  
96 6.01  
97 5.99  
98 5.92  
99 5.68  
100 5.50  
101 5.69  
102 5.70  
103 5.77  
104 5.79  
105 5.66  
106 5.91  
107 5.78  
108 5.57  
109 5.48  
110 5.47

INDEX INTENSITY

111 5.46  
112 5.25  
113 5.28  
114 5.24  
115 5.18  
116 5.26  
117 5.19  
118 5.10  
119 5.20  
120 5.24  
121 5.14  
122 5.37  
123 5.33  
124 5.54  
125 5.54  
126 5.26  
127 5.10  
128 5.13  
129 5.17  
130 5.11  
131 4.79  
132 4.74  
133 4.75  
134 4.95  
135 5.01  
136 4.75  
137 4.81  
138 4.85  
139 5.20  
140 5.41  
141 5.20  
142 5.53  
143 5.30  
144 5.36  
145 5.06  
146 5.04  
147 4.88  
148 5.00  
149 5.00  
150 5.08  
151 5.02  
152 5.10  
153 5.14  
154 5.11  
155 5.23  
156 5.26  
157 5.25  
158 5.30  
159 5.40  
160 5.26  
161 4.95  
162 4.91  
163 4.84  
164 4.78  
165 4.91

INDEX INTENSITY

166 4.77  
167 4.89  
168 4.98  
169 5.00  
170 4.87  
171 5.12  
172 4.98  
173 5.12  
174 4.76  
175 4.95  
176 4.71  
177 5.12  
178 5.15  
179 5.23  
180 4.90  
181 4.74  
182 4.85  
183 4.82  
184 4.87  
185 5.11  
186 5.12  
187 5.27  
188 4.98  
189 5.25  
190 5.11  
191 5.25  
192 5.01  
193 5.10  
194 5.01  
195 5.15  
196 4.79  
197 4.81  
198 4.86  
199 4.99  
200 4.98  
201 5.12  
202 5.07  
203 5.03  
204 5.28  
205 5.28  
206 5.21  
207 4.92  
208 4.82  
209 5.03  
210 5.30  
211 5.49  
212 5.35  
213 5.29  
214 5.31  
215 5.31  
216 5.19  
217 5.35  
218 5.16  
219 5.37  
220 5.52

INDEX	INTENSITY	INDEX	INTENSITY	INDEX	INTENSITY
221	5.79	276	8.67	331	20.64
222	5.76	277	8.35	332	21.01
223	5.60	278	8.71	333	21.75
224	5.55	279	8.68	334	22.29
225	5.61	280	8.84	335	23.25
226	5.69	281	9.09	336	24.18
227	5.58	282	9.15	337	25.20
228	5.56	283	9.43	338	26.11
229	5.67	284	9.39	339	27.07
230	5.78	285	9.42	340	28.20
231	5.89	286	9.50	341	29.66
232	5.98	287	9.77	342	31.41
233	6.17	288	9.54	343	33.37
234	5.98	289	10.35	344	35.50
235	6.05	290	10.03	345	37.52
236	5.98	291	10.31	346	39.78
237	6.11	292	10.33	347	41.78
238	6.19	293	10.58	348	44.12
239	6.41	294	10.71	349	46.16
240	6.16	295	10.99	350	48.54
241	6.32	296	11.13	351	50.36
242	6.20	297	11.16	352	52.52
243	6.30	298	11.39	353	53.91
244	6.33	299	11.54	354	55.82
245	6.29	300	11.71	355	56.73
246	6.32	301	11.56	356	57.92
247	6.48	302	11.48	357	58.68
248	6.54	303	11.16	358	59.33
249	6.64	304	11.53	359	59.87
250	6.61	305	11.66	360	59.92
251	6.70	306	11.99	361	60.11
252	6.43	307	11.68	362	59.84
253	6.61	308	11.95	363	59.86
254	6.56	309	11.98	364	59.31
255	7.03	310	12.43	365	59.09
256	7.12	311	12.67	366	58.62
257	7.09	312	12.87	367	57.98
258	7.03	313	12.93	368	57.05
259	6.89	314	13.13	369	56.08
260	6.93	315	13.34	370	55.23
261	7.17	316	13.56	371	54.21
262	7.31	317	13.96	372	53.19
263	7.14	318	14.50	373	52.28
264	7.23	319	15.03	374	51.29
265	7.30	320	15.22	375	50.53
266	7.59	321	15.67	376	49.65
267	7.62	322	15.96	377	48.76
268	7.61	323	16.80	378	47.94
269	7.68	324	17.24	379	47.27
270	7.89	325	17.65	380	46.65
271	8.30	326	18.08	381	46.13
272	8.50	327	18.31	382	45.83
273	8.67	328	19.04	383	45.42
274	8.77	329	19.75	384	45.17
275	8.40	330	20.18	385	44.87

INDEX INTENSITY

386 44.91  
387 44.84  
388 44.85  
389 44.90  
390 44.81  
391 45.21  
392 45.31  
393 45.76  
394 46.31  
395 46.86  
396 47.32  
397 47.82  
398 48.48  
399 49.15  
400 50.15  
401 50.67  
402 51.61  
403 52.87  
404 54.06  
405 55.02  
406 56.14  
407 57.59  
408 58.82  
409 60.24  
410 61.61  
411 62.54  
412 63.38  
413 64.20  
414 65.24  
415 66.07  
416 67.00  
417 67.36  
418 67.74  
419 68.10  
420 68.12  
421 68.45  
422 68.23  
423 68.05  
424 67.96  
425 67.54  
426 67.15  
427 66.37  
428 65.56  
429 64.53  
430 63.48  
431 62.36  
432 61.01  
433 59.86  
434 58.48  
435 57.26  
436 55.75  
437 54.42  
438 52.96  
439 51.69  
440 50.45

INDEX INTENSITY

441 48.93  
442 47.47  
443 46.23  
444 44.85  
445 43.56  
446 42.42  
447 41.14  
448 40.18  
449 38.98  
450 37.95  
451 36.67  
452 35.76  
453 34.75  
454 33.89  
455 32.92  
456 32.27  
457 31.16  
458 30.62  
459 30.00  
460 29.25  
461 28.72  
462 28.04  
463 27.37  
464 26.71  
465 26.22  
466 25.75  
467 25.44  
468 24.74  
469 24.43  
470 24.15  
471 23.85  
472 23.30  
473 22.93  
474 22.77  
475 22.15  
476 21.89  
477 21.57  
478 21.02  
479 20.98  
480 20.56  
481 20.30  
482 19.95  
483 19.78  
484 19.45  
485 19.24  
486 18.90  
487 18.58  
488 18.09  
489 17.71  
490 17.49  
491 17.31  
492 17.25  
493 16.75  
494 16.46  
495 15.90

INDEX INTENSITY

496 15.56  
497 15.29  
498 14.91  
499 14.59  
500 14.34  
501 14.40  
502 14.11  
503 13.71  
504 13.47  
505 13.03  
506 12.68  
507 12.48  
508 12.25  
509 11.97  
510 11.94  
511 11.82  
512 11.31  
513 11.21  
514 10.70  
515 11.15  
516 10.93  
517 10.76  
518 10.79  
519 10.92  
520 10.72  
521 10.88  
522 10.66  
523 10.42  
524 10.12  
525 9.86  
526 9.91  
527 9.35  
528 9.27  
529 9.10  
530 9.15  
531 9.10  
532 8.92  
533 9.03  
534 8.94  
535 9.24  
536 8.91  
537 8.89  
538 8.52  
539 8.61  
540 8.90  
541 9.12  
542 9.27  
543 9.07  
544 9.12  
545 8.93  
546 8.93  
547 8.89  
548 9.06  
549 9.24  
550 9.14



INDEX INTENSITY

551 8.84  
552 8.64  
553 8.77  
554 8.66  
555 8.60  
556 8.41  
557 8.47  
558 8.34  
559 8.09  
560 7.99  
561 7.74  
562 7.71  
563 7.36  
564 7.44  
565 7.04  
566 7.15  
567 6.99  
568 7.10  
569 6.86  
570 6.72  
571 6.62  
572 6.78  
573 6.73  
574 6.75  
575 6.70  
576 6.58  
577 6.54  
578 6.72  
579 6.57  
580 6.68  
581 6.24  
582 6.53  
583 6.24  
584 6.40  
585 6.44  
586 6.53  
587 6.08  
588 6.22  
589 6.27  
590 6.47  
591 6.58  
592 6.49  
593 6.55  
594 6.27  
595 6.50  
596 6.53  
597 6.56  
598 6.45  
599 6.49  
600 6.43  
601 6.62  
602 6.52  
603 6.73  
604 6.56  
605 6.33

INDEX INTENSITY

606 6.39  
607 6.35  
608 6.51  
609 6.41  
610 6.52  
611 6.50  
612 6.66  
613 6.82  
614 6.84  
615 6.56  
616 6.56  
617 6.53  
618 6.64  
619 6.41  
620 6.74  
621 6.55  
622 6.54  
623 6.81  
624 6.64  
625 6.96  
626 6.68  
627 6.85  
628 6.19  
629 6.56  
630 6.50  
631 6.68  
632 7.00  
633 6.88  
634 6.80  
635 6.89  
636 6.82  
637 6.87  
638 6.63  
639 6.68  
640 6.86  
641 6.89  
642 6.94  
643 6.96  
644 7.05  
645 6.90  
646 7.06  
647 6.95  
648 6.89  
649 6.95  
650 7.17  
651 6.89  
652 7.14  
653 7.01  
654 7.11  
655 7.01  
656 6.99  
657 7.14  
658 6.97  
659 7.17  
660 6.91

INDEX INTENSITY

661 6.82  
662 6.87  
663 7.11  
664 7.28  
665 7.24  
666 7.25  
667 7.22  
668 7.13  
669 7.29  
670 7.35  
671 7.19  
672 7.40  
673 7.08  
674 7.08  
675 7.15  
676 7.06  
677 7.07  
678 7.14  
679 7.27  
680 7.50  
681 7.42  
682 7.34  
683 7.60  
684 7.44  
685 7.52  
686 7.45  
687 7.51  
688 7.64  
689 7.77  
690 7.53  
691 7.46  
692 7.53  
693 7.59  
694 7.38  
695 7.52  
696 7.46  
697 7.88  
698 7.83  
699 8.10  
700 7.75  
701 8.07  
702 7.73  
703 7.94  
704 8.02  
705 8.01  
706 8.16  
707 7.93  
708 7.88  
709 8.08  
710 7.97  
711 7.96  
712 8.05  
713 8.07  
714 8.22  
715 8.08

INDEX INTENSITY

716 7.88  
717 7.96  
718 7.91  
719 8.08  
720 8.35  
721 8.37  
722 8.32  
723 8.38  
724 8.13  
725 8.33  
726 8.55  
727 8.71  
728 8.64  
729 8.79  
730 8.79  
731 8.80  
732 8.71  
733 8.69  
734 8.99  
735 8.89  
736 8.85  
737 8.95  
738 9.18  
739 9.48  
740 9.10  
741 9.38  
742 9.30  
743 9.33  
744 9.40  
745 9.29  
746 9.38  
747 9.49  
748 9.63  
749 9.69  
750 9.48  
751 9.85  
752 9.89  
753 10.04  
754 10.21  
755 10.06  
756 10.29  
757 10.19  
758 10.53  
759 10.49  
760 10.53  
761 10.80  
762 10.59  
763 10.81  
764 10.79  
765 10.94  
766 11.02  
767 11.19  
768 11.51  
769 11.50  
770 11.48

INDEX INTENSITY

771 11.55  
772 11.86  
773 12.00  
774 12.24  
775 12.29  
776 12.37  
777 12.45  
778 12.64  
779 12.75  
780 13.14  
781 13.01  
782 13.35  
783 13.32  
784 13.40  
785 13.77  
786 13.84  
787 14.09  
788 14.02  
789 14.33  
790 14.39  
791 14.78  
792 14.60  
793 15.03  
794 15.13  
795 15.61  
796 15.85  
797 15.92  
798 16.03  
799 16.34  
800 16.82  
801 17.24  
802 17.53  
803 17.82  
804 18.12  
805 18.39  
806 18.85  
807 19.39  
808 19.93  
809 20.20  
810 20.66  
811 20.92  
812 21.26  
813 21.95  
814 22.32  
815 22.85  
816 23.02  
817 23.34  
818 23.86  
819 23.98  
820 24.40  
821 24.79  
822 25.06  
823 25.52  
824 26.17  
825 26.77

INDEX INTENSITY

826 27.43  
827 27.63  
828 27.96  
829 28.50  
830 28.69  
831 29.05  
832 29.18  
833 29.83  
834 30.35  
835 31.12  
836 31.21  
837 31.96  
838 32.54  
839 33.26  
840 33.70  
841 34.24  
842 35.07  
843 36.13  
844 37.05  
845 38.32  
846 39.25  
847 40.36  
848 41.62  
849 43.05  
850 44.61  
851 46.17  
852 48.37  
853 49.92  
854 52.18  
855 54.37  
856 56.78  
857 59.52  
858 62.52  
859 65.61  
860 68.81  
861 72.59  
862 76.61  
863 81.10  
864 85.62  
865 90.74  
866 96.00  
867 101.90  
868 108.38  
869 114.87  
870 122.03  
871 129.41  
872 138.07  
873 146.86  
874 156.51  
875 166.92  
876 177.88  
877 189.79  
878 202.23  
879 215.31  
880 228.64

INDEX	INTENSITY	INDEX	INTENSITY	INDEX	INTENSITY
881	241.97	936	26.99	991	8.68
882	255.46	937	26.37	992	8.60
883	267.71	938	25.47	993	8.47
884	279.70	939	24.94	994	8.36
885	289.01	940	24.38	995	8.17
886	297.16	941	23.86	996	8.23
887	302.12	942	23.20	997	7.98
888	304.73	943	22.69	998	7.82
889	303.95	944	21.97	999	7.87
890	300.42	945	21.31	1000	7.71
891	293.83	946	20.50	1001	7.65
892	284.76	947	20.34	1002	7.77
893	273.57	948	19.77	1003	7.43
894	260.43	949	19.50	1004	7.41
895	245.92	950	18.37	1005	7.51
896	231.27	951	18.21	1006	7.46
897	216.03	952	17.88	1007	7.55
898	200.95	953	17.53	1008	7.22
899	186.00	954	17.14	1009	7.08
900	171.91	955	16.37	1010	7.07
901	159.06	956	16.02	1011	6.76
902	147.07	957	15.65	1012	6.92
903	135.74	958	15.61	1013	7.00
904	125.31	959	15.09	1014	6.92
905	115.95	960	14.81	1015	7.16
906	107.44	961	14.75	1016	6.94
907	99.76	962	14.44	1017	6.77
908	92.67	963	14.25	1018	6.55
909	86.40	964	13.73	1019	6.60
910	80.76	965	13.37	1020	6.45
911	75.51	966	13.22	1021	6.48
912	70.68	967	12.80	1022	6.18
913	66.59	968	13.05	1023	6.32
914	62.43	969	12.78		
915	58.92	970	12.56		
916	55.62	971	12.15		
917	52.96	972	11.80		
918	50.35	973	11.39		
919	47.83	974	11.35		
920	45.77	975	11.11		
921	43.75	976	11.05		
922	41.82	977	10.73		
923	40.24	978	10.73		
924	38.53	979	10.53		
925	37.28	980	10.34		
926	36.07	981	10.31		
927	34.95	982	10.04		
928	33.79	983	9.91		
929	32.73	984	9.88		
930	31.42	985	9.82		
931	30.62	986	9.43		
932	29.91	987	9.11		
933	28.80	988	9.10		
934	28.32	989	8.85		
935	27.58	990	8.86		

### **C) Range on which the Deconvolution will be Performed**

Generally, the deconvolution of a spectrum was not performed on the complete transferred range (appendix 2 B). In this particular example, the first 160 points of the transferred data of appendix 2 B are not included in the deconvolution. These points are not required, since no bands are present in that region (3.9 to 3.7 ppm). Thus, the removal of those points does not affect the deconvolution of the lineshape of the NMR spectrum. Moreover, it speeds up the deconvolution process. The plot, corresponding to the range on which the deconvolution was performed (161 to 1021), is given in appendix 1 C.

### **D) Supporting Data for the Deconvoluted Spectrum and Baseline**

After the deconvolution process is finished, one obtains the intensity values for the lineshape and the baseline of the spectrum. Again, for convenience, these data are given in six columns. Columns 1 and 4 are the transfer index, columns 2 and 5 are the intensity values for the lineshape of the spectrum, and columns 3 and 6 are the intensity values for the baseline. The plot corresponding to the deconvoluted spectrum can be found in appendix 1 D.

INDEX	LINESHAPE INTENSITY	BASELINE INTENSITY	INDEX	LINESHAPE INTENSITY	BASELINE INTENSITY
161	4.36	3.16	171	4.60	3.30
162	4.39	3.18	172	4.62	3.31
163	4.41	3.19	173	4.65	3.32
164	4.43	3.20	174	4.67	3.34
165	4.46	3.22	175	4.69	3.35
166	4.48	3.23	176	4.72	3.36
167	4.50	3.24	177	4.74	3.38
168	4.53	3.26	178	4.77	3.39
169	4.55	3.27	179	4.79	3.40
170	4.57	3.28	180	4.82	3.41

INDEX	LINESHAPE INTENSITY	BASELINE INTENSITY	INDEX	LINESHAPE INTENSITY	BASELINE INTENSITY
181	4.84	3.43	230	6.34	4.03
182	4.87	3.44	231	6.38	4.04
183	4.89	3.45	232	6.42	4.06
184	4.92	3.47	233	6.46	4.07
185	4.95	3.48	234	6.50	4.08
186	4.97	3.49	235	6.54	4.09
187	5.00	3.51	236	6.58	4.10
188	5.02	3.52	237	6.62	4.11
189	5.05	3.53	238	6.66	4.13
190	5.08	3.54	239	6.71	4.14
191	5.10	3.56	240	6.75	4.15
192	5.13	3.57	241	6.79	4.16
193	5.16	3.58	242	6.84	4.17
194	5.19	3.59	243	6.88	4.18
195	5.21	3.61	244	6.93	4.19
196	5.24	3.62	245	6.98	4.20
197	5.27	3.63	246	7.02	4.22
198	5.30	3.64	247	7.07	4.23
199	5.33	3.66	248	7.12	4.24
200	5.35	3.67	249	7.17	4.25
201	5.38	3.68	250	7.22	4.26
202	5.41	3.69	251	7.27	4.27
203	5.44	3.71	252	7.32	4.28
204	5.47	3.72	253	7.38	4.29
205	5.50	3.73	254	7.43	4.30
206	5.53	3.74	255	7.48	4.32
207	5.56	3.76	256	7.54	4.33
208	5.59	3.77	257	7.60	4.34
209	5.62	3.78	258	7.65	4.35
210	5.65	3.79	259	7.71	4.36
211	5.68	3.81	260	7.77	4.37
212	5.71	3.82	261	7.84	4.38
213	5.75	3.83	262	7.90	4.39
214	5.78	3.84	263	7.96	4.40
215	5.81	3.85	264	8.03	4.41
216	5.84	3.87	265	8.09	4.42
217	5.88	3.88	266	8.16	4.44
218	5.91	3.89	267	8.23	4.45
219	5.94	3.90	268	8.30	4.46
220	5.98	3.91	269	8.37	4.47
221	6.01	3.93	270	8.44	4.48
222	6.05	3.94	271	8.52	4.49
223	6.08	3.95	272	8.60	4.50
224	6.12	3.96	273	8.67	4.51
225	6.15	3.97	274	8.76	4.52
226	6.19	3.99	275	8.84	4.53
227	6.23	4.00	276	8.92	4.54
228	6.26	4.01	277	9.01	4.55
229	6.30	4.02	278	9.10	4.56

INDEX	LINESHAPE INTENSITY	BASELINE INTENSITY	INDEX	LINESHAPE INTENSITY	BASELINE INTENSITY
279	9.19	4.57	328	21.13	5.05
280	9.28	4.58	329	21.77	5.06
281	9.38	4.59	330	22.45	5.06
282	9.47	4.60	331	23.17	5.07
283	9.57	4.61	332	23.93	5.08
284	9.68	4.62	333	24.74	5.09
285	9.78	4.63	334	25.60	5.10
286	9.89	4.64	335	26.52	5.11
287	10.00	4.65	336	27.49	5.12
288	10.12	4.66	337	28.53	5.13
289	10.24	4.67	338	29.63	5.14
290	10.36	4.68	339	30.80	5.14
291	10.49	4.69	340	32.04	5.15
292	10.62	4.70	341	33.36	5.16
293	10.75	4.71	342	34.76	5.17
294	10.89	4.72	343	36.23	5.18
295	11.03	4.73	344	37.78	5.19
296	11.18	4.74	345	39.41	5.20
297	11.33	4.75	346	41.11	5.20
298	11.49	4.76	347	42.88	5.21
299	11.65	4.77	348	44.70	5.22
300	11.82	4.78	349	46.57	5.23
301	12.00	4.79	350	48.47	5.24
302	12.18	4.80	351	50.36	5.25
303	12.37	4.81	352	52.23	5.26
304	12.56	4.82	353	54.05	5.26
305	12.77	4.83	354	55.77	5.27
306	12.98	4.84	355	57.37	5.28
307	13.20	4.85	356	58.79	5.29
308	13.43	4.86	357	60.02	5.30
309	13.66	4.87	358	61.00	5.30
310	13.91	4.88	359	61.72	5.31
311	14.17	4.89	360	62.17	5.32
312	14.44	4.90	361	62.33	5.33
313	14.72	4.91	362	62.22	5.34
314	15.02	4.92	363	61.85	5.35
315	15.33	4.93	364	61.24	5.35
316	15.65	4.94	365	60.43	5.36
317	15.99	4.95	366	59.46	5.37
318	16.35	4.96	367	58.36	5.38
319	16.72	4.96	368	57.18	5.39
320	17.11	4.97	369	55.95	5.39
321	17.53	4.98	370	54.71	5.40
322	17.96	4.99	371	53.48	5.41
323	18.42	5.00	372	52.28	5.42
324	18.90	5.01	373	51.14	5.42
325	19.41	5.02	374	50.07	5.43
326	19.95	5.03	375	49.09	5.44
327	20.52	5.04	376	48.19	5.45

INDEX	LINESHAPE INTENSITY	BASELINE INTENSITY	INDEX	LINESHAPE INTENSITY	BASELINE INTENSITY
377	47.38	5.46	426	66.62	5.80
378	46.67	5.46	427	65.83	5.81
379	46.06	5.47	428	64.94	5.81
380	45.54	5.48	429	63.96	5.82
381	45.12	5.49	430	62.89	5.82
382	44.80	5.49	431	61.75	5.83
383	44.57	5.50	432	60.55	5.84
384	44.43	5.51	433	59.29	5.84
385	44.37	5.52	434	58.00	5.85
386	44.40	5.52	435	56.67	5.86
387	44.52	5.53	436	55.33	5.86
388	44.71	5.54	437	53.97	5.87
389	44.98	5.55	438	52.61	5.87
390	45.33	5.55	439	51.25	5.88
391	45.74	5.56	440	49.90	5.89
392	46.23	5.57	441	48.56	5.89
393	46.79	5.58	442	47.25	5.90
394	47.41	5.58	443	45.95	5.90
395	48.09	5.59	444	44.69	5.91
396	48.83	5.60	445	43.45	5.92
397	49.63	5.60	446	42.24	5.92
398	50.48	5.61	447	41.07	5.93
399	51.38	5.62	448	39.93	5.93
400	52.32	5.63	449	38.83	5.94
401	53.31	5.63	450	37.76	5.94
402	54.33	5.64	451	36.73	5.95
403	55.37	5.65	452	35.73	5.96
404	56.44	5.65	453	34.77	5.96
405	57.53	5.66	454	33.85	5.97
406	58.61	5.67	455	32.96	5.97
407	59.70	5.67	456	32.10	5.98
408	60.78	5.68	457	31.27	5.98
409	61.83	5.69	458	30.48	5.99
410	62.85	5.69	459	29.71	5.99
411	63.82	5.70	460	28.98	6.00
412	64.74	5.71	461	28.28	6.01
413	65.59	5.71	462	27.60	6.01
414	66.36	5.72	463	26.95	6.02
415	67.04	5.73	464	26.32	6.02
416	67.63	5.73	465	25.72	6.03
417	68.10	5.74	466	25.15	6.03
418	68.45	5.75	467	24.59	6.04
419	68.68	5.75	468	24.06	6.04
420	68.78	5.76	469	23.55	6.05
421	68.75	5.77	470	23.06	6.05
422	68.58	5.77	471	22.59	6.06
423	68.28	5.78	472	22.14	6.06
424	67.85	5.79	473	21.70	6.07
425	67.30	5.79	474	21.28	6.07

INDEX	LINESHAPE INTENSITY	BASELINE INTENSITY	INDEX	LINESHAPE INTENSITY	BASELINE INTENSITY
475	20.88	6.08	524	11.66	6.29
476	20.49	6.08	525	11.58	6.30
477	20.12	6.09	526	11.50	6.30
478	19.76	6.09	527	11.43	6.30
479	19.41	6.10	528	11.36	6.31
480	19.08	6.10	529	11.29	6.31
481	18.76	6.11	530	11.22	6.31
482	18.45	6.11	531	11.15	6.32
483	18.15	6.12	532	11.09	6.32
484	17.86	6.12	533	11.02	6.32
485	17.59	6.13	534	10.96	6.33
486	17.32	6.13	535	10.90	6.33
487	17.06	6.14	536	10.84	6.33
488	16.82	6.14	537	10.79	6.34
489	16.58	6.15	538	10.73	6.34
490	16.34	6.15	539	10.68	6.34
491	16.12	6.16	540	10.62	6.35
492	15.90	6.16	541	10.57	6.35
493	15.70	6.16	542	10.52	6.35
494	15.49	6.17	543	10.47	6.36
495	15.30	6.17	544	10.42	6.36
496	15.11	6.18	545	10.38	6.36
497	14.93	6.18	546	10.33	6.37
498	14.75	6.19	547	10.29	6.37
499	14.58	6.19	548	10.24	6.37
500	14.42	6.20	549	10.20	6.38
501	14.26	6.20	550	10.16	6.38
502	14.10	6.20	551	10.12	6.38
503	13.95	6.21	552	10.08	6.38
504	13.81	6.21	553	10.04	6.39
505	13.67	6.22	554	10.01	6.39
506	13.53	6.22	555	9.97	6.39
507	13.40	6.23	556	9.93	6.40
508	13.27	6.23	557	9.90	6.40
509	13.15	6.23	558	9.86	6.40
510	13.02	6.24	559	9.83	6.40
511	12.91	6.24	560	9.80	6.41
512	12.79	6.25	561	9.77	6.41
513	12.68	6.25	562	9.74	6.41
514	12.58	6.25	563	9.71	6.42
515	12.47	6.26	564	9.68	6.42
516	12.37	6.26	565	9.65	6.42
517	12.27	6.27	566	9.62	6.42
518	12.18	6.27	567	9.59	6.43
519	12.08	6.27	568	9.57	6.43
520	11.99	6.28	569	9.54	6.43
521	11.91	6.28	570	9.51	6.43
522	11.82	6.28	571	9.49	6.44
523	11.74	6.29	572	9.46	6.44



INDEX	LINESHAPE INTENSITY	BASELINE INTENSITY	INDEX	LINESHAPE INTENSITY	BASELINE INTENSITY
573	9.44	6.44	622	8.77	6.52
574	9.42	6.44	623	8.76	6.52
575	9.39	6.44	624	8.75	6.52
576	9.37	6.45	625	8.75	6.53
577	9.35	6.45	626	8.74	6.53
578	9.33	6.45	627	8.74	6.53
579	9.31	6.45	628	8.73	6.53
580	9.29	6.46	629	8.73	6.53
581	9.27	6.46	630	8.72	6.53
582	9.25	6.46	631	8.72	6.53
583	9.23	6.46	632	8.71	6.53
584	9.21	6.46	633	8.71	6.53
585	9.19	6.47	634	8.71	6.53
586	9.18	6.47	635	8.70	6.53
587	9.16	6.47	636	8.70	6.53
588	9.14	6.47	637	8.70	6.54
589	9.12	6.47	638	8.69	6.54
590	9.11	6.48	639	8.69	6.54
591	9.09	6.48	640	8.69	6.54
592	9.08	6.48	641	8.69	6.54
593	9.06	6.48	642	8.68	6.54
594	9.05	6.48	643	8.68	6.54
595	9.03	6.49	644	8.68	6.54
596	9.02	6.49	645	8.68	6.54
597	9.01	6.49	646	8.68	6.54
598	8.99	6.49	647	8.68	6.54
599	8.98	6.49	648	8.67	6.54
600	8.97	6.49	649	8.67	6.54
601	8.96	6.50	650	8.67	6.54
602	8.94	6.50	651	8.67	6.54
603	8.93	6.50	652	8.67	6.54
604	8.92	6.50	653	8.67	6.54
605	8.91	6.50	654	8.67	6.54
606	8.90	6.50	655	8.67	6.54
607	8.89	6.50	656	8.67	6.54
608	8.88	6.51	657	8.67	6.54
609	8.87	6.51	658	8.68	6.54
610	8.86	6.51	659	8.68	6.54
611	8.85	6.51	660	8.68	6.54
612	8.84	6.51	661	8.68	6.54
613	8.83	6.51	662	8.68	6.54
614	8.83	6.51	663	8.68	6.54
615	8.82	6.52	664	8.69	6.54
616	8.81	6.52	665	8.69	6.54
617	8.80	6.52	666	8.69	6.54
618	8.79	6.52	667	8.69	6.54
619	8.79	6.52	668	8.70	6.54
620	8.78	6.52	669	8.70	6.54
621	8.77	6.52	670	8.70	6.54

INDEX	LINESHAPE INTENSITY	BASELINE INTENSITY	INDEX	LINESHAPE INTENSITY	BASELINE INTENSITY
671	8.71	6.54	720	9.20	6.49
672	8.71	6.54	721	9.22	6.49
673	8.71	6.54	722	9.24	6.49
674	8.72	6.54	723	9.26	6.49
675	8.72	6.54	724	9.28	6.49
676	8.73	6.54	725	9.30	6.48
677	8.73	6.54	726	9.32	6.48
678	8.74	6.54	727	9.34	6.48
679	8.74	6.54	728	9.37	6.48
680	8.75	6.54	729	9.39	6.48
681	8.76	6.54	730	9.41	6.48
682	8.76	6.54	731	9.43	6.47
683	8.77	6.53	732	9.46	6.47
684	8.77	6.53	733	9.48	6.47
685	8.78	6.53	734	9.51	6.47
686	8.79	6.53	735	9.54	6.47
687	8.80	6.53	736	9.56	6.46
688	8.80	6.53	737	9.59	6.46
689	8.81	6.53	738	9.62	6.46
690	8.82	6.53	739	9.65	6.46
691	8.83	6.53	740	9.68	6.45
692	8.84	6.53	741	9.71	6.45
693	8.84	6.53	742	9.74	6.45
694	8.85	6.53	743	9.77	6.45
695	8.86	6.53	744	9.80	6.45
696	8.87	6.52	745	9.83	6.44
697	8.88	6.52	746	9.87	6.44
698	8.89	6.52	747	9.90	6.44
699	8.90	6.52	748	9.94	6.44
700	8.91	6.52	749	9.98	6.43
701	8.93	6.52	750	10.01	6.43
702	8.94	6.52	751	10.05	6.43
703	8.95	6.52	752	10.09	6.43
704	8.96	6.52	753	10.13	6.42
705	8.97	6.51	754	10.17	6.42
706	8.99	6.51	755	10.22	6.42
707	9.00	6.51	756	10.26	6.42
708	9.01	6.51	757	10.30	6.41
709	9.03	6.51	758	10.35	6.41
710	9.04	6.51	759	10.40	6.41
711	9.05	6.51	760	10.45	6.41
712	9.07	6.51	761	10.50	6.40
713	9.09	6.50	762	10.55	6.40
714	9.10	6.50	763	10.60	6.40
715	9.12	6.50	764	10.65	6.39
716	9.13	6.50	765	10.71	6.39
717	9.15	6.50	766	10.77	6.39
718	9.17	6.50	767	10.82	6.39
719	9.18	6.49	768	10.88	6.38

INDEX	LINESHAPE INTENSITY	BASELINE INTENSITY	INDEX	LINESHAPE INTENSITY	BASELINE INTENSITY
769	10.95	6.38	818	18.22	6.20
770	11.01	6.38	819	18.54	6.20
771	11.07	6.37	820	18.88	6.19
772	11.14	6.37	821	19.24	6.19
773	11.21	6.37	822	19.61	6.18
774	11.28	6.37	823	20.00	6.18
775	11.35	6.36	824	20.40	6.18
776	11.43	6.36	825	20.83	6.17
777	11.50	6.36	826	21.27	6.17
778	11.58	6.35	827	21.74	6.16
779	11.66	6.35	828	22.23	6.16
780	11.75	6.35	829	22.74	6.15
781	11.84	6.34	830	23.28	6.15
782	11.92	6.34	831	23.85	6.14
783	12.02	6.34	832	24.44	6.14
784	12.11	6.33	833	25.07	6.13
785	12.21	6.33	834	25.73	6.13
786	12.31	6.33	835	26.42	6.13
787	12.41	6.32	836	27.15	6.12
788	12.52	6.32	837	27.93	6.12
789	12.63	6.32	838	28.74	6.11
790	12.74	6.31	839	29.61	6.11
791	12.86	6.31	840	30.52	6.10
792	12.98	6.30	841	31.49	6.10
793	13.11	6.30	842	32.52	6.09
794	13.23	6.30	843	33.61	6.09
795	13.37	6.29	844	34.77	6.08
796	13.51	6.29	845	36.01	6.08
797	13.65	6.29	846	37.32	6.07
798	13.80	6.28	847	38.72	6.07
799	13.95	6.28	848	40.21	6.06
800	14.11	6.28	849	41.81	6.06
801	14.27	6.27	850	43.51	6.05
802	14.44	6.27	851	45.34	6.05
803	14.61	6.26	852	47.30	6.04
804	14.80	6.26	853	49.40	6.04
805	14.99	6.26	854	51.67	6.03
806	15.18	6.25	855	54.10	6.02
807	15.38	6.25	856	56.72	6.02
808	15.59	6.24	857	59.55	6.01
809	15.81	6.24	858	62.60	6.01
810	16.04	6.24	859	65.91	6.00
811	16.28	6.23	860	69.49	6.00
812	16.52	6.23	861	73.37	5.99
813	16.78	6.22	862	77.58	5.99
814	17.04	6.22	863	82.15	5.98
815	17.32	6.21	864	87.13	5.98
816	17.60	6.21	865	92.54	5.97
817	17.90	6.21	866	98.44	5.96

INDEX	LINESHAPE INTENSITY	BASELINE INTENSITY	INDEX	LINESHAPE INTENSITY	BASELINE INTENSITY
867	104.86	5.96	916	60.27	5.65
868	111.85	5.95	917	57.35	5.64
869	119.46	5.95	918	54.63	5.64
870	127.74	5.94	919	52.11	5.63
871	136.73	5.94	920	49.77	5.62
872	146.46	5.93	921	47.59	5.62
873	156.96	5.92	922	45.57	5.61
874	168.24	5.92	923	43.67	5.60
875	180.28	5.91	924	41.91	5.59
876	193.02	5.91	925	40.25	5.59
877	206.37	5.90	926	38.71	5.58
878	220.16	5.90	927	37.26	5.57
879	234.15	5.89	928	35.90	5.56
880	248.04	5.88	929	34.62	5.56
881	261.42	5.88	930	33.42	5.55
882	273.85	5.87	931	32.28	5.54
883	284.80	5.87	932	31.22	5.54
884	293.75	5.86	933	30.21	5.53
885	300.25	5.85	934	29.26	5.52
886	303.90	5.85	935	28.36	5.51
887	304.50	5.84	936	27.51	5.51
888	302.00	5.83	937	26.71	5.50
889	296.55	5.83	938	25.94	5.49
890	288.48	5.82	939	25.22	5.48
891	278.23	5.82	940	24.53	5.48
892	266.30	5.81	941	23.88	5.47
893	253.22	5.80	942	23.26	5.46
894	239.46	5.80	943	22.66	5.45
895	225.45	5.79	944	22.10	5.44
896	211.54	5.78	945	21.56	5.44
897	197.98	5.78	946	21.05	5.43
898	184.98	5.77	947	20.56	5.42
899	172.64	5.76	948	20.09	5.41
900	161.05	5.76	949	19.64	5.41
901	150.23	5.75	950	19.22	5.40
902	140.18	5.75	951	18.81	5.39
903	130.90	5.74	952	18.41	5.38
904	122.34	5.73	953	18.04	5.37
905	114.46	5.73	954	17.68	5.37
906	107.22	5.72	955	17.33	5.36
907	100.57	5.71	956	17.00	5.35
908	94.46	5.71	957	16.68	5.34
909	88.85	5.70	958	16.37	5.33
910	83.69	5.69	959	16.08	5.33
911	78.95	5.68	960	15.79	5.32
912	74.59	5.68	961	15.52	5.31
913	70.57	5.67	962	15.25	5.30
914	66.86	5.66	963	15.00	5.29
915	63.44	5.66	964	14.75	5.28

INDEX	LINESHAPE INTENSITY	BASELINE INTENSITY	INDEX	LINESHAPE INTENSITY	BASELINE INTENSITY
965	14.52	5.28	1014	8.50	4.84
966	14.29	5.27	1015	8.43	4.83
967	14.07	5.26	1016	8.37	4.82
968	13.85	5.25	1017	8.31	4.81
969	13.65	5.24	1018	8.25	4.80
970	13.45	5.23	1019	8.19	4.79
971	13.25	5.23	1020	8.13	4.78
972	13.07	5.22	1021	8.07	4.77
973	12.89	5.21			
974	12.71	5.20			
975	12.54	5.19			
976	12.38	5.18			
977	12.22	5.18			
978	12.06	5.17			
979	11.91	5.16			
980	11.76	5.15			
981	11.62	5.14			
982	11.48	5.13			
983	11.35	5.12			
984	11.22	5.11			
985	11.09	5.11			
986	10.97	5.10			
987	10.85	5.09			
988	10.73	5.08			
989	10.62	5.07			
990	10.51	5.06			
991	10.40	5.05			
992	10.29	5.04			
993	10.19	5.03			
994	10.09	5.02			
995	9.99	5.02			
996	9.90	5.01			
997	9.80	5.00			
998	9.71	4.99			
999	9.62	4.98			
1000	9.54	4.97			
1001	9.45	4.96			
1002	9.37	4.95			
1003	9.29	4.94			
1004	9.21	4.93			
1005	9.13	4.92			
1006	9.05	4.91			
1007	8.98	4.90			
1008	8.91	4.89			
1009	8.83	4.89			
1010	8.76	4.88			
1011	8.69	4.87			
1012	8.63	4.86			
1013	8.56	4.85			

### E) Supporting Data for the Three Independent Deconvoluted Bands

The deconvoluted lineshape is composed of three independent bands, i.e. the signal due to unshielded methoxy groups (band # 1), the signal due to the shielded methoxy groups (band # 2), and the signal due to the presence of water traces (band # 3). The addition of the intensity values of the three bands, for the range on which the deconvolution was performed, to the baseline gives rise to the deconvoluted lineshape shown in appendix 1 D. For the sake of convenience, since the intensity values of these bands reach 0 at infinity, the width of the deconvoluted bands is arbitrary set to 10 times their width at half height. The intensity data for each deconvoluted bands are reported sequentially in six columns. Columns 1, 3 and 5 are the transfer index, and columns 2, 4 and 6 are the intensity values for a given band. These data correspond to the plot shown in appendix 1 E.

INDEX	BAND #1 INTENSITY	INDEX	BAND #1 INTENSITY	INDEX	BAND #1 INTENSITY
273	6.30	293	7.65	313	10.51
274	6.35	294	7.75	314	10.73
275	6.40	295	7.84	315	10.97
276	6.45	296	7.94	316	11.21
277	6.51	297	8.05	317	11.48
278	6.57	298	8.16	318	11.75
279	6.62	299	8.27	319	12.05
280	6.68	300	8.39	320	12.36
281	6.74	301	8.51	321	12.68
282	6.81	302	8.64	322	13.03
283	6.87	303	8.77	323	13.40
284	6.94	304	8.91	324	13.79
285	7.01	305	9.06	325	14.21
286	7.08	306	9.21	326	14.65
287	7.15	307	9.37	327	15.12
288	7.23	308	9.54	328	15.62
289	7.31	309	9.71	329	16.15
290	7.39	310	9.90	330	16.72
291	7.47	311	10.09	331	17.33
292	7.56	312	10.29	332	17.98

**INDEX      BAND #1  
INTENSITY**

333      18.67  
334      19.41  
335      20.20  
336      21.04  
337      21.94  
338      22.90  
339      23.93  
340      25.03  
341      26.19  
342      27.43  
343      28.74  
344      30.12  
345      31.58  
346      33.10  
347      34.69  
348      36.32  
349      37.99  
350      39.68  
351      41.37  
352      43.02  
353      44.61  
354      46.10  
355      47.45  
356      48.63  
357      49.59  
358      50.30  
359      50.75  
360      50.90  
361      50.76  
362      50.34  
363      49.64  
364      48.69  
365      47.53  
366      46.20  
367      44.72  
368      43.15  
369      41.51  
370      39.85  
371      38.17  
372      36.52  
373      34.90  
374      33.33  
375      31.83  
376      30.39  
377      29.02  
378      27.72  
379      26.50  
380      25.35  
381      24.28

**INDEX      BAND #1  
INTENSITY**

382      23.26  
383      22.32  
384      21.43  
385      20.61  
386      19.83  
387      19.11  
388      18.43  
389      17.80  
390      17.21  
391      16.66  
392      16.14  
393      15.66  
394      15.20  
395      14.78  
396      14.38  
397      14.00  
398      13.65  
399      13.32  
400      13.01  
401      12.72  
402      12.44  
403      12.18  
404      11.93  
405      11.70  
406      11.48  
407      11.27  
408      11.08  
409      10.89  
410      10.71  
411      10.55  
412      10.39  
413      10.24  
414      10.09  
415      9.96  
416      9.83  
417      9.70  
418      9.59  
419      9.47  
420      9.37  
421      9.27  
422      9.17  
423      9.08  
424      8.99  
425      8.90  
426      8.82  
427      8.74  
428      8.67  
429      8.60  
430      8.53

**INDEX      BAND #1  
INTENSITY**

431      8.47  
432      8.40  
433      8.34  
434      8.29  
435      8.23  
436      8.18  
437      8.13  
438      8.08  
439      8.03  
440      7.99  
441      7.94  
442      7.90  
443      7.86  
444      7.82  
445      7.79  
446      7.75  
447      7.72  
448      7.68

INDEX	BAND #2 INTENSITY	INDEX	BAND #2 INTENSITY	INDEX	BAND #2 INTENSITY
275	6.81	324	9.94	373	21.45
276	6.85	325	10.05	374	21.96
277	6.90	326	10.15	375	22.48
278	6.94	327	10.26	376	23.03
279	6.98	328	10.37	377	23.60
290	7.02	329	10.49	378	24.19
281	7.07	330	10.61	379	24.80
282	7.11	331	10.73	380	25.44
283	7.16	332	10.85	381	26.11
284	7.20	333	10.98	382	26.80
285	7.25	334	11.11	383	27.53
286	7.30	335	11.24	384	28.28
287	7.35	336	11.38	385	29.06
288	7.39	337	11.53	386	29.87
289	7.44	338	11.67	387	30.71
290	7.49	339	11.82	388	31.59
291	7.55	340	11.98	389	32.49
292	7.60	341	12.14	390	33.44
293	7.65	342	12.30	391	34.41
294	7.70	343	12.47	392	35.42
295	7.76	344	12.65	393	36.47
296	7.82	345	12.83	394	37.55
297	7.87	346	13.02	395	38.66
298	7.93	347	13.21	396	39.81
299	7.99	348	13.41	397	40.99
300	8.05	349	13.61	398	42.20
301	8.11	350	13.83	399	43.44
302	8.17	351	14.04	400	44.70
303	8.24	352	14.27	401	45.98
304	8.30	353	14.50	402	47.28
305	8.37	354	14.75	403	48.60
306	8.44	355	15.00	404	49.92
307	8.51	356	15.25	405	51.24
308	8.58	357	15.52	406	52.56
309	8.65	358	15.80	407	53.86
310	8.72	359	16.09	408	55.13
311	8.80	360	16.39	409	56.38
312	8.87	361	16.69	410	57.58
313	8.95	362	17.01	411	58.73
314	9.03	363	17.35	412	59.81
315	9.11	364	17.69	413	60.82
316	9.20	365	18.05	414	61.74
317	9.28	366	18.42	415	62.56
318	9.37	367	18.80	416	63.28
319	9.46	368	19.20	417	63.88
320	9.55	369	19.62	418	64.35
321	9.65	370	20.05	419	64.70
322	9.74	371	20.50	420	64.91
323	9.84	372	20.97	421	64.99



INDEX	BAND #2 INTENSITY	INDEX	BAND #2 INTENSITY	INDEX	BAND #2 INTENSITY
422	64.92	471	21.14	520	11.03
423	64.72	472	20.71	521	10.94
424	64.39	473	20.29	522	10.86
425	63.92	474	19.89	523	10.78
426	63.33	475	19.50	524	10.71
427	62.63	476	19.13	525	10.63
428	61.81	477	18.77	526	10.56
429	60.91	478	18.43	527	10.49
430	59.91	479	18.09	528	10.42
431	58.84	480	17.78	529	10.35
432	57.70	481	17.47	530	10.29
433	56.52	482	17.17	531	10.22
434	55.28	483	16.89	532	10.16
435	54.02	484	16.61	533	10.10
436	52.73	485	16.35	534	10.04
437	51.43	486	16.09	535	9.98
438	50.12	487	15.85	536	9.93
439	48.81	488	15.61	537	9.87
440	47.51	489	15.38	538	9.82
441	46.22	490	15.16	539	9.77
442	44.95	491	14.95	540	9.72
443	43.70	492	14.74	541	9.67
444	42.48	493	14.54	542	9.62
445	41.29	494	14.35	543	9.57
446	40.12	495	14.17	544	9.53
447	38.99	496	13.99	545	9.48
448	37.89	497	13.81	546	9.44
449	36.82	498	13.65	547	9.39
450	35.79	499	13.48	548	9.35
451	34.79	500	13.33	549	9.31
452	33.83	501	13.18	550	9.27
453	32.90	502	13.03	551	9.23
454	32.00	503	12.89	552	9.19
455	31.14	504	12.75	553	9.16
456	30.31	505	12.61	554	9.12
457	29.51	506	12.48	555	9.08
458	28.75	507	12.36	556	9.05
459	28.01	508	12.24	557	9.01
460	27.30	509	12.12	558	8.98
461	26.62	510	12.00	559	8.95
462	25.97	511	11.89	560	8.92
463	25.34	512	11.79	561	8.88
464	24.74	513	11.68	562	8.85
465	24.16	514	11.58	563	8.82
466	23.61	515	11.48	564	8.79
467	23.07	516	11.38	565	8.76
468	22.56	517	11.29	566	8.74
469	22.07	518	11.20	567	8.71
470	21.60	519	11.11	568	8.68

INDEX BAND #3  
INTENSITY

818 17.83  
819 18.16  
820 18.50  
821 18.86  
822 19.23  
823 19.62  
824 20.03  
825 20.45  
826 20.90  
827 21.37  
828 21.86  
829 22.37  
830 22.91  
831 23.48  
832 24.08  
833 24.71  
834 25.37  
835 26.06  
836 26.80  
837 27.57  
838 28.39  
839 29.26  
840 30.18  
841 31.15  
842 32.18  
843 33.27  
844 34.43  
845 35.67  
846 36.98  
847 38.38  
848 39.88  
849 41.47  
850 43.18  
851 45.01  
852 46.97  
853 49.08  
854 51.34  
855 53.77  
856 56.40  
857 59.23  
858 62.28  
859 65.59  
860 69.17  
861 73.05  
862 77.26  
863 81.84  
864 86.82  
865 92.23  
866 98.13

INDEX BAND #3  
INTENSITY

867 104.55  
868 111.55  
869 119.16  
870 127.44  
871 136.42  
872 146.16  
873 156.66  
874 167.94  
875 179.98  
876 192.73  
877 206.08  
878 219.86  
879 233.86  
880 247.74  
881 261.13  
882 273.56  
883 284.51  
884 293.47  
885 299.96  
886 303.62  
887 304.22  
888 301.72  
889 296.27  
890 288.21  
891 277.95  
892 266.03  
893 252.94  
894 239.18  
895 225.18  
896 211.26  
897 197.71  
898 184.71  
899 172.37  
900 160.78  
901 149.96  
902 139.92  
903 130.63  
904 122.07  
905 114.20  
906 106.96  
907 100.30  
908 94.20  
909 88.59  
910 83.43  
911 78.69  
912 74.33  
913 70.31  
914 66.61  
915 63.19

INDEX BAND #3  
INTENSITY

916 60.02  
917 57.09  
918 54.38  
919 51.86  
920 49.52  
921 47.35  
922 45.32  
923 43.43  
924 41.66  
925 40.01  
926 38.46  
927 37.02  
928 35.66  
929 34.38  
930 33.18  
931 32.05  
932 30.98  
933 29.98  
934 29.03  
935 28.13  
936 27.28  
937 26.47  
938 25.71  
939 24.99  
940 24.30  
941 23.65  
942 23.03  
943 22.44  
944 21.87  
945 21.34  
946 20.83  
947 20.34  
948 19.87  
949 19.42  
950 19.00  
951 18.59  
952 18.20  
953 17.82  
954 17.46  
955 17.11  
956 16.78

## Appendix 3

### Formatting Program Written in Fortran, for the Transferred NMR Files.

This Fortran program performs four modifications on the original file containing the intensity values for a transferred NMR spectrum. First, it removes all the extra (non-numerical) characters. Second, it creates an alternate chemical shift axis, which is, in fact, directly related to the number of transferred points. The third modification is introduced when a smoothing (moving average) operation is performed on the intensity values. Finally, it rescales the intensity in order to obtain a maximum value less than 1000.

```
$TITLE:'NMRMOD: FORMAT OUTPUT DATA FILES FROM NMR'
$SUBTITLE:'INTO A FILE FOR FIT PGM'
$DEBUG
C-----
C      PROGRAM NMRMOD
C      NMRMOD:  MODIFIES AN EXISTING SEQUENTIAL FILE TO THE
C                FORMAT ACCEPTED BY THE PROGRAM FIT
C
C      F. BOSSE                      NOVEMBER 1988
C-----
C
C      ***** DEFINITION OF THE VARIABLES AND THE CONSTANTS *****
C
C      LOGICAL*2      LIOFLG,BATCH
C      INTEGER*2      NPT, ICH, ITOP
C      REAL*4         YD,DSTRT,DEND,YMIN,YMAX,DINCR
C      CHARACTER*1     KEY,BELL,C
C      CHARACTER*2     EX1,EX2,EX3,EX4
C      CHARACTER*10    STING1,STING2
C      CHARACTER*30    WRTFLE,FIENME,PRCFLE,INLNE,SYD1,SYD2
C
C      PARAMETER (MAXPTS=5000)
C      DIMENSION YD(MAXPTS),ITOP(MAXPTS)
C      COMMON      /DT1COM/ YD,ITOP
C      BELL=CHAR(07)
C
C      *****
C      ** START OF MAIN PROGRAM **
C      *****
```

```

C      ASK OPERATOR THE NAME OF THE BATCH FILE TO BE PROCESSED
C
0010 CALL ECRAN(0,0,12)
      WRITE(0,90000)
90000 FORMAT(' DATA WILL BE READ FROM A BATCH FILE (Y)ES OR (N)O? '\)
      CALL GETKEY(KEY,1)
      IF (KEY.EQ. 'Y') THEN
        CALL ECRAN(0,0,12)
        WRITE(0,90010)
90010  FORMAT(' ENTER FULL BATCH FILE NAME: '\)
        READ(0,90020) PRCFILE
90020  FORMAT(A30)
        WRITE(0,90020) PRCFILE
        INQUIRE(FILE=PRCFLE,EXIST=LIOFLG)
        IF (.NOT. LIOFLG) THEN
          CALL ECRAN(0,0,12)
          WRITE(0,90030) PRCFILE,BELL
90030  FORMAT(2X,A30,' DOES NOT EXIST.',A1/)
          CALL GETKEY(KEY,0)
          GOTO 0010
        ENDIF
        OPEN(4,FILE=PRCFLE,STATUS=' OLD',ACCESS=' SEQUENTIAL')
        BATCH=.TRUE.
        ICH=4
      ELSE
        BATCH=.FALSE.
        ICH=0
      ENDIF

C
C      ASK OPERATOR FOR THE NMR DATA FILE-NAME
C
0100 IF(.NOT. BATCH) THEN
      CALL ECRAN(0,0,12)
      WRITE(0,90110)
90110  FORMAT(' ENTER FULL FILE-NAME OF NMR SPECTRUM: '\)
      READ(ICH,90020,END=9992) FLENME
      ELSE
        READ(ICH,90120,END=9992) FLENME
90120  FORMAT(A16)
        WRITE(0,90121) FLENME
90121  FORMAT(' READING FILE: ',A30)
      ENDIF
      INQUIRE(FILE=FLENME,EXIST=LIOFLG)
      IF (.NOT. LIOFLG) THEN
        CALL ECRAN(0,0,12)
        WRITE(0,90030) FLENME,BELL
        IF (.NOT. BATCH) CALL GETKEY(KEY,0)
        GOTO 0100
      ENDIF
      OPEN(1,FILE=FLENME,STATUS=' OLD',ACCESS=' SEQUENTIAL')

C
C      READ NMR SPECTRUM DATA (X,Y) FROM THE DISK FROM CHANNEL #1

```

```

C
  NPT=2
  WRITE(0,90129)
90129 FORMAT('    FORMATTING FILE(S)')
  DO 0500 I=1,8
    READ(1,90130) INLNE
  0500 CONTINUE
  0505 READ(1,90130,ERR=0550,END=0550) INLNE
90130 FORMAT(A30)
  READ(INLNE,90140,ERR=0550,END=0550) C,STING1,C,EX1,C,STING2,C,EX2
90140 FORMAT(2(A1,A10,A1,A2))
  EX3=EX1
  EX4=EX2
  WRITE(SYD1,90150,ERR=0550) STING1,EX1
  WRITE(SYD2,90150,ERR=0550) STING2,EX2
90150 FORMAT(A10,A2)
  READ(SYD1,*,ERR=0550,END=0550) YD(NPT-1)
  READ(SYD2,*,ERR=0550,END=0550) YD(NPT)
  READ(EX3,90145) ITOP(NPT-1)
  READ(EX4,90145) ITOP(NPT)
90145 FORMAT(I2)
  NPT=NPT+2
  GOTO 0505
0550 CLOSE(1)
C
C    DO A SMOOTHING TO REDUCE THE NOISE
C
  NPT=NPT-4
  WRITE(0,90151) NPT
90151 FORMAT('    PROCESSED DATA -> ',I5)
  DO 0600 I=1,NPT-2
    YD(I)=0.5*YD(I)+0.25*YD(I+1)+0.25*YD(I+2)
  0600 CONTINUE
  DINCR=1
  DEND=NPT
  DSTRT=DINCR
0625 YMIN=YD(1)
  YMAX=YMIN
  DO 0650 I=2,NPT
    IF (YMIN .GT. YD(I)) YMIN=YD(I)
    IF (YMAX .LT. YD(I)) YMAX=YD(I)
  0650 CONTINUE
  IEXMAX=ITOP(1)
  DO 0651 I=2,NPT
    IF (IEXMAX .LT. ITOP(I)) IEXMAX=ITOP(I)
  0651 CONTINUE
  ID=0
  IF (IEXMAX .GT. 2) THEN
    ID=1
    IMAX=IEXMAX-2
    XDIV=10**IMAX
    DO 0655 I=1,NPT

```

```

        YD(I)=YD(I)/XDIV
0655    CONTINUE
    ENDIF
    IF (IEXMAX .LT. 2) THEN
        ID=1
        IMAX=IABS(IEXMAX)-2
        XDIV=10**IMAX
        DO 0700 I=1,NPT
            YD(I)=YD(I)*XDIV
0700    CONTINUE
    ENDIF
    IF (ID .EQ. 1) THEN
        YMIN=YD(1)
        YMAX=YMIN
        DO 0750 I=2,NPT
            IF (YMIN .GT. YD(I)) YMIN=YD(I)
            IF (YMAX .LT. YD(I)) YMAX=YD(I)
0750    CONTINUE
    ENDIF

C
C    IF NMR DATA FILES ARE NOT READ FROM A BATCH FILE,
C    REQUEST FROM THE OPERATOR THE OUTPUT FILE NAME
C
    IF (.NOT. BATCH) THEN
0800    CALL ECRAN(0,0,12)
        WRITE(0,90210)
090210    FORMAT(' ENTER FULL FILE NAME FOR OUTPUT FILE: '\)
        READ(0,90020) WRTFLE
        INQUIRE(FILE=WRTFLE,EXIST=LIOFLG)
        IF (LIOFLG) THEN
            WRITE(0,90220) WRTFLE
090220    FORMAT(2X,A30,' EXISTS. OVERWRITE? '\)
            CALL GETKEY(KEY,1)
            IF (KEY .EQ. 'Y') THEN
                OPEN(2,FILE=WRTFLE,STATUS='OLD',ACCESS='SEQUENTIAL')
            ELSE
                GOTO 0800
            ENDIF
        ELSE
            OPEN(2,FILE=WRTFLE,STATUS='NEW',ACCESS='SEQUENTIAL')
        ENDIF
    ELSE
        WRTFLE=FLENME
        OPEN(2,FILE=WRTFLE,STATUS='OLD',ACCESS='SEQUENTIAL')
    ENDIF

C
C    WRITE REFORMATTED FILE TO DISK
C
    WRITE(2,94200,ERR=9990) DSTRT,DEND,DINCR,NPT
094200    FORMAT(3(G14.6,2X),I4,2X)
    DO 4210 I=1,NPT
        WRITE(2,*) YD(I)

```

```

4210 CONTINUE
      WRITE(2,*) YMAX,YMIN
      WRITE(0,94300) FLENME
94300 FORMAT( 2X,A30,' IS REFORMATTED AND SAVED')
      CLOSE(2)
      IF (BATCH) GOTO 0100
      CALL GETKEY(KEY,0)
C
C   PROGRAM CONTINUATION OPTIONS
C
      4500 CALL ECRAN(0,0,12)
      WRITE(0,94500)
94500 FORMAT(30X,'OPTIONS: '/')
      WRITE(0,94510)
94510 FORMAT(25X,'A',4X,'DO ANOTHER FILE' /
      3      25X,'B',4X,'TERMINATE PROGRAM' /)
      CALL QCMOV(0,7)
      4510 WRITE(0,94520)
94520 FORMAT(30X,'INPUT OPTION: '\)
      4520 CALL GETKEY(KEY,1)
      IF (KEY .EQ. 'A') GOTO 0010
      IF (KEY .EQ. 'B') GOTO 9999
      CALL QCMOV(0,7)
      WRITE(0,94540) BELL
94540 FORMAT(20X,'INVALID CHOICE - INPUT OPTION: ',A1\))
      GOTO 4520
C
C   ERROR READING PROCESS FILE
C
      9990 CALL ECRAN(0,0,12)
      WRITE(0,99900) FLENME,BELL
99900 FORMAT(' UNEXPECTED END OF FILE. RUN ABORTED.' /
      1      ' IN: ',A30,A1/)
      CALL GETKEY(KEY,0)
      IF (BATCH) GOTO 0100
      GOTO 4500
C
C   END OF A BATCH FILE
C
      9992 CLOSE(4)
      WRITE(0,99910) BELL,BELL
99910 FORMAT(2A1,' ALL THE FILES ARE REFORMATTED!!!')
      CALL GETKEY(KEY,0)
      GOTO 4500
      9999 STOP
      END
C
C   *****
C   ** END OF MAIN PROGRAM **
C   *****
C-----

```

```

C          *****
C          **  START OF SUBROUTINES  **
C          *****
C
C          SUBROUTINE ECRAN(IX,IY,IZ)
C
C          ECRAN : SCREEN MANAGEMENT
C
C          IX : GRAPHIC MODE OF THE SCREEN
C          IY : CURSOR COLUMN
C          IZ : CURSOR LINE
C
C          CALL QSMODE(IX)
C          CALL QCMOV(IY,IZ)
C          RETURN
C          END
C-----
C          SUBROUTINE GETKEY(KEY,KEYFLG)
C
C          GETKEY : WAITS FOR A KEYBOARD INPUT THEN INPUT KEY WILL BE PUT
C                   IN UPPERCASE.
C
C          KEY   : INPUT CHARACTER FROM KEYBOARD
C          KEYFLG: TASK FLAG
C                   0 = WAIT FOR ANY KEY THEN RETURN
C                   1 = WAIT FOR ANY KEY THEN RETURN CHARACTER
C
C          INTEGER*2  CKKEY,KEYVAL,KEYFLG
C          CHARACTER*1 KEY,BELL
C
C          BELL=CHAR(#07)
C          IF (KEYFLG .EQ. 0) THEN
C              WRITE(0,99999) BELL
C          99999  FORMAT(20X,A1,'HIT ANY KEY TO CONTINUE: '\)
C              CALL QINPUT(KEY,0)
C              RETURN
C          ENDIF
C          1000 KEYVAL=CKKEY(0)
C              IF (KEYVAL .EQ. 0) GOTO 1000
C              KEY=CHAR(KEYVAL)
C              IF (ICHAR(KEY) .GE. #60) KEY=CHAR(ICHAR(KEY)-#20)
C              RETURN
C              END

```



## Appendix 4

### Deconvolution Program Written in Fortran.

The program FIT written in Fortran deconvolutes a given lineshape by performing a non-linear least-squares estimation of a combination of two common idealized band shapes, Lorentzian and Gaussian. Those two distributions are modeled using three non-linear parameters, i.e. the mean, the standard deviation and the relative height, which can be related, respectively, to the position, the half width at half height ( $v_{1/2}$ ) and the height of an experimental band. The deconvolution process is based on the algorithm developed by Marquardt,<sup>52,53</sup> which was explained in greater detail in section 5.3 of Chapter 2.

```
$NOTSTRICT
$NOFLOATCALLS
$STORAGE:2
$SUBTITLE:''
$TITLE:'FIT: FITS LORENTZIAN OR GAUSSIAN BANDS'
$DEBUG
C-----
C      PROGRAM FIT
C
C      FIT:  FITS GAUSSIAN OR LORENTZIAN BANDS OF A SPECTRUM
C
C              F. BOSSE                                MAY, 1989
C-----
C
C      ***** DEFINITION OF THE VARIABLES AND THE CONSTANTS *****
C
C      LOGICAL*2  FLG, FLGK, FLGFIT, FLGSCL, FAX, FAL, MIN, MAJ, BOX, ILN, PLT
C      LOGICAL*2  OPINT, RSTFLG, LBLPK, FIRST
C      INTEGER*2  FITLST, FITIND, MAXPM, MAXBND, PLTNO, NOSTEP
C      INTEGER*2  FITLO, FITHI, BEGCHN, ENDCHN, NITER, NPARMS, NBANDS, ILIB, ND
C      INTEGER*2  IXL, IXH, IYL, IYH, IXALBL, IXFMT, IXLNG, IYALBL, IYFMT, IYLANG
C      INTEGER*2  IXPB, IYPK, NPADJ, ICHR, IPN, IPNA, HDRING, PXL, PXH, PYL, PYH
C      REAL*4     YD, XD, SGMY, YFT, PARM, CHISQ, BPRM, SUMBND, NPARM
C      REAL*4     XMN, XMN, YMN, YMX, YADD, OX, OY, XMAX, XMIN, BND
C      REAL*4     ALPHA, COVAR, CHRWDH, CHRHHG, DST, DND, DNK, ALANDA
C      CHARACTER*1  KEY, BTYP, BKGTP
C      CHARACTER*7  DEV
```

```

CHARACTER*10    CORMSG
CHARACTER*12    WRTFLE,FLENME
CHARACTER*20    LABELT
CHARACTER*80    HDRLNE,CXLBL,CYLBL,OUTLNE,BLNK
PARAMETER (MAXPTS=4000,MAXBND=33,MAXPM=3*MAXBND+3)
PARAMETER (ITCYCL=3,ITMAX=50)

```

```

DIMENSION OY(MAXPTS),OX(MAXPTS)
DIMENSION YD(MAXPTS),YFT(MAXPTS),XD(MAXPTS),SGMY(MAXPTS)
DIMENSION COVAR(MAXPM,MAXPM),ALPHA(MAXPM,MAXPM)
DIMENSION PARM(MAXPM),NPARM(MAXPM)
DIMENSION FITLST(MAXPM),BTYP(MAXBND),BPRM(3),YADD(MAXPTS)
DIMENSION IXPB(MAXBND),IYPB(MAXBND),BND(MAXBND)

```

```

COMMON /B,KIND/  BTYP
COMMON /IPPLT/   IXL,IXH,IYL,IYH,HDRLNE,HDRLNG,
1               IXALBL,IXFMT,CXLBL,IXLNG,
2               IYALBL,IYFMT,CYLBL,IYLNG
COMMON /DTPSCL/  FLGSCL
COMMON /DTPAXS/  PXL,PXH,PYL,PYH
COMMON /DTPFRM/  ICHR,IPN,ILN,CHRWDH,CHRHGH,FAX,IPNA,FAL,BOX
COMMON /DT1COM/  YD,YFT,XD
COMMON /DT2COM/  COVAR,ALPHA
COMMON /DT3COM/  BEGCHN,ENDCHN,NPDSF
COMMON /DT4COM/  MAJ,MIN
COMMON /DT5COM/  FLGK,FLGFIT
COMMON /DT6COM/  YMN,YMX
COMMON /DT7COM/  FLENME,WRTFLE
COMMON /DT8COM/  XMN,XMX
COMMON /DT9COM/  PLT,DEV
COMMON /DTSZMY/  SZMY
COMMON /DTWRT /  OUTLNE,BLNK
COMMON /DTYADD/  YADD
COMMON /DZ1COM/  NPTS,ILIB,CHISQ,NPADJ,NITER
COMMON /DZ2COM/  OX,OY
COMMON /DZ3COM/  ND,DST,DND,DNK
COMMON /DZ4COM/  NBANDS,PARM,NPARMS,FITLST
COMMON /DZ5COM/  BND,SUMBND
COMMON /DZ7COM/  FITLO,FITHI,CORMSG
COMMON /DZ8COM/  XMIN,XMAX
COMMON /DZ9COM/  IXPB,IYPB
EXTERNAL NMRBND, ZGET

```

```

C
C      INITIALIZATION OF THE CONSTANTS AND THE VARIABLES
C

```

```

DATA      PLTNO/0/
DATA      BPRM/0.0,0.0,1.0/
WRITE (BLNK,90001)
90001 FORMAT(80(' '))
DO 0005 I=1,MAXPTS
      SGMY(I)=1
0005 CONTINUE

```

```

IPN = 2
IPNA= 1
IXL = 150
IXH = 650
IYL = 50
IYH = 300
PXL=1500
PYL=1000
PXH=9000
PYH=7000
ICHR =42
CHRWDH=0.1
CHRHGH=0.2
IXALBL=1
IXFMT =2
IYALBL=1
IYFMT =2
CXLBL ='X AXIS'
IXLNG =15
CYLBL ='INTENSITY'
IYLNG =9
ILN  =.FALSE.
PLT  =.FALSE.
FLG  =.FALSE.
FLGK =.FALSE.
FLGFIT=.FALSE.
FLGSCL=.TRUE.
FAX  =.TRUE.
FAL  =.TRUE.
MAJ  =.TRUE.
MIN  =.TRUE.
BOX  =.TRUE.
DEV  ='SCREEN'
HDLRNE='EXP #1'
HDLRNG=6
FLENME='Z1'
WRTFLE='Z1.FIT'

```

```

C
C
C
C
C
C
C
*****
** START OF MAIN PROGRAM **
**      MENU 1      **
*****
0010 CALL ECRAN(0,0,20)
      WRITE(0,*)
      WRITE(0,90000)
      WRITE(0,90002)
      WRITE(0,90003)
      WRITE(0,90004)
90000 FORMAT(32X,'MENU #1'/)
90002 FORMAT(22X,'1-  LOAD DATA FROM DISK'/)
90003 FORMAT(22X,'2-  MENU #2'/)

```

```

90004 FORMAT(22X,'3- END PROGRAM' /)
KEY=ZGET(1)
IF (KEY.EQ. '1') THEN
    CALL LOAD(FLG)
    GOTO 0020
ENDIF
IF ((KEY.EQ. '2') .AND. (FLG)) GOTO 0020
IF (KEY.NE. '3') THEN
    GOTO 0010
ELSE
    GOTO 9999
ENDIF

```

```

C -----
C          ***** MENU2 *****
C          MAJOR OPTIONS FOR THE USER
C -----

```

```

0020 CALL ECRAN(0,0,20)
    WRITE(0,*)
    WRITE(0,90010)
    WRITE(0,90011)
    WRITE(0,90012)
    WRITE(0,90014)
    WRITE(0,90015)
90010 FORMAT(27X,'MENU #2' /)
90011 FORMAT(22X,'1- FIT A GRAPH' /)
90012 FORMAT(22X,'2- DO A GRAPH' /)
90014 FORMAT(22X,'3- SAVE DATA' /)
90015 FORMAT(22X,'4- MENU #1' /)
    KEY=ZGET(1)
    IF (KEY.EQ. '1') GOTO 0040
    IF (KEY.EQ. '2') GOTO 0030
    IF (KEY.EQ. '3') CALL SAVE
    IF (KEY.EQ. '4') GOTO 0010
    GOTO 0020

```

```

C -----
C          ***** GRAPHIC MENU *****
C          GRAPHIC OPTIONS FOR THE USER
C -----

```

```

0030 CALL ECRAN(0,0,20)
    WRITE(0,90020) DEV
    WRITE(0,*)
    WRITE(0,90021)
    WRITE(0,90022)
    WRITE(0,90023)
    WRITE(0,90024)
    WRITE(0,90025)
    WRITE(0,90026)
    WRITE(0,90027)
90020 FORMAT(27X,'GRAPH OPTIONS      [' ,A7,' ]' /)
90021 FORMAT(23X,'1- PLOT POINTS' /)
90022 FORMAT(23X,'2- DRAW THE CURVE' /)
90023 FORMAT(23X,'3- NEW TITLE' /)

```

```

90024 FORMAT(23X,'4- NEW SCALE'/)
90025 FORMAT(23X,'5- PLOTTER VS SCREEN'/)
90026 FORMAT(23X,'6- PLOT OPTIONS'/)
90027 FORMAT(23X,'7- MENU #2'/)
      KEY=ZGET(1)
      IF (KEY .EQ. '1') CALL PLTPNT(XMN,XMX)
      IF (KEY .EQ. '2') THEN
        IF (PLT) THEN
          CALL PLTPNT(XMN,XMX)
          GOTO 6000
        ELSE
          CALL NWPLTS
          GOTO 3500
        ENDIF
      ENDIF
      IF (KEY .EQ. '3') CALL INTTL
      IF (KEY .EQ. '4') CALL NWSCL
      IF (KEY .EQ. '6') CALL PLTOPT
      IF (KEY .EQ. '5') THEN
        IF (PLT) THEN
          PLT=.FALSE.
          DEV='SCREEN'
        ELSE
          PLT=.TRUE.
          DEV='PLOTTER'
        ENDIF
        GOTO 0030
      ENDIF
      IF (KEY .EQ. '1') THEN
        IF (.NOT. PLT) THEN
          KEY=ZGET(2)
        ELSE
          CALL ZFINIS
        ENDIF
      ENDIF
      IF (KEY .EQ. '7') GOTO 0020

      GOTO 0030

```

```

C -----
C          ***** FIT MENU *****
C -----
0040 CALL ECRAN(0,0,20)
      WRITE(0,90040)
      WRITE(0,*)
      WRITE(0,90041)
      WRITE(0,90043)
      WRITE(0,90045)
      WRITE(0,90046)
      WRITE(0,90047)
      KEY=ZGET(1)
      IF (KEY .EQ. '1') GOTO 0500
      IF (KEY .EQ. '2') THEN

```

```

        CALL OUT(I)
        GOTO 4400
    ENDIF
    IF (KEY .EQ. '3') GOTO 0030
    IF (KEY .EQ. '4') GOTO 0020
    IF (KEY .EQ. '5') GOTO 0010
    GOTO 0040
90040 FORMAT(30X,'FIT MENU'/)
90041 FORMAT(23X,'1- FIT BANDS'/)
90043 FORMAT(23X,'2- PRINT FITTED DATA'/)
90045 FORMAT(23X,'3- GRAPH OPTIONS'/)
90046 FORMAT(23X,'4- MENU #2'/)
90047 FORMAT(23X,'5- MENU #1'/)
C -----
C          START OF DECONVOLUTION PROCESS
C -----
0500 FIRST=.TRUE.
    BEGCHN=1
    ENDCHN=ND
    CALL YMAX(1,ND)
    YMN=YMN-0.1*(YMX-YMN)
    YMX=YMX*1.1
    XMN=XD(1)
    XMX=XD(ND)
    NPDSP=ENDCHN-BEGCHN+1
    FLGSCL=.TRUE.

C
C          PLOTTING DATA TO THE MONITOR SCREEN
C
0810 CALL NWPLTS
    CALL QTABL(1,ND,XD,YD)
    CALL QPTXT(80,BLNK,1,0,22)

C
C          ASK OPERATOR TO DEFINE FITTING REGION
C
    CALL QPTXT(38,'DEFINE FITTING REGION WITH TWO CURSORS',1,2,22)
    CALL GRINPO(X1,DNK)
    CALL GRINPO(X2,DNK)
    FITLO=ITAB(X1)
    FITHI=ITAB(X2)
    IF (FITLO .EQ. FITHI) GOTO 0810
    IF (FITLO .GE. FITHI) CALL SWAPI(FITLO,FITHI)
    NFPTS=FITHI-FITLO+1
    XMAX=XMX
    XMIN=XMN
    XMX=X2
    XMN=X1

C
C          FIND MAXIMUM AND MINIMUM OF DEFINED PLOT LIMITS, REPLOT DATA
C
    CALL YMAX(FITLO,FITHI)
    YMN=YMN-0.1*(YMX-YMN)

```

```

YMX=YMX*1.1
CALL NWPLTS
CALL QTABL(1,NFPTS,XD(FITLO),YD(FITLO))

```

```

C
C      ASK OPERATOR FOR NUMBER OF BANDS TO FIT AND INITIAL ESTIMATES
C

```

```

2000 CALL OPTXT(80,BLNK,1,2,22)
      CALL OPTXT(24,'NUMBER OF BANDS TO FIT? ',1,2,22)
      CALL QINNUM(26,22,4,NBANDS,0)
      IF (NBANDS .LE. 0) GOTO 0810

```

```

2002 FITIND=1
      NPARMS=3*NBANDS+3
      PARM(NPARMS-2)=0.0
      PARM(NPARMS-1)=0.0
      PARM(NPARMS)=0.0
      BPRM(1)=1.0
      DO 2050 I=1, NBANDS
        IBZ=3*(I-1)+1
        CALL OPTXT(80,BLNK,1,2,22)
        WRITE(OUTLINE,92005) I

```

```

C
C      DEFINITION OF THE BANDS
C

```

```

92005  FORMAT('MOVE CURSOR TO ESTIMATED PEAK POSITION ',I2,'.')
      CALL OPTXT(41,OUTLINE,1,2,22)
      CALL GRINPO(PARM(IBZ+1),DNK)
      CALL OPTXT(80,BLNK,1,2,22)
      CALL OPTXT(28,'ESTIMATE OF THE HALF WIDTH? ',1,2,22)
      CALL QINNUM(30,22,10,PARM(IBZ+2),1)
      CALL OPTXT(37,'BAND TYPE (G)AUSSIAN OR (L)ORENTZIAN ',1,2,22)
      BTYP(I)=ZGET(1)
      IF ((BTYP(I) .NE. 'G') .AND. (BTYP(I) .NE. 'L')) BTYP(I)='L'
      IPK=ITAB(PARM(IBZ+1))
      BPRM(3)=PARM(IBZ+2)
      PARM(IBZ)=0.70*(YD(IPK)-YMX)/
1      XBND(PARM(IBZ+1)-XD(IPK),BPRM,PARM(NPARMS-2),BTYP(I))
2003  CALL OPTXT(80,BLNK,1,2,22)
      CALL OPTXT(33,'(F)IX OR (V)ARY BAND PARAMETERS? ',1,2,22)
      KEY=ZGET(1)
      IF (KEY .EQ. 'V') THEN
        DO 2005 J=0,2
          FITLST(FITIND+J)=IBZ+J
2005  CONTINUE
          FITIND=FITIND+3
        ELSE
          IF (KEY .EQ. 'F') THEN
            CALL OPTXT(80,BLNK,1,2,22)
            CALL OPTXT(26,'FIX HEIGHT (Y)ES OR (N)O? ',1,2,22)
            KEY=ZGET(1)
            IF (KEY .EQ. 'N') THEN
              FITLST(FITIND)=IBZ
              FITIND=FITIND+1

```

```

        ENDIF
        CALL QPTXT(80,BLNK,1,2,22)
        CALL QPTXT(28,'FIX POSITION (Y)ES OR (N)O? ',1,2,22)
        KEY=ZGET(1)
        IF (KEY.EQ.'N') THEN
            FITLST(FITIND)=IBZ+1
            FITIND=FITIND+1
        ENDIF
        CALL QPTXT(80,BLNK,1,2,22)
        CALL QPTXT(30,'FIX HALF WIDTH (Y)ES OR (N)O? ',1,2,22)
        KEY=ZGET(1)
        IF (KEY.EQ.'N') THEN
            FITLST(FITIND)=IBZ+2
            FITIND=FITIND+1
        ENDIF
    ELSE
        GOTO 2003
    ENDIF
ENDIF
ENDIF
2050 CONTINUE
    BKGTYP='P'
    FITIND=FITIND+2
    FITLST(FITIND-2)=NPARMS-2
    FITLST(FITIND-1)=NPARMS-1
    FITLST(FITIND)=NPARMS
    NPADJ=0
    PARM(NPARMS-2)=YMN
    BPRM(1)=0.0
    BPRM(2)=0.0
    BPRM(3)=0.0
2200 CALL PLTPNT(XD(FITLO),XD(FITHI))
    CALL QSETUP(0,1,-2,0)
    DO 2210 I=FITLO,FITHI
        CALL NMRBND(XD(I),PARM,YFT(I),DUM,NPARMS,-1)
        YFT(I)=AMIN1(YFT(I),YMX)
2210 CONTINUE
    CALL QTABL(1,NFPTS,XD(FITLO),YFT(FITLO))
    CALL QPTXT(80,BLNK,1,2,22)
C
C     ENTER CORRECTION TO INPUT BANDS
C
    CALL QPTXT(37,'CHANGE ANY PARAMETERS (Y)ES OR (N)O? ',1,2,22)
    KEY=ZGET(1)
    IF (KEY.NE.'Y') GOTO 2900
    WRITE(OUTLINE,92300) NBANDS
92300 FORMAT('CHANGE PARAMETERS FOR WHICH BAND (1-',I2,',')? ')
    CALL QPTXT(41,OUTLINE,1,2,22)
    CALL QINNUM(43,22,4,IFX,0)
    IPK=IFX
    IF (IPK.LE.0) GOTO 2900
    IFX=3*(IFX-1)+1
    CALL QRTOI(PARM(IFX+1),YMN,IX1,IX2)

```



```

CALL QRTOI(PARM(IFX+1),YMX,IX3,IX4)
CALL QLINE(IX1,IX2,IX3,IX4,2)
CALL QPTXT(80,BLNK,1,2,22)
WRITE(OUTLINE,92310)
92310 FORMAT('MULTIPLYING FACTOR FOR BAND HEIGHT (<CR>-NO CHANGE)?')
CALL QPTXT(53,OUTLINE,1,2,22)
CALL QINNUM(55,22,14,DUM,1)
IF (DUM .NE. 0.0) PARM(IFX)=DUM*PARM(IFX)
CALL QPTXT(80,BLNK,1,2,22)
WRITE(OUTLINE,92320) PARM(IFX+1)
92320 FORMAT('CURRENT POSITION = ',F8.3,'. (<CR>-NO CHANGE)?')
CALL QPTXT(48,OUTLINE,1,2,22)
CALL QINNUM(62,22,10,DUM,1)
IF (DUM .NE. 0.0) PARM(IFX+1)=DUM
CALL QPTXT(80,BLNK,1,2,22)
WRITE(OUTLINE,92330) PARM(IFX+2)
92330 FORMAT('CURRENT WIDTH = ',F8.3,'. NEW WIDTH (<CR>-NO CHANGE)?')
CALL QPTXT(54,OUTLINE,1,2,22)
CALL QINNUM(56,22,10,DUM,1)
IF (DUM .NE. 0.0) THEN
  IF (BTYP(IPK) .EQ. 'G') THEN
    PARM(IFX+2)=DUM
  ELSE
    TMP1=PARM(IFX)*XBND(PARM(IFX+1),PARM(IFX),BPRM,'L')
    PARM(IFX+2)=DUM
    PARM(IFX)=TMP1/XBND(PARM(IFX+1),PARM(IFX),BPRM,'L')
  ENDIF
ENDIF
CALL QLINE(IX1,IX2,IX3,IX4,2)
GOTO 2200

C
C   SETS UP VARIABLES FOR MARQUARDT ALGORITHM, PERFORM ONE
C   ITERATION TO INITIALIZE ROUTINE
C
2900   ALAMDA=-1.0
      CALL MRQMIN(XD(FITLO),YD(FITLO),SGMY(FITLO),
1         NPPTS,PARM,NPARMS,FITLST,FITIND,COVAR,
2         ALPHA,MAXPM,CHISQ,NMRBND,ALAMDA)
      NITER=1
      NOSTEP=0

C
C   IF ALAMDA = -1.0 ON EXIT FROM MRQMIN, THEN FITLIST WAS INVALID.
C   REFILL FITLIST TO FIT ALL PARAMETERS AND TRY AGAIN
C
      IF (ALAMDA .EQ. -1.0) THEN
        DO 2910 I=1,NPARMS-NPADJ
          FITLST(I)=I
2910    CONTINUE
        FITIND=NPARMS-NPADJ
        GOTO 2900
      ENDIF

```

```

C
C      PLOTS EXPERIMENTAL AND FITTED SPECTRUM AFTER EACH ITCYCL (3)
C      ITERATIONS UNTIL DECONVOLUTION, OR OPERATOR INTERRUPTED
C
3000 CALL PLTPNT(XD(FITLO),XD(FITHI))
      CALL QSETUP(0,1,-2,0)
      DO 3010 I=FITLO,FITHI
          CALL NMRBND(XD(I),PARM,YFT(I),DUM,NPARMS,-1)
          YFT(I)=AMIN1(YFT(I),YMX)
3010 CONTINUE
      CALL QTABL(1,NFPTS,XD(FITLO),YFT(FITLO))
3020 IF (CHISQ .LT. 9.0E6) THEN
      WRITE(OUTLNE,93010) NITER,CHISQ
93010  FORMAT('PRESS <Esc> TO INTERRUPT. NUMBER OF ITERATIONS = ',
1      I3,'.',4X,'CHISQR = ',F10.2)
      ELSE
          WRITE(OUTLNE,93020) NITER,CHISQ
93020  FORMAT('PRESS <Esc> TO INTERRUPT. NUMBER OF ITERATIONS = ',
1      I3,'.',4X,'CHISQR = ',1PE10.3)
      ENDIF
      CALL QPTXT(80,OUTLNE,1,2,22)
      OCHISQ=CHISQ
      OLAMDA=ALAMDA
      CALL MRQMIN(XD(FITLO),YD(FITLO),SGMY(FITLO),
1          NFPTS,PARM,NPARMS,FITLST,FITIND,COVAR,
2          ALPHA,MAXPM,CHISQ,NMRBND,ALAMDA)
      NITER=NITER+1
      DIF=ABS(POCHISQ-CHISQ)
      IF ((DIF .LT. 0.1) .OR. (DIF/POCHISQ .LT. 0.001)) .AND.
1      (ALAMDA .LE. OLAMDA) THEN
          OPINT=.FALSE.
          GOTO 3500
      ENDIF
      IF (NITER .GT. ITMAX) THEN
          OPINT=.FALSE.
          GOTO 3500
      ENDIF
      IF (CKKEY(0) .EQ. #1B) THEN
          OPINT=.TRUE.
          GOTO 3500
      ENDIF
      IF (CHISQ .EQ. OCHISQ) THEN
          NOSTEP=NOSTEP+1
      ELSE
          NOSTEP=0
      ENDIF
      IF (NOSTEP .GT. 10) THEN
          OPINT=.FALSE.
          GOTO 3500
      ENDIF
      DO 3030 I=1,3*NBANDS
          IF ((MOD(I,3) .NE. 2) .AND. (PARM(I) .LT. 0.0)) THEN

```

```

        PARM(I)=ABS(PARM(I))
        ALAMDA=-1.0
    ENDIF
    IF (MOD(I,3) .EQ. 0) THEN
        RSTFLG=.FALSE.
        IF ((DNK .LT. 0) .AND. ((PARM(I) .GT. NFPTS*ABS(DNK))
1          .OR. (PARM(I-1)-10.0*PARM(I) .GT. XD(FITLO)) .OR.
2          (PARM(I-1)+10.0*PARM(I) .LT. XD(FITHI)))) THEN
            RSTFLG=.TRUE.
            PARM(I)=ABS(DNK)
            PARM(I-1)=XD(ENDCHN)-2.0*DNK
            PARM(I-2)=0.0
            NFIX=0
        ENDIF
        IF ((DNK .GT. 0) .AND. ((PARM(I) .GT. NFPTS*DNK) .OR.
1          (PARM(I-1)+10.0*PARM(I) .LT. XD(FITLO)) .OR.
2          (PARM(I-1)-10.0*PARM(I) .GT. XD(FITHI)))) THEN
            PARM(I)=DNK
            RSTFLG=.TRUE.
            PARM(I-1)=XD(ENDCHN)-2.0*DNK
            PARM(I-2)=0.0
            NFIX=0
        ENDIF
        IF (RSTFLG) THEN
            DO 3023 J1=FITIND,1,-1
                IF ((FITLST(J1) .GE. I-2) .AND. (FITLST(J1) .LE. I)) THEN
                    DO 3022 J2=J1+1,FITIND-NFIX
                        FITLST(J2-1)=FITLST(J2)
3022                CONTINUE
                        NFIX=NFIX+1
                    ENDIF
3023                CONTINUE
                        FITIND=FITIND-NFIX
                        ALAMDA=-1.0
                ENDIF
            ENDIF
3030        CONTINUE
            IF (ALAMDA .EQ. -1.0) THEN
                IF (MOD(NITER,ITCYCL) .EQ. 0) THEN
                    GOTO 3000
                ELSE
                    GOTO 3020
                ENDIF
            ENDIF
            IF (MOD(NITER,ITCYCL) .EQ. 0) GOTO 3000
            GOTO 3020
3500        BPRM(1)=0.0
            BPRM(3)=1.0
            DO 3510 I=FITLO,FITHI
                CALL NMRBND(XD(I),PARM,YFT(I),DUM,NPARMS,-1)
                IF (YFT(I) .GT. YMX) YMX=YFT(I)
                YADD(I)=YFT(I)

```

```

      YMN=AMIN1 (YMN, XBND (XD (I) , BPRM, PARM (NPARMS-2) , 'G' ) )
3510 CONTINUE
      CALL PLTPNT (XD (FITLO) , XD (FITHI) )
      CALL QSETUP (0,1,-2,0)
      CALL QTABL (0,NFPTS,XD (FITLO) , YD (FITLO) )
      CALL QTABL (1,NFPTS,XD (FITLO) , YFT (FITLO) )
      BPRM(1)=0.0
      BPRM(3)=1.0
      DO 3520 I=FITLO,FITHI
        YFT (I) =XBND (XD (I) , BPRM, PARM (NPARMS-2) , 'G' )
3520 CONTINUE
      CALL QTABL (1,NFPTS,XD (FITLO) , YFT (FITLO) )
      SUMBND=0
      DO 3540 I=1,NPARMS-3,3
        IF (BTYP (I/3+1) .EQ. 'G' ) THEN
          XBEG=AMAX1 (PARM (I+1) -3*PARM (I+2) , XD (FITLO) )
          XEND=AMIN1 (PARM (I+1) +3*PARM (I+2) , XD (FITHI) )
        ELSE
          XBEG=AMAX1 (PARM (I+1) -5*PARM (I+2) , XD (FITLO) )
          XEND=AMIN1 (PARM (I+1) +5*PARM (I+2) , XD (FITHI) )
        ENDIF
        IBEG=ITAB (XBEG)
        IEND=ITAB (XEND)
        IF ((IBEG .GT. ENDCHN) .OR. (IEND .LT. BEGCHN) ) GOTO 3540
        DO 3530 J=IBEG, IEND
          YFT (J) =XBND (XD (J) , PARM (I) , PARM (NPARMS-2) , BTYP (I/3+1) )
3530 CONTINUE
        BND (I/3+1) =AREA (IBEG, IEND, DNK)
        SUMBND=SUMBND+BND (I/3+1)
        CALL QTABL (1, IEND-IBEG+1, XD (IBEG) , YFT (IBEG) )
3540 CONTINUE
        IF (.NOT. FIRST) THEN
          KEY=ZGET (2)
          GOTO 0040
        ENDIF
C
C      END OF THE DECONVOLUTION PROCESS
C
3550 CALL OPTXT (80,BLNK,1,2,22)
      CALL OPTXT (34,'(C)ONTINUE, (R)EFIT OR (F)INISHED?',1,2,22)
      KEY=ZGET (1)
      IF (KEY .EQ. 'C' ) GOTO 3020
      IF (KEY .EQ. 'R' ) GOTO 0500
      IF (KEY .NE. 'F' ) GOTO 3550
      CALL ECRAN (0,0,22)
      ALAMDA=0.0
      CALL MRQMIN (XD (FITLO) , YD (FITLO) , SGMY (FITLO) ,
1          NFPTS, PARM, NPARMS, FITLST, FITIND, COVAR,
2          ALPHA, MAXPM, CHISQ, NMRBND, ALAMDA)
C
C      OUTPUT DECONVOLUTED BANDS PARAMETERS TO DISK
C

```

```

      OPEN(1,FILE=WRITE,STATUS='NEW',ACCESS='SEQUENTIAL')
4000 WRITE(1,94200) FLENME,DST,DND,DNK,ND
94200 FORMAT(A12:3(2X,F14.6),2X,I4)
      WRITE(1,94210) XD(FITLO),XD(FITHI),NBANDS,'1',FITLO,FITHI,NFPTS
94210 FORMAT(2(F14.6,2X),I3,2X,A1:3X,'DATA POINTS: ',3I7)
      DO 4210 I=1,NPARMS-3,3
          WRITE(1,94220) PARM(I),PARM(I+1),PARM(I+2),BTYP(I/3+1),
1              SIGN(SQRT(ABS(COVAR(I,I))),COVAR(I,I)),
2              SIGN(SQRT(ABS(COVAR(I+1,I+1))),COVAR(I+1,I+1)),
3              SIGN(SQRT(ABS(COVAR(I+2,I+2))),COVAR(I+2,I+2))
94220 FORMAT(3(F12.3,1X),A1:2X,'(' ,F12.3,')',2(1X,'( ,F8.4,')'))
4210 CONTINUE
      WRITE(1,94230) (PARM(I), I=NPARMS-2,NPARMS),BKGTF,
1              (SIGN(SQRT(ABS(COVAR(I,I))),COVAR(I,I)),
2              I=NPARMS-2,NPARMS)
94230 FORMAT(3(1PE12.5,1X),A1:2X,'(' ,0PF10.3,')',2(2X,'( ,F8.4,')'))
      WRITE(1,94235) (FITLST(I), I=1,FITIND),0
94235 FORMAT(20(I3,1X))
      WRITE(1,94240) CHISQ,NITER
94240 FORMAT(F14.4,5X,I3)
      TSTK=TSTCOR(YADD)
      WRITE(1,94245) TSTK,CORMSG
94245 FORMAT(F7.3,2X,A10)
      WRITE(1,*)
      DO 4220 I=1,NPARMS-NPADJ
          WRITE(1,94250) (COVAR(I,J), J=1,I-1), 1.0
94250 FORMAT(5(F14.4,1X))
4220 CONTINUE
      WRITE(1,*)
      I=0
4400 CALL ECRAN(0,0,22)
      ILIB=NFPTS-FITIND
      IF (I.EQ. 0) CALL ECRAN(0,0,12)
      IF (FIRST) THEN
          WRITE (0,94314)
C
C      PEAK LABELING
C
94314 FORMAT(2X,'LABEL THE PEAK (Y)ES OR (N)O? '\)
      KEY=ZGET(1)
      LBLPK=.FALSE.
      OPEN(3,FILE='LABEL.FIT',STATUS='NEW',ACCESS='SEQUENTIAL')
      IF (KEY.EQ. 'Y') LBLPK=.TRUE.
      WRITE(0,*)
      ENDIF
      DO 4404 I1=1,NBANDS
          IF (FIRST) THEN
              LABELT='-----'
              IF (LBLPK) THEN
                  WRITE(0,94316) I1
94316 FORMAT (2X,'ENTER LABEL FOR PEAK ',I2,' '/')
                  READ(0,94317) LABELT

```

```

94317          FORMAT(A20)
              ENDIF
              WRITE(3,94317) LABELT
              ENDIF
4404 CONTINUE
REWIND 3

C
C          OUTPUT DECONVOLUTION RESULTS TO SCREEN AND DISK
C
WRITE(I,*)
IF (I.EQ. 0) CALL ECRAN(0,0,22)
WRITE(I,*) HDRLNE
WRITE(I,94300) FLENME
94300 FORMAT(20X,'FILE: ',A12,/)
WRITE(I,94305) CHISQ
94305 FORMAT(5X,'TIME:      min.',30X,'Kh1^2: ',F11.3/)
WRITE(I,94306) CHISQ,ILIB,NFPTS,NPARMS-NPADJ,NITER
94306 FORMAT(F14.3,' CHISQ BASED ON ',I4,' DEGREES OF FREEDOM' /
1          '      FITTING ',I4,' POINTS WITH ',I2,' PARAMETERS IN ',
2          I3,' ITERATIONS')
WRITE(I,94307) TSTK,CORMSG
94307 FORMAT (3X,'CORRELATION FOR THE FIT= ',F6.2,'% [' ,
1          A10,'FIT BETWEEN THE CURVES']')
WRITE(I,*)
WRITE(I,94310)
94310 FORMAT(2X,'PEAK' ,6X,'PEAK' ,8X,'PEAK' ,8X,'RATIO' ,7X,
1          'WIDTH' ,5X,'PEAK LABEL' /)
WRITE(I,94312)
94312 FORMAT(3X,'(%)' ,4X,'POSITION' ,6X,'AREA' ,9X,' (%)' /)
WRITE(I,*)
DO 4405 J=1,NBANDS
    READ(3,94317) LABELT
    DUM=BND(J)/SUMBND*100
    WRITE(I,94320) J,PARM(J*3-1),BND(J),DUM,PARM(J*3),LABELT
94320    FORMAT(3X,I2,3X,F10.4,2X,F10.2,5X,F6.2,2X,F10.4,5X,A20/)
4405 CONTINUE
WRITE(I,94340) SUMBND
94340 FORMAT(2X,'Totals' ,10X,F12.2,5X,'100.00' /)
IF (FIRST) THEN
    KEY=ZGET(0)
    FIRST=.FALSE.
    I=1
    GOTO 4400
ENDIF
IF (I.EQ. 0) KEY=ZGET(0)
GOTO 0040

C-----
C          PLOTTING ROUTINE
C-----
6000 WRITE(OUTLINE,94427) CHISQ,NFPTS,NPARMS
94427 FORMAT('SUMSQR = ',F14.2,' fitting ',I4,' points with ',I3,
1          ' parameters')

```

```

CALL ZSPRLB(OUTLINE,80,5182,7100,0,0.125,0.1875)
DO 4410 I=FITLO,FITHI
    CALL NMRBND(XD(I),PARM,YFT(I),DUM,NPARMS,-1)
4410 CONTINUE

CALL ZSETUP(-1,3,0,0)
CALL ZTABL(1,NFPTS,XD(FITLO),YFT(FITLO))
CALL ZSETUP(-1,4,0,0)
YMDPNT=(YMN+YMX)/2
CALL ZDI(0.0,1.0,1)
NPK=0
DO 4430 I=1,NPARMS-3,3
    IF (BTYP(I/3+1) .EQ. 'G') THEN
        XBEG=AMAX1(PARM(I+1)-3.0*PARM(I+2),XD(FITLO))
        XEND=AMIN1(PARM(I+1)+3.0*PARM(I+2),XD(FITHI))
    ELSE
        XBEG=AMAX1(PARM(I+1)-5.0*PARM(I+2),XD(FITLO))
        XEND=AMIN1(PARM(I+1)+5.0*PARM(I+2),XD(FITHI))
    ENDIF
    IBEG=(XBEG-DST)/DNK+1
    IEND=(XEND-DST)/DNK+1
    IF ((IBEG .GT. ENDCHN) .OR. (IEND .LT. BEGCHN)) GOTO 4430
    DO 4420 J=IBEG,IEND
        YFT(J)=XBND(XD(J),PARM(I),PARM(NPARMS-2),BTYP(I/3+1))
4420 CONTINUE
        CALL ZTABL(1,IEND-IBEG+1,XD(IBEG),YFT(IBEG))
        IPK=(PARM(I+1)-DST)/DNK+1
        IF (YD(IPK) .GT. YMDPNT) THEN
            CALL ZRTOI(XD(IPK),PARM(NPARMS),IX1,IX2)
            IX2=IX2+200
        ELSE
            CALL ZRTOI(XD(IPK),YD(IPK),IX1,IX2)
            IX2=IX2+400
        ENDIF
        NPK=NPK+1
        DO 4425 J=1,NPK-1
            IF (IABS(IX1-IXPK(J)) .GE. 375) GOTO 4425
            IF (IABS(IX2-IYPK(J)) .GE. 1125) GOTO 4425
            IX2=IYPK(J)+1125
4425 CONTINUE
            IXPK(NPK)=IX1
            IYPK(NPK)=IX2
            CALL ZPU
            CALL ZPA(IX1,IX2)
            CALL ZCP(0.0,0.25,1)
            WRITE(OUTLINE,94430) PARM(I+1)
94430 FORMAT('POS = ',F7.2)
            CALL ZSPRLB(OUTLINE,13,0,0,-1,0.0,0.0)
            CALL ZCP(0.0,0.0,0)
            WRITE(OUTLINE,94440) PARM(I+2)
94440 FORMAT('WDT = ',F7.2)
            CALL ZSPRLB(OUTLINE,13,0,0,-1,0.0,0.0)

```

CCCCCCCC

```
*****
**  START OF SUBROUTINES  **
*****
```

CCCCCCCCCCCC

**INPUT :**

```

INTEGER*2 IBEG, IEND, I, J
REAL*4 DNK, Y1, Y2, X, YFT, Y, C, D
PARAMETER (MAXPTS=4000)
DIMENSION Y (MAXPTS), YFT (MAXPTS), X (MAXPTS)
COMMON /DT1COM/ Y, YFT, X

```

```

1000 CONTINUE
      AREA=DNK/3*(Y1+(C*4)+D*2+Y2)
      RETURN
      END

```

c c c c c

**PLTPNT :** ROUTINE THAT DISPLAYS OR PLOTS THE DATA POINTS  
OF A SPECTRUM.



C  
C  
C  
C

INPUT :

R\*4            X1,X2            X AXIS VALUES OF THE FIRST AND LAST POINTS

LOGICAL\*2    PLT,FAX,FAL,BOX,ILN  
INTEGER\*2    ND,IPN,IPNA,ICHR,J1,J2,I1,I2  
REAL\*4       Y,X,YD,CHH,CHW,DST,DD,DNK,OW,OH,X1,X2  
CHARACTER\*1 CHR  
CHARACTER\*7 DEV  
PARAMETER (MAXPTS=4000)  
DIMENSION Y(MAXPTS),YD(MAXPTS),X(MAXPTS)  
COMMON /DT1COM/ Y,YD,X  
COMMON /DT9COM/ PLT,DEV  
COMMON /DTPFRM/ ICHR,IPN,ILN,CHW,CHH,FAX,IPNA,FAL,BOX  
COMMON /DZ3COM/ ND,DST,DD,DK

CHR=CHAR(ICHR)  
I1=ITAB(X1)  
I2=ITAB(X2)  
IPT=I2-I1+1  
IF (PLT) THEN  
  CALL NWPLTP  
  IF (ND .GT. 100) THEN  
    OW=CHW  
    OH=CHH  
    CHW=0.1/(ND/200)  
    CHH=2\*CHW  
    CALL QTABL(1,IPT,X(I1),Y(I1))  
    CHW=OW  
    CHH=OH  
    GOTO 9999  
  ENDIF  
  DO 1000 I=I1,I2  
    J1=ISCLP(X(I),0)-40  
    J2=ISCLP(Y(I),1)-70  
    CALL ZPTXT(1,CHR,IPN,J1,J2)  
    IF (ILN) THEN  
      CALL ZSETUP(-1,IPN,0,IPN)  
      CALL ETABL(1,ND,X,Y)  
    ENDIF  
  1000 CONTINUE  
  ELSE  
    CALL NWPLTS  
    IF (ND .GT. 100) THEN  
      CALL QTABL(0,IPT,X(I1),Y(I1))  
      GOTO 9999  
    ENDIF  
    DO 2000 I=I1,I2  
      J1=ISCLS(X(I),0)-5  
      J2=ISCLS(Y(I),1)-5  
      CALL QGTXT(1,CHR,IPN,J1,J2,0)  
      IF (ILN) THEN

```

                CALL QSETUP(0,IPN,-2,IPN)
                CALL QTABL(1,ND,X,Y)
            ENDIF
2000    CONTINUE
        ENDIF
9999    RETURN
        END
C -----
C    SUBROUTINE PPM
C
C    PPM      :  MODIFIES THE X AXIS SCALING AND THE PARAMETERS OF THE
C                DECONVOLUTED BANDS.
C
LOGICAL*2    PLT,FLG
INTEGER*2    ND,I
REAL*4       DST,DD,DK,XMN,XX,XD,YD,YDF,BND1,BND2,YMN,YMX
CHARACTER*7   DEV
CHARACTER*80  OUTLINE,BLNK
PARAMETER     (MXPT=4000)
DIMENSION     YD(MXPT),XD(MXPT),YDF(MXPT),OX(MXPT),OY(MXPT)
COMMON /DT1COM/ YD,YDF,XD
COMMON /DT6COM/ YMN,YMX
COMMON /DT8COM/ XMN,XX
COMMON /DT9COM/ PLT,DEV
COMMON /DTPSCL/ FLG
COMMON /DTWRT / OUTLINE,BLNK
COMMON /DZ2COM/ OY,OX
COMMON /DZ3COM/ ND,DST,DD,DK
CALL YMAX(1,ND)
CALL XMAX(1,ND)
FLG=.TRUE.
YMX=1.1*YMX
YMN=YMN*0.9
0020    CALL NWPLTS
        CALL QTABL(1,ND,XD,YD)
        CALL QPTXT(80,BLNK,1,2,22)
        WRITE(OUTLINE,92005)
92005    FORMAT('MOVE CURSOR TO FIRST POSITION')
        CALL QPTXT(29,OUTLINE,1,2,22)
        CALL GRINPO(X1,DK/10)
        CALL QPTXT(80,BLNK,1,2,22)
        WRITE(OUTLINE,92010)
92010    FORMAT('ENTER NEW VALUE ')
        CALL QPTXT(16,OUTLINE,1,2,22)
        CALL QINNUM(20,22,10,BND1,1)
        CALL QPTXT(80,BLNK,1,2,22)
        WRITE(OUTLINE,92020)
92020    FORMAT('MOVE CURSOR TO SECOND POSITION')
        CALL QPTXT(37,OUTLINE,1,2,22)
        CALL GRINPO(X2,DK/10)
        CALL QPTXT(80,BLNK,1,2,22)
        WRITE(OUTLINE,92010)

```

```

CALL QPTXT(16,OUTLINE,1,2,22)
CALL QINNUM(20,22,10,BND2,1)
IF (BND1 .GT. BND2) CALL SWAP(BND1,BND2)
IF (X1 .GT. X2) CALL SWAP(X1,X2)
DK=ABS((BND2-BND1)/(X2-X1))
DST=BND1-(DK*(X1-1))
DD=DST+(ND-1)*DK
XMX=DD
XMN=DST
DO 0450 I=1,ND
    XD(I)=DST+(DK*(I-1))
    OX(I)=XD(I)
0450 CONTINUE
1111 RETURN
END
C -----
REAL*4 FUNCTION XBND(X,BPRM,BKGRND,BTYP)
C
C   XBND:    FUNCTION THAT CALCULATES THE VALUE IN INTENSITY
C             FOR A GAUSSIAN OR A LORENTZIAN BAND TO WHICH
C             THE BACKGROUND IS ADDED.
C
C   INPUT:
C
C       R*4      X          POINT FOR WHICH CALCULATION IS DESIRED
C       R*4      BPRM(3)    BAND PARAMETERS:  HEIGHT, POSITION, WIDTH
C       R*4      BKGRND(3)  PARAMETERS FOR PARABOLIC BACKGROUND
C       C*1      BTYP      TYPE OF BAND
C                       G    GAUSSIAN
C                       L    LORENTZIAN
C
C   CHARACTER*1  BTYP
C   REAL*4       X,BPRM,BKGRND
C   DIMENSION BPRM(3),BKGRND(3)
C
C   XBND=(BKGRND(3)*X+BKGRND(2))*X+BKGRND(1)
C   IF (BTYP .EQ. 'G') THEN
C       Z=(X-BPRM(2))/BPRM(3)
C       IF (ABS(Z) .LT. 9.0) XBND=XBND+BPRM(1)*EXP(-Z*Z/2.0)
C       RETURN
C   ENDIF
C   IF (BTYP .EQ. 'L') THEN
C       Z=(X-BPRM(2))*(X-BPRM(2))+BPRM(3)*BPRM(3)
C       XBND=XBND+BPRM(1)/Z
C       RETURN
C   ENDIF
C   RETURN
C   END
C -----
LOGICAL*2 FUNCTION ZBLNKF(STRING)
C
C   ZBLNKF :    LOGICAL FUNCTION THAT VERIFIES IF THE VALIDITY
C               AND THE LENGTH OF A FILE NAME.

```

```

C
C      OUTPUT :   .TRUE.   IF THE FILE NAME IS VALID
C                .FALSE.  IF THE FILE NAME IS NOT VALID
C
CHARACTER*1  A1,A2,A3,A4,A5,A6,A7,A8,A9,A10,A11,A12
CHARACTER*4  FILL
CHARACTER*12 FLE,WRT,STRING
COMMON /DT7COM/ FLE,WRT
FILL=' .FIT'
ZBLNKF=.TRUE.
ILN=0
READ (STRING,97500) A1,A2,A3,A4,A5,A6,A7,A8,A9,A10,A11,A12
IF ((A1 .LT. 'A') .OR. (A1 .GT. 'z')) GOTO 8000
  ILN=1
IF ((A2 .LT. '0') .OR. (A2 .GT. 'z')) GOTO 8000
  ILN=2
IF ((A3 .LT. '0') .OR. (A3 .GT. 'z')) GOTO 8000
  ILN=3
IF ((A4 .LT. '0') .OR. (A4 .GT. 'z')) GOTO 8000
  ILN=4
IF ((A5 .LT. '0') .OR. (A5 .GT. 'z')) GOTO 8000
  ILN=5
IF ((A6 .LT. '0') .OR. (A6 .GT. 'z')) GOTO 8000
  ILN=6
IF ((A7 .LT. '0') .OR. (A7 .GT. 'z')) GOTO 8000
  ILN=7
IF ((A8 .LT. '0') .OR. (A8 .GT. 'z')) GOTO 8000
  ILN=8
8000 IF (ILN .EQ. 0) THEN
  ZBLNKF=.FALSE.
  GOTO 9999
ENDIF
FLE=STRING
IF (ILN .EQ. 1) WRITE(WRT,99001) A1,FILL
IF (ILN .EQ. 2) WRITE(WRT,99002) A1,A2,FILL
IF (ILN .EQ. 3) WRITE(WRT,99003) A1,A2,A3,FILL
IF (ILN .EQ. 4) WRITE(WRT,99004) A1,A2,A3,A4,FILL
IF (ILN .EQ. 5) WRITE(WRT,99005) A1,A2,A3,A4,A5,FILL
IF (ILN .EQ. 6) WRITE(WRT,99006) A1,A2,A3,A4,A5,A6,FILL
IF (ILN .EQ. 7) WRITE(WRT,99007) A1,A2,A3,A4,A5,A6,A7,FILL
IF (ILN .EQ. 8) WRITE(WRT,99008) A1,A2,A3,A4,A5,A6,A7,A8,FILL
9999 RETURN
97500 FORMAT(12(A1))
98000 FORMAT(8(A1))
99001 FORMAT(A1,A4)
99002 FORMAT(2(A1),A4)
99003 FORMAT(3(A1),A4)
99004 FORMAT(4(A1),A4)
99005 FORMAT(5(A1),A4)
99006 FORMAT(6(A1),A4)
99007 FORMAT(7(A1),A4)
99008 FORMAT(8(A1),A4)

```

END

```
C-----
C      INTEGER*2 FUNCTION  ITAB (VALUE)
C
C      ITAB   : RETURNS THE INTEGER VALUE OF THE ARRAY INDEX
C               FOR AN INPUT VALUE.
C
C      INPUT :
C
C      R*4      VALUE      REAL X AXIS VALUE
C
C      REAL*4    VALUE,DST,DD,DK
C      COMMON    /DZ3COM/ INP,DST,DD,DK
C
C      ITAB=NINT((VALUE-DST)/DK+1)
C      IF (ITAB .LT. 1) ITAB=1
C      IF (ITAB .GT. INP) ITAB=INP
C      RETURN
C      END
```

```
C-----
C      INTEGER*2 FUNCTION  ILNG (STRNG1,MAXLNG)
C
C      ILNG : RETURNS THE LENGTH (INTEGER VALUE) OF A STRING.
C
C      INPUT :
C
C      C*80      STRING1  CHARACTER STRING TO BE ANALYZED
C      I*2        MAXLNG   MAXIMUM LENGTH OF THE STRING
C
C      INTEGER*2  MAXLNG
C      CHARACTER*1 A1,A2,A3,A4,A5,A6,A7,A8,A9,A0,B1,B2,B3,B4,B5
C      CHARACTER*1 B6,B7,B8,B9,B0,C1,C2,C3,C4,C5,C6,C7,C8,C9,C0,D1,
1      D2,D3,D4,D5,D6,D7,D8,D9,D0,E1,E2,E3,E4,E5,E6,E7,
2      E8,E9,E0,F1,F2,F3,F4,F5,F6,F7,F8,F9,F0
C      CHARACTER*80 STRNG1
C
C      READ (STRNG1,98000) A1,A2,A3,A4,A5,A6,A7,A8,A9,A0,B1,B2,B3,B4,B5,
1      B6,B7,B8,B9,B0,C1,C2,C3,C4,C5,C6,C7,C8,C9,C0,D1,
2      D2,D3,D4,D5,D6,D7,D8,D9,D0,E1,E2,E3,E4,E5,E6,E7,
3      E8,E9,E0,F1,F2,F3,F4,F5,F6,F7,F8,F9,F0
C      IF (MAXLNG .LE. 50) GOTO 0005
C      IF (MAXLNG .LE. 30) GOTO 0030
C      IF (MAXLNG .LE. 20) GOTO 0120
C      IF ((F0 .GT. ' ') .AND. (F0 .LE. '~')) THEN
C          ILNG=60
C          GOTO 9999
C      ENDIF
C      IF ((F9 .GT. ' ') .AND. (F9 .LE. '~')) THEN
C          ILNG=59
C          GOTO 9999
C      ENDIF
C      IF ((F8 .GT. ' ') .AND. (F8 .LE. '~')) THEN
```

```

        ILNG=58
        GOTO 9999
    ENDIF
    IF ((F7 .GT. ' ') .AND. (F7 .LE. '~')) THEN
        ILNG=57
        GOTO 9999
    ENDIF
    IF ((F6 .GT. ' ') .AND. (F6 .LE. '~')) THEN
        ILNG=56
        GOTO 9999
    ENDIF
    IF ((F5 .GT. ' ') .AND. (F5 .LE. '~')) THEN
        ILNG=55
        GOTO 9999
    ENDIF
    IF ((F4 .GT. ' ') .AND. (F4 .LE. '~')) THEN
        ILNG=54
        GOTO 9999
    ENDIF
    IF ((F3 .GT. ' ') .AND. (F3 .LE. '~')) THEN
        ILNG=53
        GOTO 9999
    ENDIF
    IF ((F2 .GT. ' ') .AND. (F2 .LE. '~')) THEN
        ILNG=52
        GOTO 9999
    ENDIF
    IF ((F1 .GT. ' ') .AND. (F1 .LE. '~')) THEN
        ILNG=51
        GOTO 9999
    ENDIF
0005 IF ((E0 .GT. ' ') .AND. (E0 .LE. '~')) THEN
        ILNG=50
        GOTO 9999
    ENDIF
    IF ((E9 .GT. ' ') .AND. (E9 .LE. '~')) THEN
        ILNG=49
        GOTO 9999
    ENDIF
    IF ((E8 .GT. ' ') .AND. (E8 .LE. '~')) THEN
        ILNG=48
        GOTO 9999
    ENDIF
    IF ((E7 .GT. ' ') .AND. (E7 .LE. '~')) THEN
        ILNG=47
        GOTO 9999
    ENDIF
    IF ((E6 .GT. ' ') .AND. (E6 .LE. '~')) THEN
        ILNG=46
        GOTO 9999
    ENDIF
    IF ((E5 .GT. ' ') .AND. (E5 .LE. '~')) THEN

```

```

        ILNG=45
        GOTO 9999
    ENDIF
    IF ((E4 .GT. ' ') .AND. (E4 .LE. '~')) THEN
        ILNG=44
        GOTO 9999
    ENDIF
    IF ((E3 .GT. ' ') .AND. (E3 .LE. '~')) THEN
        ILNG=43
        GOTO 9999
    ENDIF
    IF ((E2 .GT. ' ') .AND. (E2 .LE. '~')) THEN
        ILNG=42
        GOTO 9999
    ENDIF
    IF ((E1 .GT. ' ') .AND. (E1 .LE. '~')) THEN
        ILNG=41
        GOTO 9999
    ENDIF
    IF ((D0 .GT. ' ') .AND. (D0 .LE. '~')) THEN
        ILNG=40
        GOTO 9999
    ENDIF
    IF ((D9 .GT. ' ') .AND. (D9 .LE. '~')) THEN
        ILNG=39
        GOTO 9999
    ENDIF
    IF ((D8 .GT. ' ') .AND. (D8 .LE. '~')) THEN
        ILNG=38
        GOTO 9999
    ENDIF
    IF ((D7 .GT. ' ') .AND. (D7 .LE. '~')) THEN
        ILNG=37
        GOTO 9999
    ENDIF
    IF ((D6 .GT. ' ') .AND. (D6 .LE. '~')) THEN
        ILNG=36
        GOTO 9999
    ENDIF
    IF ((D5 .GT. ' ') .AND. (D5 .LE. '~')) THEN
        ILNG=35
        GOTO 9999
    ENDIF
    IF ((D4 .GT. ' ') .AND. (D4 .LE. '~')) THEN
        ILNG=34
        GOTO 9999
    ENDIF
    IF ((D3 .GT. ' ') .AND. (D3 .LE. '~')) THEN
        ILNG=33
        GOTO 9999
    ENDIF
    IF ((D2 .GT. ' ') .AND. (D2 .LE. '~')) THEN

```

```

        ILNG=32
        GOTO 9999
    ENDIF
    IF ((D1 .GT. ' ') .AND. (D1 .LE. '~')) THEN
        ILNG=31
        GOTO 9999
    ENDIF
0030 IF ((C0 .GT. ' ') .AND. (C0 .LE. '~')) THEN
        ILNG=30
        GOTO 9999
    ENDIF
    IF ((C9 .GT. ' ') .AND. (C9 .LE. '~')) THEN
        ILNG=29
        GOTO 9999
    ENDIF
    IF ((C8 .GT. ' ') .AND. (C8 .LE. '~')) THEN
        ILNG=28
        GOTO 9999
    ENDIF
    IF ((C7 .GT. ' ') .AND. (C7 .LE. '~')) THEN
        ILNG=27
        GOTO 9999
    ENDIF
    IF ((C6 .GT. ' ') .AND. (C6 .LE. '~')) THEN
        ILNG=26
        GOTO 9999
    ENDIF
    IF ((C5 .GT. ' ') .AND. (C5 .LE. '~')) THEN
        ILNG=25
        GOTO 9999
    ENDIF
    IF ((C4 .GT. ' ') .AND. (C4 .LE. '~')) THEN
        ILNG=24
        GOTO 9999
    ENDIF
    IF ((C3 .GT. ' ') .AND. (C3 .LE. '~')) THEN
        ILNG=23
        GOTO 9999
    ENDIF
    IF ((C2 .GT. ' ') .AND. (C2 .LE. '~')) THEN
        ILNG=22
        GOTO 9999
    ENDIF
    IF ((C1 .GT. ' ') .AND. (C1 .LE. '~')) THEN
        ILNG=21
        GOTO 9999
    ENDIF
0120 IF ((B0 .GT. ' ') .AND. (B0 .LE. '~')) THEN
        ILNG=20
        GOTO 9999
    ENDIF
    IF ((B9 .GT. ' ') .AND. (B9 .LE. '~')) THEN

```



```

        ILNG=19
        GOTO 9999
    ENDIF
    IF ((B8 .GT. ' ') .AND. (B8 .LE. '~')) THEN
        ILNG=18
        GOTO 9999
    ENDIF
    IF ((B7 .GT. ' ') .AND. (B7 .LE. '~')) THEN
        ILNG=17
        GOTO 9999
    ENDIF
    IF ((B6 .GT. ' ') .AND. (B6 .LE. '~')) THEN
        ILNG=16
        GOTO 9999
    ENDIF
    IF ((B5 .GT. ' ') .AND. (B5 .LE. '~')) THEN
        ILNG=15
        GOTO 9999
    ENDIF
    IF ((B4 .GT. ' ') .AND. (B4 .LE. '~')) THEN
        ILNG=14
        GOTO 9999
    ENDIF
    IF ((B3 .GT. ' ') .AND. (B3 .LE. '~')) THEN
        ILNG=13
        GOTO 9999
    ENDIF
    IF ((B2 .GT. ' ') .AND. (B2 .LE. '~')) THEN
        ILNG=12
        GOTO 9999
    ENDIF
    IF ((B1 .GT. ' ') .AND. (B1 .LE. '~')) THEN
        ILNG=11
        GOTO 9999
    ENDIF
    IF ((A0 .GT. ' ') .AND. (A0 .LE. '~')) THEN
        ILNG=10
        GOTO 9999
    ENDIF
    IF ((A9 .GT. ' ') .AND. (A9 .LE. '~')) THEN
        ILNG=9
        GOTO 9999
    ENDIF
    IF ((A8 .GT. ' ') .AND. (A8 .LE. '~')) THEN
        ILNG= 8
        GOTO 9999
    ENDIF
    IF ((A7 .GT. ' ') .AND. (A7 .LE. '~')) THEN
        ILNG= 7
        GOTO 9999
    ENDIF
    IF ((A6 .GT. ' ') .AND. (A6 .LE. '~')) THEN

```

```

        ILNG= 6
        GOTO 9999
    ENDIF
    IF ((A5 .GT. ' ') .AND. (A5 .LE. '~')) THEN
        ILNG= 5
        GOTO 9999
    ENDIF
    IF ((A4 .GT. ' ') .AND. (A4 .LE. '~')) THEN
        ILNG= 4
        GOTO 9999
    ENDIF
    IF ((A3 .GT. ' ') .AND. (A3 .LE. '~')) THEN
        ILNG= 3
        GOTO 9999
    ENDIF
    IF ((A2 .GT. ' ') .AND. (A2 .LE. '~')) THEN
        ILNG= 2
        GOTO 9999
    ENDIF
    IF ((A1 .GT. ' ') .AND. (A1 .LE. '~')) THEN
        ILNG= 1
        GOTO 9999
    ENDIF
    ILNG=0
9999 RETURN
98000 FORMAT(60(A1))
END

```

```

-----
C-----
C      INTEGER*2 FUNCTION ISCLP(X,I)
C
C      ISCLP :   SCALING FUNCTION THAT RETURNS THE PLOTTER PEN
C                COORDINATE FOR AN X OR Y DATA POINT.
C
C      INPUT :
C
C      I*2      I      INTEGER FLAG RELATED TO THE AXIS TO BE SCALED
C                0      X AXIS
C                1      Y AXIS
C
C      R*4      X      X OR Y AXIS DATA POINT TO BE SCALED
C
C      INTEGER*2 IXL,IXH,IYL,IYH,I
C      REAL*4    XMN,XMX,YNM,YMY,X
C      COMMON /DT6COM/  YMN,YMX
C      COMMON /DT8COM/  XMN,XMX
C      COMMON /DTPAXS/  IXL,IXH,IYL,IYH
C
C      IF (I .EQ. 0) THEN
C          ISCLP=NINT(((X-XMN)*(IXH-IXL)/(XMX-XMN))+IXL)
C      ELSE
C          ISCLP=NINT(((X-YNM)*(IYH-IYL)/(YMY-YNM))+IYL)
C      ENDIF

```

```

RETURN
END
-----
C
C      INTEGER*2 FUNCTION ISCLS(X,I)
C
C      ISCLS :   SCALING FUNCTION THAT RETURNS THE SCREEN PIXEL
C                COORDINATE FOR AN X OR Y DATA POINT.
C
C      INPUT :
C
C      I*2      I      EXECUTION FLAG RELATED TO THE AXIS TO BE SCALED
C                0      X AXIS
C                1      Y AXIS
C
C      R*4      X      X OR Y AXIS DATA POINT VALUE TO BE SCALED
C
C      INTEGER*2 IXL,IXH,IYL,IYH,HDRLNG
C      INTEGER*2 I,IXALBL,IXFMT,IXLNG,IYALBL,IYFMT,IYLANG
C      REAL*4     XMN,XMX,YNM,YMY,X
C      CHARACTER*80 HDRLNE,CXLBL,CYLBL
C      COMMON      /DTPPLT/ IXL,IXH,IYL,IYH,HDRLNE,HDRLNG,
1                    IXALBL,IXFMT,CXLBL,IXLNG,
2                    IYALBL,IYFMT,CYLBL,IYLANG
C      COMMON      /DT6COM/ YNM,YMY
C      COMMON      /DT8COM/ XMN,XMX
C
C      IF (I .EQ. 0) THEN
C          ISCLS=NINT(((X-XMN)*(IXH-IXL)/(XMX-XMN))+IXL)
C      ELSE
C          ISCLS=NINT(((X-YNM)*(IYH-IYL)/(YMY-YNM))+IYL)
C      ENDIF
C      RETURN
C      END
-----
C
C      SUBROUTINE DISK(FL)
C
C      DISK :   OPENS THE FILES FOR A READ OR WRITE OPERATION TO DISK.
C
C      INPUT :
C
C      B*2      FLG      LOGICAL FLAG FOR THE DISK OPERATION
C                .TRUE.  READ OPERATION
C                .FALSE. WRITE OPERATION
C
C      LOGICAL*2  FLG,OK,LIOFLG
C      CHARACTER*1 KEY
C      CHARACTER*12 FLE,WRT,STRING
C      COMMON /DT7COM/  FLE,WRT
C
C      0010 CALL ECRAN(0,0,20)
C      WRITE(0,90010) FLE
C      WRITE(0,90020) WRT
C      WRITE(0,*)

```

```

WRITE(0,*)
IF (FLG) THEN
    WRITE(0,90030)
    WRITE(0,90040)
    KEY=ZGET(1)
    IF (KEY .EQ. 'E') THEN
C
C      GET NAME OF FILE TO PROCESS THEN CHECK FOR ITS EXISTENCE
C
0500      WRITE(0,*)
          WRITE(0,90050)
          READ(0,90060) STRING
          OK=ZBLNKF(STRING)
          IF (.NOT. OK) GOTO 0500
          INQUIRE(FILE=WRT,EXIST=LIOFLG)
          IF (LIOFLG) THEN
              WRITE(0,90220) WRT
              KEY=ZGET(1)
              IF (KEY .EQ. 'Y') THEN
                  OPEN(1,FILE=WRT,STATUS='OLD',ACCESS='SEQUENTIAL')
              ELSE
                  GOTO 0500
              ENDIF
          ELSE
              OPEN(1,FILE=WRT,STATUS='NEW',ACCESS='SEQUENTIAL')
          ENDIF
      ELSE
          OPEN(1,FILE=WRT,STATUS='NEW',ACCESS='SEQUENTIAL')
      ENDIF
ELSE
    WRITE(0,90070)
    WRITE(0,90040)
    KEY=ZGET(1)
    IF (KEY .EQ. 'E') THEN
1500      WRITE(0,*)
          WRITE(0,90050)
          READ(0,90060) STRING
          OK=ZBLNKF(STRING)
          IF (.NOT. OK) GOTO 1500
      ENDIF
      INQUIRE(FILE=FLE,EXIST=LIOFLG)
      IF (.NOT. LIOFLG) THEN
          WRITE(0,91000) FLE
          KEY=ZGET(0)
          GOTO 0010
      ENDIF
      OPEN(1,FILE=FLE,STATUS='OLD',ACCESS='SEQUENTIAL')
    ENDIF
    RETURN
90010 FORMAT(2X,'ACTIVE FILE: ',A12/)
90020 FORMAT(2X,'WRITE FILE: ',A12/)
90030 FORMAT(2X,'(E)NTER NEW NAME FOR WRITE FILE'/)

```

```

90040 FORMAT(2X,'(K)EEP CURRENT NAME'/)
90050 FORMAT(2X,'ENTER NEW NAME: '\)
90060 FORMAT(A12)
90070 FORMAT(2X,'(E)NTER NEW NAME FOR LOAD FILE')
90220 FORMAT(2X,A12,' EXISTS. OVERWRITE? (Yes or No) '\)
91000 FORMAT(2X,A12,' DOES NOT EXISTS. ENTER NEW NAME'/)
END

```

```

C-----
SUBROUTINE ECRAN (IX,IY,IZ)

```

```

C
C      ECRAN : SCREEN MANAGEMENT
C
C      IX : GRAPHIC MODE OF THE MONITOR
C      IY : CURSOR COLUMN
C      IZ : CURSOR LINE
C
C      CALL QSMODE (IX)
C      CALL QCMOV (IY,IZ)
C      RETURN
C      END

```

```

C-----
SUBROUTINE NMRBND (X,PARM,YFT,DYDA,NPARM,INIT)

```

```

C
C      NMRBND : CALCULATES THE INTENSITY OF A DATA POINT AND THE
C                PARTIAL DERIVATIVES FOR TWO THEORETICAL FUNCTIONS,
C                I.E. THE GAUSSIAN OR THE LORENTZIAN FUNCTIONS.
C
C      INPUT:
C
C      X          POINT FOR WHICH CALCULATION IS DESIRED
C      PARM(NPARM) BAND PARAMETERS STORED LINEARLY SUCH THAT
C                  PARM(I), PARM(I+1) AND PARM(I+2) ARE
C                  PARAMETERS FOR BAND (I-1)/3. ORDERING
C                  OF PARAMETERS IS HEIGHT, CENTER, WIDTH.
C                  PARM(NPARM-2), PARM(NPARM-1), PARM(NPARM)
C                  ARE PARAMETERS FOR A PARABOLIC BACKGROUND.
C      NPARM      NUMBER OF PARAMETERS
C      INIT       EXECUTION CONTROL FLAG
C                  - -1      DO NOT CALCULATE PARTIAL
C                           DERIVATIVES
C                  - 0      INITIALIZE ROUTINE
C                  - 1      ALL OTHER TIMES (ROUTINE SETS
C                           TO 1 AFTER INITIALIZATION)
C
C      OUTPUT:
C
C      YFT        INTENSITY VALUE OF THE FUNCTION AT X
C      DYDA (NPARM) ARRAY OF PARTIAL DERIVATIVES WITH RESPECT TO
C                  PARAMETERS EVALUATED AT X
C      INIT       SET TO .FALSE. AFTER FIRST CALL
C
C      CHARACTER*1 BTYP
C      INTEGER*2   INIT,NPARM,MAXBND

```

```

REAL*4      X,YFT,DYDA
REAL*4      Z,EX,G,L,HGT,POS,WDT
PARAMETER (MAXBND=33)
DIMENSION PARM(NPARM),BTYP(MAXBND),DYDA(NPARM)
COMMON /BKIND/ BTYP

YFT=(PARM(NPARM)*X+PARM(NPARM-1))*X+PARM(NPARM-2)
IF (INIT.NE.-1) THEN
  DYDA(NPARM-2)=1.0
  DYDA(NPARM-1)=X
  DYDA(NPARM)=X*X
ENDIF
DO 1000 I=1,NPARM-3,3
  HGT = PARM(I)
  POS = PARM(I+1)
  WDT = PARM(I+2)
  IF (BTYP(I/3+1).EQ.'G') THEN
    Z = (X-POS)/WDT
    IF (ABS(Z).GE.7.0) THEN
      IF (INIT.NE.-1) THEN
        DYDA(I)=0.0
        DYDA(I+1)=0.0
        DYDA(I+2)=0.0
      ENDIF
    ELSE
      EX = EXP(-Z*Z/2.0)
      G = HGT*EX
      YFT = YFT+G
      IF (INIT.NE.-1) THEN
        DYDA(I) = EX
        DYDA(I+1) = G*Z/WDT
        DYDA(I+2) = DYDA(I+1)*Z
      ENDIF
    ENDIF
    GOTO 1000
  ENDIF
  IF (BTYP(I/3+1).EQ.'L') THEN
    Z = (X-POS)*(X-POS)+WDT*WDT
    L = HGT/Z
    YFT = YFT+L
    IF (INIT.NE.-1) THEN
      DYDA(I) = 1.0/Z
      DYDA(I+1) = 2.0*L*(X-POS)/Z
      DYDA(I+2) = -2.0*L*WDT/Z
    ENDIF
  ENDIF
1000 CONTINUE
RETURN
END

```

```

C -----
C SUBROUTINE GRINPO(GO,DK)

```

```

C      GRINPO : GRAPHICALLY INPUTS THE X AXIS VALUE.
C
C      GO      : OUPUT AXIS VALUE
C      DK      : AXIS INCREMENT
C
      INTEGER*2      CKKEY
      INTEGER*2      IAN,LNG,LNE,COL,IMIN,IMAX,IDUM
      REAL*4         GO,VMIN,VMAX,DK,FMIN,FMAX
      CHARACTER*10    FMT
      CHARACTER*80     OUTLNE,BLNK
      COMMON /DT6COM/  FMIN,FMAX
      COMMON /DT8COM/  VMIN,VMAX
      COMMON /DTWRT /  OUTLNE,BLNK
      COMMON /ZAP/     IMIN,IMAX

      FMT=' (F8.3)'
      LNG=8
      COL=70
      LNE=22
      IF (LNG .GT. 0) CALL QPTXT(LNG,BLNK,1,COL,LNE)
      XPOS=VMIN
      CALL QRTOI(0.0,FMIN,IDUM,IMIN)
      CALL QRTOI(0.0,FMAX,IDUM,IMAX)
      CALL SWITCH(XPOS)
1000 WRITE(OUTLNE,FMT) XPOS
      CALL QPTXT(LNG,OUTLNE,1,COL,LNE)
1005 IAN=CKKEY(0)
      IF (IAN .EQ. 0) GOTO 1005
C
C      MOVE TO THE LEFT SIDE OF THE SCREEN, <HOME> PRESSED
C
1010 IF (IAN .EQ. -71) THEN
      CALL SWITCH(XPOS)
      XPOS=VMIN
      CALL SWITCH(XPOS)
      GOTO 1000
ENDIF
C
C      MOVE TO THE RIGHT SIDE OF THE SCREEN, <END> PRESSED
C
      IF (IAN .EQ. -79) THEN
      CALL SWITCH(XPOS)
      XPOS=VMAX
      CALL SWITCH(XPOS)
      GOTO 1000
ENDIF
C
C      MOVE LEFT, <LEFT ARROW> PRESSED
C
      IF (IAN .EQ. -75) THEN
      CALL SWITCH(XPOS)
      XPOS=AMAX1(XPOS-DK,VMIN)

```

```

        CALL SWITCH(XPOS)
        GOTO 1000
    ENDIF
C
C     MOVE RIGHT, <RIGHT ARROW> PRESSED
C
1025 IF (IAN .EQ. -77) THEN
        CALL SWITCH(XPOS)
        XPOS=AMIN1(XPOS+DK,VMAX)
        CALL SWITCH(XPOS)
        GOTO 1000
    ENDIF
C
C     MOVE 10 UNIT RIGHT, <RIGHT ARROW> PRESSED
C
    IF (IAN .EQ. -72) THEN
        CALL SWITCH(XPOS)
        XPOS=AMIN1(XPOS+10*DK,VMAX)
        CALL SWITCH(XPOS)
        GOTO 1000
    ENDIF
C
C     MOVE 10 UNIT LEFT, <LEFT ARROW> PRESSED
C
    IF (IAN .EQ. -80) THEN
        CALL SWITCH(XPOS)
        XPOS=AMAX1(XPOS-10*DK,VMIN)
        CALL SWITCH(XPOS)
        GOTO 1000
    ENDIF
C
C     MOVE 50 UNIT LEFT, <Pg Dn> PRESSED
C
    IF (IAN .EQ. -81) THEN
        CALL SWITCH(XPOS)
        XPOS=AMAX1(XPOS-50*DK,VMIN)
        CALL SWITCH(XPOS)
        GOTO 1000
    ENDIF
C
C     MOVE 50 UNIT RIGHT, <Pg Up> PRESSED
C
    IF (IAN .EQ. -73) THEN
        CALL SWITCH(XPOS)
        XPOS=AMIN1(XPOS+50*DK,VMAX)
        CALL SWITCH(XPOS)
        GOTO 1000
    ENDIF
C
C     RETURN HAVE BEEN PRESS SO RETURN LINE POSITIN VALUE TO MAIN PGM
C
    IF (IAN .EQ. 13) THEN

```



```

        GO=XPOS
        RETURN
    ENDIF
    GOTO 1000
    END
C -----
    SUBROUTINE INTTL
C
C    INTTL :   INPUTS NEW TITLES STRINGS FOR A PLOT.
C
    INTEGER*2 IXL,IXH,IYL,IYH,HDRLNG
    INTEGER*2 IXALBL,IXFMT,IXLNG,IYALBL,IYFMT,IYLNG
    CHARACTER*1 KEY
    CHARACTER*80 HDRLNE,CXLBL,CYLBL
    COMMON /DTPPLT/ IXL,IXH,IYL,IYH,HDRLNE,HDRLNG,
1                IXALBL,IXFMT,CXLBL,IXLNG,
2                IYALBL,IYFMT,CYLBL,IYLNG

    CALL ECRAN(0,0,20)
    WRITE(0,90010) CXLBL
    WRITE(0,90015)
    KEY=ZGET(1)
    IF (KEY.EQ. 'N') THEN
        WRITE(0,*)
        WRITE(0,90020)
        READ(0,90120) CXLBL
        IXLNG=ILNG(CXLBL,30)
    ENDIF
    WRITE(0,*)
    WRITE(0,90030) CYLBL
    WRITE(0,90015)
    KEY=ZGET(1)
    IF (KEY.EQ. 'N') THEN
        WRITE(0,*)
        WRITE(0,90040)
        READ(0,90125) CYLBL
        IYLNG=ILNG(CYLBL,20)
    ENDIF
    WRITE(0,*)
    WRITE(0,90050) HDRLNE
    WRITE(0,90015)
    KEY=ZGET(1)
    IF (KEY.EQ. 'N') THEN
        WRITE(0,*)
        WRITE(0,90060)
        READ(0,90070) HDRLNE
        HDRLNG=ILNG(HDRLNE,50)
    ENDIF
    RETURN
90010 FORMAT(2X,A30,/' IS THE CURRENT X AXIS LABEL'/)
90015 FORMAT(2X,'DO YOU WANT TO KEEP THIS LABEL (Y)ES OR (N)O '\)
90020 FORMAT(2X,'ENTER NEW X LABEL THEN <CR>'/)

```

```

90030 FORMAT(2X,A20,/' IS THE CURRENT Y AXIS LABEL'/)
90040 FORMAT(2X,'ENTER NEW Y LABEL THEN <CR>'/)
90050 FORMAT(2X,A50,/' IS THE CURRENT TITLE'/)
90060 FORMAT(2X,'ENTER NEW TITLE THEN <CR>'/)
90070 FORMAT(A50)
90120 FORMAT(A30)
90125 FORMAT(A24)
      END

```

```

C -----
C SUBROUTINE LOAD (FLG)

```

```

C
C LOAD :   READS SPECTRUM DATA FILE FROM DISK.
C

```

```

C INPUT :
C      B*2   FLG   FLAG THAT INDICATES THAT DATA WERE RETRIEVED
C              .TRUE.  DATA WERE SUCCESSFULLY RETRIEVED
C              .FALSE. DATA WERE NOT SUCCESSFULLY RETRIEVED
C

```

```

      LOGICAL*2 FLGK,FLG,FLGFIT,FLAG
      INTEGER*2 ND,N,I
      REAL*4     YD,XD,OX,OY,YDF,DST,DND,DNK,XCNTR,XMX,XMN,YMX,YMN
      PARAMETER (MAXPTS=4000)
      DIMENSION YD (MAXPTS),YDF (MAXPTS),XD (MAXPTS)
      DIMENSION OY (MAXPTS),OX (MAXPTS)
      COMMON /DT1COM/  YD,YDF,XD
      COMMON /DT5COM/  FLGK,FLGFIT
      COMMON /DT6COM/  YMN,YMX
      COMMON /DT8COM/  XMN,XMX
      COMMON /DZ2COM/  OY,OX
      COMMON /DZ3COM/  ND,DST,DND,DNK

```

```

      FLAG=.FALSE.
      CALL DISK (FLAG)

```

```

C
C READ DATA FILE
C
      READ (1,*,ERR=0721) DST,DND,DNK,ND
      XCNTR=DST
      DO 0718 I=1, ND
          XD(I)=XCNTR
          OX(I)=XCNTR
          XCNTR=XCNTR + DNK
          READ (1,*,ERR=0721) YD(I)
          OY(I)=YD(I)
0718 CONTINUE
      READ (1,*,ERR=0721) YMX,YMN
      IF (YMN .LT. 0) THEN
          Y=2*ABS (YMN)
          DO 0720 I=1,ND
              YD(I)=YD(I)+Y
0720 CONTINUE
          YMN=ABS (YMN)

```

```

        YMX=YMXX+Y
    ENDIF
    CALL SMOOTH
    XMX=DND+10*DNK
    XMN=DST-10*DNK
    YMX=YMXX*1.1
    YMN=YMN*0.9
    GOTO 0722
C
C    DATA FILE NOT OK!
C
    0721 WRITE(0,91000)
    91000 FORMAT(2X,'THE FILE FORMAT IS NOT COMPATIBLE!!'/)
    KEY=ZGET(0)
    GOTO 9999
C
C    DATA FILE OK!
C
    0722 FLG=.TRUE.
    FLGFIT=.FALSE.
    FLGK=.FALSE.
    9999 RETURN
    END
C-----
    SUBROUTINE NBTIC(XMN,XMX,NTICS,MAJOR,MINOR)
C
C    NBTIC: AUTOSCALING ROUTINE THAT FIND THE PROPER SCALING AND
C           AXIS INCREMENTS FOR PLOT.
C
C    XMN : OUTPUT CORRECTED MINIMUM FOR  AXIS
C    XMX : OUTPUT CORRECTED MAXIMUM FOR  AXIS
C    NTICS: NUMBER OF MAJOR TICS ON AXIS
C    MAJOR: INCREMENT BETWEEN 2 MAJOR TICS ON  AXIS
C    MINOR: NUMBER OF MINOR TICS BETWEEN 2 MAJOR TICS
C
    INTEGER*2 NTICS,MINOR,ITSPCE
    REAL*4    XMN,XMX,TSPCE,TSPFRC,MAJOR
    IF (NTICS .EQ. 0.0) THEN
        MAJOR=0.0
        MINOR=0
        RETURN
    ENDIF
    TSPCE=ALOG10 (ABS ((XMX-XMN)/(NTICS-1)))
    ITSPCE=INT (TSPCE)
    TSPFRC=TSPCE-ITSPCE
    IF (TSPFRC .LT. 0.0) THEN
        TSPFRC=TSPFRC+1.0
        ITSPCE=ITSPCE-1
    ENDIF
    IF (TSPFRC .LT. 0.322) THEN
        MAJOR=2.0*10.0**ITSPCE
        MINOR=3
    
```

```

      GOTO 1000
    ENDIF
    IF (TSPFRC .LT. 0.415) THEN
      MAJOR=2.5*10.0**ITSPCE
      MINOR=4
      GOTO 1000
    ENDIF
    IF (TSPFRC .LT. 0.491) THEN
      MAJOR=3.0*10.0**ITSPCE
      MINOR=2
      GOTO 1000
    ENDIF
    IF (TSPFRC .LT. 0.613) THEN
      MAJOR=4.0*10.0**ITSPCE
      MINOR=3
      GOTO 1000
    ENDIF
    IF (TSPFRC .LT. 0.708) THEN
      MAJOR=5.0*10.0**ITSPCE
      MINOR=4
      GOTO 1000
    ENDIF
    IF (TSPFRC .LT. 0.785) THEN
      MAJOR=6.0*10.0**ITSPCE
      MINOR=5
      GOTO 1000
    ENDIF
    IF (TSPFRC .LT. 0.851) THEN
      MAJOR=7.0*10.0**ITSPCE
      MINOR=6
      GOTO 1000
    ENDIF
    IF (TSPFRC .LT. 0.881) THEN
      MAJOR=7.5*10.0**ITSPCE
      MINOR=4
      GOTO 1000
    ENDIF
    IF (TSPFRC .LT. 0.908) THEN
      MAJOR=8.0*10.0**ITSPCE
      MINOR=3
      GOTO 1000
    ENDIF
    IF (TSPFRC .GE. 0.908) THEN
      MAJOR=1.0*10.0** (ITSPCE+1)
      MINOR=4
    ENDIF
1000 IF (AMOD(XMN,MAJOR) .NE. 0.0) THEN
      IF (XMN .LE. 0.0) THEN
        XMN=MAJOR*(INT(XMN/MAJOR)-1)
      ELSE
        XMN=MAJOR*INT(XMN/MAJOR)
      ENDIF

```

```

ENDIF
IF (AMOD(XMX,MAJOR) .NE. 0.0) THEN
  IF (XMX .LE. 0.0) THEN
    XMX=MAJOR*INT(XMX/MAJOR)
  ELSE
    XMX=MAJOR*(INT(XMX/MAJOR)+1)
  ENDIF
ENDIF
NTICS=NINT(ABS(XMX-XMN)/MAJOR)+1
RETURN
END

-----
C SUBROUTINE NWSCL
C
C NWSCL : SPECIFIES AND CALCULATES TWO TYPES OF SCALING FOR A
C PLOT, I.E. MANUAL OR AUTO SCALED.
C
LOGICAL*2 FLG
REAL*4 XMX, YMN, YMX, XMN, DST, DD, DK
CHARACTER*1 KEY
COMMON /DTPSCL/ FLG
COMMON /DT6COM/ YMN, YMX
COMMON /DT8COM/ XMN, XMX
COMMON /DZ3COM/ ND, DST, DND, DNK
0010 CALL ECRAN(0,0,20)
WRITE(0,90010)
KEY=ZGET(1)
IF (KEY .EQ. 'N') THEN
  CALL PPM
  GOTO 9999
ENDIF
IF (KEY .EQ. 'M') THEN
  FLG=.TRUE.
  WRITE(0,*)
  WRITE(0,90020)
  READ(0,*,ERR=1000) XMN
  WRITE(0,90030)
  READ(0,*,ERR=1000) XMX
  WRITE(0,90040)
  IF (XMX .EQ. XMN) GOTO 1000
  IF (XMX .LT. XMN) CALL SWAP(XMX,XMN)
  READ(0,*,ERR=1000) YMN
  WRITE(0,90050)
  READ(0,*,ERR=1000) YMX
  IF (YMX .EQ. YMN) GOTO 1000
  IF (YMX .LT. YMN) CALL SWAP(YMX,YMN)
ELSE
  CALL XMAX(1,ND)
  CALL YMAX(1,ND)
  FLG=.FALSE.
ENDIF
GOTO 9999

```

```

1000 WRITE(0,*)
      WRITE(0,99020)
      KEY=ZGET(0)
      GOTO 0010
9999 RETURN
90010 FORMAT (2X,'(A)UTO OR (M)ANUAL SCALING OR (N)EW X AXIS SCALE')
90020 FORMAT (2X,'ENTER X AXIS MINIMUM: '\)
90030 FORMAT (2X,'ENTER X AXIS MAXIMUM: '\)
90040 FORMAT (2X,'ENTER Y AXIS MINIMUM: '\)
90050 FORMAT (2X,'ENTER Y AXIS MAXIMUM: '\)
99020 FORMAT (2X,'BAD ENTRY!!!'\)
      END
-----C-----
      SUBROUTINE NWPLTP
C
C      NWPLTP : AUTOMATED PLOTTING ROUTINE FOR THE PLOTTER.
C
      LOGICAL*2 FLGMAN,FAX,PLTSLW,FAL,PLT,MAJ,MIN,BOX,ILN
      INTEGER*2 IXL,IXH,IYL,IYH,IXALBL,IXFMT,IXLNG,IYALBL,IYFMT,IYLNG
      INTEGER*2 IXNTIC,IYNTIC,IXMN,IYMN,HDRLNG,PXH,PXL,PYL,PYH
      INTEGER*2 ICHR,IPN,IPNA,IH,IB,ND
      REAL*4     XMN,XXM,YMN,XXY,XMAJOR,YMAJOR,YD,YFT,XD,YADD
      REAL*4     CHRWDH,CHRHGH,CK,DD,DST
      CHARACTER*7 DEV
      CHARACTER*80 HDRLNE,CXLBL,CYLBL,BLNK,LNE,OUTLNE
      PARAMETER  (MXPT=4000)
      DIMENSION  YD(MXPT),YADD(MXPT),XD(MXPT),YFT(MXPT)
      COMMON /DT1COM/  YD,YFT,XD
      COMMON /DT4COM/  MAJ,MIN
      COMMON /DT6COM/  YMN,XXY
      COMMON /DT8COM/  XMN,XXM
      COMMON /DT9COM/  PLT,DEV
      COMMON /DZ3COM/  ND,DST,DND,DNK
      COMMON /DTPPLT/  IXL,IXH,IYL,IYH,HDRLNE,HDRLNG,
1                      IXALBL,IXFMT,CXLBL,IXLNG,
2                      IYALBL,IYFMT,CYLBL,IYLNG
      COMMON /DTPSCL/  FLGMAN
      COMMON /DTPFRM/  ICHR,IPN,ILN,CHRWDH,CHRHGH,FAX,IPNA,FAL,BOX
      COMMON /DTPAXS/  PXL,PXH,PYL,PYH
      COMMON /DTWRT /  OUTLNE,BLNK
      COMMON /DTYADD/  YADD
      IB=1450
      IH=565
      PLT=.FALSE.
      PLT=.TRUE.
      CALL QPTXT(80,BLNK,1,0,22)
      CALL QPTXT(47,'ARE YOU PLOTTING TRANSPARENCIES (Y)ES OR (N)O? '
1              ,1,2,22)
      KEY=ZGET(1)
      PLTSLW=.FALSE.
      IF (KEY.EQ. 'Y') PLTSLW=.TRUE.
      CALL QPTXT(80,BLNK,1,0,22)

```

```

WRITE (LNE, 90000)
CALL QPTXT (61, LNE, 1, 2, 22)
CALL QINPUT (KEY, 0)
IF (FLGMAN) THEN
    XMAJOR = (XMX - XMN) / 5
    YMAJOR = (YMX - YMN) / 5
ELSE
    CALL YMAX (1, ND)
    XMN = XD (1)
    XMX = XD (ND)
    XMX = XMX + 0.30 * ABS (XMX - XMN)
    YMX = YMX + 0.30 * ABS (YMX - YMN)
    IXNTIC = 5
    IYNTIC = 5
    CALL NBTIC (XMN, XMX, IXNTIC, XMAJOR, IXMN)
    CALL NBTIC (YMN, YMX, IYNTIC, YMAJOR, IYMN)
ENDIF
IF (.NOT. MAJ) THEN
    XMAJOR = 0
    YMAJOR = 0
ENDIF
IF (MIN) THEN
    IXMN = 1
    IYMN = 1
ELSE
    IXMN = 0
    IYMN = 0
ENDIF
CALL ZINIT (2, 1, ' ')
CALL ZSETUP (-1, IPN, ICHR, IPN)
CALL ZPLOT (PXL, PXH, PYL, PYH, XMN, XMX, YMN, YMX, XMN, YMN)
IF (PLTSLW) CALL ZVS (10.0)
CALL ZIW (0, 0, 10365, 7962.1)
IF (FAX) THEN
    CALL ZSI (CHRWDH, CHRHGH)
    CALL ZXAXIS (XMN, XMX, XMAJOR, IXMN, IXALBL, IXFMT)
    CALL ZYAXIS (YMN, YMX, YMAJOR, IYMN, IYALBL, IYFMT)
    IF (BOX) THEN
        CALL ZLINE (PXH, PYL, PXH, PYH, IPNA)
        CALL ZLINE (PXH, PYH, PXL, PYH, IPNA)
        CALL ZLINE (PXL + IB, PYH, PXL + IB, PYH + IH, IPNA)
        CALL ZLINE (PXL + IB, PYH + IH, PXH - IB, PYH + IH, IPNA)
        CALL ZLINE (PXH - IB, PYH + IH, PXH - IB, PYH, IPNA)
    ENDIF
ENDIF
ENDIF
IF (FAL) THEN
    CALL ZSP (IPNA)
    CALL ZDI (0.0, 1.0, 1)
    CALL ZSI (0.16, 0.27)
    CALL ZSPRLB (CYLBL, IYLANG, 400, 4000, 0, 0.0, 0.0)
    CALL ZDI (0.0, 0.0, 0)
    CALL ZSPRLB (CXLBL, IXLNG, 5182, 400, 0, 0.0, 0.0)

```

```

        CALL ZSPRLB(HDRLNE,HDRLNG,5182,PYH+225,0,0.0,0.0)
    ENDIF
9999 RETURN
90000 FORMAT
1('LOAD PENS, PAPER AND TURN PLOTTER ON. HIT A KEY TO CONTINUE!')
    END
C -----
    SUBROUTINE NWPLTS
C
C     NWPLTS : AUTOMATED PLOTTING ROUTINE FOR THE MONITOR SCREEN.
C
    LOGICAL*2 FLGMAN,FAX,FAL,MIN,MAJ,BOX,ILN
    INTEGER*2 IXL,IXH,IYL,IYH,IXALBL,IXFMT,IXLNG,IYALBL,IYFMT,IYLANG
    INTEGER*2 IXNTIC,IYNTIC,IXMN,IYMN,HDRLNG
    INTEGER*2 ICHR,IPN,IPNA,ICOLOR,ILNE,ND
    REAL*4     XMN,XXM,YMN,XXM,XMAJOR,YMAJOR,XD,YFT,YD,YADD
    REAL*4     CHRWDH,CHRRGH,DK,DD,DST
    CHARACTER*80 HDRLNE,CXLBL,CYLBL
    PARAMETER (MXPT=4000)
    DIMENSION YD(MXPT),YADD(MXPT),XD(MXPT),YFT(MXPT)
    COMMON /DT1COM/ YD,YFT,XD
    COMMON /DT4COM/ MAJ,MIN
    COMMON /DT6COM/ YMN,XXM
    COMMON /DT8COM/ XMN,XXM
    COMMON /DZ3COM/ ND,DST,DND,DNK
    COMMON /DTPPLT/ IXL,IXH,IYL,IYH,HDRLNE,HDRLNG,
1                  IXALBL,IXFMT,CXLBL,IXLNG,
2                  IYALBL,IYFMT,CYLBL,IYLANG
    COMMON /DTPSCL/ FLGMAN
    COMMON /DTPFRM/ ICHR,IPN,ILN,CHRWDH,CHRRGH,FAX,IPNA,FAL,BOX
    COMMON /DTYADD/ YADD

    CALL QSMODE(4)
    IF (FLGMAN) THEN
        XMAJOR=(XXM-XMN)/5
        YMAJOR=(YMN-XXM)/5
    ELSE
        CALL YMAX(1,ND)
        XMN=XD(1)
        XXM=XD(ND)
        XXM=XXM+0.30*ABS(XXM-XMN)
        YMN=XXM+0.30*ABS(YMN-XXM)
        IXNTIC=5
        IYNTIC=5
        CALL NBTIC(XMN,XXM,IXNTIC,XMAJOR,IXMN)
        CALL NBTIC(YMN,XXM,IYNTIC,YMAJOR,IYMN)
    ENDIF
    IF (.NOT. MAJ) THEN
        XMAJOR=0
        YMAJOR=0
    ENDIF
    IF (MIN) THEN

```



```

        IXMN=1
        IYMN=1
    ELSE
        IXMN=0
        IYMN=0
    ENDIF
    ICOLOR=0
    ILNE=1
    IF (ILN) THEN
        ICOLOR=IPN
        ILNE=0
    ENDIF
    CALL QSETUP (ILNE, ICOLOR, ICHR, IPN)
    CALL QPLOT (IXL, IXH, IYL, IYH, XMN, XMX, YMN, YMX, XMN, YMN,
1      0,1.0,1.5)
    IF (FAX) THEN
        CALL QXAXIS (XMN, XMX, XMAJOR, IXMN, IXALBL, IXFMT)
        CALL QYAXIS (YMN, YMX, YMAJOR, IYMN, IYALBL, IYFMT)
        IF (BOX) THEN
            CALL QLINE (IXH, IYH, IXH, IYL, IPNA)
            CALL QLINE (IXH, IYH, IXL, IYH, IPNA)
            CALL QLINE (IXH-1, IYL, IXH-1, IYH, IPNA)
            CALL QLINE (IXH, IYH-1, IXL, IYH-1, IPNA)
        ENDIF
    ENDIF
    IF (FAL) THEN
        IF (IXLNG .NE. 0) CALL QGTXT (IXLNG, CXLBL, IPNA,
1      (IXH+IXL-9*IXLNG)/2,10,0)
        IF (IYLANG .NE. 0) CALL QGTXT (IYLANG, CYLBL, IPNA, 50,
1      (IYH+IYL+14*IYLANG)/2,-1)
        IF (HDRLNG .NE. 0) CALL QGTXT (HDRLNG, HDRLNE, IPNA,
1      (IXH+IXL-9*HDRLNG)/2,330,0)
    ENDIF
    RETURN
    END

```

```

C-----
C      SUBROUTINE OUT(I)
C
C      OUT :   READS NEW OUTPUT DEVICE FOR THE DECONVOLUTION RESULTS.
C
C      INPUT, OUTPUT :
C      I*2      I      EXECUTION CONTROL FLAG, CHANNEL FOR OUTPUT
C                  1    OUTPUT TO SCREEN, CHANNEL 0
C                  2    OUTPUT TO PRINTER, CHANNEL 6
C
C      INTEGER*2  I
C      CHARACTER*1 KEY
C      CALL ECRAN(0,0,20)
C      WRITE(0,90010)
C      WRITE(0,*)
C      WRITE(0,90020)
C      WRITE(0,90030)

```

```

KEY=ZGET(1)
IF (KEY .EQ. '2') THEN
    I=6
    OPEN(6,FILE='PRN')
ELSE
    I=0
    CALL ECRAN(0,0,20)
ENDIF
RETURN
90010 FORMAT(22X,'OUTPUT DEVICE'//)
90020 FORMAT(22X,'1- Screen')
90030 FORMAT(22X,'2- Printer')
END
C -----
C SUBROUTINE PLTOPT
C
C PLTOPT : MENU CONTAINING ALL THE PLOTTING OPTIONS THAT CAN
C          BE MODIFIED (PEN, SYMBOLS, TYPE OF LINE, ...).
C
LOGICAL*2 FAX,FAL,GOOD,PLT,MAJ,MIN,BOX,ILN
INTEGER*2 ICHR,IPN,IPNA,ICH,HDRLNG
INTEGER*2 IXL,IXH,IYL,IYH,IXALBL,IXFMT,IXLNG,IYALBL,IYFMT,IYING
REAL*4    CHRWDH,CHRHGH,XH,XW
CHARACTER*1 KEY,CH
CHARACTER*3 STATX,STATL,LNETYP,STTMAJ,STTMIN,STTBOX
CHARACTER*7 DEV
CHARACTER*80 HDRLNE,CXLBL,CYLBL
COMMON /DTPPLT/ IXL,IXH,IYL,IYH,HDRLNE,HDRLNG,
1              IXALBL,IXFMT,CXLBL,IXLNG,
2              IYALBL,IYFMT,CYLBL,IYING
COMMON /DTPFRM/ ICHR,IPN,ILN,CHRWDH,CHRHGH,FAX,IPNA,FAL,BOX
COMMON /DT4COM/ MAJ,MIN
COMMON /DT9COM/ PLT,DEV

0030 CALL ECRAN(0,0,24)
WRITE(0,90020) DEV
CH=CHAR(ICH)
STATX='OFF'
IF (FAX) STATX='ON '
STATL='OFF'
IF (FAL) STATL='ON '
STTBOX='OFF'
IF (BOX) STTBOX='ON '
STTMAJ='OFF'
STTMIN='OFF'
IF (MAJ) STTMAJ='ON '
IF (.NOT. (MAJ) .AND. (MIN)) MIN=.NOT. MIN
IF (MIN) STTMIN='ON '
LNETYP='OFF'
IF (ILN) LNETYP='ON '
WRITE(0,90021) CH
WRITE(0,90022) IPN

```

```

WRITE(0,90023) CHRWDH,CHRHGH
WRITE(0,90024) IXFMT,IYFMT
WRITE(0,90025) LNETYP
WRITE(0,90026) STATX,STATL
WRITE(0,90027) STTMAJ,STTMIN
WRITE(0,90031) STTBOX
WRITE(0,90028)
KEY=ZGET(1)
WRITE(0,*)
WRITE(0,*)
IF (KEY .EQ. '1') THEN
    GOOD=.FALSE.
    WRITE(0,90030)
1000    ICH=CKKEY(0)
        IF (ICH .EQ. 0) GOTO 1000
        CH=CHAR(ICH)
        IF (CH .EQ. '+') GOOD=.TRUE.
        IF (CH .EQ. '#') GOOD=.TRUE.
        IF (CH .EQ. '*') GOOD=.TRUE.
        IF (CH .EQ. 'O') GOOD=.TRUE.
        IF (CH .EQ. 'o') GOOD=.TRUE.
        IF (CH .EQ. 'X') GOOD=.TRUE.
        IF (CH .EQ. 'x') GOOD=.TRUE.
        IF (GOOD) ICHR=ICHAR(CH)
    ENDIF
    IF (KEY .EQ. '2') THEN
        WRITE(0,90040)
        READ(0,99999,ERR=0030) ICH
        IF ((ICH .LE. 3) .AND. (ICH .GE. 1)) IPN =ICH
    ENDIF
    IF (KEY .EQ. '3') THEN
        WRITE(0,90041)
        READ(0,*,ERR=0030) XW
        IF ((XW .LE. 2.0) .AND. (XW .GT. 0)) CHRWDH=XW
        WRITE(0,*)
        WRITE(0,90042)
        READ(0,*,ERR=0030) XH
        IF ((XH .LE. 2.0) .AND. (XH .GT. 0)) CHRHGH=XH
    ENDIF
    IF (KEY .EQ. '4') THEN
        WRITE(0,90045)
        READ(0,99999,ERR=0030) ICH
        IF ((ICH .LE. 5) .AND. (ICH .GE. 0)) IXFMT=ICH
        WRITE(0,*)
        WRITE(0,90047)
        READ(0,99999,ERR=0030) ICH
        IF ((ICH .LE. 5) .AND. (ICH .GE. 0)) IYFMT=ICH
    ENDIF
    IF (KEY .EQ. '5') ILN=.NOT. ILN
    IF (KEY .EQ. '6') FAX=.NOT. FAX
    IF (KEY .EQ. '7') FAL=.NOT. FAL
    IF (KEY .EQ. '8') MAJ=.NOT. MAJ

```

```

      IF (KEY .EQ. '9') MIN=.NOT. MIN
      IF (KEY .EQ. 'B') BOX=.NOT. BOX
      IF (KEY .NE. '0') GOTO 0030
90020 FORMAT(27X,'PLOT OPTIONS      [' ,A8,']' /)
90021 FORMAT(23X,'1-  POINT  SYMBOL : ' ,A1/)
90022 FORMAT(23X,'2-  PEN FOR CURVE : ' ,I2/)
90023 FORMAT(23X,'3-  CHARACTER FORMAT (WIDTH,HIGH): ' ,2(2X,I4.2) /)
90024 FORMAT(23X,'4-  X # OF DIGITS : ' ,I2,6X, '      Y # OF DIGITS : ' ,I2/)
90025 FORMAT(23X,'5-  LINE BETWEEN POINTS IS ' ,A3/)
90026 FORMAT(23X,'6-  AXIS          ARE ' ,A3,5X, '7-  LABELS      ARE ' ,A3/)
90027 FORMAT(23X,'8-  MAJOR TICS ARE ' ,A3,5X, '9-  MINOR TICS ARE ' ,A3/)
90028 FORMAT(23X,'0-  MENU #2' /)
90030 FORMAT(23X,'TYPE IN NEW SYMBOL: ' /)
90031 FORMAT(23X,'B-  BOX      IS      ' ,A3/)
90040 FORMAT(23X,'TYPE IN NEW PEN NUMBER (1-3): ' \)
90041 FORMAT(23X,'CHARACTER WIDTH IN CM (0.1): ' \)
90042 FORMAT(23X,'CHARACTER HIGH IN CM (0.2): ' \)
90045 FORMAT(23X,'X AXIS # OF DIGITS      (0-5): ' \)
90047 FORMAT(23X,'Y AXIS # OF DIGITS      (0-5): ' \)
90050 FORMAT(23X,'TYPE IN NEW LINE TYPE (0-6): ' \)
99999 FORMAT(I2)
      RETURN
      END

```

```

C -----
C SUBROUTINE SAVE
C
C SAVE :   WRITES SPECTRUM DATA FILE TO DISK.
C
      LOGICAL*2  FLAG
      INTEGER*2  ND
      REAL*4      OX,OY,YMN,YMX,DST,DND,DNK
      PARAMETER (MAXPTS=4000)
      DIMENSION  OY(MAXPTS),OX(MAXPTS)
      COMMON /DT6COM/  YMN,YMX
      COMMON /DZ2COM/  OY,OX
      COMMON /DZ3COM/  ND,DST,DND,DNK

      FLAG=.TRUE.
      CALL DISK(FLAG)
      WRITE (1,*) DST,DND,DNK,ND
      DO 1000 I=1,ND
        WRITE(1,*) OY(I)
1000 CONTINUE
      WRITE (1,*) YMX,YMN
      END

```

```

C-----
C      SUBROUTINE SMOOTH
C
C      SMOOTH : SMOOTHING ROUTINE FOR Y AXIS DATA (MOVING AVERAGE) .
C
C      INTEGER*2    I,ND
C      REAL*4       YD,XD,YDF,DST,DND,DNK
C      PARAMETER    (MAXPTS=4000)
C      DIMENSION    YD (MAXPTS) , YDF (MAXPTS) , XD (MAXPTS)
C      COMMON /DT1COM/ YD,YDF,XD
C      COMMON /DZ3COM/ ND,DST,DND,DNK
C
C      DO 0100 I=2,ND-1
C          YD(I-1)=0.25*YD(I+1)+0.50*YD(I)+0.25*YD(I-1)
C          XD(I-1)=XD(I)
C      0100 CONTINUE
C
C      CORRECTION OF THE X AXIS DATA DUE TO THE SMOOTHING PROCESS
C
C      ND=ND-2
C      DST=DST-DK
C      DND=DND-DK
C      RETURN
C      END
C-----
C      SUBROUTINE SWAP (X1,X2)
C
C      SWAP : EXCHANGES THE CONTENT OF 2 REAL VARIABLES.
C
C      INPUT :
C      R*4    X1, X2    VARIABLE #1, #2
C
C      XDUM = X1
C      X1    = X2
C      X2    = XDUM
C      RETURN
C      END
C-----
C      SUBROUTINE SWAPI (I1,I2)
C
C      SWAP : EXCHANGES THE CONTENT OF 2 INTEGER VARIABLES.
C
C      INPUT :
C      I*2    I1, I2    VARIABLE #1, #2
C
C      IDUM = I1
C      I1    = I2
C      I2    = IDUM
C      RETURN
C      END

```

```

C-----
SUBROUTINE SWITCH(XPOS)
C
C   SWITCH: ERASES OLD LINE ON SCREEN AND DRAW A NEW ONE FOR GRINPO.
C
C   INPUT :
C   R*4     XPOS     CURRENT X POSITION OF THE THRESHOLD ON SCREEN
C
C   IMPLICIT REAL*4      (A-Z)
C   INTEGER*2  IPOS, IMIN, IMAX, IDUM
C   COMMON     /ZAP/      IMIN, IMAX
C
C   CALL QRTOI(XPOS, 0.0, IPOS, IDUM)
C   CALL QLINE(IPOS, IMIN, IPOS, IMAX, 2)
C   RETURN
C   END
C-----
REAL*4 FUNCTION TSTCOR
C
C   TSTCOR : RETURNS THE REAL VALUE OF THE CORRELATION COEFFICIENT
C            BETWEEN THE DATA AND THE FITTED CURVE
C
C   REAL*4      YD, YDF, XD, YADD, YAVG
C   REAL*8      EX, TOT, DUM
C   CHARACTER*10 MSG
C   PARAMETER    (MP=4000)
C   DIMENSION    YD(MP), YDF(MP), XD(MP), YADD(MP)
C   COMMON       /DT1COM/  YD, YDF, XD
C   COMMON       /DTYADD/  YADD
C   COMMON       /DZ7COM/  IMIN, IMAX, MSG
C
C   EX=0.0
C   TOT=EX
C   DUM=EX
C   INP=IMAX-IMIN+1
C   DO 0050 I=IMIN, IMAX
C       DUM=DUM+YD(I)
0050 CONTINUE
C   YAVG=DUM/INP
C   DO 1000 I=IMIN, IMAX
C       EX=EX+(YADD(I)-YAVG)**2
C       TOT=TOT+(YD(I)-YAVG)**2
1000 CONTINUE
C   TSTCOR=ABS(EX/TOT)*100
C   IF ( TSTCOR .GT. 100) TSTCOR=100.0
C   IF ( TSTCOR .LT. 0.0) TSTCOR= 0.0
C   IF ( TSTCOR .EQ. 100.0) MSG='PERFECT '
C   IF ((TSTCOR .LT. 100) .AND. (TSTCOR .GE. 80)) MSG='VERY HIGH '
C   IF ((TSTCOR .LT. 80 ) .AND. (TSTCOR .GE. 60)) MSG='HIGH '
C   IF ((TSTCOR .LT. 60 ) .AND. (TSTCOR .GE. 40)) MSG='MODERATE '
C   IF ((TSTCOR .LT. 40 ) .AND. (TSTCOR .GE. 20)) MSG='LOW '
C   IF ( TSTCOR .LT. 20 ) MSG='NO '

```

```

      RETURN
      END
C-----
      SUBROUTINE XMAX(I1,I2)
C
C   XMAX :   FINDS THE MINIMUM AND MAXIMUM FOR THE X AXIS DATA.
C
C   INPUT :
C
C       I*2      I1,I2      ARRAY INDEX OF THE FIRST AND LAST POINTS
C
      REAL*4      YD,XD,YDF
      PARAMETER (MAXPTS=4000)
      DIMENSION YD (MAXPTS), YDF (MAXPTS), XD (MAXPTS)
      COMMON /DT1COM/ YD,YDF,XD
      COMMON /DT8COM/ XMN,XXM

      XMN=XD(I1)
      XXM=XMN
      DO 1000 I=I1,I2
         IF (XD(I) .GE. XXM) XXM=XD(I)
         IF (XD(I) .LT. XMN) XMN=XD(I)
1000 CONTINUE
      RETURN
      END
C-----
      SUBROUTINE YMAX(I1,I2)
C
C   YMAX :   FINDS THE MINIMUM AND MAXIMUM FOR THE Y AXIS DATA.
C
C   INPUT :
C
C       I*2      I1,I2      ARRAY INDEX OF THE FIRST AND LAST POINTS
C
      REAL*4      YD,XD,YDF,YMX,YMN
      PARAMETER (MAXPTS=4000)
      DIMENSION YD (MAXPTS), YDF (MAXPTS), XD (MAXPTS)
      COMMON /DT1COM/ YD,YDF,XD
      COMMON /DT6COM/ YMN,YMX

      YMX=YD(I1)
      YMN=YMX
      DO 1000 I=I1,I2
         IF (YD(I) .GE. YMX) YMX=YD(I)
         IF (YD(I) .LT. YMN) YMN=YD(I)
1000 CONTINUE
      RETURN
      END

```

```

C -----
C CHARACTER*1 FUNCTION ZGET(KEYFLG)
C
C ZGET : FUNCTION THAT READS ONE CHARACTER FROM THE KEYBOARD.
C
C INPUT :
C I*2 KEYFLG INTEGER EXECUTION CONTROL FLAG
C 2 WAIT FOR A DUMMY KEY WHEN THE SCREEN
C IS IN GRAPHIC MODE (4) THEN RETURN
C 1 WAIT FOR A CHARACTER WHEN THE SCREEN
C IS IN TEXT MODE (0) THEN RETURN
C 0 WAIT FOR A DUMMY KEY WHEN THE SCREEN
C IS IN GRAPHIC MODE (0) THEN RETURN
C
C
C INTEGER*2 CKKEY, KEYVAL, KEYFLG
C CHARACTER*1 KEY
C CHARACTER*80 BLNK, OUTLNE
C COMMON /DTWRT / OUTLNE, BLNK
C
C IF (KEYFLG .EQ. 2) THEN
C CALL OPTXT(80,BLNK,1,0,22)
C CALL OPTXT(24,'HIT ANY KEY TO CONTINUE!',1,2,22)
C CALL QINPUT(KEY,0)
C ZGET=' '
C RETURN
C ENDIF
C IF (KEYFLG .EQ. 0) THEN
C WRITE(0,99999)
C CALL QINPUT(KEY,0)
C ZGET=' '
C RETURN
C ENDIF
C IF (KEYFLG .GT. 1) CALL QCMOV(IGCOL(KEYFLG), IGROW(22))
1000 KEYVAL=CKKEY(0)
C IF (KEYVAL .EQ. 0) GOTO 1000
C KEY=CHAR(KEYVAL)
C IF (ICHAR(KEY) .GE. #60) KEY=CHAR(ICHAR(KEY)-#20)
C ZGET=KEY
C RETURN
99999 FORMAT(20X,'HIT ANY KEY TO CONTINUE! '\)
C END

```



## Appendix 5

### Calculation of the Mean Distances Between Two Coils in Solution.

In chapter 4 and 5, the mean distances between two dissimilar coils were used to illustrate the type of regime which was operative in the copolymer solutions, i.e. separated or overlapped region. The calculations are outlined in this appendix. The list of symbols used for the dimensions of the polymer molecules, follows the nomenclature from Tanford.<sup>71</sup> Since coil dimension for the PS in DMSO at temperature higher than 70°C are not known and three significant figures are not needed in this calculation, an approximation is introduced. The only restriction for this approximation is a fixed bond angle.

Consider, for the sake of simplicity, that the mixtures are composed of polymers of which the repeat units have a average mass of 100 and a bond length of 1.54 Å. Thus, for the PS-SSA (MW=12000 and 100000) and PMMA-4VP (MW=100000), one can calculate the average end-to-end distance of the polymer chains using this equation

$$h_{av} = (\bar{h}^2)^{1/2} = \sigma^{1/2} l (1 + \cos \Theta / 1 - \cos \Theta)^{1/2}$$

where  $h_{av}$  is the average end-to-end distance of a polymer chain,  $(\bar{h}^2)^{1/2}$  is the rms average of the separation between the two ends of the polymer chain,  $l$  is the bond length,  $\sigma$  is the number of segments (MW/average mass) and  $\Theta$  the angle between the positive direction of successive bonds ( $\Theta = 180^\circ - 109.5^\circ$ ). Rearrangement of this equation gives

$$h_{av} = \sigma^{1/2} l (2)^{1/2}$$

The radius of these polymer coils will be considered equal to  $h_{av}$ .<sup>71</sup> For the PS-SSA with a molecular weight equal to 12000 and 100000,  $h_{av}$  is 24 Å and 69 Å, respectively. For the PMMA-4VP (MW=100000)  $h_{av}$  is equal to 69 Å. If these polymer

coils (assumed spherical) are treated as points arranged on a cubic lattice in the solution, then the average nearest-neighbor distance between two dissimilar polymer coils is the cube root of the volume of one unit cell from which the radii of the two dissimilar coils are subtracted. For equimolar mixtures of 0.05 M, 0.10 M and 0.15 M, containing the PS-SSA (MW=12000) and the PMMA-4VP (MW=100000), the average nearest-neighbor distances are 88 Å, 50 Å and 31 Å, respectively. While, for equimolar mixtures of 0.05 M, 0.10 M and 0.15 M, containing the PS-SSA (MW=100000) and the PMMA-4VP (MW=100000), this average distances are equal to 181 Å, 114 Å and 80 Å, respectively. From this one can conclude that for mixtures containing PS-SSA chains of MW=10<sup>4</sup>, the interpenetration of the PS-SSA and PMMA-4VP coils starts for a total polymer concentration of the order of 0.20 M. While for mixtures containing PS-SSA chains of MW=10<sup>5</sup>, it occurs for total concentrations of ~ 0.30 M.

## Appendix 6

### Supporting Data

Section A of this appendix contains the supporting data for the figures 4.1 to 5.1, which are results obtained from the application of a distinct equation.

#### A) Data for the Figures

**Figure 4.1** Determination of the true order ( $n_c$ ) for equimolar blends of PMMA-4VP 11 mole % (MW=10<sup>5</sup>) with PS-SSA 10 mole % (MW=10<sup>4</sup>, MW=10<sup>5</sup>) at 85°C in DMSO<sub>d6</sub>.

i) For the mixtures containing the PS-SSA with a MW=10<sup>4</sup>

$\ln a_o$	$\ln v$
-3.00	-7.25
-2.30	-5.78
-1.90	-4.93

ii) For the mixtures containing the PS-SSA with a MW=10<sup>5</sup>

$\ln a_o$	$\ln v$
-3.00	-7.25
-2.30	-5.78
-1.90	-4.93

**Figure 4.2** Time-concentration curves for various equimolar starting concentrations of PMMA-4VP 11 mole % of MW= $10^5$  with PS-SSA 10 mole % of MW= $10^5$ , at 85°C. The concentration on the vertical axis refers to the unshielded methoxy groups signal.

i) Filled Circles ([0.15]M)

Time (min)	[Unshielded Methoxy Groups] (M)
0.0	0.148
3.0	0.148
6.0	0.148
9.6	0.148
11.7	0.143
13.7	0.134
17.8	0.124
22.9	0.104
28.0	0.089
33.1	0.074
43.1	0.051
53.2	0.037
78.4	0.034
109	0.035
124	0.036
169	0.033

ii) Filled Triangles ([0.10]M)

Time (min)	[Unshielded Methoxy Groups] (M)
0.0	0.105
3.3	0.098
5.4	0.069
7.5	0.056
9.6	0.047
11.7	0.040
13.7	0.037
17.8	0.029
22.9	0.028
28.0	0.026
33.1	0.024
53.2	0.017
78.4	0.016
109	0.016
182	0.014

iii) Filled Squares ([0.05]M)

Time (min)	[Unshielded Methoxy Groups] (M)
0.0	0.051
3.8	0.041
5.3	0.040
6.8	0.036
8.3	0.032
9.8	0.026
14.3	0.023
15.9	0.021
17.2	0.020
22.8	0.017
27.9	0.013
38.8	0.008
43.1	0.007
48.2	0.006
53.2	0.005
88.7	0.004
98.8	0.003
109	0.003
337	0.003

**Figure 4.3** Time-concentration curves for equimolar mixtures of PMMA-4VP 11 mole % with PS-SSA of MW=10<sup>5</sup> at 85°C. Each curve represents a distinct sulfonation level. The solution contains 5 mg of both copolymers per 0.5 ml of DMSO<sub>d6</sub> (0.10 M). The concentration on the vertical axis refers to the unshielded methoxy groups signal.

i) Filled Squares (7.7%)

Time (min)	[Unshielded Methoxy Groups] (M)
0.0	0.105
3.3	0.094
5.4	0.078
7.5	0.075
9.6	0.068
11.7	0.063
13.7	0.057
17.8	0.053
22.9	0.050
28.0	0.044
33.1	0.042
53.2	0.038
78.4	0.038
109	0.041
139	0.038

ii) Filled Triangles (10.0%)

Time (min)	[Unshielded Methoxy Groups] (M)
0.0	0.105
3.3	0.098
5.4	0.069
7.5	0.056
9.6	0.047
11.7	0.040
13.7	0.037
17.8	0.029
22.9	0.028
28.0	0.026
33.1	0.024
53.2	0.017
78.4	0.016
109	0.016
182	0.014

iii) Filled Squares (14.7%)

Time (min)	[Unshielded Methoxy Groups] (M)
0.0	0.105
5.3	0.062
7.4	0.033
9.5	0.023
11.6	0.018
13.7	0.014
15.7	0.013
19.8	0.011
29.5	0.005
45.1	0.003
55.2	0.002
65.3	0.002
80.4	0.003
109	0.005
141	0.005

**Figure 4.4** Time-concentration curves for equimolar mixtures of PMMA-4VP 11 mole % with PS-SSA 10 mole % of MW= $10^5$  at various temperatures. The DMSO<sub>d6</sub> solution contains 5 mg of both copolymers per 0.5 ml (0.10 M). Vertical shifts of 0.025, 0.05, 0.02, 0 and 0 were respectively introduced on the curves from 70°C to 95°C. The concentration on the vertical axis refers to the unshielded methoxy groups signal.

i) Inverse Filled Triangles (70°C)

Time (min)	[Unshielded Methoxy Groups] (M)
0.0	0.155
3.3	0.139
5.4	0.142
7.5	0.143
9.6	0.141
11.7	0.140
13.7	0.138
17.8	0.137
22.9	0.133
28.0	0.131
33.1	0.119
43.1	0.117
63.3	0.111
78.4	0.106
93.5	0.102
109	0.098
124	0.094
139	0.092
179	0.096
199	0.095



ii) Filled Circles (75°C)

Time (min)	[Unshielded Methoxy Groups] (M)
0.0	0.130
3.3	0.130
5.4	0.130
7.5	0.129
11.7	0.126
13.7	0.123
28.0	0.119
43.1	0.104
53.2	0.094
63.3	0.089
93.5	0.082
124	0.082
139	0.083
154	0.080
169	0.078
199	0.078

iii) Filled Squares (80°C)

Time (min)	[Unshielded Methoxy Groups] (M)
0.0	0.125
5.4	0.118
7.5	0.110
9.6	0.077
11.7	0.073
13.7	0.070
17.8	0.061
22.9	0.055
28.0	0.051
33.1	0.050
43.1	0.048
63.3	0.049
78.4	0.047
93.5	0.041
109	0.035
124	0.031
139	0.031
182	0.031

iv) Filled Triangles (85°C)

Time (min)	[Unshielded Methoxy Groups] (M)
0.0	0.105
3.3	0.098
5.4	0.069
7.5	0.056
9.6	0.047
11.7	0.040
13.7	0.037
17.8	0.029
22.9	0.028
28.0	0.026
33.1	0.024
53.2	0.017
78.4	0.016
109	0.016
182	0.014

v) Filled Diamonds (95°C)

Time (min)	[Unshielded Methoxy Groups] (M)
0.0	0.105
3.9	0.064
5.9	0.050
7.9	0.043
10.1	0.039
12.2	0.037
14.3	0.031
18.3	0.028
23.4	0.028
33.6	0.021
43.6	0.019
53.7	0.019
63.8	0.016
109	0.017
139	0.016

**Figure 4.5** Time-concentration curves for mixtures of various equimolar starting concentrations of PMMA-4VP 11 mole % of MW= $10^5$  with PS-SSA 10 mole % of MW=  $10^4$ , at 85°C . Vertical shifts of 0, 0.01 and 0.020 were respectively introduced on the curves from 0.15 M to 0.05 M. The concentration on the vertical axis refers to the unshielded methoxy groups signal.

i) Filled Circles ([0.05]M)

Time (min)	[Unshielded Methoxy Groups] (M)
0.0	0.029
2.9	0.028
3.9	0.027
5.1	0.026
6.2	0.026
7.3	0.023
8.4	0.022
10.1	0.019
19.8	0.016
35.2	0.015
59.5	0.012
106	0.004
126	0.002
136	0.001
146	0.000
157	0.000
187	0.000
197	0.000

ii) Filled Triangles ([0.10]M)

Time (min)	[Unshielded Methoxy Groups] (M)
0.0	0.095
3.3	0.088
4.7	0.069
6.2	0.068
7.7	0.058
9.2	0.053
10.7	0.052
12.2	0.048
15.9	0.046
22.2	0.037
27.3	0.030
32.3	0.025
37.9	0.022
47.6	0.021
52.6	0.019
160	0.019

iii) Filled Squares ([0.15]M)

Time (min)	[Unshielded Methoxy Groups] (M)
0.0	0.168
5.0	0.142
6.6	0.109
7.8	0.076
8.6	0.075
9.5	0.074
14.3	0.071
15.7	0.070
20.2	0.069
21.9	0.068
36.1	0.068
110	0.067
182	0.067

**Figure 4.6** Time-concentration curves for equimolar mixtures of PMMA-4VP 11 mole % with a PS-SSA of MW=10<sup>4</sup> at 85°C. Each curve represents a distinct sulfonation level. The solution contains 5 mg of both copolymers per 0.5 ml of DMSO<sub>d6</sub> (0.10 M). The concentration on the vertical axis refers to the unshielded methoxy groups signal.

i) Filled Circles (13%)

Time (min)	[Unshielded Methoxy Groups] (M)
0.0	0.071
3.3	0.068
4.7	0.042
6.2	0.031
7.7	0.029
9.2	0.021
10.7	0.019
13.7	0.016
15.9	0.015
22.2	0.008
32.3	0.007
42.5	0.007
47.6	0.005
52.7	0.004
62.7	0.002
67.8	0.001
78.0	0.001
182	0.001

ii) Filled Triangles (10%)

Time (min)	[Unshielded Methoxy Groups] (M)
0.0	0.095
3.3	0.088
4.7	0.069
6.2	0.068
7.7	0.058
9.2	0.053
10.7	0.052
12.2	0.048
15.9	0.046
22.2	0.037
27.3	0.030
32.3	0.025
37.9	0.022
47.6	0.021
52.6	0.019
160	0.019

iii) Filled Diamonds (9%)

Time (min)	[Unshielded Methoxy Groups] (M)
0.0	0.137
4.8	0.110
6.9	0.109
9.0	0.105
11.1	0.101
13.1	0.098
24.4	0.093
29.5	0.085
34.6	0.083
44.6	0.065
54.7	0.050
64.8	0.043
95.0	0.039
125	0.041
140	0.039
200	0.039

iv) Filled Squares (8%)

Time (min)	[Unshielded Methoxy Groups] (M)
0.0	0.140
4.2	0.135
5.7	0.139
7.2	0.136
8.7	0.135
10.2	0.133
16.2	0.136
23.2	0.129
33.3	0.128
43.5	0.119
48.6	0.108
63.8	0.102
68.8	0.098
84.0	0.093
94.1	0.091
104	0.086
109	0.085
169	0.084

v) Inverse Filled Triangles (5%)

Time (min)	[Unshielded Methoxy Groups] (M)
0.0	0.175
2.3	0.175
4.8	0.153
6.9	0.148
9.0	0.144
11.1	0.146
13.2	0.145
17.2	0.144
22.3	0.141
27.4	0.140
32.5	0.140
52.6	0.139
77.8	0.138
108	0.137
138	0.137
168	0.137
198	0.137

**Figure 4.7** Time-concentration curves for equimolar mixtures of PMMA-4VP 11mole % with PS-SSA 10 mole % of MW=10<sup>4</sup> at various temperature. The solution of DMSO<sub>d6</sub> (0.5 ml) contained 5 mg of both copolymers. The concentration on the vertical axis refers to the unshielded methoxy groups signal.

i) Inverse Filled Triangles (70°C)

Time (min)	[Unshielded Methoxy Groups] (M)
0.0	0.090
4.3	0.090
6.4	0.082
8.5	0.055
10.6	0.046
12.7	0.039
14.7	0.034
18.8	0.020
29.0	0.018
34.1	0.013
54.2	0.007
79.4	0.006
110	0.004
140	0.004
170	0.003



ii) Filled Circles (75°C)

Time (min)	[Unshielded Methoxy Groups] (M)
0.0	0.090
4.3	0.061
6.4	0.053
8.5	0.049
10.6	0.037
12.7	0.021
14.7	0.018
18.8	0.012
23.9	0.008
29.0	0.006
34.1	0.004
54.2	0.001
79.4	0.000
110	0.000
140	0.000

iii) Filled Squares (80°C)

Time (min)	[Unshielded Methoxy Groups] (M)
0.0	0.105
4.3	0.105
6.4	0.073
8.5	0.063
10.6	0.054
12.7	0.050
14.7	0.048
18.8	0.042
23.9	0.035
29.0	0.034
34.1	0.031
54.2	0.029
64.3	0.027
95.0	0.029

iv) Filled Triangles (85°C)

Time (min)	[Unshielded Methoxy Groups] (M)
0.0	0.095
3.3	0.088
4.7	0.069
6.2	0.068
7.7	0.058
9.2	0.053
10.7	0.052
12.2	0.048
15.9	0.046
22.2	0.037
27.3	0.030
32.3	0.025
37.9	0.022
47.6	0.021
52.6	0.019
160	0.019

v) Filled Diamonds (95°C)

Time (min)	[Unshielded Methoxy Groups] (M)
0.0	0.145
4.3	0.125
6.4	0.112
8.5	0.101
10.6	0.099
12.7	0.098
14.7	0.097
18.8	0.096
23.9	0.091
29.0	0.090
34.1	0.088
39.1	0.086
44.2	0.085
49.3	0.085
54.4	0.085
64.4	0.087
84.6	0.086
94.7	0.087
105	0.086

**Figure 4.8** Plot of equations 3.5 and 3.8 for an equimolar mixture of PMMA-4VP 11 mole % with PS-SSA 10 mole % of MW=10<sup>5</sup>, at 85°C. The DMSO<sub>d6</sub> solution contains 2.5 mg of both copolymers per 0.5 ml (0.05 M).

Time (min)	Equation 3.5 ( $K_1$ )	Equation 3.8 ( $K_T$ )
0.0	0.00	0.00
3.8	0.00	0.00
5.3	0.03	0.04
6.8	0.12	0.16
8.3	0.20	0.27
9.8	0.39	0.53
14.2	0.47	0.64
15.9	0.56	0.76
17.2	0.60	0.82
22.8	0.76	1.03
27.9	1.05	1.43
38.8	1.61	2.17
43.1	1.67	2.26
48.2	1.86	2.52

Linear Regression for  $K_1$  :  $y = 0.042 x - 0.14$

Linear Regression for  $K_T$  :  $y = 0.057 x - 0.18$

**Figure 4.9** Plot of equation 3.11 for an equimolar mixture of PMMA-4VP 11 mole % with PS-SSA 10 mole % of MW= $10^5$ , at 85°C, The DMSO<sub>d6</sub> solution contains 2.5 mg of both copolymers per 0.5 ml (0.05 M).

Time (min)	Equation 32 ( $K_1$ )
0.0	0.0
3.8	0.0
5.3	1.1
6.8	4.1
8.3	6.9
9.8	13.0
14.2	15.7
15.9	18.5
17.2	19.7
22.8	24.6
27.9	33.3
38.8	49.3
43.1	51.1
48.2	56.7

Linear Regression :  $y = 1.29 x - 3.38$

**Figure 4.10** Time-concentration curve for the equimolar mixture (0.05 M) of PMMA-4VP 11 mole % of MW= $10^5$  with PS-SSA 10 mole % of MW=  $10^4$ , at 85°C. The concentration on the vertical axis refers to the shielded methoxy groups signal.

Time (min)	[Shielded Methoxy Groups] (M)
0.0	0.0000
2.9	0.0013
3.9	0.0023
5.1	0.0029
6.2	0.0033
7.3	0.0060
8.4	0.0070
10.1	0.0100
19.8	0.0132
35.2	0.0140
59.5	0.0176
106	0.0256
126	0.0276
136	0.0280
146	0.0298
157	0.0303
187	0.0302
197	0.0303

**Figure 5.1** Plot of  $\ln(X_e/X_e - X)$  vs time for an EQB (0.10M) containing PMMA-4VP 11 mole % (MW=10<sup>5</sup>) with PS-SSA 10 mole % (MW= 10<sup>5</sup>), at 80°C.

Time (min)	$\ln(X_e/X_e - X)$
0.0	0.00
5.0	0.16
10.0	0.49
13.4	0.76
18.0	1.01
22.0	1.29
26.5	1.60
35.0	2.04

Linear Regression :  $y = 0.058 x + 0$

## B) <sup>1</sup>H NMR Spectra Data Files Access

This section contains two type of data files, as obtained on the Varian XL-300 spectrometer, or the deconvolution program (FIT). The first type of files contains the <sup>1</sup>H NMR spectra, and are only accessible through the spectrometer or the work station. These files are labeled with six characters (no extension). and are included on two high density disks. The other type of File contains the results from the deconvolution and are labeled with the extension ".FIT". These IBM-PC compatible ASCII files can be displayed by the DOS command "TYPE", or accessed by any word processor program.

**Figure 2.2** <sup>1</sup>H NMR spectrum for the methoxy groups from PMMA-4VP at 120°C

File Name: PMMA120

**Figure 2.3** <sup>1</sup>H NMR spectrum for the methoxy groups from PMMA-4VP at 85°C

File Name: PMMA85

**Figure 2.4** <sup>1</sup>H NMR spectrum for the methoxy groups for a blend of PS-SSA 10% of Mw = 10<sup>4</sup> with PMMA-4VP 11% of Mw = 10<sup>5</sup> in DMSO<sub>d6</sub> at 85°C (contact time = 30 min.).

File Name: MCON05

**Figure 2.5** Example of <sup>1</sup>H NMR stack spectra for a typical shielding experiment for a blend of PS-SSA (5 mole %) of Mw = 10<sup>4</sup> with PMMA-4VP (11 mole %) of Mw = 10<sup>5</sup> in DMSO<sub>d6</sub> at 85°C.

File Name: MIC05

**Figure 3.1** Spectrum obtained by the addition of  $D_2O$  to the equilibrated polymer solution; elapsed time 1.5 hrs at  $T = 85^\circ C$ . The percentage in figures refer to volume  $D_2O / DMSO_{d6} \times 100$ .

% of $D_2O$	File Name
0.2	CW1
0.8	DW1
2.0	EW1



**Table 2.5** Deconvoluted shoulder area for the methoxy  $^1\text{H}$  NMR signal of PMMA-4VP as a function of temperature.

Temperature ( $^{\circ}\text{C}$ )	File Name
60	PMMA60.FIT
65	PMMA65.FIT
70	PMMA70.FIT
75	PMMA75.FIT
80	PMMA80.FIT
85	PMMA85.FIT
90	PMMA90.FIT
95	PMMA95.FIT
100	PMMA100.FIT
105	PMMA105.FIT
110	PMMA110.FIT
115	PMMA115.FIT
120	PMMA120.FIT

**Table 3.1** Summary of  $\Gamma$  and  $\Delta\Gamma$  values for blends containing a PS-SSA of low MW, with no observable shielded methoxy group signal.

MW	Blends Composition				File Name
	PS-SSA Ion Content (%)	Weight (mg)	PMMA-4VP Ion Content (%)	(MW=10 <sup>5</sup> ) Weight (mg)	
2000	25	2.2	11	5.0	M2000A
2000	25	5.0	11	5.0	M2000B
5000	10	5.1	11	5.0	M5000A
5000	15	3.7	11	5.0	M5000B
5000	15	5.0	11	5.0	M5000C
5000	20	2.8	11	5.0	M5000D
5000	20	5.0	11	5.0	M5000E

**Table 3.2** Summary of  $\Gamma$  and  $\Delta\Gamma$  values for blends containing a PMMA-4VP of low SSA content, with no observable shielded methoxy group signal.

MW	Blends Composition				File Name
	PS-SSA Ion Content (%)	Weight (mg)	PMMA-4VP Ion Content (%)	(MW=10 <sup>5</sup> ) Weight (mg)	
10 <sup>5</sup>	10	3.2	5	6.8	M5EQ
10 <sup>5</sup>	10	5.0	5	5.0	M5NEQ
10 <sup>5</sup>	10	4.3	7	5.8	M7EQ
10 <sup>5</sup>	10	5.0	7	5.0	M7NEQ

C) Data Files Access for the Quantitative Shielding Runs

The data collected by the  $^1\text{H}$  NMR of the polymers mixtures studied in the present work are included as part of the supporting data in the form of four 3 1/2" high density computer diskettes. The files contained on these diskettes are self-extracting files, i.e. they are files that have been compressed by the program PKZIP 1.1 (PKWARE Inc.), and then transformed to self-extracting files by the program ZIP2EXE (tm from PKWARE Inc.). The size of the files contained in one compressed file is of the order of one Mb. The more convenient procedure to decompress these files is to copy a compressed file (name.EXE) to a temporary directory on our hard disk and then type the name of the file without the extension.

A compressed file contains three types of data files. First, the files with the extension ".NMR", which are the those obtained from the data transfer from the NMR work station to the AST AT compatible. Second, the files with the extension ".DAT" are those that are compatible with the deconvolution program (FIT), i.e the transferred NMR files that have been modified by the program NMRMOD. Finally, the last type of files is labeled with the ".FIT" extension, and contains the results from the deconvolution process. All these IBM-PC compatibles files are saved as ASCII characters and can be displayed by the DOS command "TYPE", or accessed by any word processor program. These data files are the supporting data for the chapter 4 to 5.

Summary of the data files for the polymer blends.

BLEND DESCRIPTION				FILE NAME		
PS-SSA CONCENTRATION (M)	PS-SSA MW	PS-SSA ION CONTENT (mole %)	TEMPERATURE (°C)	DATA TRANSFERRED FROM THE NMR WORK STATION TO THE IBM PC	TRANSFERRED DATA MODIFIED BY THE PROGRAM NMRMOD	DECONVOLUTION RESULTS
0.05	10 <sup>5</sup>	10.0	85	HMW05 .NMR	HMW05 .DAT	HMW05 .FIT
0.15	10 <sup>5</sup>	10.0	85	HMW15 .NMR	HMW15 .DAT	HMW15 .FIT
0.10	10 <sup>5</sup>	10.0	70	HVT70 .NMR	HVT70 .DAT	HVT70 .FIT
0.10	10 <sup>5</sup>	10.0	75	HVT75 .NMR	HVT75 .DAT	HVT75 .FIT
0.10	10 <sup>5</sup>	10.0	80	HVT80 .NMR	HVT80 .DAT	HVT80 .FIT
0.10	10 <sup>5</sup>	10.0	85	HVT85 .NMR	HVT85 .DAT	HVT85 .FIT
0.10	10 <sup>5</sup>	10.0	95	HVT95 .NMR	HVT95 .DAT	HVT95 .FIT
0.10	10 <sup>5</sup>	7.7	85	HIC08 .NMR	HIC08 .DAT	HIC08 .FIT
0.10	10 <sup>5</sup>	14.7	85	HIC15 .NMR	HIC15 .DAT	HIC15 .FIT
0.05	10 <sup>4</sup>	10.0	85	MMW05 .NMR	MMW05 .DAT	MMW05 .FIT
0.15	10 <sup>4</sup>	10.0	85	MMW15 .NMR	MMW15 .DAT	MMW15 .FIT
0.10	10 <sup>4</sup>	10.0	70	MVT70 .NMR	MVT70 .DAT	MVT70 .FIT
0.10	10 <sup>4</sup>	10.0	75	MVT75 .NMR	MVT75 .DAT	MVT75 .FIT
0.10	10 <sup>4</sup>	10.0	80	MVT80 .NMR	MVT80 .DAT	MVT80 .FIT
0.10	10 <sup>4</sup>	10.0	85	MVT85 .NMR	MVT85 .DAT	MVT85 .FIT
0.10	10 <sup>4</sup>	10.0	95	MVT95 .NMR	MVT95 .DAT	MVT95 .FIT
0.10	10 <sup>4</sup>	5.3	85	MIC05 .NMR	MIC05 .DAT	MIC05 .FIT
0.10	10 <sup>4</sup>	8.3	85	MIC08 .NMR	MIC08 .DAT	MIC08 .FIT
0.10	10 <sup>4</sup>	9.2	85	MIC09 .NMR	MIC09 .DAT	MIC09 .FIT
0.10	10 <sup>4</sup>	13.8	85	MIC13 .NMR	MIC13 .DAT	MIC13 .FIT